

A Bioelectronic Approach to Post-surgical Anastomotic Leakage Diagnosis

Joshua Antony Paulinus

A thesis presented for the degree of
Doctor of Engineering

Department of Biomedical Engineering
University of Strathclyde
United Kingdom

Declaration

This thesis is the result of the author's original research. It has been composed by the author and has not been previously submitted for examination which has led to the award of a degree.

The copyright of this thesis belongs to the author under the terms of the United Kingdom Copyright Acts as qualified by University of Strathclyde Regulation 3.50. Due acknowledgement must always be made of the use of any material contained in, or derived from, this thesis.

Signed:

Date:

Acknowledgements

First, I wish to express my gratitude to my primary supervisor, Professor P. Connolly, for letting me carry out this project, as well as providing valuable advice and support during this EngD project. In addition, I would like to thank the Medical Devices group at the University of Strathclyde for providing help and support, as well as providing good company in the lab. I would like to acknowledge the EPSRC for providing the funding to allow the project to be conducted.

I would like to thank my clinical advisor, Professor S. Moug, for proposing the project as well as providing support and advice throughout its duration. I wish to further thank the clinicians at the Royal Alexandra Hospital for their help during the period when patient samples were being collected, in particular, Dr. Nicole McLaughlin who was invaluable in identifying and organising collection of samples.

I also thank the GGC Biorepository for approving the ethics for collection of patient samples.

Finally, I would like to thank my family and friends who have encouraged and supported me throughout this thesis.

Abstract

Colorectal cancer is a disease that afflicts a substantial number of people globally. One of the methods of removing the cancer is to surgically resect the tumourous section. In many cases, the remaining healthy sections of the colon/rectum are reattached to form what is known as an anastomosis. In some cases, this anastomosis can leak, often referred to as anastomotic leakage, leading to longer hospital stays and costs and can lead to patient mortality if not detected and treated at an early stage. However, there is no universal method of detecting anastomotic leakage at an early stage, with clinicians often requiring patients to exhibit symptoms before even suspecting anastomotic leakage, which is often too late for diagnosis.

Delays in diagnosis has been shown to increase the likelihood of patient mortality, therefore the aim of this thesis was to determine a method of detecting anastomotic leakage reliably at an early stage. Glucose, lactate and pH, as well as electrochemical diagnostic techniques (electrochemical impedance spectroscopy - EIS and cyclic voltammetry - CV) were used to investigate their usefulness in indicating anastomotic leakage.

Initially, methods needed to be developed to allow for testing of patient peritoneal fluid. Glucose and lactate commercial assays were modified for use with these samples and found to have a linear region of up to 20mM for lactate and 25mM for glucose. EIS and CV techniques were also developed

using platinum working and counter electrodes. Initially, these techniques were tested with a simulated wound fluid and indicated the need for a fixed volume for testing. Further testing with a more complex simulated fluid that is more similar to the expected patient samples. When spiked with bacteria and blood, EIS showed its potential at distinguishing between differing components of the fluid whereas results from CV indicated a lower utility for clinical monitoring.

Methods which were developed and tested were then used on patient samples. Though no useful data was collected with regards to anastomotic leakage, other useful information about patients who underwent an uncomplicated post-op and some on patients who experienced other post-op complications was gained. Glucose was found to peak at shortly after surgery and drop over time with a strong trend being determined. In addition, some of the patients who had post-op condition caused anomalous results which could indicate its potential at determining post-op conditions. EIS results also showed potential with determining other post-op complications. However, lactate, pH and CV showed to be of limited/no use of diagnosing post-op conditions.

Further work in the area should focus on larger scale studies looking at glucose and EIS as well as performing micro-biology studies to confirm trends in this thesis.

List of Publications

This thesis has been presented at the following conferences:

Early stage detection of post-operative complications after colorectal surgery using drain fluid

ASGBI Centenary Free Paper Series - Aug 2020

Biomarkers of Leakage after Anastomotic Dehiscence Evolution

BioMedEng 2018 - Sept 2018

Nomenclature

Abbreviations

Ag/AgCl	Silver/Silver Chloride
APE	Artificial Peritoneal Exudate
ASA	American Society of Anaesthesiologists
ATP	adenosine-tri-phosphate
COPD	Chronic Obstructive Pulmonary Disease
CPE	Constant Phase Element
CRP	C-Reactive Protein
CT	Computer Tomography
CV	Cyclic Voltammetry
dH ₂ O	Deionised Water
EGFRs	Epidermal Growth Factor Receptors
EIS	Electrochemical Impedance Spectroscopy
GCP	Good Clinical Practice
GOD	Glucose Oxidase
GORD	Gastro-Oesophageal Reflux Disease

HB	Horse blood
IHP	Inner Helmholtz Plane
IL-1 β	Interleukin 1 β
IL-10	Interleukin 10
IL-6	Interleukin 6
KCl	Potassium Chloride
LB	Lysogeny Broth
LOD	Limit of Detection
LPS	Lipopolysaccharide
LRTI	Lower Respiratory Tract Infection
MMP	Matrix Metalloproteinase
MSC-2	Micro Safety Cabinet - Level 2
NaCl	Sodium Chloride
NICE	National Institute of Clinical Excellence
OHP	Outer Helmholtz Plane
PCR	Polymerase Chain Reaction
PTFE	Polytetrafluoroethylene
SISG	Surgical Infection Study Group
TIMP	Tissue Inhibitor of Matrix Metalloproteinase
TNF- α	Tumour Necrosis Factor Alpha

TOOS N-ethyl-N-(2 hydroxy-3-sulphopropyl)m-toluidine

VEGF Vascular Endothelial Growth Factor

Constants

k_B Boltzmann's Constant ($1.38 \times 10^{-23} J K^{-1}$)

F Faraday's number ($9.648 \times 10^4 C M^{-1}$)

R Gas Constant ($8.314 J M^{-1} K^{-1}$)

Mathematical Notation

$[H^+]$ Concentration of Hydrogen ions

$\angle\theta$ Phase angle

β Charge-transfer coefficient

ΔG Gibb's Free Energy

δ Length of diffusion layer

ΔE Potential Perturbation

ϵ molecular extinction coefficient

η Overpotential

$\frac{dv}{dt}$ Acceleration

$|Z|$ Modulus of the Impedance

ω Radial Velocity

\vec{F} Force vector

ϕ Deviation from capacitance in CPE

ϕ_1	Phase shift in initial voltage perturbation
σ_b	Standard deviation of the blank
τ	Average time between collisions
τ	Relaxation Time
ϵ	Permittivity
ϵ_0	Low-frequency Relative Permittivity
ϵ_∞	High-frequency Relative Permittivity
A	Area
a	Particle Radius
$a(H_3O^+)$	Activity of Hydronium ions
a_B	Activity of the base
a_j	Activity of species j
a_{H^+}	Activity of the hydrogen ions
a_{HA}	Activity of the acid
c	Concentration
c_0	Concentration at electrode surface
c_j	Concentration of species j
c_{bulk}	Concentration in bulk solution
d	Distance
D_j	Diffusion Coefficient(Diffusivity) of species j

E^0	Constant offset potential
E_0	Amplitude of signal
E_0	Standard Electrode Potential
E_a	Activation Energy
E_e	Equilibrium Potential
E_{anode}	Potential at Anode
$E_{cathode}$	Potential at Cathode
E_{cell}	Cell Potential
$E_{solution}$	Solution Potential
I_0	Incident light intensity
i_0	Equilibrium current
I_{max}	Maximum current
j	Complex number $\sqrt{-1}$
J_j	Flux of species j
K_a	acid dissociation/acidity constant
K_b	acid basicity/association constant
m	mass
N	Number of collisions
q^d	Excess charge density
q^E	Charge of electrode

q^i	Charge of ion
q^S	Charge of solution
R_s	Solution Resistance
R_{eq}	Equivalent Resistance
t_j	Transport number of species j
v	Drift Velocity
v_s	Scan rate
w'_i, w''_i	Weights applied for EIS modelling (Resistance and Reactance)
x	Direction of movement
Z	Impedance
Z'	Real part of the impedance (Resistance)
Z''	Imaginary part of the impedance (Reactance)
Z_f	Faradaic Resistance
Z'_i, Z''_i	Experimental values of Resistance and Reactance at frequency, i
Z_s	Solution Impedance
$Z'_{i,cal}, Z''_{i,cal}$	Calculated values of Resistance and Reactance at frequency, i
A	Absorbance/Pre-exponential Factor
b	Light path length/y-intercept

C	Capacitance
E	Potential
I	Current/Exiting light intensity
IQR	Interquartile Range
k	Gradient of curve/Rate constant
m	Surface Mobility on the ion/mass flow rate
n	Number of Electrons
q	Charge
Q1	First Quartile
Q3	Third Quartile
R	Resistance
S	Sum of squares
SD, σ	Standard Deviation
T	CPE capacitance term/Transmittance/Temperature
z	Number of electrons transferred in a reaction
Units	
Ω	Ohms
A	Ampere
C	Coulombs
CFU	Colony Forming Units

F	Farads
g	Gram
K	Kelvin
L	Litre
M	Moles
V	Voltage
°C	Degrees Celcius

Contents

Declaration	i
Nomenclature	ii
Acknowledgements	ii
Abstract	iii
List of Publications	v
List of Figures	xxvii
List of Tables	xxix
1 Literature Review and Rationale	1
1.1 Introduction and Problem Statement	2
1.2 Large Intestine	6
1.2.1 Structure	6
1.2.2 Walls of the Large Intestine	7
1.3 Colorectal Cancer	9
1.3.1 Types	9
1.3.2 Classification and Staging	10
1.3.3 Treatment	12
1.4 Anastomotic Leakage	18

1.4.1	Definition	18
1.4.2	Causes of Anastomotic Leakage	20
1.4.3	Incidence Rates	23
1.4.4	Complications of Anastomotic Leakage	25
1.4.5	Risk Factors for Anastomotic Leakage	26
1.4.6	Current Clinical Diagnosis Methods	31
1.4.7	Time to Diagnosis	34
1.4.8	Management of Colorectal Anastomotic Leakage	35
1.4.9	Economic Cost of Anastomotic Leakage	38
1.5	Other Investigated Markers	38
1.5.1	Biomarkers for Ischaemia	38
1.5.2	Inflammation Markers	44
1.5.3	Matrix Metalloproteinases (MMPs)	50
1.5.4	Bacterial Markers	51
1.5.5	Impedance Measurements	53
1.5.6	Summary	57
1.6	Aims and Objectives	58
2	Background Theory	61
2.1	Introduction	62
2.2	Electrochemical Theory	62
2.2.1	Movement of Ions - Mass Transfer	64
2.2.2	Interactions at the Electrode Surface	68
2.3	Electrical Theory	74
2.3.1	Resistance and Capacitance	74
2.3.2	Impedance	76
2.3.3	Dielectric Properties of Biological Material	77

2.4	Electrochemical Techniques	81
2.4.1	Diagnostic Techniques	81
2.4.2	Potential Controlled Techniques	90
2.4.3	Potentiometry	92
2.5	Colorimetric Assays	94
2.5.1	Characterisation of Assays	97
2.6	Summary	99
3	Materials and Methods	100
3.1	Introduction	101
3.2	Materials and Solutions	103
3.2.1	Solution A	103
3.2.2	Artificial Peritoneal Exudate (APE)	103
3.2.3	pH Buffer Solutions	105
3.2.4	Lysogeny Broth Media and Agar Plates	106
3.2.5	Sodium and Potassium Chloride Solutions	106
3.2.6	Lactate and Glucose Reagents	106
3.2.7	Microbial Species	107
3.2.8	Clinical Samples	108
3.3	Lactate and Glucose Measurements	111
3.3.1	Equipment and Materials	111
3.3.2	Assay Characterisation	112
3.3.3	Clinical Lactate and Glucose Testing Procedure	114
3.4	pH Testing	115
3.4.1	Equipment	115
3.4.2	Clinical Testing	116
3.5	Electrochemical Testing - EIS and CV	117

3.5.1	Equipment	118
3.5.2	Electrode Selection	119
3.5.3	EIS Set-up and Testing	121
3.5.4	CV Set-up and Testing	121
3.5.5	Volume Experiments	122
3.5.6	Preliminary Modelling of Peritoneal Fluid	123
3.5.7	Clinical Testing	124
3.6	Analysis	126
3.6.1	Outliers	126
3.6.2	Normalisation	126
3.6.3	Modelling	127
3.6.4	Cyclic Voltammetry	128
3.6.5	Bacterial Colony Counting	128
3.6.6	Statistical Analysis	129
3.7	Summary	130
4	Preliminary Testing	131
4.1	Introduction	132
4.2	Lactate Assay Characterisation	134
4.3	Glucose Assay Characterisation	137
4.4	Electrochemical Impedance Spectroscopy (EIS)	140
4.4.1	Initial Testing with Varying Volume	141
4.4.2	Artificial Peritoneal Exudate (APE)	144
4.5	Cyclic Voltammetry	157
4.5.1	Initial Testing	158
4.5.2	Artificial Peritoneal Fluid	159
4.6	Summary	160

5	Clinical Results	161
5.1	Introduction	162
5.2	Ethics and Patient Demographics	162
5.3	Lactate	165
5.4	Glucose	168
5.4.1	Unfiltered Samples	169
5.4.2	Filtered Samples	172
5.5	pH	175
5.6	EIS	178
5.6.1	Patients with Uncomplicated Post-op	179
5.6.2	Post-operative Conditions	189
5.6.3	Modelling	193
5.6.4	Timed Experiment	197
5.7	Cyclic Voltammetry	201
5.8	Summary	202
6	Discussion and Conclusions	203
6.1	Introduction	204
6.2	Ischaemic Markers	205
6.2.1	Lactate	205
6.2.2	Glucose	214
6.2.3	pH	221
6.3	Electrochemical Testing	225
6.3.1	EIS	225
6.3.2	Cyclic Voltammetry	241
6.4	Conclusions and Future Work	243

References	247
Appendix 1 : Biorepository Ethics Approval	284

List of Figures

1.1	(Left) Schematic drawing of the large intestines. Reprinted from Blausen.com staff (2014) under a Creative Commons Licence BY 3.0 Licence. (Right) CT Image of the large intestines. Image courtesy of The Royal Alexandra Hospital Radiology Department, Paisley.	6
1.2	Representation of walls of the Large intestine. Reprinted from U. S. National Institutes of Health - National Cancer Institute (2001) (Public domain image)	7
1.3	Visual representation of how the tumour (T) is categorised in the TNM system. Image reprinted from Cancer Research UK / Wikimedia Commons (2014 <i>b</i>) under a Creative Commons BY-SA 4.0 license.	10
1.4	Local resection of colorectal tumour. Image reprinted from Cancer Research UK / Wikimedia Commons (2014 <i>a</i>) under a Creative Commons BY-SA 4.0 license.	15
1.5	Cancer removal and anastomosis formation	16

1.6	(Top) Lateral scan of gastrografin enema shows leakage of low anterior resection as shown by contrast in the presacral space (Radiopaedia 2014). (Bottom) Transverse plane CT image (with contrast) of abdomen showing anastomotic leakage, shown by red arrow, with contrast material in the presacral space (Radiopaedia 2017). Images reprinted under a Creative Commons BY-NC-SA 3.0 Licenses.	33
2.1	Basic Electrochemical Cell	63
2.2	Model of the electrical double layer. 1) Inner Helmholtz layer, 2) outer Helmholtz layer, 3) diffusion layer, 4) solvated ions, 5) adsorped ions and 6) solvent molecule. Reprinted from Wikimedia Commons (2008) under a Creative Commons BY 3.0 license	69
2.3	Effect of overpotential on current on an electrochemical system. i_c and i_a are the cathodic and anodic current components.	72
2.4	Concentration profile from the electrode. δ is the diffusion layer	73
2.5	Resistors in series	74
2.6	Resistors in parallel	74
2.7	Typical changes in permittivity due to frequency in biological material. Based on Schwan (1957).	77
2.8	Relationship between potential and current when a potential perturbation (ΔE) is applied	81
2.9	Example Nyquist plot	83
2.10	Randles Circuit Diagram	84
2.11	Example potential wave used for cyclic voltammetry	88
2.12	Example Cyclic Voltammetry Graph	89

2.13 (Top) Potential waveform used in chronoamperometry and (Bottom) the resultant current measurement	91
2.14 Basic principal of colorimetric measurements	95
2.15 Example assay profile with linear and non-linear regions defined	97
3.1 (Left) Passive drainage bag (Right) Suction drainage bag	109
3.2 UN3373 packaging used for transferring samples from the hospital to the University	110
3.3 Labsystems Multiskan Ascent (and connected PC) used to measure the absorbance of samples at specific wavelengths	111
3.4 Example schematic 96-well plate used to characterise the glucose and lactate assays	113
3.5 Probe and meter used to measure pH in clinical samples	116
3.6 pH probe schematic diagram for measuring samples	117
3.7 Solartron 1260 set up for use in Electrochemical Impedance Spectroscopy (EIS) measurements	118
3.8 Solartron 1287 set up for Cyclic Voltammetry (CV) experiments	119
3.9 Set-up used to produced Ag/AgCl wires	120
3.10 Schematic drawing of EIS electrode set-up in 24 well plate well during testing	121
3.11 Top down view of electrode set-up for CV experiments	122
3.12 Order of testing clinical sample by pH, EIS and CV	125
3.13 Example removal of baseline non-faradaic current using Origin	128
3.14 Example of colony counting of <i>E.coli</i> (DSM30083). In this case, colony counting can be done at a 10^6 dilution	129

4.1	Measurements of different lactate concentrations by the photometer (n=5). Results were fitted between 0-20mM as shown by the red line	136
4.2	Measured lactate concentrations (mean±SD), using the developed lactate assay methodology, of a known industrially manufactured lactate standard (n=4 done in triplicate)	137
4.3	Measurements of different glucose concentrations by the photometer (n=5). Results were fitted between 0-25mM as shown by the red line	138
4.4	Measured glucose concentrations (mean±SD), using the developed glucose assay methodology, of a known industrially manufactured lactate standard (n=4 done in triplicate)	140
4.5	Nyquist plot of EIS measurements of Solution A with differing volumes (n=5, mean ± SD)	142
4.6	Modulus plot of EIS experiments of Solution A with differing volumes (n=5, mean ± SD)	142
4.7	Phase plot of EIS experiments of Solution A with differing volumes (n=5, mean ± SD)	143
4.8	Nyquist plot of spiked artificial peritoneal exudate (APE) with horse blood (HB), <i>P. aeruginosa</i> (PA14) and <i>E. coli</i> (DSM30083). Mean ± SD, n=4	145
4.9	Graph showing significant differences between fluid spiked with horse blood(HB) and bacteria, <i>P. aeruginosa</i> and <i>E. coli</i> (DSM30083), over a frequency range of 0.1 and 1MHz	146

4.10	Averaged (\pm SD) modulus plot of spiked artificial peritoneal exudate (APE) with horse blood (HB), <i>P.aeruginosa</i> (PA14) and <i>E.coli</i> (DSM30083). Mean \pm SD	149
4.11	Averaged (\pm SD) phase plot of spiked artificial peritoneal exudate (APE) with horse blood (HB), <i>P.aeruginosa</i> (PA14) and <i>E.coli</i> (DSM30083). Mean \pm SD	149
4.12	Graph showing significant differences in modulus and phase between fluid spiked with horse blood(HB) and bacteria, <i>P.aeruginosa</i> and <i>E. coli</i> (DSM30083), over a frequency range of 0.1 and 1MHz	150
4.13	Normalised modulus results of variously spiked artificial peritoneal exudate (APE) vs unspiked APE. HB - Horse Blood, DSM - <i>E.coli</i> Strain, PA - <i>P.aeruginosa</i> strain PA14	152
4.14	Normalised phase results of variously spiked artificial peritoneal exudate (APE) vs unspiked APE. HB - Horse Blood, DSM - <i>E.coli</i> Strain, PA - <i>P.aeruginosa</i> strain PA14	153
4.15	(Top) Circuit diagram of selected model of simulated fluid. R_s is solution resistance, R_f is faradaic resistance and CPE is the constant phase element. (Bottom) Example fitting of model to data gained from EIS measurement of APE + <i>E.coli</i>	154
4.16	Solution resistance of spiked artificial peritoneal exudate(APE) with horse blood (HB), <i>P.aeruginosa</i> (PA14) and <i>E.coli</i> (DSM30083). Mean \pm SD, n=4.	154
4.17	Faradaic resistance of spiked artificial peritoneal exudate(APE) with horse blood (HB), <i>P.aeruginosa</i> (PA14) and <i>E.coli</i> (DSM30083). Mean \pm SD, n=4.	155

4.18	Capacitance term of CPE of spiked artificial peritoneal exudate(APE) with horse blood (HB), <i>P.aeruginosa</i> (PA14) and <i>E.coli</i> (DSM30083). Mean \pm SD, n=4.	156
4.19	Phi (ϕ) term of CPE of spiked artificial peritoneal exudate(APE) with horse blood (HB), <i>P.aeruginosa</i> (PA14) and <i>E.coli</i> (DSM30083). Mean \pm SD, n=4.	157
4.20	Cyclic Voltammetry of Solution A with different volumes in a 24 well plate. Scan rate of 25mV/s (n=3)	158
4.21	Cyclic Voltammetry (25mV/s scan rate) of variously spiked samples of artificial peritoneal exudate(APE) with horse blood(HB), <i>P.aeruginosa</i> (PA14) and <i>E.coli</i> (DSM30083)	160
5.1	Measured lactate concentrations of patients from drain fluid. Points in red diamonds are outliers. Average line is mean \pm SD.	166
5.2	Polynomial fitting of normalised lactate results. Red line is the polynomial fitting (order=2) of the results ($R^2=0.145$) Outliers (patients 6 and 12) not included in the analysis	167
5.3	Glucose change over time for patient drain samples. Points shown as a red diamond are considered outliers. Mean \pm SD is of patients who did not have post-op complications.	170
5.4	Fitting of glucose results from patient samples. Red line shows fitting of equation $y = mx + c$. Outliers (patients 8 and 12) not included in line fitting	171
5.5	Glucose concentrations found in filtered patient samples. Red diamonds indicate points that were considered outliers.	172
5.6	Glucose concentrations found in filtered patient samples. Outliers not included in line fitting	173

5.7	Unfiltered clinical pH results	176
5.8	pH change versus day 1 values in clinical samples.	177
5.9	Filtered clinical pH results	177
5.10	Average (\pm SD) Z' vs Z'' of clinical samples from uncomplicated post-op patients on each post-op day.	179
5.11	Average (\pm SD) modulus of clinical samples from uncomplicated post-op patients on each post-op day.	180
5.12	Average (\pm SD) phase of clinical samples from uncomplicated post-op patients on each post-op day.	181
5.13	Average (\pm SD) Nyquist plot of filtered clinical samples from uncomplicated post-op patients on each post-op day.	182
5.14	Resistance changes in regions that showed significance in filtered samples (Average \pm SE).	183
5.15	Reactance changes in regions that showed significance in filtered uncomplicated post-op patient samples (Average \pm SE). . .	184
5.16	Average (\pm SD) modulus plot of filtered clinical samples from uncomplicated post-op patients on each post-op day.	184
5.17	Average (\pm SD) phase plot of filtered clinical samples from uncomplicated post-op patients on each post-op day.	185
5.18	Modulus changes in regions that showed significance in filtered uncomplicated post-op patient samples (Average \pm SE).	185
5.19	Regions where significant difference was found between unfiltered and filtered results for modulus and phase results of patient samples using 2-way repeated-measures ANOVA tests.	186
5.20	Changes in phase at 1kHz as a result of filtering over time. Significant differences occurred on Days 2 and 3. Bars are mean \pm SE.	187

5.21	Changes in phase at 1Hz as a result of filtering over time. Significant differences occurred on Day 4 (indicated by star). Bars are mean±SE.	187
5.22	Changes in modulus at 0.1Hz as a result of filtering over time. Significant differences occurred on Days 2,3 and 4. Bars are mean±SE.	188
5.23	Nyquist Plots of unfiltered samples from Patients 1, 5 and 12. .	189
5.24	Nyquist Plots of unfiltered samples from Patients 18, 19 and 21.	190
5.25	Modulus Plots of unfiltered samples from patients 1, 12 and 19.	191
5.26	Phase plots of unfiltered samples from patients 1, 12, 19 and 21	192
5.27	Phase plots of filtered samples from patient 19 versus uncomplicated cases	192
5.28	Normalised phase plots for patient 19	193
5.29	Example of modelling patient data	194
5.30	Calculated solution resistances from modelling	194
5.31	Calculated faradaic resistances from modelling	195
5.32	Calculated capacitance term of constant phase element from modelling	196
5.33	Calculated phi term of constant phase element from modelling	196
5.34	3D Z' vs Z'' of timed experiment	198
5.35	3D modulus of timed experiment	198
5.36	3D phase of timed experiment	199
5.37	Normalised modulus of timed experiment	200
5.38	Normalised phase of timed experiment	201
5.39	Example of patient cyclic voltammetry result (patient 17 day 1)	202
6.1	Potential device for post-op monitoring	245

List of Tables

1.1	World Health Organisation Colorectal Tumour Types (Jessup et al. 2017).	9
1.2	TNM Category Definitions. Taken from Jessup et al.(2017).	11
1.3	Staging of colorectal cancers using the TNM classification system. Taken from Jessup et al.(2017).	12
1.4	Definitions of different types of colorectal resections. Definitions based on Martin (2015) and Cancer Research UK (2015 <i>b</i>). Percentages based on National Bowel Cancer Audit Annual Report 2019 (2020) values of patients in England and Wales where suitable follow-up occurred.	17
1.5	Complications that can occur after colorectal resections (not an exhaustive list) (Kirchhoff et al. 2010, Longo et al. 2000). SSIs - Surgical Site Infections	18
1.6	Anastomotic leakage and mortality rates from various papers - Values were standardised to percentages (patient numbers in brackets). Mortality rate percentages are based on number of patients who had anastomotic leakage and not on total number of patients. *Highest value found when reviewing	25

1.7	Risk factors associated with colorectal anastomotic leakage. *Reference indicates that significant trend is only found in low (close to the anal verge) anastomoses. Factors in bold indicate higher importance.	30
1.8	Symptoms used to determine if anastomotic leakage is potentially present (Not Exhaustive). Adapted from den Dulk et al. (2009)	31
1.9	Summaries of investigated markers in literature	57
3.1	Chemicals used for artificial peritoneal exudate	104
3.2	Solutions used to characterise glucose and lactate assays. Na-L=Sodium Lactate	112
5.1	Demographics and procedures undergone by patients included in the study	164
5.2	Post-operative complications in patients in study groups	165
6.1	Calculated parameter values of spiked solutions (mean±SD) . .	229
6.2	Average modelling parameter values obtained from clinical samples. Mean±SD	237
6.3	Changes found possibly due to post-op complications	244

Chapter 1

Literature Review and Rationale

1.1 Introduction and Problem Statement

Colorectal cancer is a prevalent disease that affects over a million people globally. It is the third most common cancer in males and second most common in women. In the UK, there are approximately 40,000 new cases each year (Cancer Research UK 2015*b*). Survival rates of patients with colorectal cancer have improved over many years due to significant improvements in treatment of which surgery plays a major role (Mitry et al. 2008, Brouwer et al. 2018). Often, the surgery involves the resection of the cancerous section of the colon/rectum, with the remaining healthy sections being reattached to form what is known as an anastomosis. However, the surgery itself can result in life-changing consequences for a patient, especially if they experience a post-operative complication. Anastomotic leakage is one such complication where healing of the anastomosis does not occur correctly, resulting in a tear/hole causing the contents of the colon to leak. This can result in unwanted symptoms such as abdominal pain, fever, rigid abdomen and, if untreated, can be fatal (Epstein & Parrillo 1993, Toutouzas et al. 2009, Weledji & Ngowe 2013). Currently, diagnosis of anastomotic leakage can be difficult with no universal method to identify the problem and often relying on patients having to exhibit symptoms before clinicians suspect anastomotic leakage. This often requires confirmation by a CT scan (den Dulk et al. 2009). However, this can be problematic with radiation risks, as well as been shown in literature to have reduced levels of sensitivity in confirming leakage (Habib et al. 2015, Hyman et al. 2007) (see Section 1.4.6 for more information on diagnosis of anastomotic leakage). Delays in treatment have been shown to increase the chances of mortality (den Dulk et al. 2013) and therefore it is important that a

method of detecting anastomotic leakage at an early stage (before symptoms occur) be established to improve patient outcomes and reduce the chances of mortality. In addition, the development of a reliable method of detecting anastomotic leakage can result in lower costs and reduced hospital stays (Ashraf et al. 2013, Gessler et al. 2017).

Therefore, the aim of this thesis was to research approaches that might be used for early detection of anastomotic leakage, preferably at the point of care. Particularly work was carried out to determine if reliable biomarker(s) could be used to determine anastomotic leakage at an early stage and if detection of such markers could be implemented in a device that could monitor the patient in real-time during their post-op recovery. It was hypothesized, based on the literature and discussions with clinicians, that monitoring of drain fluid from drains placed during surgery could provide information to determine anastomotic leakage due to the close proximity of the drain to the anastomosis, allowing drain to collect abdominal fluid from the zone of the anastomosis. Thus, any breakdown of the anastomosis might result in an early marker being detected in the drain fluid.

While the causes of anastomotic leakage are not well known, ischaemia, which is where damage to tissues occurs due to the reduction of oxygen from low blood supply, is often quoted as one of the main reasons for this complication occurring (Vignali et al. 2000, Hallböök et al. 1996) (see Section 1.4.2 for more details). Three major biomarkers that change as a result of this are glucose, lactate and pH (Matthiessen et al. 2007) (see Section 1.5.1 for more details). Therefore, it was hypothesized that monitoring of these markers could provide a method to diagnose anastomotic leakage. While some literature has found that there maybe a link between changes in these markers and anasto-

motoc leakage, methods used in these studies may not be accurately measuring these parameters, for example, microdialysis tubes that have been used to measure glucose and lactate have been noted that measured values are a fraction of the actual concentration of the area they are measuring (Chefer et al. 2009, Shippenberg & Thompson 1997, Turkina et al. 2017). In addition, some techniques used to monitor these parameters have been invasive and not practical for use in a clinical setting, for example, balloon tonometry for pH measurement (Millan et al. 2006)(more detail provided in Section 1.5.1). Therefore, unlike previous studies, lactate and glucose measurements in this study were performed directly on drain fluid collected from patients using colorimetric assays.

In addition, electrochemical techniques, Electrochemical Impedance Spectroscopy - EIS and cyclic voltammetry - CV, were also chosen to study the drain fluid. Both EIS and CV have been used to monitor various substances, for example, EIS has been used to monitor bacterial species and differentiate between cancerous and non-cancerous tissues and CV can be used to monitor redox reactions and substances such as urea (Patzner et al. 1989, Ward et al. 2018, Halter et al. 2007). Neither of these techniques have been used with regards to characterising drain fluid or to determining whether it is possible for use in diagnosing anastomotic leakage. It was hypothesized that changes in the composition of drain fluid could be detected by these techniques and differences between patients without leakage versus patients with leakage could be established.

In this chapter, an initial background to the large intestine, colorectal cancer and treatment is given to provide context to the problem. After this, more detail is given about anastomotic leakage including how it is currently clinically

diagnosed and its problems and a literature review of markers that have been looked into previously to try to solve this problem, leading to the aims and objectives of the project.

1.2 Large Intestine

1.2.1 Structure

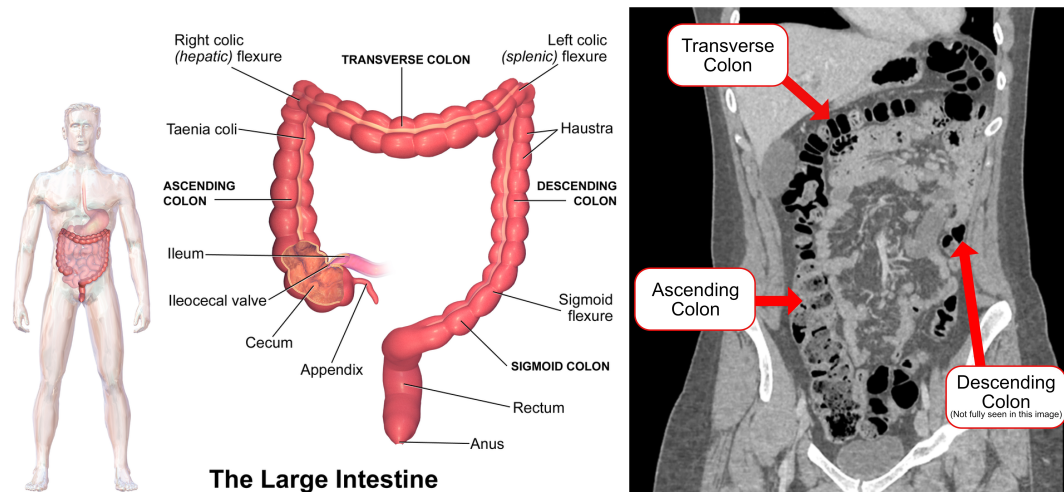


Figure 1.1: (Left) Schematic drawing of the large intestines. Reprinted from Blausen.com staff (2014) under a Creative Commons Licence BY 3.0 Licence. (Right) CT Image of the large intestines. Image courtesy of The Royal Alexandra Hospital Radiology Department, Paisley.

The large intestine is an organ, approximately 1.5m long and 7.5cm wide, found in the abdominal cavity and surrounds the small intestines. The large intestine starts at the terminus of the ileum of the small intestine and ends at the anus and can be generally divided into 3 sections; caecum, colon and rectum (Figure 1.1).

The caecum is where contents from the small intestine (ileum) enter the large intestine via the ileocaecal valve. The caecum is where collection and compaction of material known as chime begins (Martini et al. 2015, McGrath 2005). This feeds into the colon which generally divided into 4 sections (dependent on location); the ascending colon, the transverse colon, the descending colon, and the sigmoid colon (Martini et al. 2015, Steele et al. 2016). The colon

has two main functions. The first is digestion, either by mechanical means, through contraction and peristalsis, and by chemical means, through fermentation by the abundant bacterial population present. The second function is the absorption of water and electrolytes (Shroyer & Kocoshis 2011, Betts et al. 2018, Szmulowicz & Hull 2011, Wood 2019) . The final part of the large intestine (approx. 15cm) is the rectum. The rectum lies beneath the peritoneal reflection and is able to expand to act as a temporary storage of faeces before its expulsion (Christensen 1991, Martini et al. 2015, Steele et al. 2016).

1.2.2 Walls of the Large Intestine

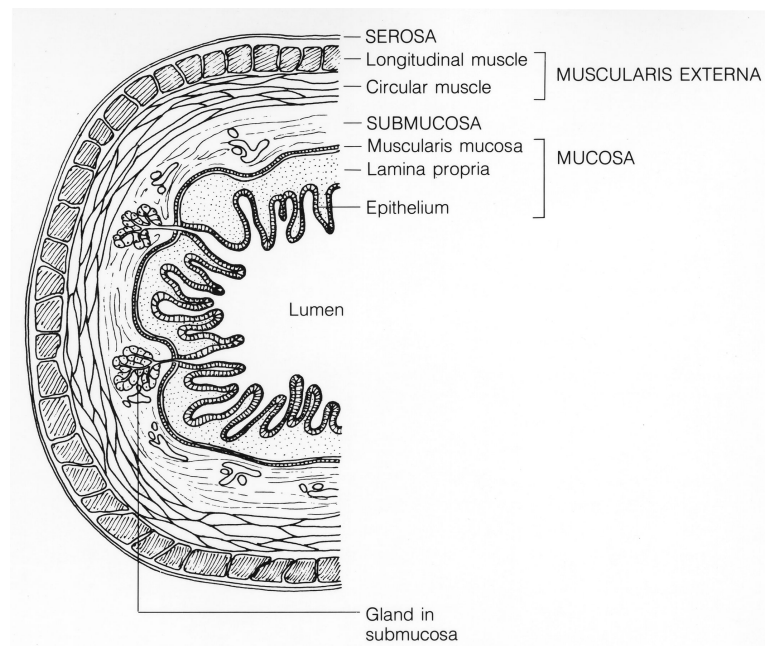


Figure 1.2: Representation of walls of the Large intestine. Reprinted from U. S. National Institutes of Health - National Cancer Institute (2001) (Public domain image)

There are 4 different layers in the walls of the large intestines: the mucosa, the submucosa, the muscularis propria(externa) and the serosa (Figure 1.2) (Christensen 1991, McGrath 2005, Shroyer & Kocoshis 2011).

The mucosa is the innermost layer and consists of 3 components: the ep-

ithelium, muscularis mucosa (a layer of smooth muscle cells) and the lamina propria (mesh containing collagen) (Christensen 1991, Moran et al. 2008, Betts et al. 2018, Shroyer & Kocoshis 2011, Uchida & Kamikawa 2007, Wood 2019).

The next layer is the submucosa which contains the blood vessels, fibroblasts, collagen and other cell types including nerves (Martini et al. 2015, Christensen 1991). It has been found that this layer is responsible for the majority of the tensile strength of the colon and as a result, most suturing of anastomoses is through the submucosa and has been shown to improve anastomotic healing (Matheson 1992, Leslie & Steele 2003) (Colorectal healing explained further in later sections).

Below the submucosa is the muscularis propria which is composed of two layers of smooth muscle fibres. The layer closest to the submucosa is orientated transverse to the large intestine, whereas the second layer is orientated longitudinally. Between these two layers is an intermuscular space which is abundant in nerves and blood vessels (Martini et al. 2015, Betts et al. 2018, Christensen 1991, Shroyer & Kocoshis 2011).

The final layer is the serosa/adventitia. This layer, composed of epithelial cells and connective tissue, reduces the friction between the large intestine and other organs and therefore, provides a layer of protection (Christensen 1991, Betts et al. 2018). This layer is called the serosa in the transverse and sigmoid colon and adventitia for the rest of the large intestine. This is due to the location of these parts relative to a closed membrane structure known as the peritoneum, which is made up of epithelium and connective tissues, covers many abdominal structures. Some of the large intestine is retroperitoneal, where the section of the colon is behind the peritoneum and only the anterior part of the colon is in contact with the peritoneum, for which the outer layer

of the wall is known as the adventitia. On the other hand, the transverse and sigmoid colon is intraperitoneal meaning it is located within the peritoneal cavity. The outer layer of these sections of the large intestines are known as serosa (Marieb & Hoehn 2013, McGrath 2005).

The peritoneum is composed of two layers: the parietal peritoneum that lines the abdomen and; the visceral peritoneum that covers the outer surface of many abdominal surfaces. Between the two layers, there is a space, known as the peritoneal cavity. This cavity contains peritoneal fluid which acts as a lubricant. This fluid is normally present in small quantities but can become more abundant as a result of disease. When the volume is greater than 25mL, it is known as ascites (or ascitic fluid).

1.3 Colorectal Cancer

1.3.1 Types

There are several histological types of primary cancer that can occur in the colon/rectum. The most common are adenocarcinomas which account for approximately 95% of all colorectal cancers. Other types of cancer that can form in the large intestine are listed in Table 1.1 (Chu 2010).

Table 1.1: World Health Organisation Colorectal Tumour Types (Jessup et al. 2017).

Adenocarcinoma <i>in situ</i>	Medullary carcinoma
Adenocarcinoma	Mucinous carcinoma
Signet ring cell carcinoma	Squamous cell carcinoma
Adenosquamous carcinoma	Neuroendocrine carcinoma
Small cell neuroendocrine carcinoma	Large cell neuroendocrine carcinoma
Undifferentiated carcinoma	Carcinoma, NOS (Not Otherwise Specified)

1.3.2 Classification and Staging

Cancers are staged to help identify the best course of treatment for each case. In order to determine what stage a colorectal cancer is, tumours are first classified by the TNM system. The letter 'T' refers to the extent at which the primary tumour has spread through the cell. A visual representation of the 'T' definitions can be seen in Figure 1.3. The letter 'N' refers to whether regional lymph nodes have cancer present. Finally, the letter 'M' refers to cancer metastasis. The full classification can be found in Table 1.2). By using the TNM classification, the cancer then can be staged (see Table 1.3).

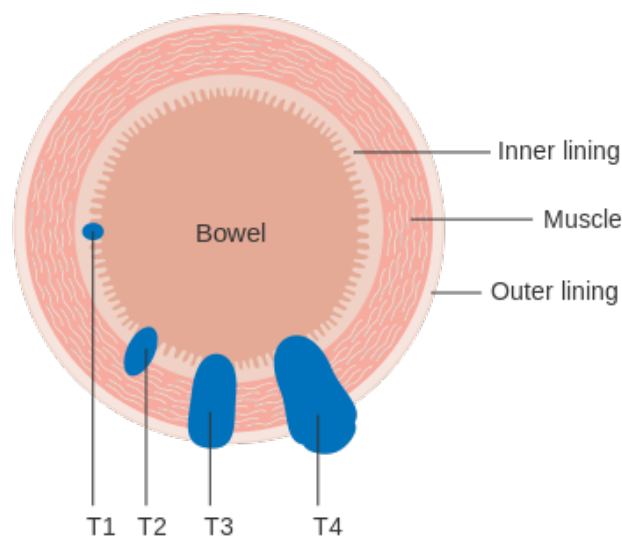


Figure 1.3: Visual representation of how the tumour (T) is categorised in the TNM system. Image reprinted from Cancer Research UK / Wikimedia Commons (2014b) under a Creative Commons BY-SA 4.0 license.

Table 1.2: TNM Category Definitions. Taken from Jessup et al.(2017).

Tumour (T)
TX - Tumour cannot be assessed
T0 - No evidence of primary tumour
Tis - Carcinoma <i>in situ</i>
T1 - Tumour invades submucosa
T2 - Tumour invades muscularis propria
T3 - Tumour invades through muscularis propria into pericorectal tissues
T4a - Tumour invades through peritoneum
T4b - Tumour invades/adheres to surrounding structures/organs
Lymph Node (N)
NX - Regional lymph nodes cannot be assessed
N0 - No lymph node metastasis
N1a - 1 regional lymph nodes positive
N1b - 2/3 lymph nodes positive
N1c - Tumour deposits present in the mesentery, subserosa or non-peritonealised pericolic or perirectal/mesorectal tissues.
N2a - 4-6 lymph nodes positive
N2b - 7+ lymph nodes positive
Metastasis (M)
M0 - No distant metastasis identified
M1a - Metastasis identified in one distant site/organ. No peritoneal metastasis.
M1b - Metastasis identified in 2+ distant sites/organs. No peritoneal metastasis.
M1c - Metastasis identified on peritoneal surface with or without metastasis in other sites/organs.

Table 1.3: Staging of colorectal cancers using the TNM classification system. Taken from Jessup et al.(2017).

Stage	T Category	N Category	M Category
0	Tis	N0	M0
1	T1/2	N0	M0
2A	T3	N0	M0
2B	T4a	N0	M0
2C	T4b	N0	M0
3A	T1/2	N1	M0
or	T1	N2a	M0
3B	T3/T4a	N1	M0
or	T2/T3	N2a	M0
or	T1/T2	N2b	M0
3C	T4a	N2b	M0
or	T3/T4a	N2a	M0
or	T4b	N2b	M0
4A	Any T	Any N	M1a
4B	Any T	Any N	M1b
4C	Any T	Any N	M1c

1.3.3 Treatment

There are several treatments that can be used to treat colorectal cancer. Survival rates are highly dependent on the stage of the cancer when treatment occurs, with patients at stage 1 having a 91.7% 5 year survival rate which reduces to 10.3% for patients at stage 4 (Office for National Statistics 2019).

Chemotherapy

Chemotherapy is where patients are given cytotoxic agents to kill off cancerous cells. The agents used affect a cell's ability to replicate as well as trigger cell death. This can be achieved in numerous ways, often by interfering with the cell cycle, for example, by producing reactive oxygen species or affecting enzymes that are required for cell division (Dickens & Ahmed 2018, Sak

2012). Chemotherapy is used either; after initial treatment by another modality; for advanced cases, where some studies have shown that chemotherapy may allow shrinkage of a tumour to the point that it could be then surgically resected; or as a palliative treatment (Dickens & Ahmed 2018, Tobias & Hochhauser 2014).

The treatment is not able to differentiate between healthy and cancerous cells and relies on the higher frequency of cancer cells replicating in order to be effective. Slow-growing cancerous cells can survive this treatment and can result in new strains of the cancer occurring weeks or months after remission of cancer. It has been found that the higher the use of chemotherapy in a patient, the more likely that the potential relapse becomes more aggressive with a more resistant cancer cell types occurring (Sak 2012). In the UK, about 31.2% of patients with colon cancer and 41.9% of patients with rectal cancer undergo chemotherapy (National Cancer Registration and Analysis Service & Cancer Research UK 2017).

Radiotherapy

Radiation therapy is a treatment modality where ionising radiation is focused on cancer cells to cause irreparable damage. When the cells are exposed to this radiation, they become impaired as a result of two mechanisms: direct or indirect. Direct radiation is where the high energy of the treatment directly affects cells, damaging DNA. The second mechanism is by indirect means using free radicals. Free radicals are produced as a result of ionisation/excitation of water within a cell. These free radicals then interact with DNA in cells causing damage to them and therefore inhibiting their function to divide. When lower energy beams are used, such as X-rays and gamma rays, the majority

of damage tends to be caused by indirect actions.

The radiation dose must be calculated precisely to effectively kill cancerous cells while not causing much damage to surrounding normal cells. As this is often complex to calculate, due to the random nature that radiation kills cells, multiple treatments are usually required to get the desired result. Radiotherapy can be done externally via the use of machines (external beam therapy) or by placing radioactive material near the cancerous cells (internal radiation therapy, also known as brachytherapy) and is usually applied over numerous sessions (up to 8) in low doses to minimise unwanted side effects (Ahmad et al. 2012, Baskar et al. 2014). The use of radiotherapy is heavily dependent on the stage and location of the cancer. In the UK, approximately 3.4% of colon cancer patients and 40.8% of rectal cancer patients receive radiotherapy (National Cancer Registration and Analysis Service & Cancer Research UK 2017).

Biological Treatment

Biological treatment is a relatively new option for treatment. At the moment, the National Institute of Clinical Excellence (NICE) allows this treatment for metastatic colorectal cancers with several criteria needing to be fulfilled.

There are several types of biological treatments available, where monoclonal antibodies are used to inhibit cell function in various ways. There are two main functions that can be inhibited by these monoclonal antibodies. The first is to disrupt cell proliferation the antibodies targeting and by attaching to epidermal growth factor receptors (EGFRs), which are usually overexpressed in cancerous cells. The other method of disruption is to bind to the anti-vascular endothelial growth factor (VEGF) receptors, which causes inhibition

of angiogenesis (Jonker et al. 2007, Noel 2017).

Surgery

The mainstay of treatment for colorectal cancer is surgical resection, where the cancerous section is removed alongside the mesentery to achieve complete oncological clearance. The type of surgery that is offered depends on the stage of the cancer.

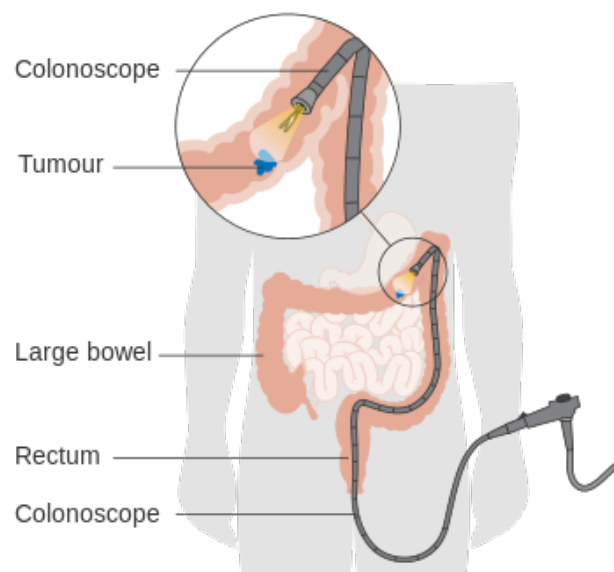


Figure 1.4: Local resection of colorectal tumour. Image reprinted from Cancer Research UK / Wikimedia Commons (2014a) under a Creative Commons BY-SA 4.0 license.

For polyp cancers with no venous invasions, surgeons can perform resection of the polyp via colonoscopy (Figure 1.4). For early stage rectal cancers (T1), local resection/excision via the anus (Trans Anal MicroSurgery – TAMiS) is considered optimal. For tumours staged T2 and beyond (or if the patient wishes), segmental resection of the large intestine is performed with the accompanying mesentery (to remove blood vessels and lymph nodes). This can be done either laparoscopically or at open surgery. Resections can be cate-

gorised by the anatomy of the colon and/or rectum removed (Table 1.4). The level of resection is dependent on how far the cancer has spread and may include lymph nodes (Althumairi & Gearhart 2015, Cancer Research UK 2015a, NICE 2011).

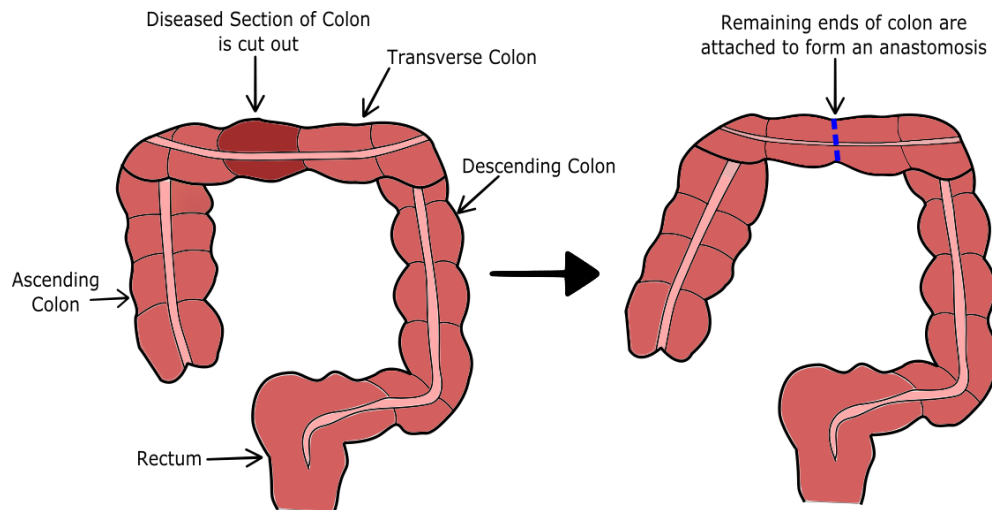


Figure 1.5: Cancer removal and anastomosis formation

In most cases, there is enough healthy colon/rectum left for which the surgeon is able to reattach, using sutures or staples, to form what is known as an anastomosis as shown in Figure 1.5 (Cancer Research UK 2015a).

Table 1.4: Definitions of different types of colorectal resections. Definitions based on Martin (2015) and Cancer Research UK (2015*b*). Percentages based on National Bowel Cancer Audit Annual Report 2019 (2020) values of patients in England and Wales where suitable follow-up occurred.

Procedure	Section of the large intestine removed	Percentage of patients undergoing procedure (Primary Treatment)
Total Colectomy	Whole colon	3.2%
Right Hemicolectomy	Ascending colon	41.7%
Left Hemicolectomy	Descending colon	4.2%
Transverse colectomy	Transverse colon	0.4%
Sigmoid colectomy	Sigmoid colon	3.6%
Anterior Resection	Sigmoid colon and a section of the rectum	32.8%
Proctosigmoidectomy	Rectum and sigmoid colon	7.5%
Abdominoperineal Resection	Anus, anal sphincter, rectum and part of the sigmoid colon	6.27%
Pelvic Exenteration	Removal of all organs in pelvic cavity	0.4%

Some patients may require a stoma to be formed after resection of the large intestine. A stoma is where either the end of the ileum of the small intestine (ileostomy) or a section of the large intestine (colostomy) is brought through the abdominal wall to the external part of the abdomen to which faeces can pass through. The use of a stoma may be to protect the anastomosis and allow for healing among other reason and could be reversed at a later date. In certain cases however, such as in abdominoperineal resections, a permanent stoma is required as the patient has insufficient residual large intestine to remove waste products (Pine & Stevenson 2017). In the UK, approximately 65% of patient undergo surgery for cancer removal (National Cancer Registration and Analysis Service & Cancer Research UK 2017).

There are many complications that can occur as a result of colorectal surgery. Some of these are listed in Table 1.5. One complication that is particularly worrying for surgeons is known as anastomotic leakage. This occurs when

the anastomosis deteriorates, allowing the contents of the colon to leak into the peritoneum which can rapidly lead to a patient's post-surgical condition deteriorating.

Table 1.5: Complications that can occur after colorectal resections (not an exhaustive list) (Kirchhoff et al. 2010, Longo et al. 2000). SSIs - Surgical Site Infections

Infections (including SSIs)	Postoperative Bleeding
Bowel Dysfunction	Ileus
Wound Complications	Anastomotic Leakage
Renal Failure	Cardiovascular/Respiratory Complications
Urethral/Bladder complications	Neurological Complications

1.4 Anastomotic Leakage

1.4.1 Definition

There is no universally accepted definition for anastomotic leakage. In 1991, the Surgical Infection Study Group (SISG) in the UK attempted to provide a standardised definition to allow for valid comparisons between differing centres. Their definition of an anastomotic leak was; “... a leak of luminal contents from surgical join between two hollow viscera. The luminal contents may emerge either through the wound or at the drain site, or they may collect near the anastomosis, causing fever, abscess, septicaemia, metabolic disturbance and/or multiple-organ failure. The escape of luminal contents from the site of the anastomosis into an adjacent localised area, detect by imaging, in the absence of clinical symptoms and signs should be recorded as a subclinical leak” (Peel & Taylor 1991). This definition was proposed over two decades ago and is cited by the Association of Surgeons

of Great Britain and Ireland & The Association of Coloproctology of Great Britain and Ireland (2016) but was not universally accepted.

Often, papers that refer to anastomotic leakage provide their own definition which usually contains elements of the definition proposed by SISG. Bruce et al. (2001) performed a review regarding the definition of an anastomotic leak in relation to gastrointestinal surgery. They found that in the 97 studies that were used for the review, there were 56 differing definitions for the term anastomotic leakage. Based on the papers used in the review, key points for a definition were noted and three broad categories were established depending on how an anastomotic leak could be diagnosed and the level of severity; radiological, clinical minor and clinical major. Radiological detection refers to leaks that were detected by imaging such as Computer Tomography (CT) scans. Clinical minor diagnosis of an anastomotic leak refers to a diagnosis made based on tests and observations such as fever, high white blood cell count, etc. and clinical major is where a diagnosis is made on a similar level as clinical minor leaks but there is more disturbances at the anastomotic site and would be detectable with imaging techniques.

Another attempt to define anastomotic leakage was performed by the International Study Group of Rectal Cancer, which they defined as *“a defect of the intestinal wall at the anastomotic site (including suture and staple lines of neorectal reservoirs) leading to a communication between the intra- and extraluminal compartments”*. They also introduced a grading system to indicate the severity of the leakage but were based on the level of intervention required. Grade A leaks are leaks where no active intervention was required; grade B leaks are where active intervention is required without re-laparotomy and grade C leaks are where active intervention requiring re-laparotomy (Rahbari et al.

2010). Again, the definition was not widely used verbatim, but some papers do refer a grading system or use a modified system to indicate the severity of the leak.

Though Bruce et al. (2001) and Rahbari et al. (2010) highlighted key points that are used in definitions of anastomotic leakage, it also brings up the point that much of the tools used to define leakage are quite subjective which makes direct comparison of studies regarding this topic particularly difficult.

1.4.2 Causes of Anastomotic Leakage

The cause of why anastomotic leakage occurs is still relatively unknown, even with numerous studies that have looked into it.

In terms of healing of anastomoses, there is a three stage process: 1) The inflammatory stage, 2) the proliferation stage and 3) the tissue remodelling stage.

In the inflammatory stage, which starts immediately after the wound is formed and lasts for approximately 3 days, haemostasis (the cessation of bleeding) is achieved by vasoconstriction and increased permeability of blood vessels. In addition, inflammatory cells enter the wound and release tissue growth factors and white blood cells fight any infections and aid in the removal of dead cells. As mentioned in section 1.2.2, the tensile strength of colon is mostly contributed by the collagen found in the submucosa. During the early wound healing process, collagen is low due to the fact there is high level of collagenase activity. As a result, during this time, the anastomosis is weak and its strength is highly dependent on the sutures/staples and the remaining collagen. The proliferation stage follows this, where new tissue is formed

with collagen synthesis occurring, vastly improving the strength of the anastomosis, as well as angiogenesis improving oxygen supply to the tissue and providing vitamins and minerals required for healing. The deposited collagen in the proliferation stage is further improved (thicker bundles) and tissue is remodelled in the tissue remodelling stage. This stage usually lasts for weeks/months. Disruption of healing processes are thought to cause leakage and there are 3 commonly cited reasons for why this disruption occurs: bacteria, ischaemia and tension (Daams et al. 2013, Thompson et al. 2006, Bosmans et al. 2015).

A notable difference between the large intestine and other organs (e.g. skin) is presence of the large population of bacteria within the large intestine, for which some groups have claimed is the cause of leakage occurring. In rats that had anastomoses (performed surgically), Schardey et al. (1994) found that anastomotic leakage occurred in 95% of rats which were inoculated with *Pseudomonas aeruginosa* (on day 1 by oral dose), a bacteria often associated with hospital acquired infections and can cause intestinal infections (Okuda et al. 2010, Markou & Apidianakis 2014). This could indicate that bacteria have some role in leakage, possibly through endo- and exo- toxins interfering with normal healing pathways, where endotoxins are large molecules that form part of the outer membrane of Gram-negative bacteria and exotoxins are proteins that are excreted from bacteria, both of which are harmful to tissues (Baker et al. 2011, Alcamo & Warner 2010). In another rat-based study, it was found that in rats that exhibited anastomotic leakage, higher levels of organisms that cause collagen degradation, production of which is required in the healing of tissues, were present, particularly strains of *Enterococcus faecalis*. As mentioned previously, collagen deposition is important in providing the

colon its strength (Shogan et al. 2013).

However, other studies have suggested that bacteria have a role in healing of anastomoses. Bacteria play a major role in digestion. One of the products produced by some of the bacteria in the colon are short-chain fatty acids. One of these fatty acids, butyrate, has been shown to be involved in epithelial healing by modulating the inflammatory response and a few studies have shown (in rats) that with infusions of butyrate, the strength of anastomoses increased (Mathew et al. 2010, Liu et al. 2018). In addition, some recent research has found that some types of bacteria found in the mucosa of the anastomosis after surgery were correlated to improved anastomotic healing (Li et al. 2019).

Though it has been shown that some bacteria can contribute to the cause of anastomotic leakage, not all bacteria do and could contribute to the healing of anastomoses. More research is required to understand how the bacterial environment affects healing of anastomoses, particularly in humans as opposed to rats.

Another commonly cited reason for anastomotic leakage occurring is the reduction of blood flow/reduced oxygen perfusion. Adequate blood flow is required for healing; otherwise, ischaemia occurs. However, what is meant by adequate is still under debate. Ischaemia occurs when tissues do not receive enough oxygen, due to reduced blood flow, and therefore become hypoxic. This has been indicated by several studies such a study by Hallböök et al. (1996). In the study, laser Doppler flowmetry was used. In this technique, a laser was used on tissues which causes light beams from the laser to be scattered by the movement of red blood cells in accordance to the Doppler effect. Some of the light is backscattered which can be detected by a photodetector and the output of this voltage levels can be related to red blood cell

concentrations and velocity. In the study, this arrangement was used to monitor blood flow during surgery at the anastomotic site and it was found that uninterrupted blood flow (i.e. higher levels of red blood cell flow as indicated by higher output voltages) allowed for better healing of the anastomosis. Vignali et al. (2000), who also used Doppler techniques also found that reduced proximal perfusion of an anastomosis was linked to anastomotic leakage. It should be noted though, that during the beginning phases of wound healing, tissues need to be some level of hypoxic in order to trigger the healing processes to form new blood vessels (Castilla et al. 2012). This was shown by Boyle et al. (2000) who found, using Doppler, that oxygen levels could drop by 57% and healing of anastomoses could still occur. Further work is still needed to understand how perfusion affects healing.

The last commonly cited reason is leakage occurs due to incorrect surgical technique (e.g. incorrect suturing technique) or that the two ends of the bowel are pulled together such that increased stresses and strains are applied onto the tissues (Shogan et al. 2013). In skin wounds, it has been seen that when this occurs, tissues have reduced microperfusion and oxygen supply (Guo & DiPietro 2010, Wilson & Clark 2004). While some work has found that measuring and ensuring good microperfusion at the site of the anastomosis improves outcomes (Gröne et al. 2015), further work is required to confirm incorrect surgical technique as a cause of colorectal anastomotic leakage.

1.4.3 Incidence Rates

The number of people affected by anastomotic leakage varies greatly in literature. Incidence rates range from as low as 1.8% of patients (Choi et al. 2006) to as high as 33% (Komen et al. 2008) though often it tends to be up to 20%

(Association of Surgeons of Great Britain and Ireland & The Association of Coloproctology of Great Britain and Ireland 2016). An overview of the range of values stated in papers can be seen in Table 1.6. One of the reasons for the large variations could be attributed to the different definitions of anastomotic leakage (as mentioned earlier) and what type of surgical resection is being performed as it is well established that rectal surgery anastomoses carry a significantly higher leak rate than colonic surgery. Why rectal anastomoses have a higher leak rate has been associated with the fact the rectum has a relatively poor blood supply and therefore the risk of ischaemia is increased (Wang & Gu 2010, Bruce et al. 2001, Komen et al. 2008).

The mortality rate, like the incidence rate, varies a lot in literature from as low as 0.7% (Alves et al. 2002) to just over 50% of patients affected by anastomotic leakage dying (Vignali et al. 1997) as shown in Table 1.6. More recent papers also have a large variation with one paper by Popescu et al. (2017) reporting a mortality rate of 28.6% and another by the 2015 European Society of Coloproctology Collaborating Group (2020) reporting a rate of 10.6%.

Mortality has been shown to be affected by delays to treating the leakage due to the problems regarding confirming diagnosis of leakage. When using a standardised protocol to reduce the time required to diagnosis (reduced from 4 days to 1.5 days), den Dulk et al. (2013) found that the mortality rate reduced from 39% to 24%.

Table 1.6: Anastomotic leakage and mortality rates from various papers - Values were standardised to percentages (patient numbers in brackets). Mortality rate percentages are based on number of patients who had anastomotic leakage and not on total number of patients. *Highest value found when reviewing

Paper	Number of Patients	Leakage Rate	Mortality Rate
Kockering et al. (1999)	1143	4.2%(48)	4.2%(2)
Dulk et al. (2009)	223	9.4%(21)	24%(5)
Alves et al. (1999)	655	6% (39)	13% (5)
Hyman et al. (2007)	1223	2.7% (33)	6.1% (2)
Boccola et al. (2011)	1576	7%	-
Alves et al. (2002)	707	6% (43)	11.6%(5)
Vignali et al. (1997)	1014	2.9%(29)	55.2%(16)
Sørensen et al. (1999)	333	15.9%(53)	-
Konishi et al. (2006)	391	2.8% (11)	-
Choi et al. (2006)	1417	1.8% (25)	32% (8)
Khan et al. (2008)	1421	2.9% (41)	12.2% (5)
Ramphal et al. (2018)	1984	7.5%(149)	-
Komen et al. (2008)	-	33%*	-
Kornmann et al. (2014)	524	10.9%(57)	21.1% (12)

1.4.4 Complications of Anastomotic Leakage

The effects of anastomotic leakage can be devastating and fatal if not treated in time. The main cause of mortality is as a result of sepsis/septic shock. This can occur because the contents of the colon, that leaks into the abdomen, contains colonic bacteria, which become pathogenic outside their normal environment, leading to an infection such as peritonitis as well as potentially causing abscesses to form. These microorganisms multiply and release endotoxins and exotoxins. As a result, a local response is triggered with cytokines being released and cells, such as macrophages, being recruited to combat the infection. When the infection cannot be cleared with this initial response, a systemic inflammatory response occurs, with further cytokine and other me-

diators such as nitric oxide and free radicals being released. This prolonged response causes damage to cells as well as affecting the cardiovascular system as these released substances increase vasodilation, vessel permeability, leukocyte aggregation and activation of coagulation pathways to name a few effects. If the response is not stopped, this can lead to refractory hypotension and organ failure due to microthrombi formation, resulting in the patient mortality. This mechanism can lead to patients experiencing several symptoms including abdominal pain, increased heart rate, fever and a rigid abdomen among others (Epstein & Parrillo 1993, Toutouzas et al. 2009, Weledji & Ngowe 2013).

Patients who experience anastomotic leakage often need emergency treatment (management options further elaborated in section 1.4.8) requiring longer hospital stays, with Gessler et al. (2017) showing that patients with leakage had significantly longer time in hospital on average versus patients without (on average 29 vs 9.4 days). In addition, anastomotic leakage has been shown to increase the chances of permanent stoma formation as well as being associated with reduced survival rates (Jutesten et al. 2019, Walker et al. 2004).

1.4.5 Risk Factors for Anastomotic Leakage

There have been several studies that have found risk factors that have been associated with this complication. A summary of these risk factors can be found in Table 1.7.

Non-modifiable Risk Factors

There are several non-modifiable risk factors with regards to anastomotic leakage. One of the main non-modifiable risk factors is gender where it has been found that being male increases the chances of leakage. Why this oc-

curs is not completely understood but some reasons that have been forward includes a narrower pelvis meaning surgery is more difficult and hormonal differences (Law et al. 2000, Walker et al. 2004, Rullier et al. 1998).

Another major non-modifiable risk factor that is associated with leakage is the location where the anastomosis is performed. A study by Vignali et al. (1997) found that there was a higher risk of leakage if the anastomosis was within 7cm of the anal verge. Similar results were found by Mäkelä et al. (2003), who found risk was increased if the anastomosis was within 5 cm of anal verge. This has been associated with the fact that there is a reduced blood supply in this area (Wang & Gu 2010).

Fitness and cardiovascular disease are the other main non-modifiable risk factor. Fitness is assessed using the American Society of Anesthesiologist (ASA) score. It has been seen that a score of 3 or greater (ASA score of 3 is one where the patient has severe systemic disease) increases the risk of leakage (Mäkelä et al. 2003, Choi et al. 2006, Alves et al. 2002).

Another non-modifiable risk factor is emergency surgery. It has been seen that compared to elective procedures, emergency surgery has a higher risk of leakage occurring. However, it has been noted that it is more likely the case that it is not the emergency surgery that carries a higher risk, but rather for these emergency procedures the patients are sicker compared to patients with elective procedures. Therefore, emergency surgery is not as important a risk factor (Choi et al. 2006, Constantinides et al. 2007, McDermott et al. 2014).

Modifiable Risk Factors

There are several modifiable risk factors linked to anastomotic leakage. These include alcohol consumption, where $>105\text{g}$ of alcohol per week increases risk,

as well as smoking, where if the patient is a smoker (Sørensen et al. 1999, Mäkelä et al. 2003, Richards et al. 2012) or has had a long history of smoking (>40 years) increases risk (Kim et al. 2011). Obesity has also been seen to be risk factor, however, definitions in studies are not well defined but measurement of waist has been seen to be more sensitive in determining anastomotic leakage (Rullier et al. 1998, Benoist et al. 2000, Senagore et al. 2003). There are many studies that have looked at medication as a risk factor, but the majority of medication has not been seen to increase risk. However, exceptions are immunosuppressant drugs which have been seen to increase risk (Zeeh et al. 2001, Alves et al. 2002). Patients who experience hypoalbuminemia and malnutrition prior to surgery have also been seen to have an increased risk of them developing leakage and lastly, radiation, in particular pelvic irradiation also increases risk (Alves et al. 2002, Mäkelä et al. 2003).

Intraoperative conditions

Surgical skill has been seen to be important in anastomotic healing and that poor technique increases the chances of leakage occurring. In addition to this, increased blood loss which requires transfusions to occur, as well as longer surgical times (319mins vs 269mins quoted in Mäkelä et al. has also been associated with poorer outcomes (Alves et al. 2002, Mäkelä et al. 2003, Vignali et al. 1997, Konishi et al. 2006).

The use of drainage tubes as a risk factor is still questionable. Some papers such as one published by Vignali et al. (1997) found that there was an increased chance of anastomotic leak occurring with the use of drainage tubes, however, later studies such as Mäkelä et al. (2003) and Denost et al. (2017) did not find any significant trends. There are arguments for and against the use

of drains. As a result surgeons currently use drains at their own discretion and in the era of enhanced recovery after surgery overall usage has declined (Kehlet 1997, Emile & Abd El-Hamed 2017).

Postoperative conditions

The use of non-steroidal anti-inflammatory drugs (NSAIDs) has been cautioned with evidence showing its use during the post-op period with one study showing the likelihood of leakage increased by 24% (Hakkarainen et al. 2015).

Table 1.7: Risk factors associated with colorectal anastomotic leakage. *Reference indicates that significant trend is only found in low (close to the anal verge) anastomoses. Factors in bold indicate higher importance.

Risk Factors	Reference(s)
Alcohol	Sørensen et al. (1999), Mäkelä et al. (2003)
ASA Score	Mäkelä et al. (2003), Choi et al. (2006), Alves et al. (2002)
Blood Transfusion	Alves et al. (2002), Mäkelä et al. (2003)
Cardiovascular Disease	Mäkelä et al. (2003), Warschkow et al. (2011)
Emergency Operation	Choi et al. (2006), McDermott et al. (2014), Constantinides et al. (2007)
Gender	Law et al. (2000), Rullier et al. (1998), Walker et al. (2004)
Hypoalbuminemia	Mäkelä et al. (2003)
Immunosuppressant Drugs	Alves et al. (2002), Zeeh et al. (2001)
Location of Anastomosis	Vignali et al. (1997), Mäkelä et al. (2003), Alves et al. (2002), Rullier et al. (1998)
Malnutrition	Mäkelä et al. (2003)
Obesity	Rullier et al. (1998)*, Benoist et al. (2000), Senagore et al. (2003)
Operating Time	Konishi et al. (2006), Mäkelä et al. (2003), Alves et al. (2002)
Pelvis Irradiation	Alves et al. (2002)
NSAIDs Use	Hakkarainen et al. (2015)
Smoking	Sørensen et al. (1999) Richards et al. (2012)
Surgical Skill	Vignali et al. (1997)

1.4.6 Current Clinical Diagnosis Methods

Symptoms

Currently, the earliest way to detect anastomotic leakage is by clinicians looking at symptoms and biochemical parameters that develop in patients which are associated with the complication. The Association of Surgeons of Great Britain and Ireland & The Association of Coloproctology of Great Britain and Ireland (2016) suggests looking at a departure of expected recovery as a way of diagnosing anastomotic leakage. Many of the symptoms associated with leakage have been noted by den Dulk et al. (2009). These are listed in Table 1.8.

Table 1.8: Symptoms used to determine if anastomotic leakage is potentially present (Not Exhaustive). Adapted from den Dulk et al. (2009)

Fever > 38°C	Ileus Present
Heart Rate > 100bpm	Gastric Retention
Respiratory Rate > 30/min	Fascial dehiscence
Urine Production < 30ml/h	Abdominal Pain
Agitated or lethargic mental state	Infection (based on increased leukocyte numbers or C-Reactive Protein levels)
Deteriorating Condition	Increased urea or creatinine levels

However, it should be noted that these symptoms are not necessarily specific to anastomotic leakage and may not present at all until much later in the postop period. Den Dulk et al. (2013) admitted that there was a particularly low positive predictive value when using the systems developed in the papers, with 1 of 6 patients who tested positive using the scoring system actually having leakage. Erb et al. (2014) found that monitoring vital signs could not be used reliably to diagnose anastomotic leakage with patients who had an un-

complicated post-op also exhibiting tachycardia and several of the symptoms mentioned previously. It was also found that the positive predictive value of using vital signs or white blood cell count to diagnose anastomotic leakage was 4-11%. Additionally, patients have found to be discharged with having postoperative abscesses and the diagnosis of anastomotic leakage being missed completely in other cases (Costedio & Hyman 2008). Often, radiography or contrast enhanced CT needs to be performed to allow for confirmation of diagnosis (Hyman et al. 2007).

Radiography

Imaging is often used only when a clinician suspects that an anastomotic leakage has occurred (unless it is considered obvious, i.e. the patient is very unwell) and requires confirmation of diagnosis. Two types of radiographic examinations can be used. The first method that can be used to detect leakage is using water-soluble enema, where a contrast substance is put into the colon and X-rays are taken to detect leaks. This is not used in the acute setting as it requires contrast to be passed through the lumen. The second type is computed tomography (CT) imaging where high resolution 2D X-ray images are taken to build up an overall image of the area of interest and can be used with the aid of a contrast material to optimise the images.

Though imaging has shown to be valuable in diagnosis of various conditions, its use in detecting anastomotic leakage has been brought into question several papers. Water-soluble enemas and CT scans have been shown to have a moderate level of sensitivity of approximately 60-80% and 55-75% but have a specificity of approximately 95-100% and 90-100% respectively (Habib et al. 2015, Hyman et al. 2007, Kornmann et al. 2014, Marres et al. 2017, Nesbakken

et al. 2005). This indicates that these methods are particularly good at ruling out anastomotic leakage rather than confirming it.

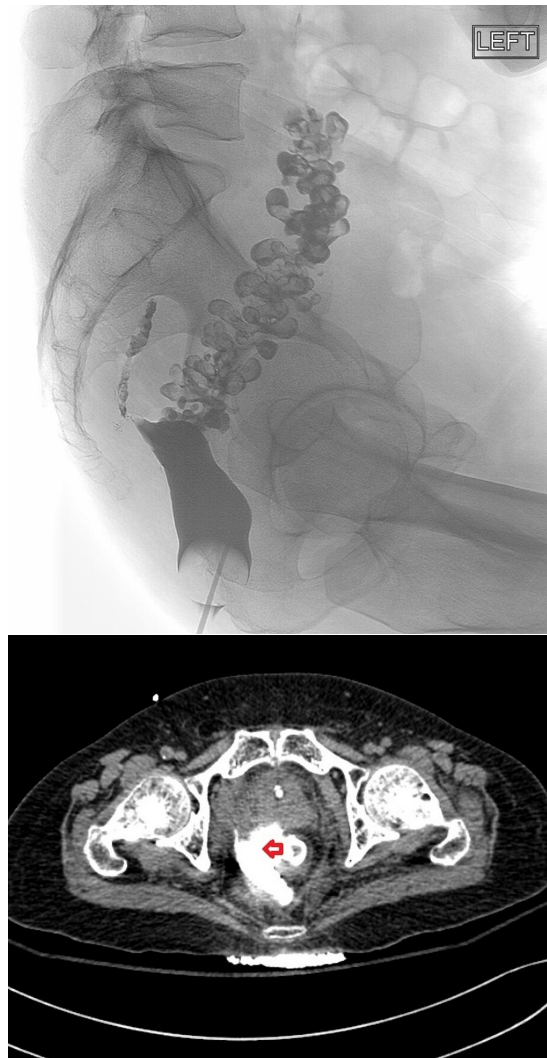


Figure 1.6: (Top) Lateral scan of gastrografin enema shows leakage of low anterior resection as shown by contrast in the presacral space (Radiopaedia 2014). (Bottom) Transverse plane CT image (with contrast) of abdomen showing anastomotic leakage, shown by red arrow, with contrast material in the presacral space (Radiopaedia 2017). Images reprinted under a Creative Commons BY-NC-SA 3.0 Licenses.

One of the reasons that was stated by Nesbakken et al. (2005) for the false negatives was the fact that imaging was done before leakage actually occurred indicating an important issue with regards to imaging; the importance of the timing of imaging. Radiology can only be used once a leak has occurred,

which can only be suspected once a patient exhibits symptoms as mentioned in the previous section. Additionally, for CT scans, it is particularly difficult to identify anastomotic leakage without experienced radiologists (see CT image in Figure 1.6) and there is no consensus for how leakage is identified, with some radiologists looking for air pockets/fluid in areas where they should not be. Another consideration that should be noted is that both CT and water-soluble contrast techniques expose the patient to radiation, a known risk factor of cancer and therefore its use is not advisable unless absolutely necessary (Kornmann et al. 2014, Nesbakken et al. 2005).

1.4.7 Time to Diagnosis

Diagnosis of an anastomotic leakage is particularly difficult due to the non-specific symptoms currently used clinically as mentioned previously (Section 1.4.6). Diagnosis often happens several days after surgery but can take a significant amount time, up to 42 days in some cases (Gessler et al. 2017, Hyman et al. 2007). This is due to the fact that anastomotic leakage can occur with little to no symptoms which doctors currently use to suspect anastomotic leakage and, as a result, often patients are sent home due to the inability to rationalise continued hospital stay and further costs. Hyman et al. (2007) found in a study they conducted, 42% of patients who had anastomotic leak were sent home before they had to be re-admitted and diagnosed. Similarly, in a report by den Dulk et al. (2009), where 3 patients were sent home due to the fact that they showed no signs of anastomotic leakage which was only diagnosed on readmission. One of these patients died due to the delay in diagnosis.

1.4.8 Management of Colorectal Anastomotic Leakage

Anastomotic leaks can be treated in various ways and is dependent on the level of leakage that has occurred and the patient's condition. The aims of management of anastomotic leakage are to try and preserve the anastomosis, control inflammation/infection and to restore the function of the large intestine (Blumetti & Abcarian 2015, Girard et al. 2014, Thomas & Margolin 2016).

Non-operative and Minimally Invasive Solutions

When possible, the first treatment often is intravenous broad-spectrum antibiotics. This is used when the patient is stable but is showing symptoms of leakage (Girard et al. 2014, Thomas & Margolin 2016).

Abscesses that are formed as a result of anastomotic leak (perforations greater than 3cm) can be drained using several methods depending on the case. Percutaneous drainage guided by interventional radiology is a commonly used technique with the aid of imaging and has been said to be effective when used correctly for appropriate patients (Chadi et al. 2016). Other techniques include transvaginal, transrectal and, for use in low anastomosis, transanal drainage, which are all done under general anaesthetic by a surgeon. If after some time, the anastomotic site has not been able to heal by itself and symptoms are either not improving or worsening, other treatment would be considered (Thomas & Margolin 2016, Vermeer et al. 2014).

The use of colorectal stents has also been looked into by several studies. These stents can be used to manage symptoms of bowel obstruction (except in cases of low anastomoses) as an alternative to a stoma and have been provided en-

couraging results at helping manage anastomotic complications (Abbas 2010, Blumetti & Abcarian 2015). Self-expanding metallic stents have provided some positive results with an 86% of anastomotic leakage cured, though it should be noted that no control was used in the study (Lamazza et al. 2015). Chopra et al. (2009) found that the use of stents accelerated anastomotic healing after healing (105 vs 173 days on average) and claimed that stents have helped in resolve anastomotic leakage by covering the anastomotic leak, diverting faecal matter and therefore reduce bacterial contamination. However, there are several drawbacks in using these stents, most significantly migration or expulsion of the stent, which has been reported to occur in 25-40% of patients. Additionally, costs associated have also been shown to be high (Abbas 2010, Blumetti & Abcarian 2015, Chopra et al. 2009, Sevim et al. 2016). Further studies are required to investigate the effectiveness of stents.

Another management strategy is the use of endoscopic clips. Most clips that are commercially available are through the scope clips which are used to control bleeding or small perforations but were not necessarily useful for anastomotic leakage due to their small size and low compression forces (Blumetti & Abcarian 2015, Sevim et al. 2016). However, newer over-the-scope clips have been developed that allow for higher forces to be applied and there is some evidence that the use of clip to have high success rate for small leaks. For example, Arezzo et al. (2012) claimed 86% of patients had their anastomotic leakage reversed with the use of over-the-scope clips with leaks less than 1.5cm. Currently, most of the studies for use of clips for reversing anastomotic leakage are relatively small studies or anecdotal, based on oesophageal studies, and larger studies are required.

A device that can be utilised in management of leakage is known as Endo-

SPONGE[®]. This is a polyurethane sponge which has shown some success in treating anastomotic leakage. The sponge is placed into the deepest part of the wound and is connected to a low suction negative vacuum. The device allows the draining of the area as well as promoting repair of anastomotic leaks (Arezzo et al. 2015, Veloso et al. 2013). Arezzo et al. (2015) and van Koperen et al. (2009) found that when endo-SPONGE[®] was used, over 70% of patients (89% and 75%) had successfully reversed their anastomotic leakage when used as an early intervention treatment. However, it should be noted that this device is particularly difficult to use where the anastomosis is present in higher parts of the large intestine and frequent changing of sponges (at least 5 returns to the theatre) are required (Blumetti & Abcarian 2015).

Surgical Intervention

For patients who do not improve with or are unsuitable for minimally invasive techniques, surgery can be performed to stop the leakage. The type of surgical intervention is dependent on several factors including the location, size of the leakage, condition of the patient, etc.

In some cases, the anastomosis can be salvaged (particularly if the leakage is small) and is preferable if possible. In combination with a loop ileostomy diversion, it has been found to be associated with lower levels of complications compared with not using a loop diversion.

However, many leakages are treated by resecting the anastomosis and an ostomy is formed, though this approach has been shown to increase the chances of permanent faecal diversion versus salvaging the anastomosis (Fraccalvieri et al. 2012, Krarup et al. 2014, Peters et al. 2019).

1.4.9 Economic Cost of Anastomotic Leakage

Patients who experience anastomotic leakage are associated with significantly higher costs versus patients who have an uncomplicated post-op course due to the longer hospital stay and further treatment required. Hammond et al. (2014) reported that the average cost of a patients who developed anastomotic leakage in the USA was approximately \$24,129 higher than patients without leakage. The approximate cost of anastomotic leak in the UK is £1.1-3.5 million in the UK (Ashraf et al. 2013).

1.5 Other Investigated Markers

While in current clinical practice, anastomotic leakage is typically diagnosed by monitoring symptoms and through the use radiology, it has been seen that these methods are not particularly great at determining anastomotic leakage with patients not necessarily presenting with symptoms and the relatively low sensitivity of radiology at detecting anastomotic leakage (Hyman et al. 2007, Marres et al. 2017, Nesbakken et al. 2005). As a result, other groups have investigated other markers that could be used to diagnose anastomotic leakage, which has been detailed in this section and as a result, justify the chosen markers for this thesis.

1.5.1 Biomarkers for Ischaemia

As mentioned previously, ischaemia has been commonly cited the major cause of anastomotic leakage. In normal cell respiration, glucose is converted into pyruvate through the Krebs cycle to produce adenosine-tri-phosphate (ATP), a molecule used to power normal physiological processes. When oxygen is

lacking, tissues switch from aerobic to anaerobic respiration and due to this switch, pyruvate is converted into lactate. As tissues start healing, the effects of ischaemia are lessened (Matthiessen et al. 2007). These markers include; glucose, lactate, pH and oxygen concentration. Therefore, there have been studies that have looked at how markers that are related to this are affected and how they change with anastomotic leakage and how they change with regards to anastomotic leakage are looked into in this section.

Glucose

Glucose is the main molecule involved in respiration and has been monitored with respect to anastomotic leakage in a few papers. Daams et al. (2014) found that glucose levels in patients stayed relatively similar over the post-op period with an average glucose level of 8.1mM and 7.8mM in patients without and with anastomotic leakage using microdialysis tubes placed near the anastomosis. However, whilst Matthiessen et al. (2007) found that in patients without leakage had a stable glucose level (of 7mM) like Daams et al. also using microdialysis, they found that in patients with leakage had a lower level of glucose of 6mM which dropped to 4mM during the post-op period, though this was not considered significantly different. Pedersen et al. (2009) also found this trend as well though this study only had two patients with leakage. In addition, measurements of glucose by previous papers have used microdialysis tubes to sample peritoneal fluid. However, this has been shown to underestimate the concentration of the sampling environment (Chefer et al. 2009, Shippenberg & Thompson 1997, Turkina et al. 2017).

Based on the small amount of literature, there could potentially be a trend with glucose that could be related to anastomotic leakage but larger scale

studies are required with more accurate measurement techniques. As a result, glucose was chosen in this thesis as one of the biomarkers to measure. This was to be done by directly measuring the glucose in clinical drain fluids using colorimetric methods, which have a high level of accuracy (Silva et al. 2016). This has not been done previously.

Lactate

Studies to date involving measuring lactate have involved the use of microdialysis catheters placed near the anastomosis. Pedersen et al. (2009) found that in patients who developed leakage, lactate concentration and lactate/pyruvate ratio increased significantly days before symptoms presented. The same group had similar findings for oesophageal anastomotic leakage (Pedersen et al. 2014). Similar results were found by Daams et al. (2014) where the levels of lactate were significantly increased in patients who had anastomotic leakage versus patients who did not (4.4 vs 3.2 mM/L) within the first few days of surgery. Matthiessen et al. (2007) measured lactate, pyruvate and glucose levels at regular intervals for 6 days post-op in patients who had anterior resections. They found that the lactate/pyruvate ratio to be significantly different on post-operative days 5 and 6 for patients with leakage vs those without. It should be noted that it is not well explained if this significance is prior to the onset of symptoms and if so, how far in advance. Additionally, these studies have used microdialysis tube to sample the environment, which has been shown to underestimate the concentration of analytes in the sampling environment (Chefer et al. 2009, Shippenberg & Thompson 1997, Turkina et al. 2017).

There is some evidence to indicate that monitoring lactate concentration can

be used as an early indicator of anastomotic leakage. However, a larger scale study is necessary to confirm the usefulness of lactate as a potential biomarker. Previous studies looking at lactate with regards to anastomotic leakage have used microdialysis tube which has been shown to underestimate the concentration of analytes in the sampling environment. Therefore, lactate was another marker that was chosen in this thesis as one of the biomarkers to measure. This was to be done by directly measuring the glucose in clinical drain fluids using colorimetric methods, which have a high level of accuracy (Yanase et al. 2018). This has not been done previously.

pH

Another potential method of diagnosing anastomotic leakage is by measuring pH levels which are lowered due to anaerobic respiration. However, there is little literature in this regard. A study by Yang et al. (2013) measured the pH of fluid from pelvic drains for 12 days post-op for 753 patients (57 developed leaks). They found that significant differences on day 3 in patients with leakage (all leakages were diagnosed between days 6 and 12) vs those without. A threshold point (pH=6.978) was determined that produced a high level of sensitivity (98.7%) and specificity (94.7%) was reported. However, only mean values were provided and nothing else (confidence intervals, standard deviations, range of measurements, etc.) with regards to anastomotic leakage.

Another paper by Millan et al. (2006) measured the pH level during the first and second 24 hours after surgery. This was done in 90 patients using tonometry, where a balloon catheter was introduced near the anastomosis and in the stomach during surgery and sutured into position. It was found that pH was significantly lower in patients with leakage compared to those without

in the first 24 hours (7.05 ± 0.1 vs 7.32 ± 0.3 , mean pH \pm SD). Using results that were gained, a threshold pH was found (7.28) which, if a patient was below, they were 22 times more likely to develop leakage. It should be noted that a negative result with this criterion does not necessarily rule out a patient having an anastomotic leakage as, according to the paper, the experiment had a negative predictive value of approximately 70% as well as having a low sensitivity of approximately 28%. In addition, the use of balloon tonometry in clinic would be impractical.

pH could potentially be valuable in diagnosing anastomotic leakage. While there is a study that does look at measuring pH in drain fluid, not enough information is provided to determine whether it can be used reliably (lack of information of range, confidence levels, etc. with regards to anastomotic leakage pH measurements). As a result, pH was also marker chosen to measure in this study to gain further information about whether it is able to diagnose leakage.

Oxygen Concentration

Reduction of oxygen to tissue is the cause of hypoxia so being able to measure this parameter could potentially be effective in detecting leakage.

One of the first studies that looked into oxygen levels as a potential predictor for anastomotic leakage was by Sheridan et al. (1987). Using an electrode-based system, oxygen tension was measured in 50 patients (5 of whom developed leakage) prior and post resection, at various sites of the bowel (caecum, transverse colon, descending colon, sigmoid colon and rectum) as well as measurements within 1cm proximal and distal of the anastomotic site. It was found that in patients who had oxygen tension levels drop either by 20mmHg

(absolute) or 50% (relative) based on the measurements taken at the anastomosis site, were significantly more likely to have anastomotic leakage. It should be noted that one of the patients who developed leakage did not exhibit reduction in oxygen tension levels.

More recent studies have used optical methods to measure oxygen supply in the colorectal region. Hirano et al. (2006) used near-infrared spectroscopy to detect oxygen saturation of colon tissue. Measuring at sites proximal and distal to the anastomosis site (soon after the anastomosis was formed in surgery), they found that the level of oxygen saturation in the body was found to be significantly lower in patients who had anastomotic leakage compared to those who did not (58% vs 71%). However, it should be noted that there was a very small number of patients had leakage (2 patients) so the reliability of this trend is questionable.

Karliczek et al. (2010) performed a similar study to Hirano et al. (2006) using visible light spectroscopy instead of infrared with an increased patient pool (77 patients, of which 14 had leakage). The use of visible light, instead of infrared, reduces the penetration of light through tissue and measurements are of blood vessels closer to the surface, which in this case is measuring saturation in the serosa layer of the colon wall. A probe was used to make measurements prior and post resection during surgery, approximately 1.5cm proximal and distal to the anastomosis as well as the caecum. It was indicated from the results that an increase in saturated oxygen levels was significantly associated with patients with leakage at the measurement site proximal to the anastomosis. Another observation that was found was that saturated oxygen levels in the caecum was significant lower in patients who presented with leakage compared to those who did not ($69.6 \pm 5.6\%$ vs $73.6 \pm 5.7\%$).

Something that should be noted is that all the studies above looked at oxygen during surgery. No studies have looked how perfusion/oxygen level changes during the post-op period.

1.5.2 Inflammation Markers

Any surgery induces some level of inflammatory response. During colorectal surgery, inflammatory markers are produced and released. These levels could be increased during prolonged inflammation/sepsis and several groups thought it would be prudent to monitor these levels with regards to anastomotic leakage.

C-Reactive Protein (CRP) and Procalcitonin

C-reactive protein (CRP) and procalcitonin are biomarkers that are released as a response to infections and inflammation. CRP is formed in the liver and its major function is to help identify and remove specific pathogens. This is attained by binding to a certain type of receptor. This triggers the complement system causing phagocytosis to occur. Additionally, this receptor is expressed on dead/dying cells so CRP may aid in removal of these cells as well. The level of CRP is relative to the level of the inflammatory response and seeing as it has a relatively short half-life (4-7 hours), some groups have thought this could be a useful marker in determining anastomotic leakage (Bray et al. 2016).

Almeida et al. (2012) found that in patients who had anastomotic leakage, serum CRP values were significantly increased from two days after surgery up to diagnosis (day 2 values: 187 vs 132 mg/L). A threshold value was established of 140mg/L which provided a sensitivity of 78% and specificity

of 86%. Matthiessen et al. (2008) also found that increases in CRP levels in serum was indicative of anastomotic leakage and could be seen from 2 days after surgery. However, it should be noted that anastomotic leakage is not the only complication that can occur after surgery. Pedrazzani et al. (2017) found that serum CRP values increase significantly at day 3 in patients who had surgery-related and severe post-operative complications including anastomotic leakage, bleeding, lymphorrhea, etc. Silvestre et al. (2014) similarly looked at post-operative infections which included urinary tract infections, central line infections, etc. as well as anastomotic leakage. A CRP value greater than 5.0mg/dl at day six was associated with a post-operative infection, with a high level of sensitivity (85%) with a moderate level of specificity (62%). Fernández et al. (2017) found also found that the surgical approach used (open vs laproscopic) also affected CRP values.

Procalcitonin is a precursor peptide to the hormone calcitonin which is involved in calcium regulation. In healthy humans, this peptide is produced by the neuroendocrine cells of the thyroid gland and concentrations in the body are low (<0.05ng/mL). However, in bacterial infections, the levels of procalcitonin increase significantly, with studies indicating values of >1µg/L as a threshold to suggest use of increased/broadening antibiotics and use of imaging. The levels of procalcitonin accumulate and are relative to the level of inflammation when this happens as, unlike neuroendocrine cells, the parenchymal tissues cannot convert it to calcitonin. This accumulation does not occur in viral infections where specific viral cytokines prevents this from happening. Levels of procalcitonin increase promptly after initial bacterial infection and has a relative short half-life of about 24 hrs. Therefore, its measurement has been used to monitor sepsis and therefore naturally some groups have looked

at its relationship with regards to anastomotic leakage (El-Azeem et al. 2013). Giaccaglia et al. (2014) found that procalcitonin values (taken from whole blood) from patients, were significantly different in patients who had anastomotic leakage for levels measured 3 days after surgery (4.97ng/ml) versus patients who had other complications (2.27ng/ml) or and those who did not suffer any complications (1.12ng/ml). Additionally, it was found that if a threshold of 5ng/ml was established (for day 3), a concentration of less than this resulted in a high negative predictive value of 96.7% and specificity of 95.7%. It should be noted that sensitivity or positive predictive value was not stated, and though similar trends were found on day 5 (measurements were done on day 1, 3 and 5), leakage results were not significant from other results. It should be noted the low levels of patients with complications (only 9 anastomotic leakage patients and <20 patients with other complications). However, a study by Garcia-Granero et al. (2013) found that procalcitonin levels in serum were only significant when a “major leak” occurred on days 3 and 5 post-op. In another study which measured procalcitonin in drain fluid from drains placed near the anastomosis, it was found there was a significant difference in levels between patients who have leakage (approx. 2.3ng/mL) vs those who did not (approx. 0.3ng/mL) at 5 day post-op (Komen et al. 2014). No comparison was made with other complications.

In general, both CRP and procalcitonin can help rule out anastomotic leakage. However, their ability to diagnose leakage is still questionable. Even with some results that show that these markers can indicate if leakage is occurring, larger studies are required to confirm any trends found.

Cytokines

Cytokines is a general name for small signalling proteins that are secreted by several different cells (particularly T-helper cells and macrophages) that affect interactions between cells. Cytokines are produced as part of a cascade; as one cytokine affects a cell, it triggers cells to produce more cytokines. There are several types of cytokines: Pro-inflammatory cytokines, that are involved in the inflammatory response; chemotactic cytokines, involved in the activation and chemotaxis of cells (particularly leukocytes); and anti-inflammatory cytokines, which regulate the activity of the inflammatory response (Zhang & An 2007). The candidate cytokines for indicating anastomotic leakage are discussed below.

Interleukin 6 (IL-6)

IL-6 is an inflammatory cytokine that is predominantly produced at lesions (Tanaka et al. 2014). Herwig et al. (2002) found, when measuring levels in peritoneal fluid (for 4 days), IL-6 was significantly different in patients with anastomotic leakage than those without on day 1 ($162,500 \pm 105,800$ vs $27,940 \pm 13,860$ pg/mL, mean \pm SD). This trend remained for 4 days post-op although this was not a significant difference on day 2. Uğraş et al. (2008) found a similar trend, though it was found to increase daily in leakage patients and there was no drop in levels on day 2 unlike Herwig et al. Both Herwig et al. (2002) and Uğraş et al. (2008) found levels in patients without leakage dropped daily from day 1. Matthiessen et al. (2007) found, using microdialysis tubes placed near the anastomotic site, that IL-6 levels were only significantly higher on days 1 and 2. However, Yamamoto et al. (2011) established in their study that concentration of IL-6 (measured in drain fluid) was

only significant after day 3. Bertram et al. (2003) and Reisinger et al. (2014) both contradicted papers that have been mentioned previously with no significant changes discovered between patients with and without anastomotic leakage.

Tumour Necrosis Factor Alpha (TNF- α)

TNF- α is another inflammatory cytokine that is produced by immune cells, particularly macrophages (Gahring et al. 1996). Herwig et al. (2002) and Uğraş et al. (2008) found significant increases in levels from day one in drain fluid in patients with leakage. Matthiessen et al. (2007) similarly found increases but established that these were only significant on days 1 and 2 (using microdialysis techniques). Both Uğraş et al. (2008) and Matthiessen et al. (2007) observed that levels increased daily in patients with leakage and levels decreased in patients without leakage. However, like with IL-6, Yamamoto et al. (2011) only observed significance from day 3 onwards and Bertram et al. (2003) did not determine any significance at any time point after surgery.

Interleukin 1 β (IL-1 β)

IL-1 β is a pro-inflammatory cytokine that is released by several different cells in the body (Lopez-Castejon & Brough 2011). It was noted by Herwig et al. (2002) that IL-1 β levels in drain fluid were low in the first couple of days after surgery and increased significantly on day 3 onwards. A similar result was found by Yamamoto et al. (2011) though values were much lower.

Interleukin 10 (IL-10)

IL-10 is an anti-inflammatory mediator which is secreted from various cells, particularly immune cells (Iyer & Cheng 2012). Uğraş et al. (2008) found significant differences between patients with and without leakage with signifi-

cant increases from day 1 in drain fluid from patients with leakage and significant decreases in patients without. Matthiessen et al. (2007) also found significant differences in the first 2 days of post-op using microdialysis catheters.

Inflammatory Biomarker Comments

There are several items that should be noted with regards to papers that have looked into cytokines. First of all, increases in the concentration of inflammatory markers after anastomotic surgery may not necessarily be indicative of anastomotic leakage. When Yamamoto et al. (2011) tested for various cytokines, one of the eight patients who developed complications did not develop anastomotic leakage but instead only developed an intraabdominal abscess. None of the papers have looked to see if other post-operative complications also cause changes in concentrations of cytokines. There are some papers that show that levels change regardless of complications such as study by van Berge Henegouwen et al. (1998) which showed that TNF- α rises were indicative of postoperative complications in general for abdominal surgery. If this is the case, it would be prudent to see whether changes in levels could be distinguished to identify anastomotic leakage.

Further to this point, other conditions that could affect levels, particularly anti-inflammatory drugs should also be considered. Yamamoto et al. (2011) excluded patients who already had inflammatory conditions prior to surgery and patients who took anti-inflammatory drugs and Reisinger et al. (2014) discounted patients who had inflammatory bowel disease as they believed that the result could be affected by this condition.

Lastly, most of the studies mentioned have low numbers of patients in the analysis and further larger studies would need to be required to confirm any

trends.

1.5.3 Matrix Metalloproteinases (MMPs)

In order for healing and tissue remodelling to occur, the extracellular matrix needs to be degraded. This is performed by several types of enzymes, most prominently matrix metalloproteinases (MMPs). These enzymes are secreted by several cell types, particularly activated macrophages, in a pro-enzyme state and then cleaved by Tissue Inhibitors of Matrix Metalloproteinases (TIMPs). The activity/levels of MMPs are controlled by these TIMPs as well as by cytokines, hormones and growth factors (Jabłońska-Trypuć et al. 2016, Quiding-Järbrink et al. 2001).

Stumpf et al. (2005) looked at how anastomotic leakage related to the amount of MMP levels, more specifically MMP-1, MMP-2, MMP-9 and MMP-13. From staining techniques on colonic tissue (near anastomotic site), MMP-1 and MMP-2 were found to be significantly more expressed in patients with anastomotic leakage versus non-leakage patients at the mucosal level. In addition to this, MMP-2 and MMP-9 were found to be more significantly higher at the submucosal layer in leakage patients. MMP-13 was not found to be significantly different in any case. As MMP expression is related to collagen, the authors also looked at the collagen I/III ratio, an indicator of tensile strength and stability of tissues, using similar staining techniques and found that there was a significant drop in the ratio in patients with leakage indicating that MMPs reduce the chances that an anastomosis heals properly.

A similar study was performed by Pasternak et al. (2010) where levels of MMP-1, -2, -3, -7, -8, -9 and -13 were looked into as well as TIMPs in intraperitoneal fluid collected from patients, approximately 4 hours after surgery. They

found that only MMP-8 and -9 were the only variables that were significantly increased in patients with anastomotic leakage than those without (median increases of 58% and 29% respectively).

However, it should be noted that MMPs and TIMPs levels have been shown to be affected by other post-operative complications. Baker et al. (2003) found that there were significant differences in MMP-2 (on days 3 and 6) and MMP-9 (on days 6 and 7) being elevated and a significant negative correlation with TIMP-1 (day 7) and TIMP-2 (days 2 and 3) between patients with post-operative complications (including wound infections, haemorrhage, etc.) and those without. Additionally, it was also noted that the level of severity and blood loss significantly affected the MMP-3 levels for the first 2 days after post-op and stoma formation increased levels of several MMPs as well. Considering that levels of MMPs and TIMPs seems to change inconsistently and the affects other conditions can have, they may not be effective in detecting anastomotic leakage.

1.5.4 Bacterial Markers

Bacteria have also been suggested as a method to detect anastomotic leakage. The colon is host to a large number of bacteria (3-40 trillion) which includes species of *Clostridia*, *Enterococcus* and *Bacteroides* to name a few (Webb et al. 2016). When the colon is ruptured, the contents of the colon are released into the surrounding area which, in this case, is the peritoneal cavity. There have been several studies that have looked into detecting various bacteria that are known to be present in the colon.

Komen et al.(2014, 2009) used polymerase chain reaction (PCR) to detect *Escherichia coli* (*E. coli*) or *Enterococcus faecalis* (*E. faecalis*) in drain fluid (measured

for 4 days). These bacteria were used to give an indication of whether leakage was occurring and were standardised using day 1 values. For *E. coli*, increases in Colony Forming Units (CFU) values versus day 1, on days 4 and 5 were significantly different in patients with and without leakage. However, though the results gave a relatively good specificity (day 4 value=83.5%) and negative predictive value (day 4 value=95.2%) for both days, the sensitivity was found to be moderate (day 4 value=69.2%) and the positive predictive value was quite low (day 4 value=36.0%). For *E. faecalis*, significant increases were found on days 2 to 4. Better sensitivities were found (day 2=71.4%, day 3=92.9%, day 4=75.0%), low positive predictive values were also found (day 2=27.8%, day 3=30.2%, day 4=25.7%). The method also gave false positives meaning the system requires more refinement.

Junger et al. (1996) measured the concentration of lipopolysaccharide (LPS), which is found on the walls of Gram-negative bacteria, in drain fluid. They found that patients with anastomotic leakage had significantly higher concentration on day one and three compared to patients without leakage. Day 3 results gave results that could be used to determine threshold levels where values were above 5000pg/ml in patients with leakage whereas patients without leakage had values below 2000pg/ml. However, due to the low number of patients used for the study (only three patients presented with anastomotic leakage), more research would need to be undertaken to confirm the results in this study.

A major drawback of measuring bacteria is the level of difficulty and/or length of time required for measurement by traditional means. Culturing and identification of bacteria can take days to complete with the use of either colony counting methods (which can take 48 hours or longer) or requiring

expensive equipment for polymerase-chain reactions or flow cytometry. In addition, trained staff are required to perform the complex tasks required for most of the techniques (Nemati et al. 2016). However, new emerging techniques such as electrochemical impedance spectroscopy are showing promise in bacterial detection with potential to substantially reduce times to diagnosis (explained further in the next section).

Lysozyme

Lysozyme is a polypeptide that targets and destroys Gram-negative bacteria cell walls. Miller et al. (1996) investigated how lysozyme levels were affected by anastomotic leakage. Using drainage fluid, taken from patients who had undergone low anterior resections, the samples (collected for 4 days) were subject to electrophoresis to allow separation of lysozyme and then was tested using a lysozyme testing kit. The results found showed that patients who were diagnosed radiological, when compared to no leakage patients, had a significant difference in lysozyme levels from day 1 onwards (approx.15 vs 6mg/dl). Though a significant trend was established, it must be noted that the sample size was relatively small (n=42 of which 6 diagnosed radiologically).

1.5.5 Impedance Measurements

An alternate technique that has been looked into by DeArmond et al. (2013, 2010) for the detection of anastomosis is the use of electrical impedance. In a paper published in 2010, the group looked into whether measuring impedance of the peritoneal fluid could be used to measure leakage with the aid of an electrolyte-contrast solution. The idea was that if leakage occurred, electrolyte solution, given orally, would leak into the abdomen and be picked up as a significant impedance change.

For the experiment, involving rats that had a gastrotomy to mimic leakage, pacing leads were placed near the gastrotomy site, to allow measurement of peritoneal fluid resistance. For direct current measurements, 2 leads were sutured on either side of the gastrotomy site and for alternating current measurements, leads (4 electrodes) were attached to scaffold placed near the gastrotomy site. Electrolyte contrast solution (sodium chloride solution) was delivered through a tube placed in the oesophagus and measurements were taken between leads in their respective configuration. DC measurements were taken passively using a multimeter and for AC measurements, an applied AC current of $800\mu\text{A}$ at 50 kHz delivered by a bio-impedance device. Once measurements were complete, the rats were opened up to allow removal of contrast material and the previous gastrotomy (imitating anastomotic leakage) was closed up by suture and the experiment was repeated to act as a control.

For direct current measurements, there was a significant difference in resistance between leakage and control results as shown by the mean maximum resistant change ($-340\pm 125\Omega$ vs $-30\pm 30\Omega$, mean \pm SD) and maximum rate of change ($-310\pm 140\Omega/10\text{s}$ vs $-15\pm 15\Omega/10\text{s}$, mean \pm SD) over a 70 second time frame. With regards to the alternating current measurements, it was found that the maximum change in resistance was significantly different for all increments of 0.9% NaCl used when comparing leakage results to control ($-11.3\pm 4.7\Omega$ vs $-2.6\pm 0.5\Omega$ at 1ml, mean \pm SD). However, there were only significant differences in the maximum rate of change at increments larger than 2ml ($-10.9\pm 5.8\Omega/\text{s}$ vs $-0.73\pm 0.15\Omega/\text{s}$ at 3ml, mean \pm SD). These results suggest that measuring impedance in the peritoneum could be a viable method to detect the onset of anastomosis. However, there are several drawbacks that are mentioned, one being obtaining consistent readings. The baseline readings for

the sensor were shown to vary a fair amount, direct and alternating current readings gave results that varied from 300-750 Ω and 38.4-141.8 Ω respectively for local impedance.

Further testing was done by DeArmond et al. (2013) by comparing the impedance method they developed in 2010 to barium fluoroscopy. Impedance testing was done in a similar manner to the 2010 paper but the leads were attached inside a foam sandwich, saturated with saline, to allow for stabilised baseline readings. When comparing the two methods, it was found that both had given similar results in terms of detecting leakage, although there were one or two barium fluoroscopy results that were misdiagnosed by the blinded radiologist. No experiments involving human patients have been performed with this methodology. Though not necessarily testing for colorectal anastomoses, the approach of measuring impedance of leaking contrast fluid may have some utility as an alternative to CT-scanning. However, similarly to CT scanning, an issue with this approach would be that of timing, that is, the patient would have to be constantly intaking contrast fluid in order for early detection to occur which is not feasible.

However, no literature exists on the study of the impedance of colorectal drain fluid in humans. There could potentially be some changes to the impedance (e.g. due to increases in bacteria) that may be observed.

Methods have been developed to measure changes in impedance of biological samples as an aid to diagnosis, such as for rapid detection of bacteria. In particular, the Medical Devices group at the University of Strathclyde, where this study has been carried out, have shown that the use of Electrochemical Impedance Spectroscopy (EIS) could be used to detect bacteria. EIS is the application of small potential perturbations to a system for which the re-

sponse at different frequencies are measured. Using the technique, it has been found that it is possible to detect various bacteria considerably faster than traditional methods using relatively cheap printed electrodes which could be used as point-of-care devices. For example, Ward et al. (2018, 2014) found that *Staphylococcus aureus* and *Pseudomonas aeruginosa* could be detected using cheap screen-printed electrodes much faster than traditional methods. Other groups have used EIS for use in identifying other responses such as differentiating between cancerous and non-cancerous prostate tissues (Halter et al. 2007) as well as determining changes in tissue activities due to events such as ischaemia (Gersing 1998).

Another technique that could be used is cyclic voltammetry (CV), where current changes are monitored when voltage being ramped up and down in a system. This can be used to detect and monitor changes in various substances such as urea, uric acid, adenosine etc. These substances are present in drain fluid and their levels change in the post-op period (Patzner et al. 1989, Nguyen & Venton 2015, Ernst & Knoll 2001).

Neither of these techniques have been used to characterise drain fluid in patients with an uncomplicated post-op course. In addition, neither technique has been looked at to see whether changes in results found with these techniques could be used to determine anastomotic leakage. Considering changes in the fluid occurs over the post-op period with regards to anastomotic leakage (e.g. inflammatory markers), it maybe worth looking at using these techniques to determine whether results could be used to diagnose anastomotic leakage at an early stage.

1.5.6 Summary

A summary of the various markers of anastomotic leakage following colorectal surgery is presented in the Table 1.9.

Table 1.9: Summaries of investigated markers in literature

Marker	Summary
Glucose	<ul style="list-style-type: none"> - Some work that may indicate decrease with AL over post-op period - Further work is required
Lactate	<ul style="list-style-type: none"> - Detected early when AL occurs (within 5 days) - Small numbers used in studies so further work is required
Oxygen	<ul style="list-style-type: none"> - Oxygen levels monitored during surgery showed changes could be related to anastomotic leakage (most likely due to reduced micro-perfusion due to increased tension in healing tissues by incorrect surgical technique) - No papers have measured oxygen levels of the anastomotic site during post-op period
pH	<ul style="list-style-type: none"> - pH changes can be the effect of other problems - V. little literature which only shows risk increasing past a certain point which does not necessarily rule out leakage in the event of a negative result
CRP and Procalcitonin	<ul style="list-style-type: none"> - CRP and procalcitonin have literature some that indicate changes with leakage but more useful at ruling it out - Need more studies to determine differences between anastomotic leakage and other conditions that could cause changes in levels
Cytokines	<ul style="list-style-type: none"> - Levels shown to increase straight after surgery but levels usually reduce in normal circumstances - Need more studies to determine differences between anastomotic leakage and other conditions that could cause changes in levels
Lysozymes	<ul style="list-style-type: none"> - Only 1 study that shows some changes, but more studies required
MMPs	<ul style="list-style-type: none"> - Some evidence that changes could be attributed with leakage - Takes significant amount of times to test for these markers
Bacterial Markers	<ul style="list-style-type: none"> - Moderate sensitivity with anastomotic leakage - Only looked at certain bacteria/LPS. May have more success with other species
Electrical Impedance	<ul style="list-style-type: none"> - Could be used to detect contrast material but no human studies have been performed - No studies that have looked directly at the electrochemical signature of abdominal drain fluid with regards to anastomotic leakage - Potential for use in measuring changes due to disease

1.6 Aims and Objectives

Due to the potentially devastating consequences of anastomotic leakage, the current inherent lack of detection before symptoms develop and the inability of detecting this complication consistently, it would be prudent to develop a system to detect anastomotic leakage as early as possible. Therefore, the aim of this project was to determine a reliable biomarker(s) that could be used to detect anastomotic leakage at an early stage so clinicians can take appropriate action before further problems occur.

A driving principle was to select potential markers that might be included in a personal monitoring device for patients immediately following surgery. Point-of-care testing can be used to improve patient outcomes (when implemented correctly) due to reduced diagnosis times, which is particularly important for time-sensitive complications such as for the problem presented in this thesis. Additional benefits also could include improved patient satisfaction and reduced costs (Price 2001).

As a result and following a review of the literature, an approach based on monitoring fluid from drains placed close to the anastomotic site was selected for further research during the course of this study. It was hypothesised that if such a system could be developed, it would have a high potential to yield a method that could be used to detect anastomotic leakage, as well as potentially being developed into a point-of-care device that can provide early warning of complications of occurring. Normally, drains are placed in patients during the surgery to allow excess peritoneal fluid, produced from the body's response to surgical response, and often removed within a week post-op (prior to the patient being discharged) (Tsujinaka & Konishi 2011).

This also coincides with the time period with when the majority of leaks occurs (Hyman et al. 2007), thus thus supported performing measurement with drain fluid.

Several biomarkers were chosen based on previous literature: Glucose, lactate and pH. There is some evidence glucose and lactate levels are affected by anastomotic leakage (Section 1.5.1). However, techniques used to measure these parameters have issues with microdialysis tubes been shown to underestimate analytes in the sampling environment (Chefer et al. 2009, Shippenberg & Thompson 1997, Turkina et al. 2017). Therefore, in this thesis, both lactate and glucose were measured directly from drain fluid and measured using colorimetric assays, which has not been done previously. This should provide a more accurate representation of how glucose and lactate levels change over the post-op period and potentially allow diagnosis of leakage. While a couple of studies has looked at pH as a marker indicating it could be used to diagnose leakage, there are either issues with the measurement technique (not practical for clinical use) or not provided enough information (e.g. range of values, confidence intervals, etc.). Therefore, pH was chosen to garner more information that has not previously been provided in terms of measurement of pH in drain fluid.

In addition, electrochemical impedance spectroscopy (EIS) and cyclic voltammetry (CV) techniques were also chosen to monitor changes in drain fluid. Neither of these techniques have been used previously in relation to drain fluid in detection of anastomotic leakage. Both techniques have utility to detect changes which can be related to a component in fluid they are testing. For example, EIS has been used to detect bacterial species and CV can be used to find changes in urea and other molecules (Ward et al. 2018, Patzer et al. 1989)

(see Section 1.5.5). It was hypothesized that these techniques could detect changes in the fluid during the post-op period and that deviations between patients with and without anastomotic leakage could be observed.

In order to achieve the aims of this study, several objectives were established:

- To develop and test methods of monitoring glucose, lactate and pH in drain fluid
- To develop and test methods to analyse drain fluid using EIS and CV techniques to try and identify specific markers of anastomosis such as presence of lactate or bacteria
- To test patient drain fluids with the developed methods (under ethical permissions)
- To analyse data gained from testing patient drain fluids to determine whether anastomotic leakage could be reliably diagnosed by monitoring the chosen biomarkers/techniques
- To consider, for future work, how such measurement techniques could be incorporated in a non-invasive device for bedside monitoring of the post-surgery patient.

The following chapters of this thesis will provide information on the background theory of the modalities of measuring the chosen biomarkers (Chapter 2), the methods and material employed (Chapter 3) for which the results are presented in Chapter 4 and Chapter 5. Results from these chapters are discussed and conclusions drawn in Chapter 6.

Chapter 2

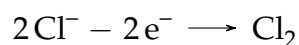
Background Theory

2.1 Introduction

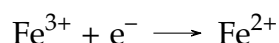
In the previous chapter, a research aim and objectives were established and a number of parameters of potential interest with regards to detection of anastomotic leakage were established; lactate, glucose, pH and electrochemical methods. In this chapter, the underpinning theories behind these parameters are provided.

2.2 Electrochemical Theory

Electrochemistry is the study of the electron transfer as a result of chemical reactions. Chemical reactions that happen in a cell cause movement of electrons which allows a current (measured as Ampere, A) and potential difference (measured as Voltage, V) to occur. These chemical reactions involve ions changing from one state to another by the loss/gain of electrons. The loss of electrons from a substance is known as oxidation, for example;



The gain of electron by a substance is known as reduction, for example;



Electrochemical cells can be formed by placing electrodes in a solution containing electrolytes (Figure 2.1) for which, the electrodes act as sites of oxidation/reduction of electrolytes. Each electrode is considered a half cell; one is called an anode, where oxidation of electrochemical species occurs; and one is called a cathode, where reduction of an electrochemical species occurs.

The total cell potential of the system (E_{cell}) is given by the summation of the

potential of the anode, cathode and solution. In other words;

$$E_{cell} = E_{anode} + E_{cathode} + E_{solution} \quad (2.1)$$

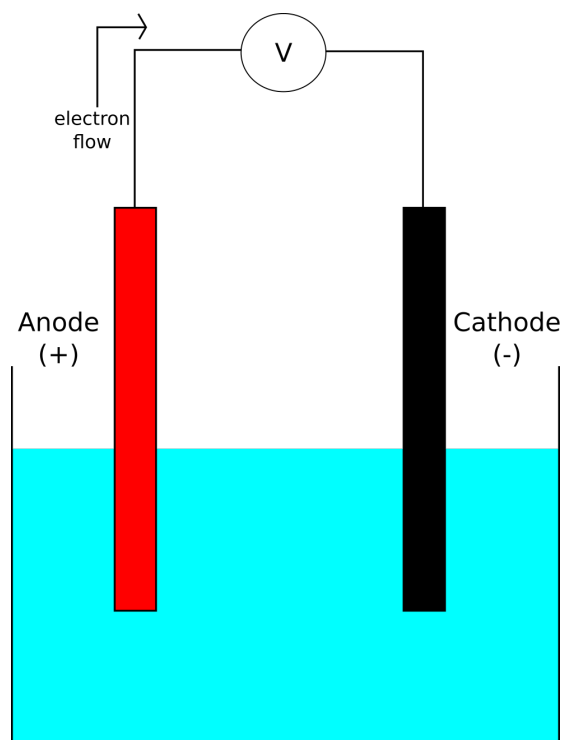


Figure 2.1: Basic Electrochemical Cell

In order to measure absolute voltage, the cell is measured relative to a reference electrode with a known fixed potential (relative to the standard hydrogen cell which is explained further in 2.2.2).

The maximum work that the total system (ΔG) can provide is given by the Gibbs free energy equation;

$$\Delta G = -zFE_{Cell} \quad (2.2)$$

Where z is the number electrons transferred in a reaction and F is Faraday's

number ($9.648 \times 10^4 \text{ C M}^{-1}$). The rate at which a species reacts can be described as:

$$\text{Rate} = kc_j \quad (2.3)$$

Where c_j is the concentration of a species (in Moles, M), j , and k is known as the rate constant. It has been found from observations that the rate constant can be defined by the Arrhenius equation:

$$k = Ae^{-E_a/RT} \quad (2.4)$$

Where E_a is the minimum energy required for a substance to react to form a product (also known as the activation energy and expressed in joules per mole, J M^{-1}) and A is known as a pre-exponential factor which considers various factors such as collision frequency of ions, T is the temperature (in Kelvin, K) and R is the gas constant ($8.314 \text{ J M}^{-1} \text{ K}^{-1}$).

In order to understand electrochemical cells further, it is best to understand how interaction of ions within a solution and with the electrode occurs.

2.2.1 Movement of Ions - Mass Transfer

The movement of ions in a solution occurs in one of three ways; diffusion, migration(conduction) and convection. Convection is the movement of ions due to mechanical methods (e.g. stirring). Effects due to convection are assumed to be zero in this thesis.

Diffusion

Diffusion is defined as the movement of ions due to differing concentration gradients in a system. This is driven by the fact that changes in concentration causes an imbalance in chemical potential and therefore the system is not in equilibrium (Bockris & Reddy 2002). In order to reach equilibrium, regions of high concentration of a species move to regions where low concentration of the species occurs. When the system is considered close to steady state (i.e. system is close to equilibrium), diffusion can be described by the following equation;

$$J_j = -D_j \frac{\partial c_j}{\partial x} \quad (2.5)$$

This is known as Fick's first law of diffusion, where J_j is the flux of species j ($\text{M m}^{-2} \text{ s}^{-1}$), c_j is the concentration of species j (in M), x is the of direction of movement (in metres, m), $\partial c_j / \partial x$ is the concentration gradient, D_j is the diffusion coefficient (also known as diffusivity, expressed as $\text{m}^2 \text{ s}^{-1}$). The negative sign indicates the movement of species is from high to low concentrations. When a system is not in steady state, diffusion can be described instead using Fick's second law of diffusion;

$$\frac{\partial c_j}{\partial t} = D \frac{\partial^2 c_j}{\partial x^2} \quad (2.6)$$

Where $\partial c_j / \partial t$ represents the change in concentration in an area with regards to time and $\partial^2 c_j / \partial x^2$ represents the varying change of the change in concentration.

Migration

Ions in a solution have an associated positive or negative charge. When exposed to an electric field, they drift to either to the positive electrode, if they negatively charged, or towards the negative electrode, if they are positively charged. They are therefore subject to a force vector (\vec{F}) which increases their velocity (known as the drift velocity, v) in the direction of this force. From Newton's second law, it is known that;

$$\frac{\vec{F}}{m} = \frac{dv}{dt} \quad (2.7)$$

Where m is mass (kg) and dv/dt is the acceleration of the ion ($m\ s^{-2}$). As they move, ions would collide with other ions, solvent molecules, etc., meaning that the movement of the ion is not smooth, and a resistance is caused by these collisions. The average time between collisions (τ) could be defined in terms of number of collisions, N , in time period, t (in seconds, s):

$$\tau = \frac{t}{N} \quad (2.8)$$

The average drift velocity for species, j , due to application of an electric field is the acceleration due to the field multiplied by the average time between collisions, i.e.;

$$v = \frac{dv}{dt}\tau = \frac{\vec{F}}{m}\tau \quad (2.9)$$

For an ionic species, j , of concentration c_j , the flux of the species towards the electrode (J_j) can be considered to be;

$$J_j = c_j v_j \quad (2.10)$$

Faraday's law, which links electron flow present in electrodes to ion movement in solution, indicates that the number of moles of a species moved (n) is;

$$n = \frac{it}{zF} \quad (2.11)$$

Where i is the current density ($A\ m^{-2}$) and t is the time the current is applied. If this is converted to a flux, then the above equation becomes;

$$J_j = \frac{i}{Fz} \quad (2.12)$$

Replacing this into equation 2.10 gives the current contribution of species j ;

$$i_j = z_j F c_j v_j \quad (2.13)$$

As there are multiple species in a solution, the total current due to migration (I) would be the sum of the current density of all species, i.e.:

$$I = \sum_j i_j \quad (2.14)$$

Combination of Diffusion and Migration

To account for the fact that both diffusion and migration effects would occur in solutions, it has been found that combining of the equations of diffusion and migration results in the following equation:

$$J = \frac{Dc}{RT} zFX - D \frac{dc}{dx} \quad (2.15)$$

This is known as the Nernst-Planck equation (effects due to convection is considered zero). While this unifies the migration and diffusion of ions in a solution, it does not consider that movement of ions affect the movement of other ions. Some ions migrate at a higher rate than others when an electric field is applied (due to size, etc.) and therefore contribute more to current flow through the solution (Bockris & Reddy 2002). In order to quantify this, a number known as the transport number (t_j), is used to represent the amount of the current species j (I_j) contributes to the total current (I_T), is defined as:

$$t_j = \frac{I_j}{I_T} \quad (2.16)$$

2.2.2 Interactions at the Electrode Surface

Faradaic and Non-Faradaic Processes

At electrodes, two types of processes occur. The first type is to do with charge transfer at the electrode interface. As the reactions between the metal and the electrolyte solution follow Faraday's law (i.e. chemical reaction due to current \propto electricity passed), such as oxidation and reduction of species at the electrode surface, and therefore are called Faradaic processes (also known as charge-transfer electrodes). With changing potential or solution composition, there could be changes to the electrode such as adsorption of substances onto the electrode surface, which can cause a change to the electrode interface for which the reactions are not proportional to the electricity passed. These are known as non-faradaic processes (Bard & Faulkner 2000).

Electrical Double Layer

In a solution, the interface between an electrode and a solution has been found to act in a capacitive manner and is known as the electrical double layer.

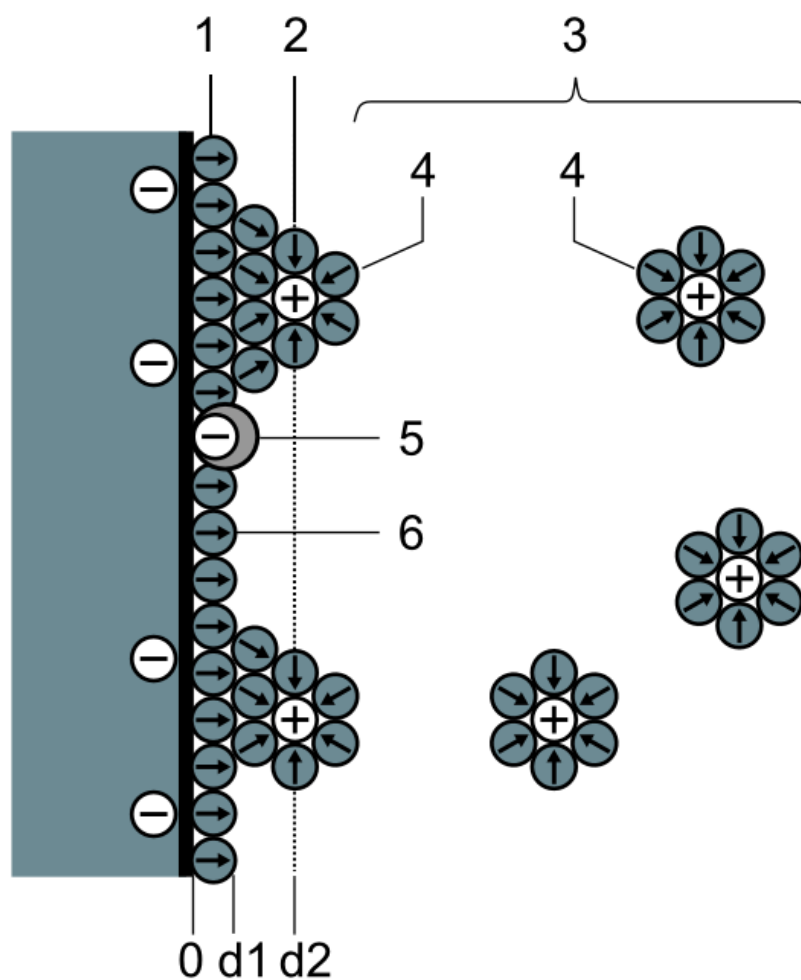


Figure 2.2: Model of the electrical double layer. 1) Inner Helmholtz layer, 2) outer Helmholtz layer, 3) diffusion layer, 4) solvated ions, 5) adsorbed ions and 6) solvent molecule. Reprinted from Wikimedia Commons (2008) under a Creative Commons BY 3.0 license

Capacitance (C), measured in Farads (F), is defined as:

$$C = \frac{q}{E} \quad (2.17)$$

where q is charge (measured in coulombs, C). When there is a potential dif-

ference, both the electrode and the solution will have a charge (q^E and q^S respectively) for which, at any given moment, are equal.

On the metal surface, the charge is due to a lack or excess of electrons on its surface. The charge at the solution side is made up of an excess of anions/cations and is thought to be made up of several layers (Figure 2.2).

The 'inner layer' of the solution, also known as the Helmholtz, compact or Stern layer, consists of two planes. The first plane is the Inner Helmholtz Plane (IHP) and is where specifically adsorbed ions are. The distance of the locus of these ions are at a distance of x_1 away from the charged metal layer with a charge of q^i . Ions present in the solution and not specifically adsorbed can interact with the electrode at a distance of at least x_2 away from the electrode, the distance between the distance x_1 and the average size of the nearest non-specifically adsorbed ions. This is known as the Outer Helmholtz Plane (OHP). The non-specifically adsorbed ions are distributed throughout the solutions, from the OHP outwards into a layer, which is known as the diffuse layer which gives an excess charge density of q^d . Therefore, the total charge density of the solution (q^s) section of the double layer is;

$$q^s = q^i + q^d = -q^E \quad (2.18)$$

Potential and Current at the Electrode

When a metal conductor is placed in a solution and no charge is applied, an equilibrium potential develops as reduction and oxidation events occurs between the conductor and the solution. For example, a simple electron transfer reaction can be given as:



Where A is an oxidised molecule and once it has accepted an electron, becomes substance D. The rate of the electrons lost must be equal to the rate at which electrons are gained, i.e. an equilibrium occurs. Therefore, the net current due to oxidation and reduction is equal to zero. This relationship leads to the formation of an equilibrium potential, E_e . This equilibrium potential can be described by Nernst's equation:

$$E_e = E^0 - \frac{RT}{zF} \ln \left(\frac{[Red]}{[Ox]} \right) \quad (2.20)$$

Where E_0 is standard electrode potential and [Red] and [Ox] are the effective concentrations of the reduced and oxidised species. As the substances in a solution can change this equilibrium potential, potentials are referenced against a standard hydrogen cell which has a defined equilibrium potential of 0V. If an additional potential, known as an overpotential (η), is added to the system, the total potential of the system (E) is:

$$E = E_e + \eta \quad (2.21)$$

The current also changes in relation to the difference between current due to reduction and the current density due to oxidation and is described by the Butler-Volmer equation as:

$$i = i_0 \left[\frac{C_{Ox}(0, t)}{C_{Ox}^*} e^{-\beta\eta F/RT} - \frac{C_{Red}(0, t)}{C_{Red}^*} e^{(1-\beta)\eta F/RT} \right] \quad (2.22)$$

Where i_0 is the current at equilibrium, the exponentials represent the current density contributions at the anode and cathode (β is known as the charge-transfer coefficient), $C_{Ox}(0, t)$ and $C_{Red}(0, t)$ is the concentration of the re-

duced/oxidised species at the electrode surface at time, t , and C_{Ox}^* and C_{Red}^* is the bulk concentration (far away from the electrode). Plotting current against overpotential gives the curve shown in Figure 2.3.

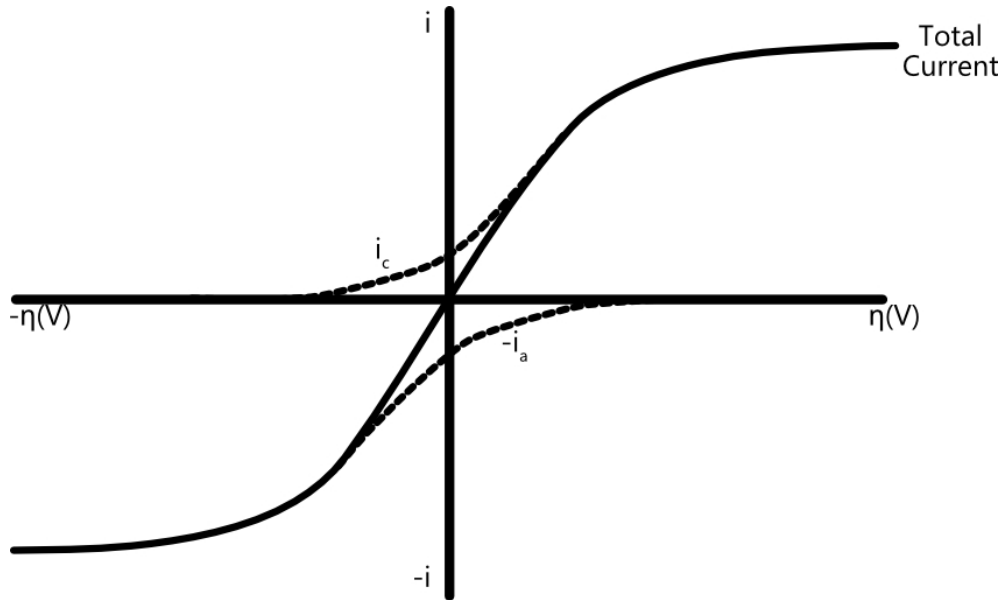


Figure 2.3: Effect of overpotential on current on an electrochemical system. i_c and i_a are the cathodic and anodic current components.

It can be seen from Figure 2.3 that at high overpotentials ($\eta \gg 0$ or $\eta \ll 0$), the current hits a limit which is dictated by mass transfer terms ($C_{Ox}(0, t)/C_{Ox}^*$ or $C_{Red}(0, t)/C_{Red}^*$) of the Butler-Volmer equation. At low overpotentials, the current is dictated by the exponential terms of the Butler-Volmer equation.

Diffusion Layer

It has been found that a concentration gradient occurs from the electrode (c_0) to bulk solution (c_{bulk}), known as the diffusion layer. This occurs due to inadequacies in the transport of ions and as a result causes the concentration of a species near the surface of the electrode to be different to the bulk solution.

At the electrode surface, the concentration of a species is at a minimum (c_0), due to immediate interaction of the species with the surface of the electrode,

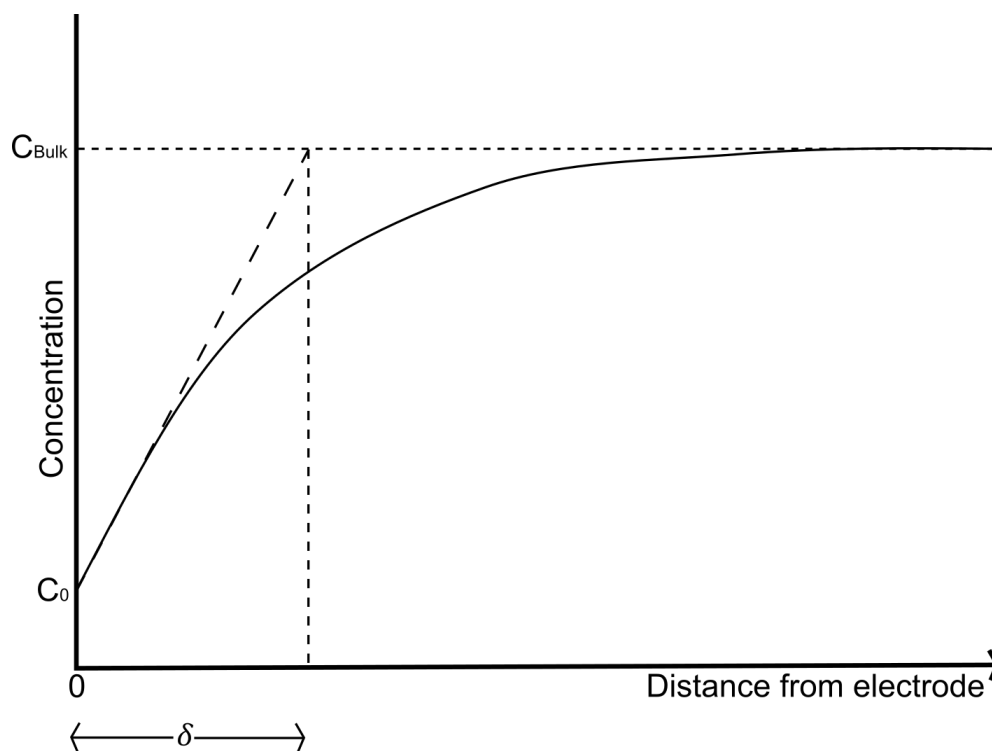


Figure 2.4: Concentration profile from the electrode. δ is the diffusion layer

and initially increases linearly small distances away from the electrode before deviating from this linearity to the bulk concentration in an asymptomatic manner. This can be seen in Figure 2.4 where the length of the diffusion layer is represented by δ .

This layer can be described by Fick's first law. For the initial linear region, Fick's first law can be changed into;

$$J_D = \frac{-D(c_0 - c_{bulk})}{\delta} \quad (2.23)$$

If a constant potential is applied to the system, it has been found that the diffusion layer thickness increases with respect to time and can be approximated as:

$$\delta = \sqrt{\pi Dt} \quad (2.24)$$

The current due to a constant potential is described by the Cottrell equation:

$$i = \frac{nFAc_{j(t=0)}\sqrt{D_j}}{\sqrt{\pi t}} \quad (2.25)$$

2.3 Electrical Theory

2.3.1 Resistance and Capacitance

Electrical resistance of a system (R), measured in ohms (Ω) is a measure of obstruction to current flow. This is defined by Ohm's law as a ratio of voltage (V) and current (I).

$$R = \frac{V}{I} \quad (2.26)$$



Figure 2.5: Resistors in series

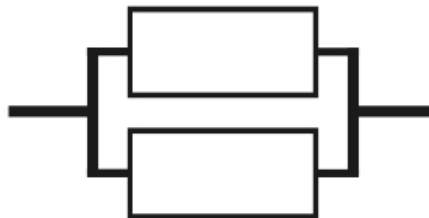


Figure 2.6: Resistors in parallel

Resistances in series (Figure 2.5), R_m ($m=1, 2, 3, \dots$) can be summed to calculate the equivalent resistance, R_{eq} . In other words;

$$R_{eq} = \sum_m R_m \quad (2.27)$$

Total equivalent resistance in parallel branches (Figure 2.6) can be calculated

from the following equation;

$$\frac{1}{R_{eq}} = \sum_m \frac{1}{R_m} \quad (2.28)$$

A capacitor is an electrical component that can store charge (Q). This is created by placing an insulated material (known as a dielectric material) between two conductors. This material becomes polarised with the application of an electric field. Voltage and charge (measured in coulombs) can be related using the following equation;

$$V = \frac{Q}{C} \quad (2.29)$$

where C is Capacitance. Charge can be related to current by;

$$Q(t) = \int_0^t i(t)dt \quad (2.30)$$

Therefore, the voltage is related to the current by combining Equation 2.29 and Equation 2.30 forming;

$$V(t) = \frac{1}{C} \int_0^t i(t)dt \quad (2.31)$$

The insulating material used in a capacitor has a permittivity (ϵ), which is a value that indicates a material's ability to store charge in an electrical field. The capacitance can be related to the permittivity by:

$$C = \frac{\epsilon A}{d} \quad (2.32)$$

Where A is the area of the capacitor plates and d is the distance between plates. Permittivity is made up to two components multiplied together: the

vacuum permittivity, ϵ_0 , the value of permittivity of a vacuum ($8.854 \times 10^{-12} \text{Fm}^{-1}$); and the relative permittivity, ϵ_r , the permittivity of a material relative to the permittivity in a vacuum.

2.3.2 Impedance

While Ohm's law is a well-known equation that describes resistance, it only works with ideal resistors, i.e. resistance is unaffected by frequency, Ohm's law holds true at any current and voltage and, for alternating current signals, current and voltage are in phase with each other. However, in practice, this is not the case and more complex behaviour is observed. Therefore, impedance (Z) is introduced as a more generalised definition which measures the resistance to the flow of current in a system. This is defined (similarly to Ohm's law) as;

$$Z = \frac{V}{I} \quad (2.33)$$

For purely resistive elements, the impedance is equal to the resistance. For capacitive elements, the impedance has been found to be:

$$Z = \frac{V}{I} = \frac{1}{j\omega C} \quad (2.34)$$

where j ($\sqrt{-1}$) indicates an imaginary number and ω is the angular velocity. Impedance of electrical components in series and parallel work the same way in Equation 2.27 and Equation 2.28;

$$Z_{series} = Z_1 + Z_2 + \dots \quad (2.35)$$

$$\frac{1}{Z_{Parallel}} = \frac{1}{Z_1} + \frac{1}{Z_2} + \dots \quad (2.36)$$

2.3.3 Dielectric Properties of Biological Material

Biological tissues have been found to exhibit a frequency dependant change when exposed to an electric field. This is due to interactions between the composition of tissues with the electric field and are categorised as α , β or γ dispersions. The typical dispersion for biological material is given in Figure 2.7.

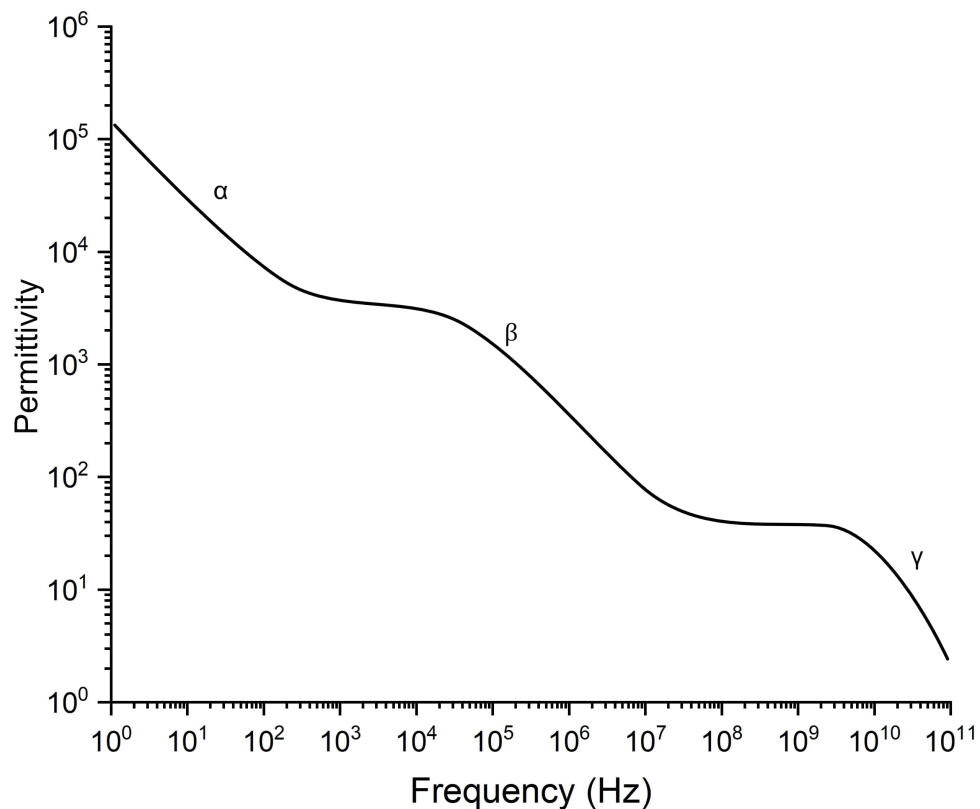


Figure 2.7: Typical changes in permittivity due to frequency in biological material. Based on Schwan (1957).

α -dispersions, which occur at low frequencies, have been found to be as a result of interactions between cell membranes and the surrounding environ-

ment. More specifically, this dispersion is thought to be affected by; metabolic exchange, the structure of the membrane and the charges on either side of the membrane. β -dispersions are as a result of cellular membranes which regulate the movement of ions between the intra and extra cellular environments. Other β -dispersions can result due to polarisation of organic molecules. γ -dispersions are due to effects of water molecules (Kuang & Nelson 1998, Schwan 1957).

Dielectric Relaxation Theories

The effects that cause α , β or γ dispersions can be related to several phenomena.

Permanent Dipoles

Many biological molecules have fixed charges that are at a fixed length away from each other resulting in a permanent dipole. When exposed to an electric field, they will orientate with regards to this field. At low frequencies, dipoles can rotate with the change in electric field and contribute to the passage of charge and the current is in phase with the voltage.

When frequencies are increased, the dipole cannot rotate in time with the changing field causing a lag to occur, resulting in changes in current (as current is not in phase with voltage) and reduction of charge that can be stored in the dielectric. The permittivity (ϵ , see Equation 2.32) can be described by the Debye equation:

$$\epsilon = \epsilon_{\infty} + \frac{\epsilon_0 - \epsilon_{\infty}}{1 + j\omega t} \quad (2.37)$$

Where ϵ_{∞} is known as the high-frequency relative permittivity (value of permittivity when a potential difference is initially applied), ϵ_0 is the low-frequency

relative permittivity (value of permittivity once the system has had time to stabilise/relax with application of a constant potential) and ω is the angular velocity.

Maxwell-Wagner Polarisation

Biological materials are composed of differing components that produce differing permittivity values. With the application of an electric field, ions and other charge carriers build up non-uniformly through the material due to this variation in permittivity for which, frequency dependence occurs. This charge build-up at the interfaces will continue until the current density between the two interfaces becomes constant. The changes in material properties maybe modelled as a circuit, for example, a 3-layer configuration using a 3 parallel RC circuits in series has been used to model bilipid membranes (Kuang & Nelson 1998, Schwan 1957).

Counterion Relaxation

The counter-ion theory is similar to the electrical double layer mentioned previously, where charged surfaces occur due to distribution of free ions within biological tissues causing a counter-ion layer to form on the surface. Application of an electric field causes counter-ion layer to change to maintain equilibrium. The time taken for biological material to achieve this this relaxation (τ) has been generally described by Schwarz as:

$$\tau = \frac{a^2}{2D} \quad (2.38)$$

where a is the particle radius and D is diffusion coefficient which can be defined by the Einstein relationship:

$$D = \frac{mk_B T}{q} \quad (2.39)$$

where m is the surface mobility on the ion and q is the charge of the ion, k_B is Boltzmann's constant ($1.38 \times 10^{-23} JK^{-1}$) and T is temperature in Kelvin (K) (Schwan 1957).

2.4 Electrochemical Techniques

Using the fundamentals of electrochemical and electrical theory, many techniques have been developed that take advantage of changing potentials. These techniques can be used to diagnose reactions in a system and determine concentrations of various species among other parameters and further discussed in this section.

2.4.1 Diagnostic Techniques

Electrochemical Impedance Spectroscopy (EIS)

Electrochemical impedance spectroscopy (EIS) is a technique used to understand and characterise electrochemical cells.

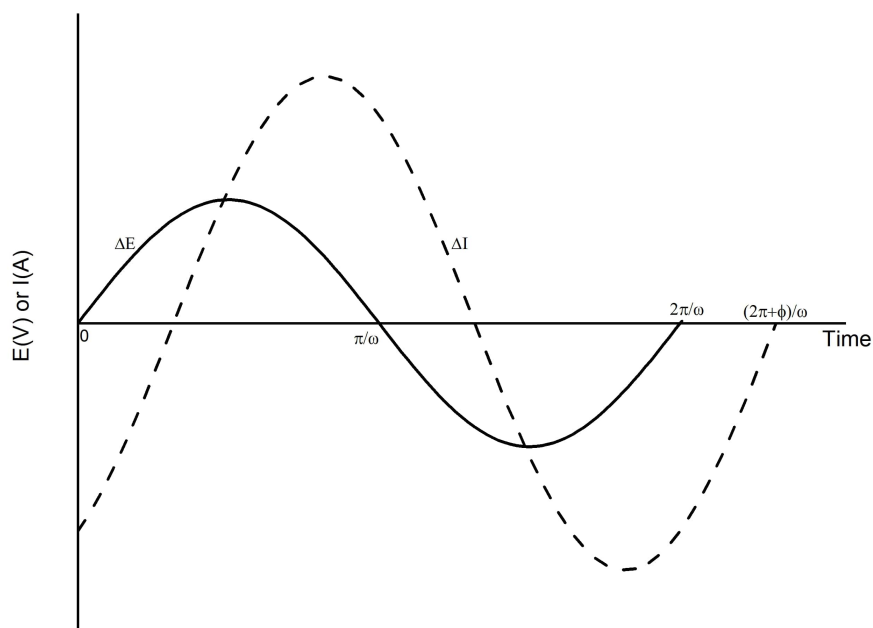


Figure 2.8: Relationship between potential and current when a potential perturbation (ΔE) is applied

In EIS, a potential perturbation (ΔE) is applied to a system where at time, t :

$$\Delta E_t = E_0 \exp[j(\omega t + \phi_1)] \quad (2.40)$$

Where E_0 is the amplitude of the signal, ω is the radial velocity (equal to 2π times the frequency) and ϕ_1 is the phase shift in the initial voltage perturbation. The measured current change corresponding to this change is;

$$\Delta I = I_0 \exp[j(\omega t + \phi)] \quad (2.41)$$

A visual representation can be seen in Figure 2.8. In practice, the phase shift in the initial voltage perturbation is assumed to be zero and other signals are measured against it, resulting in the impedance being:

$$Z(\omega) = \frac{\Delta E}{\Delta I} = Z_0 \exp(j\phi) = Z_0(\cos\phi + j\sin\phi) \quad (2.42)$$

The impedance can be represented as a complex number, in the form;

$$Z = Z' + jZ'' \quad (2.43)$$

where Z' is the real part of the impedance and is known as the resistance term and, Z'' is the imaginary part of the impedance and is known as the reactance term. This information can be displaced in a Nyquist plot as shown in Figure 2.9.

Impedance could alternately be defined in polar form as:

$$Z = |Z| \angle \theta \quad (2.44)$$

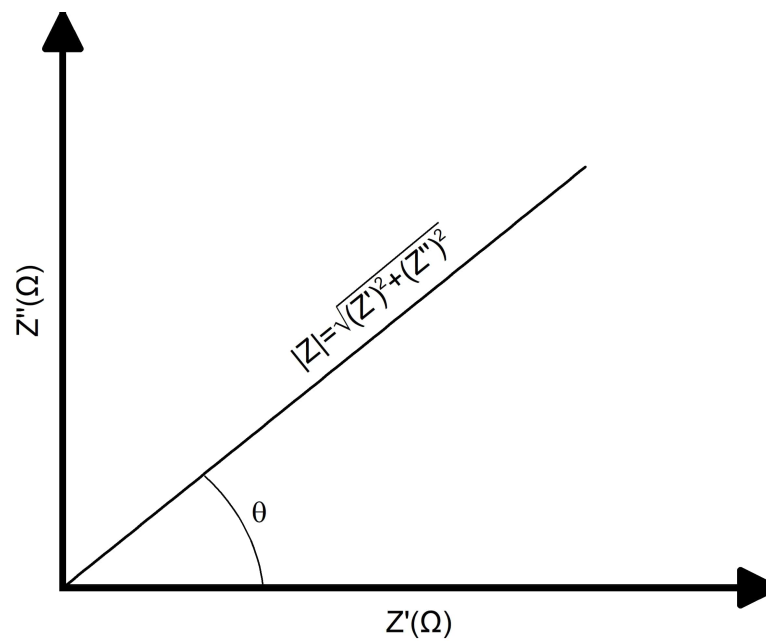


Figure 2.9: Example Nyquist plot

Where $|Z|$ is the modulus of the impedance and is defined as;

$$|Z| = \sqrt{(Z')^2 + (Z'')^2} \quad (2.45)$$

and $\angle\theta$ is known as the phase angle of the impedance and is defined as;

$$\angle\theta = \tan^{-1} \left(\frac{Z''}{Z'} \right) \quad (2.46)$$

EIS can be used to investigate a variety of substances. For example, EIS has been used to detect bacteria in solutions and detect differences between cancerous and non-cancerous tissues (Ward et al. 2014, 2018, Halter et al. 2007).

This technique has not been previously used with drain fluid or to diagnose anastomotic leakage but it was thought that this technique could detect changes in drain fluid over time which could be related to the changing composition of the fluid. This in turn could be used to distinguish between pa-

tients with and without anastomotic leakage by monitoring deviations between the two groups of patients, and as a result was a technique to be used in this thesis.

Modelling of EIS signals

Results gained from EIS experiments can be fitted by equivalent circuits. One of the commonest and simplest ways to represent an electrochemical cell is the Randles circuit (Figure 2.10). In this model, the electrode is represented by capacitor and a resistor in parallel and models the faradaic resistance and capacitance at the electrode-electrolyte interface. This parallel section is attached to another resistor which models the solution resistance.

In practice, it has been found that when using solid electrodes, a certain frequency dependent dispersion occurs which is not purely capacitive (Lasia 2014). In order to model this behaviour, a constant phase element (CPE) is used instead of a capacitor.

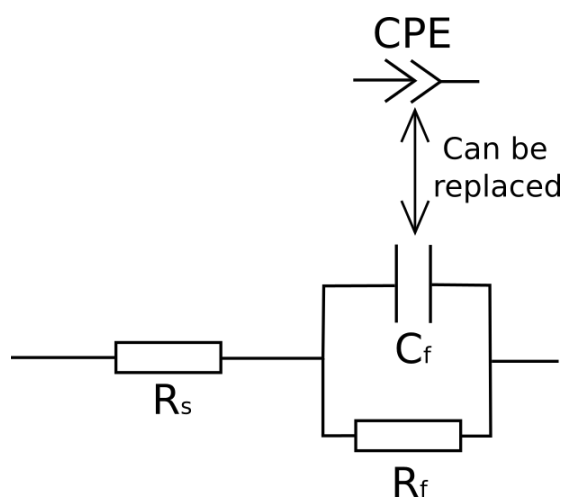


Figure 2.10: Randles Circuit Diagram

The impedance of a CPE is described by the following equation:

$$Z_{CPE} = \frac{1}{T(j\omega)^\phi} \quad (2.47)$$

Where T is value related to electrode capacitance and ϕ is a value related to the deviation from a purely capacitive component which has value of between 0 and 1. The total impedance of the Randles circuit (Z_{total}) is:

$$Z_{Total} = Z_s + Z_f \quad (2.48)$$

Where Z_s is the impedance of the solution which is purely resistive for an ionic solution;

$$Z_s = R_s \quad (2.49)$$

And Z_f is the impedance of the parallel section (also known as the faradaic impedance);

$$\frac{1}{Z_f} = \frac{1}{R_s} + \frac{1}{j\omega C} \quad (2.50)$$

Or if the CPE is used instead of the capacitor, the above equation becomes;

$$\frac{1}{Z_f} = \frac{1}{R_s} + \frac{1}{T(j\omega)^\phi} \quad (2.51)$$

In order to fit these models, non-linear least squares methods are used. Least squares methods calculate the sum of squares of the weighted differences between the calculated and experimental values (S). In other words;

$$S = \sum_{i=1}^N \left[w'_i \left(Z'_i - Z'_{i,cal} \right) + w''_i \left(Z''_i - Z''_{i,cal} \right) \right] \quad (2.52)$$

Where w'_i and w''_i are applied weights (explained further in following text),

Z'_i and Z''_i are experimental values of resistance and reactance at frequency, i , and $Z'_{i,cal}$ and $Z''_{i,cal}$ are the resistance and reactance calculated from the model at frequency, i . Minimisation can be carried out using a number of methods such as the Marquardt-Levenburg or Trust-region algorithms. For each iteration, model parameters would be changed to investigate if a better fit can be found. For a simplified Randles circuit using a CPE instead of a capacitor, there are four parameters that would be changed to improve fitting; solution resistance (R_s), faradaic resistance (R_f) and the T and ϕ parameters of the CPE (Lasia 2014).

To allow fitting of models using non-linear least squares method of EIS requires a weighting to be incorporated into the calculations. This is because without weighting, smaller features may not be approximated at all due to the large change in magnitude of frequencies that is usually performed. The two commonest types of weights used are modulus and proportional.

If resistance and reactance values are relatively similar in magnitude, modulus weighting can be used.

$$w'_i = w''_i = \sqrt{Z'^2_i + Z''^2_i} \quad (2.53)$$

Using this method ensures that, in most cases, small and large impedance contribute equally to the calculations. Modulus weightings can be implemented in 2 ways; by using experimental values, or calculated values. When possible, it is best to use calculated values to remove the possibility of random errors in experimental values affecting the fitting (Lasia 2014).

If resistance and reactance values are dissimilar to each other (order of magnitudes different), it may be useful to use proportional weighting instead as

proposed by Macdonald (1987):

$$w_i' = \frac{1}{Z_i'^2} \quad (2.54)$$

$$w_i'' = \frac{1}{Z_i''^2} \quad (2.55)$$

Similarly to modulus weighting, experimental or calculated values can be used but it is best to use calculated values when possible.

Cyclic Voltammetry

Cyclic voltammetry is a commonly used technique to diagnose electrochemical systems. Starting from a known voltage, the voltage through electrodes is ramped linearly to another known voltage at a set rate. Upon reaching this set voltage, the voltage is ramped back, usually to the initial starting point (Figure 2.11). The ramp in voltage to more positive potentials causes oxidation reactions to occur and the ramp to more negative potentials causes reduction reactions to occur. The rate of a scan can be altered to potentially gain further information.

During this process, the changes in current are recorded and then plotted against potential. The results produced shows both non-faradaic and faradaic behaviour. Non-faradaic behaviour is characterised as baseline currents. Faradaic behaviour, on the other hand, appears as increases such as peaks or decreases such as troughs. These peaks and troughs coincide with the equilibrium potential of oxidation/reduction reactions. As the equilibrium potential is approached, the species becomes reduced/oxidised resulting an increase/decrease in current. The rate of current production eventually slows down since the rate at which the reaction takes place is faster than the amount

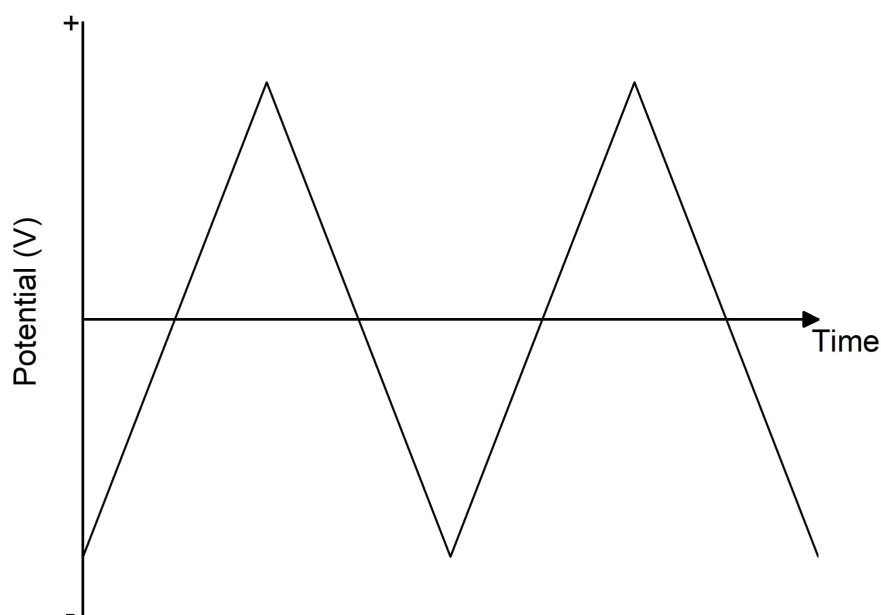


Figure 2.11: Example potential wave used for cyclic voltammetry

of the species required for the reaction is readily available. Eventually, the species required for the reaction is depleted causing the current to drop which results in a peak occurring. The peak currents can be described by the Randles-Sevcik equation:

$$I_p = 0.4463nFAc \left(\frac{nFv_s D}{RT} \right)^{\frac{1}{2}} \quad (2.56)$$

Where n is the number of electrons involved in the reaction, A the working area of the electrode, v_s is the scan rate, F is Faraday's Constant and c is concentration.

Several types of behaviour can be identified using this technique, primarily the identification of reversible (fast electron transfer) and irreversible (slow electron transfer) reactions. Reversible reactions have a reduction and oxidation peak like in Figure 2.12. If an oxidation peak occurs at potential $E_{p,a}$ with a current peak of $I_{p,a}$ and a reduction peak occurs at potential $E_{p,c}$ with a peak

of $I_{p,c}$, then the reaction is considered reversible if the following conditions are fulfilled:

1. $\left| \frac{I_{p,a}}{I_{p,c}} \right| = 1$
2. $E_{p,a} - E_{p,c} \approx \frac{57}{n} \text{mV}$
3. With changing scan rates, $E_{p,a}$ and $E_{p,c}$ do not change
4. $I_p \propto \sqrt{v_s}$

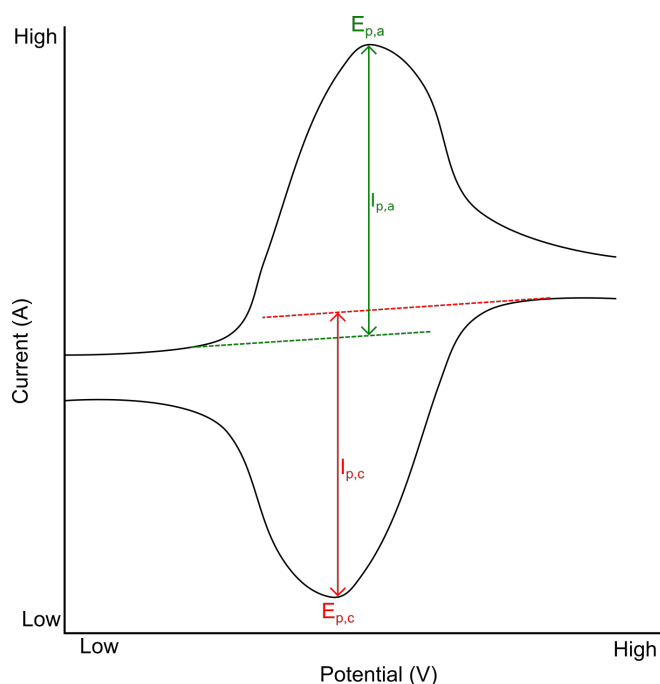


Figure 2.12: Example Cyclic Voltammetry Graph

If peaks do occur but do not fulfil these criteria or only an oxidation/reduction peak occurs, then the peak is due to an irreversible reaction. Cyclic voltammetry is a relatively qualitative technique, but the shape of the graphs can be used to determine electrochemical reversibility and understanding of reaction mechanisms.

Cyclic voltammetry has been used to monitor a variety of substance. These include urea, uric acid, adenosine, etc. that have been seen to be present in

drain fluid. Therefore, similiarly to EIS, it was thought that this technique could be used to detect changes in the composition of fluid over a patient's post-op period and that changes between patients with and without leakage could be observed and as a result was used in this thesis.

2.4.2 Potential Controlled Techniques

Chronoamperometry

Chronoamperometry is a technique for which the potential is stepped up from an initial value where no faradaic reaction happens to a value where the concentration of a species at the electrode is approximately zero for which the current is measured over time. As mentioned previously, when held at a constant potential, the diffusion layer slowly expands into the bulk fluid. The resultant current-time data is a decay over time after an initial peak when the potential is stepped. This decay can be described by the Cottrell equation (Equation 2.25). This technique can be used for several reasons, most chiefly, determination of diffusion coefficients as well as modified versions of the technique used to understand electrode processes (Wang 2006). In order to use this technique, a known electro-active species that is to be investigated needs to be established so an appropriate voltage step can be used. Currently, this information is unavailable with regards to anastomotic leakage but could be found using cyclic voltammetry. This technique was therefore not used in this thesis, but further studies could use this technique to gain further information if reactions are found using cyclic voltammetry.

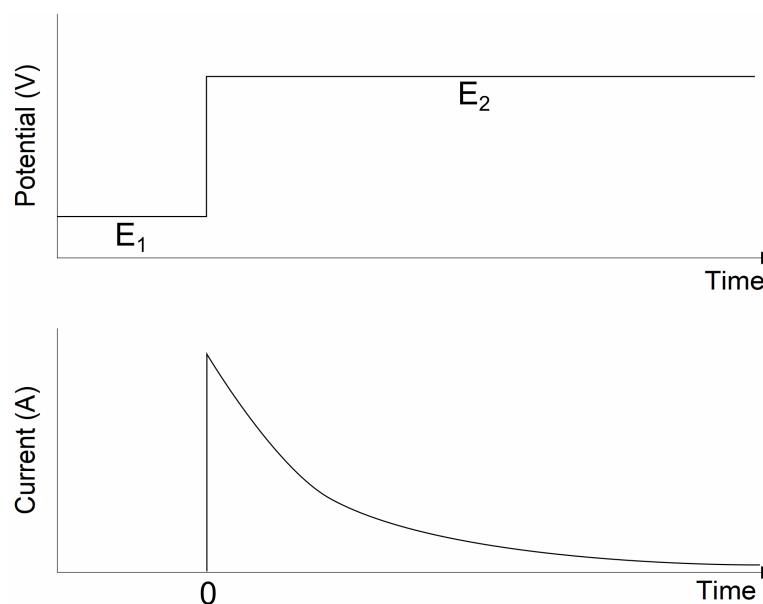


Figure 2.13: (Top) Potential waveform used in chronoamperometry and (Bottom) the resultant current measurement

Stripping Voltammetry

Stripping voltammetry is a technique to detect the concentration of analytes in a solution. Though there are many variations of the technique, they can be summarised into 2 main steps. In the first step, a potential is added to the system to cause ions to be deposited onto the working electrode. This effectively is a concentration step as the species in the large volume of fluid is now present on the smaller surface area of the electrode. Once done, the potential is reversed to strip the ions that were deposited in the first step. Any type of waveforms can be used for this step but the most common tends to be differential or square wave pulses. The current is monitored during this step and is proportional to the concentration of the analyte. The techniques have a very high level of sensitivity and as a result can be affected with the slightest of contamination (Wang 2006). Unlike EIS and CV, this technique can only monitor very specific molecules at any given time when prepared correctly.

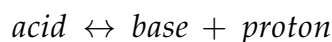
This is not what is currently required and therefore not used in this thesis. but may become a useful technique for later studies if a particular molecule is found to change with regards to anastomotic leakage.

2.4.3 Potentiometry

Potentiometry is where a system is being measured is done under static conditions using electrodes. The measured potential is described by the Nernst equation (Equation 2.20) is affected by the concentration of the measured species. Often, an ion selective electrode is required. One of the most common uses of potentiometry is the measurement of pH.

pH

Brønsted theory defines acids and bases as “substances that are capable of either donating or accepting hydrogen ions”. In other words;



By using the law of mass action (rate of reaction \propto concentration to reacting substances), the activity of the acid (a_{HA}), base (a_B) and hydrogen ions (a_{H^+}) gives the constants;

$$K_a = \frac{a_B a_{H^+}}{a_{HA}} \quad (2.57)$$

and

$$K_b = \frac{a_{HA}}{a_B a_{H^+}} \quad (2.58)$$

Where K_a is known as the acid dissociation/acidity constant and K_b is known as the basicity/association constant. Hydrogen ions are involved in all Brønsted acid-base reactions and therefore measuring its concentration is used to de-

termine the acidity or alkalinity of a substance. As the concentration scale of hydrogen can vary over several magnitudes (100 to 10^{-14} mol L^{-1}), it is prudent to represent hydrogen concentration on a logarithmic scale. Therefore, pH is defined as;

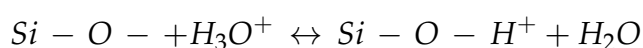
$$pH = -\log_{10} [H^+] \quad (2.59)$$

where $[H^+]$ is the effective concentration of the hydrogen ions.

Glass Bulb pH Probe

The glass bulb pH probe measures the potential change across the glass membrane. In order to measure the potential difference of the glass membrane, two measurement points are required. The first is an electrode in contact with the solution, which in this case is thin glass bulb at the end of the overall device. The second is a reference electrode in contact with a known solution, of which the potential is fixed and known. Usually, this is an Ag/AgCl electrode in a solution containing chloride ions, normally 3M KCl.

Glass is mainly composed of silicone dioxide and when exposed to water, some silicone oxide groups gain a hydrogen ion.



This reaction between the glass and the surrounding solution is what allows for pH sensing to occur and the change in potential difference at the site of the glass/solution interface is dictated by the Nernst equation:

$$E_{glass\ outer\ wall/solution} \approx \left| 2.303 \frac{RT}{F} \log a(H_3O^+) \right| \quad (2.60)$$

Where $a(H_3O^+)$ is the activity of hydronium ion and 2.303 represents the

conversion between natural and common logarithm from Equation 2.25.

The inner wall of the glass membrane also reacts with the internal solution and has a constant potential due to the sealed internal solution which effectively adds an offset. Additional offsets are caused by the potential of the reference electrode in the inner solution which is also constant.:

$$E_{glass\ electrode} = E^0 - 2.303 \frac{RT}{F} \log a(H_3O^+) \quad (2.61)$$

Where E^0 is the constant offset potential. The electrodes are connected to a voltmeter allowing direct readings of pH. Though it is mathematically given ($2.303RT/F$), it is common practice to calibrate the glass electrode in known pH values due to potentially non-ideal conditions (e.g. interfering molecules, deteriorating electrode, etc.) to determine the slope of change in pH. Additionally, several glass electrode models have temperature monitoring built in, to account for daily variations.

2.5 Colorimetric Assays

A widely established method of measuring the concentration of lactate and glucose is the use of colorimetric assays and was used in this thesis to detect lactate and glucose levels. Chemicals/substances absorb light at specific wavelength. As light at a specific wavelength is shone at the sample, the amount of light that is absorbed can be measured. Absorbance (A) is defined as:

$$A = -\log T \quad (2.62)$$

Where transmittance (T) is a ratio of the intensity of light exiting (I) and the

intensity of the incident light (I_0) and can be written as:

$$T = \frac{I}{I_0} \quad (2.63)$$

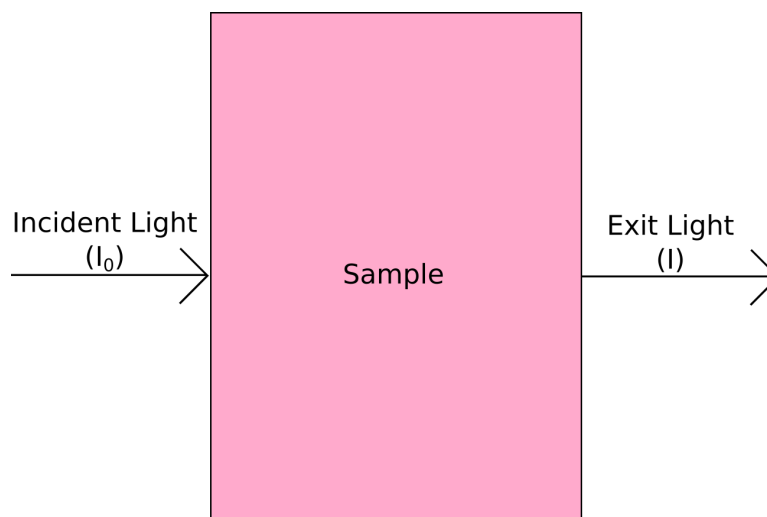


Figure 2.14: Basic principal of colorimetric measurements

Most of the reduction in intensity between the incident light and the exit light is due to absorption of the sample. When a single wavelength of light is used, this absorption process can be described by Beer's law:

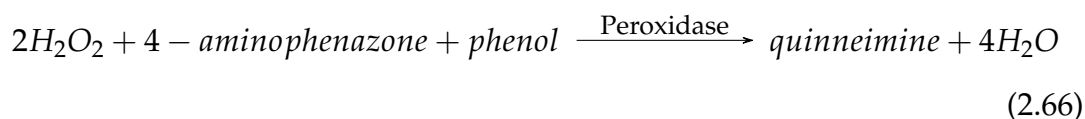
$$A = \epsilon bc \quad (2.64)$$

Where ϵ is the molecular extinction coefficient, b the path length of light and c is the concentration of the sample. However, it should be noted that some of the reduction in intensity can be due to other factors, namely reflection due to the holder the sample is held in place and scattering of some of the light in the sample. The effects of these factors can be reduced by making sure the light source is perpendicular to interface of the sample's holder and the use of a blank sample, which does not contain the light-absorbing molecule

of interest and subtracting this value from the final test values (Wu 2010).

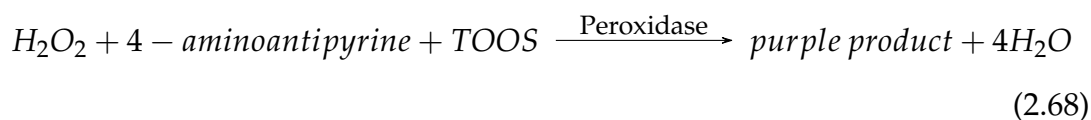
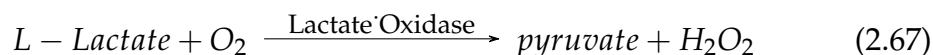
In order to calculate the levels glucose and lactate in a sample, a series of reactions are required to allow for a specific wavelength to be measured easily.

There are several methods that allows measurement of glucose. One commonly used method is through the use of the enzyme glucose oxidase (GOD).



GOD is an enzyme that interacts with glucose to create gluconic acid and hydrogen peroxide as shown in equation 2.65. This reaction does not allow absorption at a particular wavelength. Therefore, a second reaction is used (equation 2.66), where the 4-aminophenazone and phenol reacts with the hydrogen peroxide, produced in the first reaction, and catalysed by peroxidase to produce quinneimine which gives a distinctive red-violet colour for which absorbance can be measured at approximately 500nm which can be correlated to concentration of glucose.

Similarly to glucose, lactate measurement can be done through the use of an enzyme, which usually is lactate oxidase, whereby hydrogen peroxide is produced.



Where TOOS is N-ethyl-N-(2 hydroxy-3-sulphopropyl)m-toluidine.

4-aminoantipyrine and TOOS is converted into a purple product by reacting with hydrogen peroxide produced in the first step, which is catalysed by peroxidase. A purple colour is produced for which absorbance can be measured at 540nm.

2.5.1 Characterisation of Assays

In order to understand how well an assay will be at detecting an analyte, it is best to characterise its performance. This is done by measuring absorbance of solutions of known concentrations of the analyte of interest and producing a calibration curve.

Linearity and Range

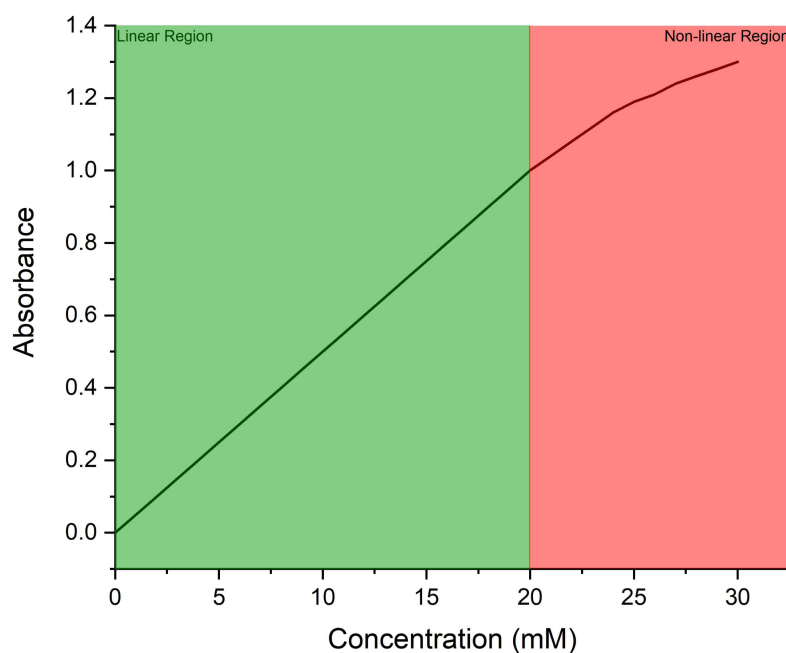


Figure 2.15: Example assay profile with linear and non-linear regions defined

The majority of assays have a linear region for which they work optimally for

which a change in concentration is proportional to absorbance. Past a certain point, assays stop being proportional to absorbance and their behaviour is not as predictable due to a lack of reagent available and therefore any measurements should be considered inaccurate (Figure 2.15). This linear relationship is in the form of:

$$A = kc + b \quad (2.69)$$

Where A is the absorbance, k is the slope of the curve and b is the background noise of the sample (y-intercept) and c is the concentration of the analyte. Linearity of an assay is determined visually. If a linear region is observed, a range can be determined for which a linear fit can be performed between and statistical tests, such as regression analysis, should be performed and stated to give an indication of goodness of fit.

Accuracy and Precision

The accuracy of an assay is how close the mean of the results is to the true value. This can be achieved by use of a reference sample or by comparing results from the proposed methodology to a known and characterised protocol.

Precision is how close each measurement is to each other when the same protocol is applied to the same sample multiple times. This can be reported in terms of standard deviation or relative standard deviation (standard deviation divided by mean).

Detection Limit

While the upper detection limit is determined by the point at which the assay ceases to be linear. However, a lower limit of detection (LOD) should be determined which allows determination of the lowest concentration that can

be measured reliably without background noise affecting the result. This can be calculated using the formula:

$$LOD = \frac{a\sigma_b}{k} \quad (2.70)$$

Where σ_b is the standard deviation of the blank (i.e. standard deviation of a sample known to have zero concentration of the analyte of interest), a is a pre-determined multiplier and k is the slope of the line of fit which is included to account for error of this fitting. Usually, a is equal to 3 as, at this value, less than 0.03% of measurements above this value should not be affected by noise.

Sensitivity

Another parameter that should be determined is the sensitivity. This is how small a change in concentration that can be detected by the system. Sensitivity can be described by 2 ways. Analytical sensitivity is the ability to distinguish between 2 distinctly different but very close concentrations of the analyte. This can be described as $\frac{k}{\sigma_b}$, where σ_b is the standard deviation of the blank. Calibration sensitivity can be described as the slope k where a higher value indicated higher sensitivity to changes in concentration.

2.6 Summary

This chapter has looked at the key theories involving electrochemistry and assays. In the following chapter, methodologies developed based on these theories are described.

Chapter 3

Materials and Methods

3.1 Introduction

In Chapter 1, it was seen that anastomotic leakage is a potentially a life changing and life-threatening complication after colorectal resection. Though these are known facts, the current methods of detecting anastomotic leakage are relatively poor with symptoms often needing to present before clinicians consider anastomotic leakage occurring. Therefore, aims and objectives were established with a view to improving methods of detecting anastomotic leakage. From literature of previous studies looking at the problem, the measurement of several biomarkers in drain fluid were identified as potentially being able to determine anastomotic leakage at an early stage; glucose, lactate and pH. In addition, electrochemical techniques (Electrochemical Impedance Spectroscopy - EIS and Cyclic Voltammetry - CV) were added as a way of gaining further information about the fluid that could also aid in the detection of anastomotic leakage (see section 2.4 for further details).

To determine whether these biomarkers could be used to detect anastomotic leakage, methodologies had to be established to determine the best way to detect these biomarkers. Previous studies looking at lactate and glucose have sampled peritoneal fluid by using microdialysis tubes. However, this method has a noted drawback that samples collected often under represents the actual concentration of the analyte of interest in the sampling area due to the fact that removal of analytes by the tubes is faster than the replenishment of the analyte at the tube's surface (Chefer et al. 2009, Shippenberg & Thompson 1997, Turkina et al. 2017). In this thesis, glucose and lactate samples were to be measured directly on drain samples which had not been done previously. By doing this, results gained should be more representative of the

environment surrounding the anastomosis. Enzymatic assays were used to detect concentrations of glucose and lactate in these drain samples as it is a well-established method of detecting these markers with a high level of accuracy (Silva et al. 2016, Yanase et al. 2018). While one study has looked at pH in drain fluid with respect to anastomotic leakage, very little information was presented (only mean pH values are provided for patients with leakage). As a result, while a similar method was to be employed, it was to provide previously unspecified data such as range, standard deviations, etc.

EIS and CV techniques have not been used previously with regards to drain fluids or to diagnose anastomotic leakage. However, these techniques have been used to monitor tissues for substances such as urea, uric acid, bacteria as well as distinguish between cancerous and non-cancerous tissues, etc. It was hypothesized that these techniques could be used to monitor changes in the composition of drain fluid over the post-op period and which could be used to differentiate between patients with and without leakage.

Before developing methodologies for these markers, it was essential to understand the theory behind these techniques, for which further information can be found in Chapter 2.

Once the theory had been understood, initial methodologies were drawn up. It was understood at the time that samples being received from patients may be small (potentially <2mL) and therefore developed methodologies had to take this into account.

It was prudent to test these methodologies prior to clinical testing to characterise the tests as well as understand the challenges that may present so any problems could be minimised before testing patient samples and was

achieved by the use of a simulated drain fluid. From these initial experiments, procedures were finalised and were then used to test clinical samples. In this chapter, the testing of initial methods and the finalised methods then used for clinical testing are explained.

3.2 Materials and Solutions

3.2.1 Solution A

Solution A refers to a solution that attempts to mimic the wound fluid environment as described by the British Pharmacopoeia (1995). To make 1L of solution A, 8.298g of sodium chloride (Sigma Aldrich, Gillingham) and 0.368g of calcium chloride dihydrate (Sigma Aldrich, Gillingham) was added to 900ml of deionised water (dH₂O) in a glass beaker. The solution was then topped up to 1L by adding 100ml deionised water. The solution was then mixed by pouring the solution back and forth from one glass beaker to another until the powders were not visible. The solution was stored in a glass bottles at 4°C prior to use.

3.2.2 Artificial Peritoneal Exudate (APE)

Though Solution A was a good starting point to test experimental protocols, it is a relatively simple fluid and is not a particularly good representation of peritoneal fluid. Therefore, it was prudent to develop a more complex solution that could give a better representation of peritoneal fluid. A paper by Kelton et al. (1978) gave details of the concentrations of various ions found in human peritoneal fluid.

In addition to the ions to be added based on this paper, it was decided that

a buffer should be incorporated to simulate the pH of peritoneal fluid, which is typically between 7.5-8 (DiZerega & Rodgers 1992). In addition to this, the buffer needed to be autoclavable. This was because solutions would be spiked with bacteria (see later sections) and therefore it was required that the solution was sterile prior to this step to prevent other bacteria from growing. Trizma buffer, an organic compound consisting of an amine group and a commonly used biological buffer (Gomori 1955), was chosen as it was able to buffer solutions within this range and was autoclavable.

Table 3.1: Chemicals used for artificial peritoneal exudate

Chemical	Supplier Ref	Qty
Trizma HCl	Sigma T3253	6.35g
Trizma Base	Sigma T6066	1.18g
Urea	Sigma U1250	1.9411g
Creatinine	Sigma C4255	0.1350g
Sodium Chloride	Sigma S7653	1.5206g
Potassium Chloride	Sigma P4504	0.0900g
Calcium Chloride Dihydrate	Sigma C5080	0.2470g
Sodium Acetate	Sigma S7545	2.0436g
Uric Acid	Sigma U2625	0.0871g
Sodium Carbonate	Sigma 71345	0.3370g
Sodium Phosphate Dibasic	Sigma S0876	0.3577g
Glucose	Sigma G8270	1.5180g

Table 3.1 shows the quantities of chemicals that were added. Chemicals were added to 900mL deionised water in a 2L glass bottle suitable for autoclaving in the order given in the table, except for glucose and sodium phosphate dibasic. Each chemical was mixed using a magnetic stirrer at approximately 800-1000rpm for at least 5 mins before adding the next chemical.

The amount of Trizma HCl and Trizma base was chosen as it would make a

0.05M buffer at a pH of 7.35 at 25°C. The addition of alkali elements, most predominantly sodium carbonate, pushed the pH of the solution to approximately 7.8 which is within normal range of peritoneal fluid. Once mixed, the solution was autoclaved at 121°C. In a separate container, glucose was added to 60mL of deionised water and then filtered through a 0.22µM syringe filter (Millipore SLGP033RS, Carrigtwohill, Ireland) in a level 2 micro-safety cabinet. Similarly, sodium phosphate dibasic was added to 60mL of deionised water and filtered through a 0.22µM syringe filter in a micro-safety cabinet. Both glucose and sodium phosphate dibasic were filter sterilised as opposed to being added to the main solution and autoclaved as there is some literature that indicate they can be affected by the autoclaving process. 50mL of both the filtered glucose and phosphate solutions were then added to the main solution in the micro-safety cabinet. Solutions were stored at room temperature and used within 24 hours.

3.2.3 pH Buffer Solutions

In order to calibrate the pH probe, buffer solutions of pH 4, 7 and 10 were used. pH 4 and pH 7 buffer tablets were purchased from Fisher Scientific (B/4765/77 and B/4760/77, Loughborough, United Kingdom). pH 4 and pH 7 buffers were made up by adding the appropriate tablet into 100mL of dH₂O. pH10 buffer solution was also purchased from Fisher Scientific (Acros Organics™ 258600010, Loughborough, United Kingdom). Buffers were stored at room temperature.

3.2.4 Lysogeny Broth Media and Agar Plates

Lysogeny Broth (LB) media was used to culture stock of *E.coli* and *P.aeruginosa*. LB media was made up by adding 2.5g of Tryptone (Fisher Scientific, 12797099), 1.25g of yeast extract (Acros Organics, 451120010) and 1.25g NaCl (Fisher Scientific, S/3160/60) to 250mL of dH₂O. Media was autoclaved in glass bottles at 121°C to ensure no other bacteria would grow in solution.

To create solid media, 5g of agar (Fisher Scientific A/1080/53) was also added to the above mixture prior to autoclaving. Once autoclaved, the media was poured into agar plates (enough to cover the surface) before the media cooled below 40°C in a level 2 micro safety cabinet (MSC-2) and left to solidify for 30 mins before being stored away at room temperature.

3.2.5 Sodium and Potassium Chloride Solutions

3M potassium chloride (KCl) solution was used to create silver chloride reference electrodes and as a storage solution for the pH probe and 1M KCl was created as a storage solution for the Silver/Silver Chloride (Ag/AgCl) wires used as reference electrodes (see following sections). 1M KCl solutions were made by adding 7.4551g KCl (Sigma P4504) to 100mL of deionised water and 3M KCl solutions were made by adding 8.9462g KCl to 40mL of deionised water. 0.9% sodium chloride (NaCl) solution was used to wash cells. This was made by adding 0.9g of NaCl (Sigma S7653) to 100mL of deionised water.

3.2.6 Lactate and Glucose Reagents

In order to detect lactate concentration, a lactate oxidase-based, commercially available kit was purchased from Randox (LC2389, Crumlin, United King-

dom). The kit is developed for large volumes of blood samples and had to be modified to allow for testing of smaller samples of peritoneal fluid which will be talked about later in this chapter. This kit contains small bottles containing the dry reagent and a buffer solution. Prior to use, the reagent must be reconstituted by adding 6mL of the buffer per bottle containing the dry reagent. Once reconstituted, the reagent is stable for two weeks after which it cannot be used. Similarly, to detect glucose concentration, a glucose oxidase-based kit was also purchased from Randox (GL2623, Crumlin, United Kingdom) and was also modified for small samples of peritoneal fluid. This kit requires no preparation and is ready to use immediately unlike the lactate kit. Both the glucose and lactate kits contained a reference solution with a known concentration. For glucose, this was at 5.56mM and for lactate, this was at 4.35mM. Both solutions were used to test the accuracy of the assays (discussed further later).

3.2.7 Microbial Species

Microorganisms used in experiments were taken from Medical Device laboratory culture stock. *E. Coli* strain DSM30083 was originally purchased from Leibniz Institute DSMZ-German Collection of Microorganisms and Cell Cultures. *Pseudomonas aeruginosa*, PA14, is a strain that was originally observed by Schroeter and then Migula in the late 1800s/early 1900s (Hugh & Leifson 1964). PA14 was taken from the Medical Devices Laboratory stocks (University of Strathclyde).

The bacteria to be used were regularly streaked onto agar plates (Section 3.2.5) under aseptic conditions. These streaked plates were placed in an incubator at 37°C overnight before being kept in fridge.

Culturing of Microbial Species

In order to culture microbial species to be added to a specific, single colonies taken from streaked agar plates were placed into 15mL of LB media in white top containers under aseptic conditions and were incubated in an orbital incubator at 37°C at 150rpm for 24 hours. The resultant cultures were then washed by first centrifuging the media at 13,400rpm for 5 mins in 1.5 mL Eppendorf tubes. The subsequent supernatant was removed and replaced with 0.9% NaCl. Cells were re-suspended in the 0.9% NaCl and centrifuged again for 5 mins. The previous step was repeated once more and then the supernatant was removed and replaced with 15mL of the chosen media and cells were re-suspended in this media.

3.2.8 Clinical Samples

In order to collect clinical drain samples from the hospital, a biorepository ethics application was submitted and successfully obtained from the West Node of the NRS Biorepositories and Tissue Services (Ref:300, see appendix for approval letter).

Clinicians identified suitable patients that were undergoing a colorectal resection and consented them using the standard biorepository form. Once consented, clinicians took peritoneal drain samples daily, starting from the morning after the surgery had taken place (post-op day 1) for as long as drain was left in the patient, which was determined by the responsible clinician. The samples were collected in white top universal containers approximately 1-2 hours after they were emptied in the morning to ensure a fresh sample. 2 types of drain bags are used in the hospital; a passive draining bag and a

suction drainage bag (Figure 3.1).

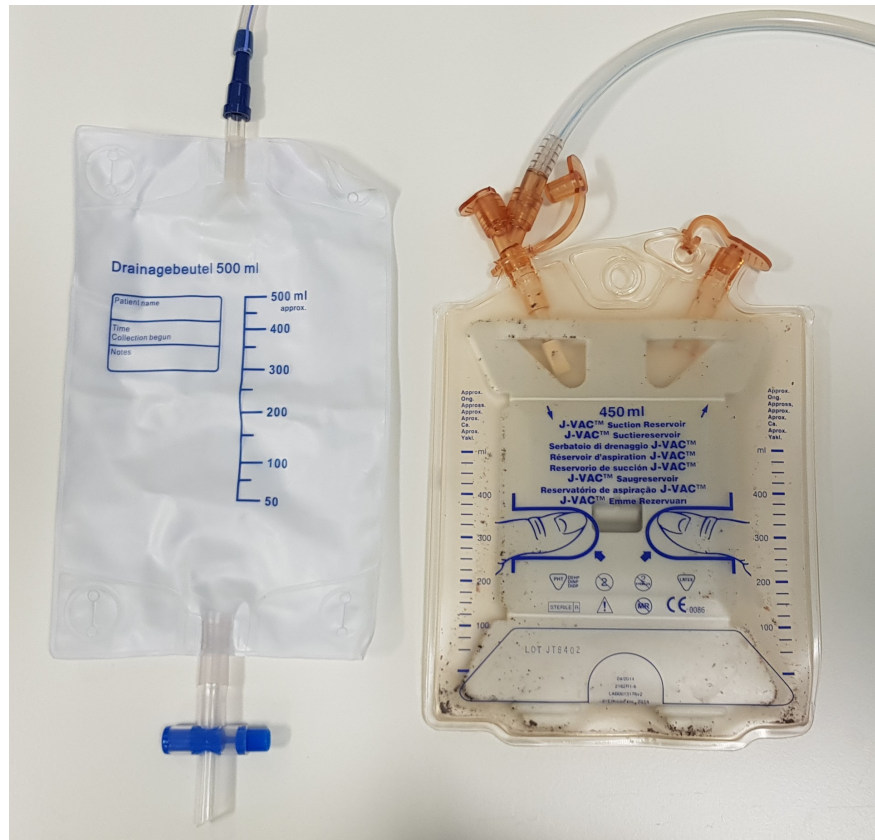


Figure 3.1: (Left) Passive drainage bag (Right) Suction drainage bag

Each patient was assigned a unique identification number to allow cross-referencing of patient history (provided at a later date) to a sample and to maintain anonymity of patients. The number also identified how many days post-op the sample had been taken.

Samples were categorised as Category B biological substances. Therefore, suitable UN3373 package was acquired from DaklaPack (Chiswick, London, 520125) and was used to transport the samples from the hospital to the university (Figure 3.2). The packaging uses a triple layer system with an adsorbent material between the first and second layers to ensure no spillage of biological material into the environment during transport. Samples were transported

within 40 mins of collection to the university (range: 24-37mins) and tested as soon as they arrived at the lab as described in upcoming Sections 3.3.3, 3.4.2 and 3.5.7.



Figure 3.2: UN3373 packaging used for transferring samples from the hospital to the University

All data collected from samples and details from patients (e.g. post-op complications experienced) were anonymised and stored in encrypted hard drives in accordance to the Biorepository ethics application. Patients were anonymised by clinicians at the hospital, therefore Strathclyde researchers did not receive any personal information in accordance with GDPR regulations.

3.3 Lactate and Glucose Measurements

As mentioned previously, ischaemia is a commonly cited cause of anastomotic leakage. Monitoring lactate and glucose was considered as a potentially valuable method of detecting anastomotic leakage in this thesis. It was decided that the best way to measure the concentrations of these molecules in drain fluid was the use of colorimetric assays, for which the theory can be found in Section 2.5.

3.3.1 Equipment and Materials



Figure 3.3: LabSystems Multiskan Ascent (and connected PC) used to measure the absorbance of samples at specific wavelengths

In order to measure the colour change of the glucose and lactate assays, a LabSystems Multiskan Ascent, a machine that can perform colorimetric measurements, was used (Figure 3.3). Samples and calibration solutions to be tested were put into 96 well plates as specified for the experiment and placed

into the machine and run using a connected PC containing Ascent software. 96 well plates were purchased from Thermo Scientific (Roskilde, Denmark).

3.3.2 Assay Characterisation

To test that this would work successfully for use with clinical samples, the assay needed to be characterised by determining parameters of linearity, range, accuracy, precision, detection limit and sensitivity (further explanation of these are found in section 2.5).

To accomplish this, spiked solutions of lactate and glucose with concentrations ranging from 0mM to 30mM were made up as specified in Table 3.2. 30mM as the upper end of the test was chosen as the kits were expected to lose linearity at about 20-25mM. Going past this expected limit allowed observation of non-linearity occurring.

Table 3.2: Solutions used to characterise glucose and lactate assays. Na-L=Sodium Lactate

Concentration	Lactate Solutions	Glucose Solutions
30mM	0.0841g Na-L + 25mL dH ₂ O	0.1351g Glucose + 25mL dH ₂ O
25mM	0.0701g Na-L + 25mL dH ₂ O	0.1126g Glucose+ 25mL dH ₂ O
20mM	0.0561g Na-L + 25mL dH ₂ O	0.0901g Glucose + 25mL dH ₂ O
15mM	10mL 30mM Na-L +10mL dH ₂ O	10mL 30mM Glucose + 10mL dH ₂ O
10mM	10mL 20mM Na-L +10mL dH ₂ O	5mL 20mM Glucose + 5mL dH ₂ O
5mM	10mL 10mM Na-L + 10mL dH ₂ O	2.5mL 10mM Glucose + 2.5mL dH ₂ O
0mM/Blank	Only dH ₂ O	Only dH ₂ O

2.5µL of each of these concentrations were pipetted into a 96 well plate, in triplicate. In addition to these solutions, reference solutions for both lactate and glucose (see section 3.2.6 for further details) were added in triplicate (2.5µL volumes as well) as it allowed for testing of accuracy versus a known reference (see section 2.5.1 for further explanation).

3.3. Lactate and Glucose Measurements

Once all concentrations had been added to the 96-well plate, 250 μ L of the lactate was added to solutions in wells containing lactate solutions and 250 μ L was added to wells containing the glucose solutions. An example plate configuration is shown in Figure 3.4.

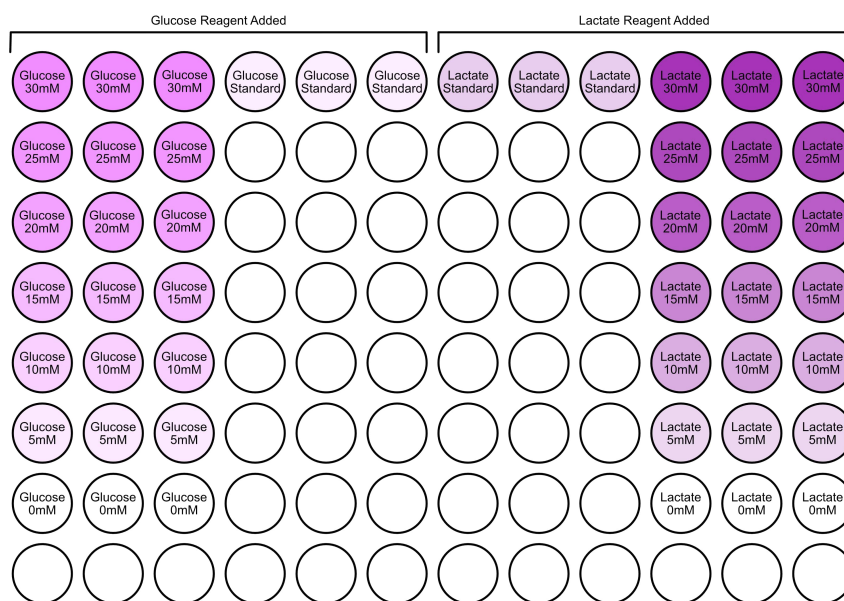


Figure 3.4: Example schematic 96-well plate used to characterise the glucose and lactate assays

The 96-well plate was then placed into the MultiSkan ascent and was programmed to incubate the plate at 37°C and shake the plate at 240rpm for 10mins. Once complete, the machine read the absorbance of each well at 560nm for lactate samples and 492nm for glucose samples. For each triplicate, absorbance values were averaged to give a final value. The calibration experiment was repeated 5 times and all results from calibration solutions were plotted on a graph of concentration vs absorbance.

3.3.3 Clinical Lactate and Glucose Testing Procedure

In order to measure the concentration of lactate or glucose in a sample, calibration solutions had to be produced, for which a calibration curve could be produced to determine the concentration of lactate and glucose in clinical samples. From the results of the characterisation of the assay (Section 4.2 and 4.3), the linearity of the assays were determined to be at 20 μ M and 25 μ M for the lactate and glucose assays respectively. To simplify the process, both lactate and glucose calibration solutions of 0, 5, 10 and 20 μ M were used in this section were made by serial dilution (see Table 3.2).

When samples were received to the lab following their transport as described in section 3.2.8, the calibration solutions were made up fresh and added to a 96 well plate in 2.5 μ L volumes in triplicate.

Most samples were expected to fall within a 0-20mM range (based on previous literature, mentioned in Section 1.5.1) but as a precaution, as there was the possibility that samples could be substantially higher than this range, samples were diluted by taking 50 μ L of samples to be tested, placing them in a white top container and adding 200 μ L of deionised water to create a 1:4 dilution. These diluted samples were added to the 96-well plate in 2 sets of triplicates; one triplicate for testing for glucose levels and one triplicate for testing lactate levels (also added in 2.5 μ L volumes). Once all calibration and diluted sample solutions were added, 250 μ L of glucose reagent was added to all wells containing glucose calibration solutions and sample triplicates which had been designated for testing glucose levels. Once complete, 250 μ L of lactate reagent was added to all wells containing lactate calibration solutions and sample triplicates that had been designated for testing lactate levels. Imme-

diately after this was finished, the plate was placed in the Multiskan and was set to incubate the plate at 37°C and shake at 240rpm for 10mins, after which the machine read the absorbance levels at 540nm for lactate and 492nm for glucose.

Modifications to Initial Methodology

After the first several samples were tested, it was noticed that the amount of blood contamination was particularly high on day 1. Red blood cells have been seen to affect the assays when present in large enough concentrations (Ginsberg 2009). Therefore, samples from patient 13 onwards were prepared as unfiltered and filtered samples. Unfiltered samples were tested as previously done but in addition, some of the sample was filtered with a 0.22µm syringe filter, prior to following the method of the unfiltered samples. The use of a 0.22µm was chosen as it has been shown in previous literature that the use of filters of this size can remove at least 96.7% of red blood cells (Bruil et al. 1995, Chen et al. 2016). It should be noted, that when 0.22µm filter is used, bacteria from a solution would also be removed.

3.4 pH Testing

Another effect of ischaemia are pH changes that occur due to the switch from aerobic to anaerobic respiration producing acidic components.

3.4.1 Equipment

In order to determine pH in a sample, a Mettler-Toledo InLab[®] Micro Pro-ISM probe was purchased from Sigma-Aldrich (Gillingham, United Kingdom). This probe was chosen as it allowed for measurements of small volumes as

well as having integrated temperature probe to account for variations in lab temperature that could affect results. The probe was connected to a Mettler-Toledo S220 SevenCompact™ pH/Ion meter, which recorded results (Figure 3.5). The probe was calibrated before every testing session using the buffer solutions mentioned in Section 3.2.3.



Figure 3.5: Probe and meter used to measure pH in clinical samples

3.4.2 Clinical Testing

In order to measure pH, 500 μ L of samples were added to 24 well plates. The pH probe was placed into a well, with the tip in contact with the sample, and held in position by use of a stand (see Figure 3.6). The probe was allowed to measure the pH of a sample and once the reading was stabilised, the pH was recorded. As much as possible, samples were added and measured in triplicate and results were averaged. The same sample was then subjected to

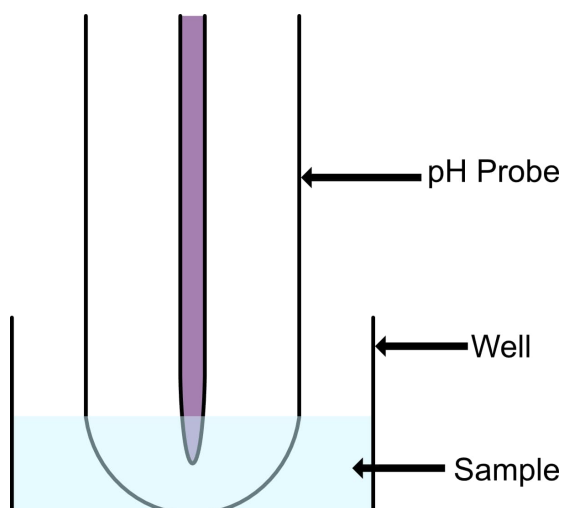


Figure 3.6: pH probe schematic diagram for measuring samples

electrochemical techniques (EIS and then cyclic voltammetry) for which the tests are described later in this chapter.

Between each measurement, the probe was cleaned by washes in Distel and ethanol, to remove biological and other contaminants before finally rinsed in deionised water. When not in use, the pH probe was stored in 3M KCl (recipe in section 3.2.5).

3.5 Electrochemical Testing - EIS and CV

In addition to looking at ischaemic markers, EIS and CV techniques were also to test the drain fluid. These techniques have been previously used to detect bacteria, changes in chemical species such as urea, uric acid, differentiate between cancerous and non-cancerous tissues, etc. (Ward et al. 2014, Patzer et al. 1989, Halter et al. 2007, Gersing 1998, Nguyen & Venton 2015) (Section 1.5.5). These techniques have not been applied previously to drain fluid so it was hypothesized that changes in drain fluid over time could be detected by these techniques and these changes could be used to differentiate between

patients with and without anastomotic leakage.

3.5.1 Equipment



Figure 3.7: Solartron 1260 set up for use in Electrochemical Impedance Spectroscopy (EIS) measurements

In order to do EIS experiments, a Solartron 1260 was used (Figure 3.7). This was connected to a PC that had the software ZPlot, which allowed initiation of EIS tests at chosen frequencies and amplitudes.

For cyclic voltammetry (CV) experiments, a Solartron 1287 was used (Figure 3.8) that was connected to a PC using Corrware software that allowed for various electrochemical tests including cyclic voltammetry.

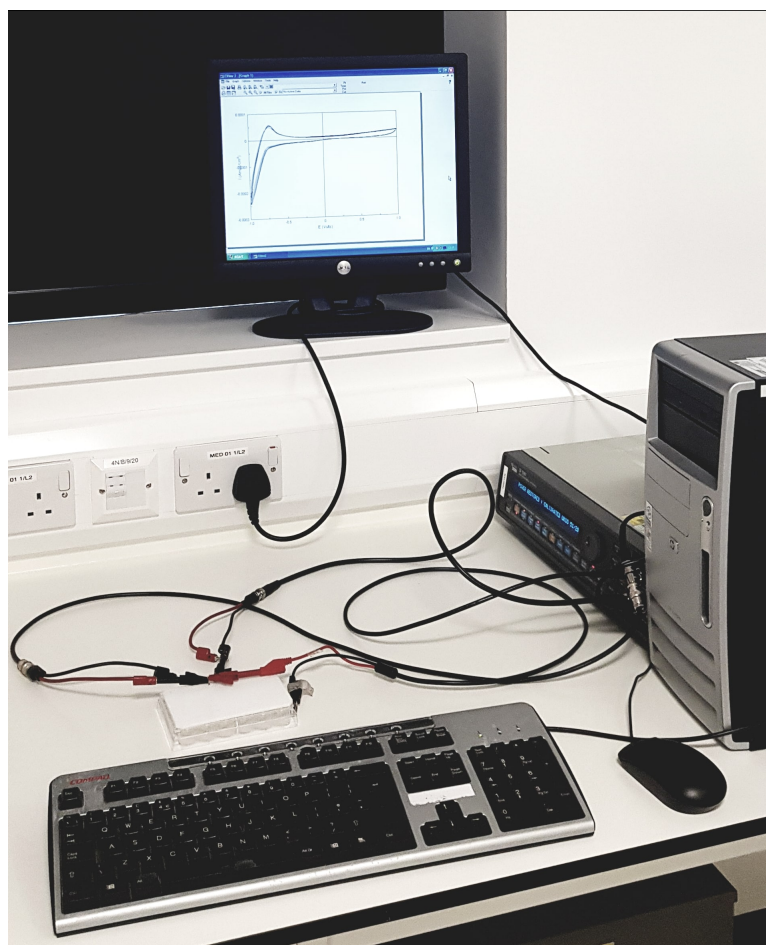


Figure 3.8: Solartron 1287 set up for Cyclic Voltammetry (CV) experiments

3.5.2 Electrode Selection

For electrochemical testing, 1mm platinum rods were chosen to be used for working and counter electrodes. This was mainly due to the fact that platinum has a low resistance, which would help increase the sensitivity of measurements. Before testing, electrodes were cleaned mechanically using 50 μ m diamond paste and rinsed thoroughly in deionised water.

For CV, an additional silver/silver chloride (Ag/AgCl) electrode was required to allow for stable readings to occur (described in the following section).

Electroplating Silver Wire

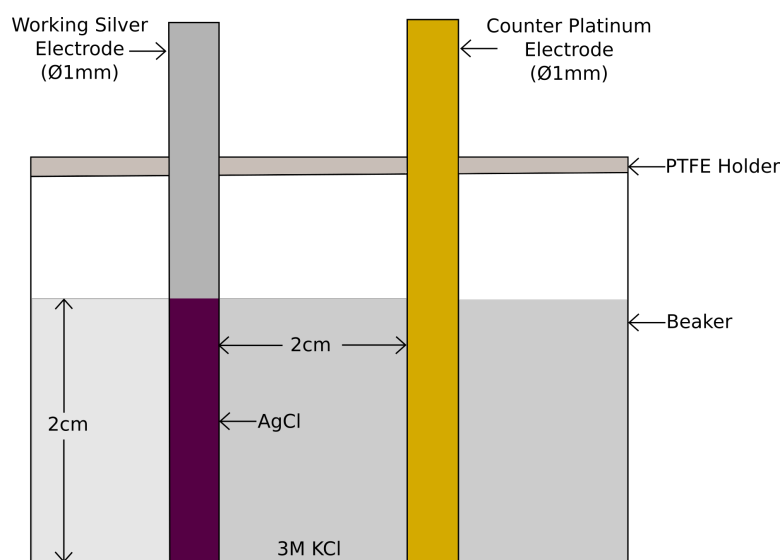


Figure 3.9: Set-up used to produced Ag/AgCl wires

In order to get stable readings for cyclic voltammetry (CV) measurements, a silver/silver chloride (Ag/AgCl) reference wire was required to which the potential delivered at the working electrode can be compared against. To create an Ag/AgCl reference electrode, a piece of silver wire (1mm diameter) was held in place inside a solution 3M KCl solution 2cm from a platinum counter electrode (1mm diameter) using a drilled PTFE sheet. Approximately 2cm (in length) was in contact with the solution (Figure 3.9). The wire was connected to the Solartron 1287 (Figure 3.8) as the working electrode and a platinum wire was connected to the machine as the counter electrode. The machine was set to deliver a constant current of approximately $1\text{mA}/\text{cm}^2$ using the software Corrware (Galvanostatic Mode) for 30 minutes, after which the silver wire was coated with chloride. The silver chloride wire was then stored in 1M KCl for at least 24hrs before first use. After use in a test, the silver wire was stripped of the silver chloride layer using fine emery paper and was re-electroplated.

3.5.3 EIS Set-up and Testing

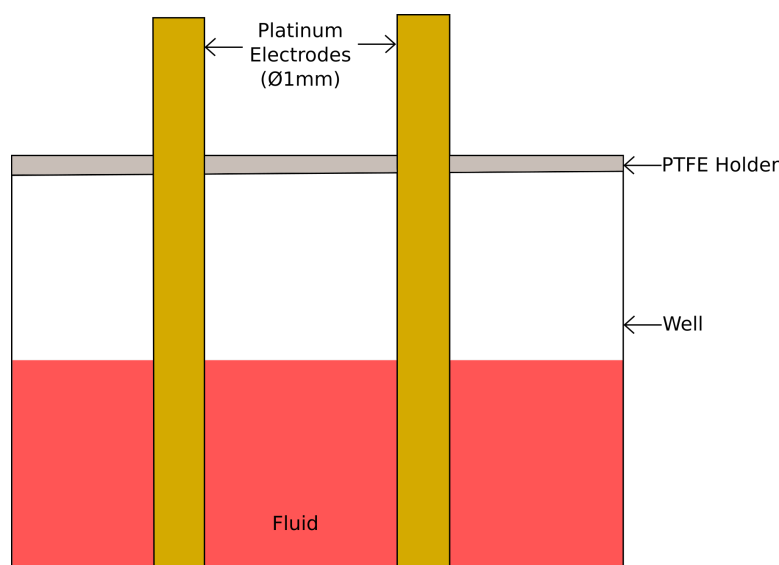


Figure 3.10: Schematic drawing of EIS electrode set-up in 24 well plate well during testing

For EIS testing, platinum electrodes were placed into the well and held in position using a PTFE holder that held the electrodes at a distance of 7mm apart as shown in Figure 3.10. This was connected to the Solartron 1260 by using crocodile clips. For testing, an amplitude of 300mV was used for measurements for a frequency range between 0.1Hz to 1MHz. Experiments were performed at 0V DC potential difference.

3.5.4 CV Set-up and Testing

For CV testing, platinum electrodes and a silver-silver chloride (Ag/AgCl) reference (see Section 3.5.2) were placed into the well where the platinum electrodes were placed 7mm apart and the Ag/AgCl reference was placed approximately 4mm from the working electrode, as shown in Figure 3.11. The electrodes were attached to the Solartron 1287 by crocodile clips and CV was run from -1V to +1V for 5 cycles at speeds of 25, 50 and 100mV/s. In

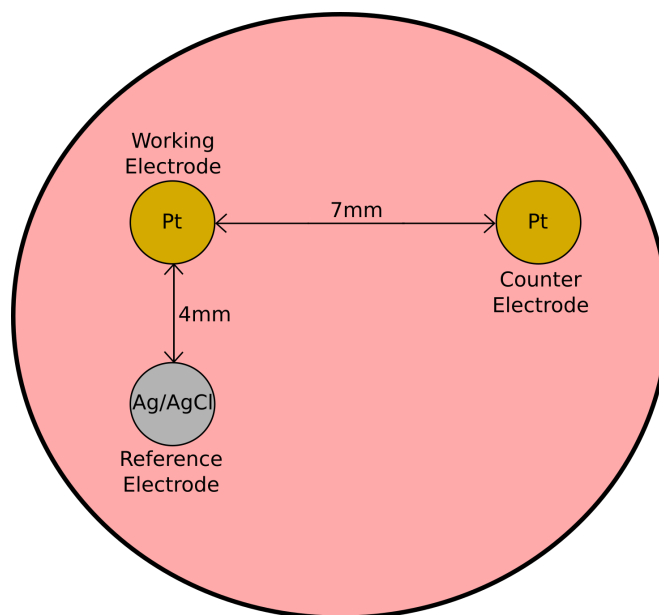


Figure 3.11: Top down view of electrode set-up for CV experiments

this range, it should be possible to detect several substances such as urea, uric acid, adenosine, etc. that can be found in drain fluid (Patzer et al. 1989, Nguyen & Venton 2015, Ernst & Knoll 2001).

3.5.5 Volume Experiments

It was expected that minimal amounts of fluid would be gained from patients (<1mL). In order to check that the technique was suitable for low amounts of fluid that were placed in a 24-well plate, a quick test was devised where small volumes of fluid were tested with both EIS and CV techniques. Volumes of 0.5, 1 and 2mL of Solution A (Section 3.2.1) were added to a 24 well plate. 0.5mL was chosen as the lowest volume to be used as it was found that this was the minimum volume required to adequately cover the bottom surface of the well. With the addition of 0.5mL resulted in the electrodes having a contact depth of 2.62mm. Addition of 1 and 2mL resulted in contact depths of 5.24mm and 10.48mm respectively. Each of the differing volumes were

tested as described in Section 3.5.3 for EIS and 3.5.4 for CV.

3.5.6 Preliminary Modelling of Peritoneal Fluid

While solution A was a good starting fluid to test methods, its main disadvantage in this case is that it does not have a similar composition to the fluid that would be received from patient samples. Therefore, an attempt was made to artificial peritoneal exudate (APE) that tried to provide similar concentration of ions that would be found in patient samples to be collected was developed as described in Section 3.2.2. By creating this exudate, it would allow for better understanding of the signals that would be produced from EIS and CV testing.

In addition to testing this artificial fluid, tests were performed where the fluid was also spiked in various ways. Two components that get released during surgery are bacteria and blood. In addition, bacterial levels have been mentioned in literature to change as a result of anastomotic leakage. Therefore, it was thought that the addition of bacteria and blood and how it affects the EIS and CV results would be useful to understand, particularly with bacteria where previous studies in the group have been able to detect bacteria using EIS quicker than traditional methods. Therefore, some of the artificial peritoneal fluid was spiked with strains of *E.coli* and *P.aeruginosa*, which are bacteria present in the colon, and blood, as described in Section 3.2.7, with the aim of determining any changes at particular frequencies/voltage that could be related to the addition to these elements.

In addition, artificial peritoneal fluid made was spiked with blood by mixing 5mL of artificial fluid with 5mL of defibrinated horse blood to create a 50-50 mixture of the two fluids. Lastly, some of the artificial fluid was spiked with

bacteria and blood. This was done by spiking both artificial peritoneal fluid and blood with either *E.Coli* and *P.aeruginosa* as described in section 3.2.7 and then mixing 5mL of the spiked blood with 5mL of the spiked artificial fluid.

In total, there were 6 fluids that were tested; Artificial peritoneal fluid, artificial peritoneal fluid spiked with *E.Coli*, artificial peritoneal fluid spiked with *P. aeruginosa*, Artificial peritoneal fluid spiked with horse blood, artificial peritoneal fluid spiked with *E.coli* and horse blood, artificial peritoneal fluid spiked with *P. aeruginosa* and horse blood. Each of these fluids was added to a 24 well plate in 0.5mL volumes and were tested in a similar manner to the volume experiment. All fluids were tested using the EIS and CV testing protocols described in section 3.5.3 and 3.5.4.

3.5.7 Clinical Testing

Patient samples were collected and transported from the hospital as described in section 3.2.8. Fluids to be tested were pipetted into a 24 well plate well in 0.5mL volumes and initially tested with a pH probe prior to testing with EIS and then by CV.

Once the pH measurement was done as detailed in section 3.4, EIS measurements were done on the same sample that was tested by the pH probe previously using the EIS testing protocol as described in section 3.5.3. Once complete, the same sample then underwent a CV experiment, as described in section 3.5.4. The reason the same sample was used for pH, EIS and CV was that due to the expected low volume of fluid, there may have not been enough fluid to perform these all these tests with fresh, untested fluid (it was expected some of the samples to be less than 2mL).

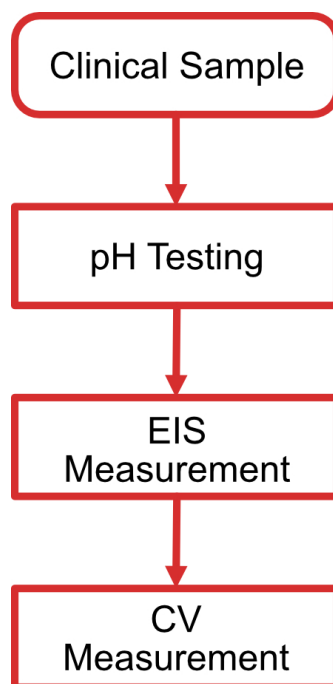


Figure 3.12: Order of testing clinical sample by pH, EIS and CV

Timed Experiment

With the last 3 samples received (Patient 19, 20 and 21), a further experiment was performed where some of the excess fluid was tested in a similar manner to the previous clinical samples but the platinum electrodes were left in the fluid, still at a fixed 7mm distance but had additional EIS measurements taken 6 and 24 hours after the initial EIS measurement. The reason for this experiment was to see if there were any biological processes occurring that may cause changes over time to the EIS signal.

3.6 Analysis

3.6.1 Outliers

In order to determine outliers in the data received from the assay data, upper and lower limits needed to be defined:

$$\text{Upper Limit} = Q3 + (1.5 \times IQR) \quad (3.1)$$

$$\text{Lower Limit} = Q1 - (1.5 \times IQR) \quad (3.2)$$

Q3 is the third quartile and Q1 is the first quartile of data. The interquartile range (IQR) is the difference between Q3 and Q1. If a data point was below the lower limit or above the upper limit, that value was considered an outlier. This outlier test was performed on for each patient day for both standardised and non-standardised data for glucose, lactate and pH data.

3.6.2 Normalisation

Previous studies have found that normalisation of data useful in identifying various components, such as bacteria, in biological substances (see Section 1.5.5) as well as making patient data more comparable. For lactate, glucose and pH results, this was done by the following equation:

$$\text{Normalised Data}_{t=n} = \frac{\text{Raw Data}_{t=n}}{\text{Raw Data}_{t=1}} \quad (3.3)$$

Where $t=n$ was the time point to be normalised and $t=1$ is the first measured data point (i.e. the result on day 1). This data normalised data was then fitted

using the various fitting functions (e.g. linear, power, etc.) on Origin where possible. The best fit was determined using regression analysis.

For EIS data, normalisation was performed as described in a patent by Connolly & Shedden (2012):

$$\text{Normalised Data}_{t=n,f=m} = \frac{\text{Raw Data}_{t=n,f=m}}{\text{Raw Data}_{t=1,f=m}} \quad (3.4)$$

Where m is the frequency of the data point.

3.6.3 Modelling

Impedance results were used to develop equivalent electrical circuit models. The theory behind this can be found in Section 2.4.1. Model fitting was performed in MATLAB. A function file was written that provided the mathematical model of an electrical circuit.

A file was then written to run a non-linear least squares model (function on MATLAB:lsqnonlin) using the mathematical function file. The least squares iteration was given lower bounds of 0 as resistance and capacitance cannot be a negative number. Prior to running the least squares, initial values were given to represent the various parameters to be determined through the algorithm. For a Randles circuit using a constant phase element (CPE), four parameters are changed; solution resistance, faradaic resistance and the capacitance and phi terms of the CPE. In this case, solution and faradaic resistance were initialised to 1Ω , capacitance was initialised to $1\text{E-}7$ and phi was initialised to 1. Due to the reasons explained in Section 2.4.1, phi is a value between 0 and 1 and constraints were added to ensure this. During iterations, calculated results were modulus weighted as described by equation 2.53.

3.6.4 Cyclic Voltammetry

In order to analyse peaks/troughs that appear in a cyclic voltammetry results, removal the non-faradaic baseline current was required. This was done in Origin using the cyclic voltammetry add-on. An example using the add-on is shown in Figure 3.13. A section is chosen to analysed (highlighted in coloured rectangles) and the program uses asymmetric least squares to find a baseline of the region of interest (Figure 3.13, middle graphs). Once accomplished, the calculated baseline is subtracted to give the only the faradaic component of the cyclic voltammetry measurement in the selected area. Peaks/troughs can be determined by finding the highest/lowest value in the region of interest.

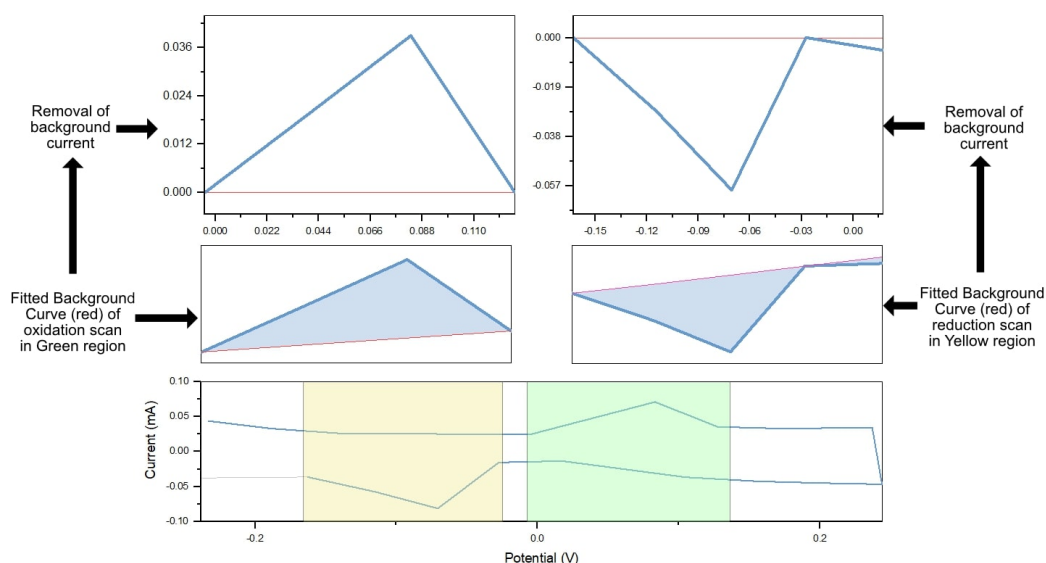


Figure 3.13: Example removal of baseline non-faradaic current using Origin

3.6.5 Bacterial Colony Counting

Colony counting of microbial species was done by the drop plate method as detailed by Herigstad et al. (2001). A series of 10-fold dilutions were performed with LB media and ten 10 μ L drops of each diluted inoculant concen-

tration was added onto LB-agar plates. Plates were then incubated overnight at 37°C. Colonies were counted at concentrations where approximately 3-30 colonies had formed (Figure 3.14).

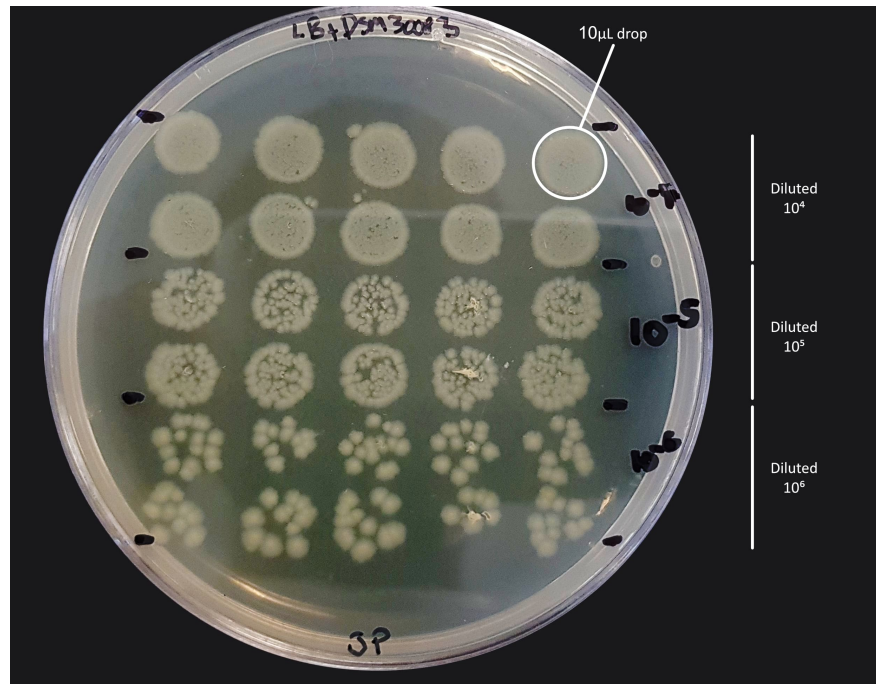


Figure 3.14: Example of colony counting of *E.coli* (DSM30083). In this case, colony counting can be done at a 10^6 dilution

Based on counting the number of single colonies and the volume placed, the colony-forming unit per mL (CFU/mL) can be calculated from:

$$\text{Bacterial Concentration (CFU/mL)} = \frac{\text{No. of Colonies (CFU)} \times \text{Dilution Factor}}{\text{Volume (mL)}} \quad (3.5)$$

3.6.6 Statistical Analysis

Line fittings were performed using Origin to determine any trends in data (Glucose, lactate and pH). In order to determine how well the lines fitted the data, R^2 regression analysis was performed. The value provided is between

0 and 1 and indicates how well the line explains the variations in data. A value of 1 indicates that the line explains all variation in data and a value of 0 indicates that the line does not explain the variation in data.

To determine the accuracy of the assays, the developed glucose and lactate assays were used to measure a known industrial standard. To determine whether there was a difference between the measured concentration and the stated concentration, a one-sample t-test was performed to determine significant differences ($\alpha = 0.05$).

To find differences between EIS solutions as described in Section 3.5.6, data was subjected to a two-way ANOVA test which looked for differences in data between the two independent variables that affect the dependent variable (frequency and fluid composition are the independent variables in this case). If significant differences were found ($\alpha = 0.05$), a Tukey post-hoc test was performed to find specifically where the differences occurred. For clinical EIS data, a repeated-measures ANOVA was used which looked differences in data. The repeated-measures model was used to take into account that data was related to different patients.

3.7 Summary

In this section, the methods and materials used to investigate potential ways to detect anastomotic leakage using glucose, lactate and pH biomarkers as well as using diagnostic electrochemical methods (EIS and CV) have been described. In the following sections, the results based on these described methodologies are shown.

Chapter 4

Preliminary Testing

4.1 Introduction

As seen in Chapter 1, anastomotic leakage can be a harmful complication of colorectal resections. There are no universal methods currently of detecting anastomotic leakage and therefore this thesis aims to determine a way to consistently determine this complication so that clinicians can be warned at an early stage and therefore plan and provide the necessary medical management.

It was hypothesized that the best approach was to monitor drain fluid from the patient during the post-operative period due to the close proximity of the drain to the anastomosis. The proximity of the drain would capture fluid that was hypothesized to change over time as a result of healing process during the post-op period. As anastomotic leakage has been associated with incorrect healing, this should provide invaluable information in determining a method of diagnosing leakage at an early stage (Thompson et al. 2006, Bosmans et al. 2015).

Ischaemia is cited as one of the reasons for why anastomotic leakage occurs (Vignali et al. 2000, Hallböök et al. 1996) (See Section 1.5.1). As a result, some groups have looked at several biomarkers related to this, more specifically; glucose, lactate and pH. While there is some evidence that these markers could have identify anastomotic leakage, there are issues with measurement techniques that have been used which have been seen to under-estimate analytes, are not practical for clinical use or not enough information has been provided to determine its usefulness. Therefore, measurement with regards to lactate and glucose were to be done directly on the drain samples which should give a more accurate representation of changes of these markers,

which had not been done previously. While pH measurements have been done previously directly on drain samples, very little information was provided (only mean values provided for patients with anastomotic leakage). As a result, pH measurements with drain fluids in this thesis were to try provide more information that has not previously been published.

In addition, electrochemical impedance spectroscopy and cyclic voltammetry techniques were also to be utilised to monitor changes in drain fluid. These techniques has not been used previously to monitor drain fluid or anastomotic leakage. However, these techniques previously have been used to detect changes in fluids such as bacteria and urea, as well as distinguish between cancerous and non-cancerous tissues, etc (Ward et al. 2014, Halter et al. 2007, Patzer et al. 1989). It was hypothesized that changes in drain fluid over time could be detected by these techniques and changes between patients with and without leakage could be observed.

However, prior to looking at clinical samples, it was best to develop methodologies to do so and test them using simulated fluids and therefore preliminary experiments were performed with the aim of testing the proposed methodologies to minimise potential experimental problems and gain better understanding of possible results that could be acquired with patient samples.

The first section of this chapter looks at characterising the glucose and lactate assays that had been modified for clinical samples to be received from the hospital (see Section 2.5 for further background). The second section of this chapter looks at the electrochemical techniques to be used and looking at effects of testing low volumes as well as better understanding what type of signal that maybe expected from the patient samples and determining the best ways of analysing these results. From these results, test methodologies

were finalised and used on clinical samples for which results are presented in Chapter 5.

4.2 Lactate Assay Characterisation

Ischaemia of tissues at the anastomotic site has been commonly cited as one of the main causes of anastomotic leakage (see section 1.4.2). In ischaemic tissues, the lack of oxygen causes anaerobic respiration to occur. Along with other processes such as cell proliferation and leucocytes combatting infections, lactate is produced as a result and accumulates. As the wound heals, angiogenesis occurs, increasing oxygen supply to tissues, causing a switch from anaerobic respiration to aerobic respiration resulting in reduced lactate production (Matthiessen et al. 2007). Monitoring this biomarker during the post-operative period was thought to be important as it has been cited that incorrect/interrupted healing causes anastomotic leakage (Thompson et al. 2006, Daams et al. 2013). This would affect lactate production occurring, which has been seen in previous work (Daams et al. 2014, Matthiessen et al. 2007, Pedersen et al. 2014) so it was hypothesized that changes in lactate levels could be related to anastomotic leakage. Unlike previous work, lactate levels were to be measured directly on drain samples using colorimetric methods. This should provide a more accurate representation of lactate levels unlike previous literature which used microdialysis tubes that have been underestimate analytes concentrations in the sampling environment (Chefer et al. 2009, Shippenberg & Thompson 1997, Turkina et al. 2017).

In order to test clinical samples for levels of lactate present, an initial methodology was proposed (see Section 3.3) and tested over a range of concentrations

up to 30mM to test the limitations of the kit. The expected range of the kit was up to 20-25mM and by going up to a concentration higher than this would allow observation of non-linearity to occur and determination of an upper limit of the modified kit (see Section 2.5.1) for further explanation). Five repeats were performed for which the results can be seen in Figure 4.1.

From the results shown in Figure 4.1, a linear relationship between concentration and absorbance was observed between 0 to 20mM with a relatively tight range of absorbance values indicating a high level of precision in this range. There was a noticeably larger range of absorbance values at 25 and 30mM with larger standard deviations being found (absorbance SD at 25mM was 0.2906 and at 30mM was 0.1518) versus concentrations lower than 25mM such as the absorbance standard deviation at 20mM being 0.0810. Due to these large variations in absorbance values at 25 and 30mM indicating a reduced precision of the assay in these ranges, it was decided that the upper limit of the lactate assay would be 20mM. Based on previous literature, it was expected that measured lactate concentration gained from clinical results would fall within this 0-20mM range. However, as there was a chance that results could be higher than this range for clinical testing, samples were diluted prior to testing and then multiplied to reflect the dilution (see Section 3.3.3). It was found later that some of the clinical samples had measured lactate concentrations of over 40mM (see Section 5.3).

Based on the upper limit of linearity that was determined from Figure 4.1, a calibration curve was fitted with all values up to 20mM (as shown in Figure 4.1 by the red line). A linear relationship was determined with the equation of the fitted line being $y = 0.1213x + 0.0092$ with the R^2 value calculated to be 0.9977. The average standard deviation of the blanks was calculated to be

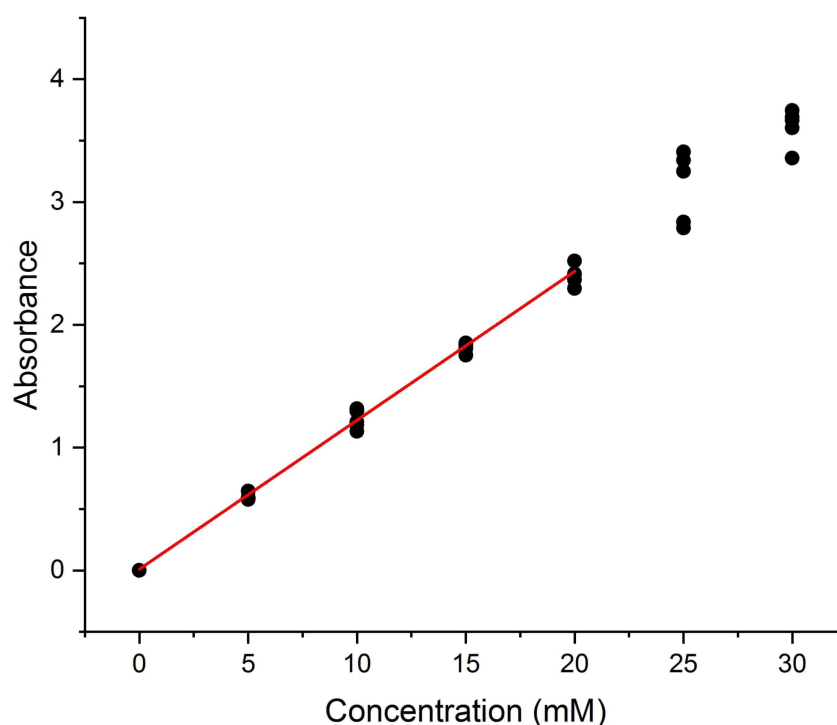


Figure 4.1: Measurements of different lactate concentrations by the photometer (n=5). Results were fitted between 0-20mM as shown by the red line

0.0001 (absorbance value). Using this value, the limit of detection (LOD) was determined to be 3.24 μ M (using the equation detailed in Section 2.5.1).

To check the accuracy of the assay, the results were used to measure a known industrially produced reference (see Section 2.5.1). The reference standard was produced by Randox and was stated to be 4.35mM.

It can be seen in Figure 4.2, using the calibration curves produced, the measured concentration of the reference sample was close to the stated value. A one sample t-test was performed to check whether the measured samples were similar or significantly different to the known concentration. It was found not to be significantly different (p-value=0.645, 95% confidence limits =4.205 - 4.550) indicating that the modified assay had a similar accuracy to a known industrially produced reference. Based on the results gained here, it

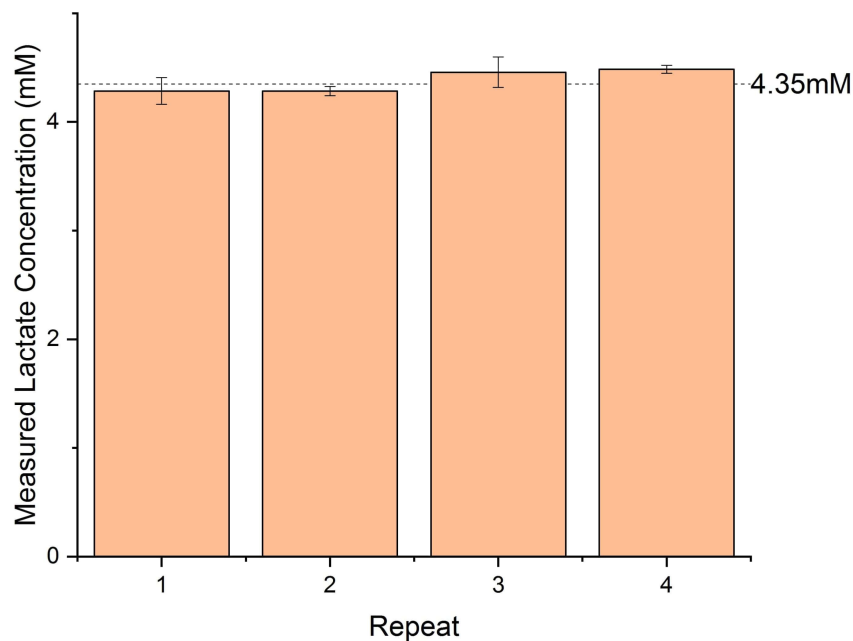


Figure 4.2: Measured lactate concentrations (mean \pm SD), using the developed lactate assay methodology, of a known industrially manufactured lactate standard (n=4 done in triplicate)

was found that the modified lactate assay developed could be used accurately for a range of up to 20mM and was considered suitable for use with clinical drain samples. To ensure samples fell within this range, it was decided that drain fluid received would be diluted and the resultant concentration would be multiplied up to reflect the dilution.

4.3 Glucose Assay Characterisation

Glucose is an important molecule involved in respiration which, in anaerobic respiration, is converted into lactate. Similarly to lactate therefore, glucose was monitored to see how its levels change with regards to the healing process and whether anastomotic leakage and/or other post-operative complications could be related to this.

An initial methodology of a glucose assay was developed and tested up to 30mM, as described in Section 3.3.2, to allow for testing of glucose in clinical samples. Like the lactate assay, the upper limit of the assay was expected to be at approximately 20-25mM. Therefore, testing past the limit at 30mM would allow observation of non-linearity and the upper limit of the assay.

Five repeats were performed, for which results can be seen in Figure 4.3. A linear relationship between concentration and absorbance can be seen up to 25mM. Between 25-30mM, it was observed that the gradient of the graph changes and there was a more noticeably larger range in results with a standard deviation of 0.0534 at 30mM versus at 25mM with a standard deviation of 0.0237, so 25mM was decided to be the upper limit of the kit indicating a reduction in precision and linearity above 25mM. The standard deviations from measurements 0 to 25mM were small indicating a high level of precision.

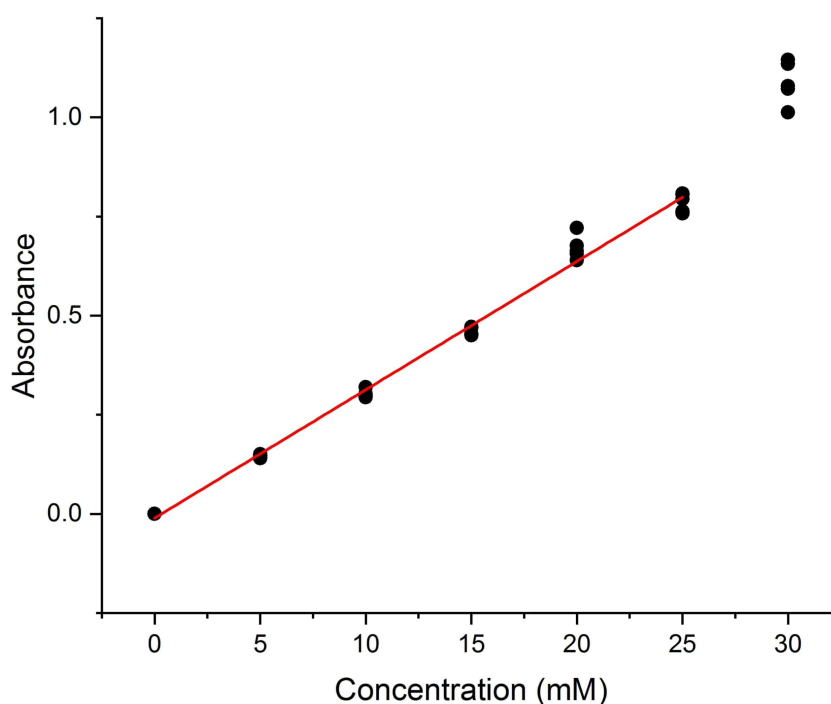


Figure 4.3: Measurements of different glucose concentrations by the photometer (n=5). Results were fitted between 0-25mM as shown by the red line

The few studies that have looked at glucose levels found that the average glucose levels in peritoneal fluid was at about 10mM, which is within the range of the kit. However, as there was the possibility glucose levels could be above the 25mM limit, clinical samples were diluted and then multiplied up to reflect the dilution (see section 3.3.3). It was later found that some of the glucose concentrations measured in patient samples were reaching a maximum of approximately 35mM.

The results were fitted between 0 and 25mM in Origin (as shown on Figure 4.3 by a red line) and a linear relationship was determined, with the equation of the fitted line being $y = 0.0324x - 0.0104$ and the R^2 value calculated to be 0.9930. The average standard deviation of the blanks was calculated to be 0.0016. Using this value, the limit of detection (LOD) was determined to be 0.67mM.

To check the accuracy of the assay, the calibration results were used to measure a known industrially produced reference standard. The reference was stated to be 5.56mM.

It was observed in Figure 4.4 that the concentration measured using the calibration curves were similar to the stated value. A one sample t-test was performed, and results were found not to be significantly different (p-value=0.254, 95% confidence limits=5.459 - 5.822) indicating that the modified assay had a similar level of accuracy to a known industrial standard. Therefore, it was decided that the modified glucose assay was suitable for clinical use for up to 25mM. To ensure clinical samples were within the range of the kit, it was decided that drain fluid would be diluted and the measured concentration would be multiplied up to account for the dilution.

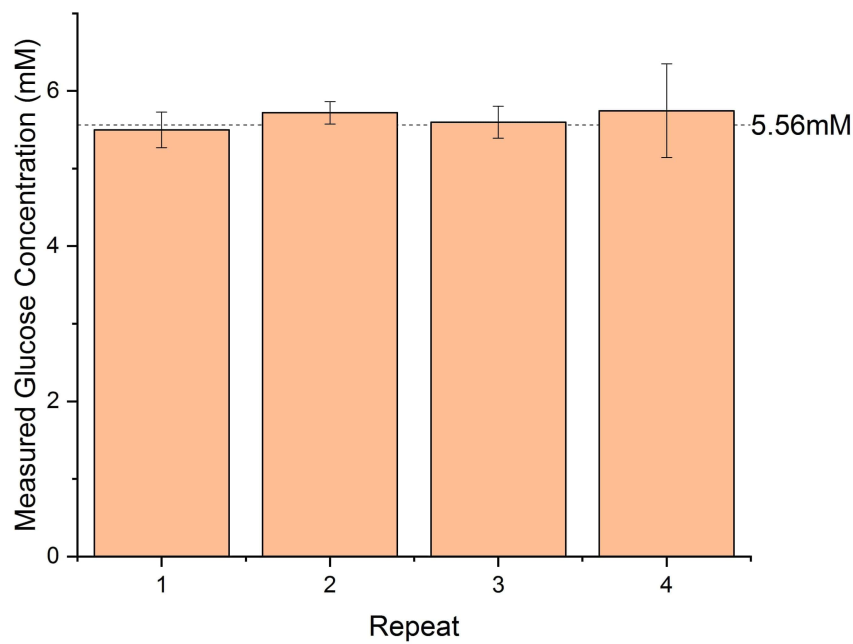


Figure 4.4: Measured glucose concentrations (mean \pm SD), using the developed glucose assay methodology, of a known industrially manufactured lactate standard (n=4 done in triplicate)

4.4 Electrochemical Impedance Spectroscopy (EIS)

Electrochemical impedance spectroscopy is a technique that has been used to understand/characterise biological systems. Previous uses have investigated, for example, identifying bacteria in samples, differentiating between cancerous and non-cancerous tissue, changes in metabolites, etc. (Ward et al. 2014, Halter et al. 2007, Gersing 1998) (see Section 1.5.5). Therefore, in this thesis, EIS was employed to try to identify the normal signal produced by patients with uncomplicated post-op and to also determine any items in the fluid that may change the signal in response to complicated post-op which has not been done previously.

4.4.1 Initial Testing with Varying Volume

Due to the proposed low volume of sample to be tested (potentially <1mL), experiments were performed to check whether results could be gained using the minimal obtainable volume and how these results would compare to higher volume samples. This experiment also gave an opportunity to test the initially proposed methodology, initially on a simple simulated fluid (Solution A - Section 3.2.1). EIS was performed on samples according to the method outlined in Section 3.5.3.

The minimum volume that covered the bottom of a 24 well plate was approximated to 500 μ L which produced of a depth of approximately 2.62mm of electrode contact. Therefore, using Solution A, 500 μ L was placed into the well and tested using the impedance technique described in section 3 (see Figure 3.10). This was then done with 1mL and 2mL volumes (contact depth of approx. 5.24mm and 10.48mm respectively) and compared (5 repeats).

4.4. Electrochemical Impedance Spectroscopy (EIS)

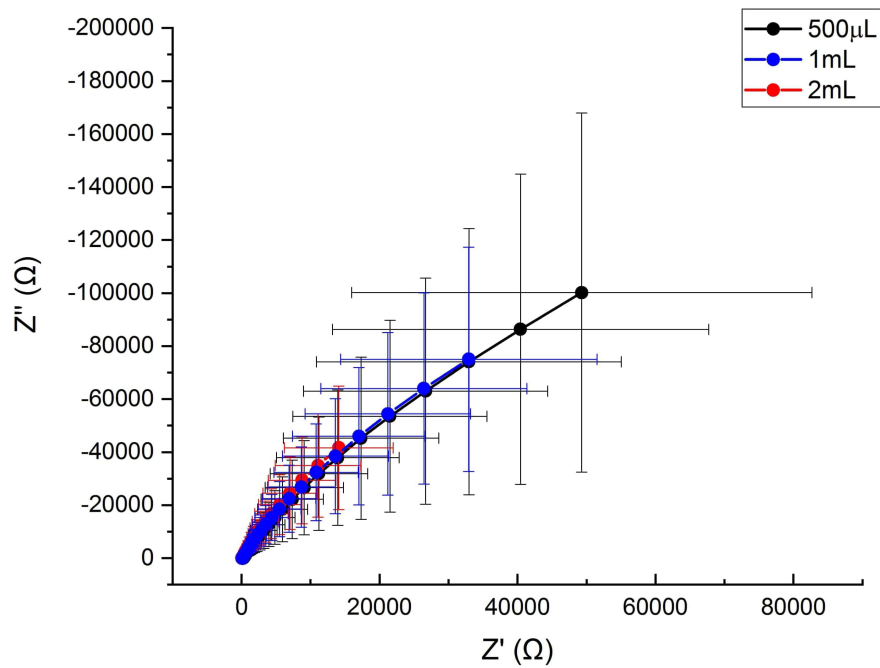


Figure 4.5: Nyquist plot of EIS measurements of Solution A with differing volumes (n=5, mean \pm SD)

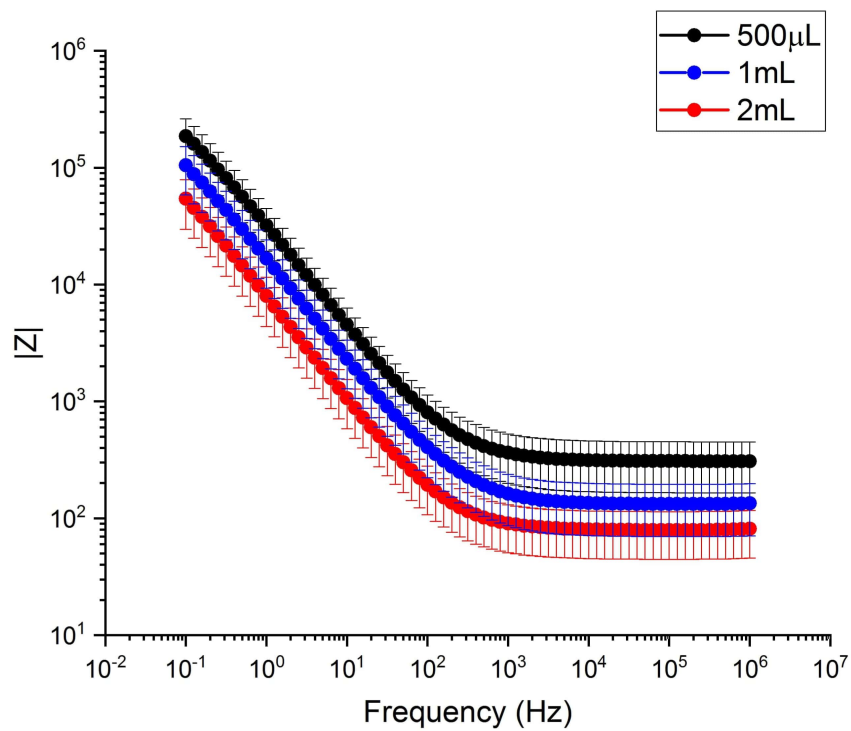


Figure 4.6: Modulus plot of EIS experiments of Solution A with differing volumes (n=5, mean \pm SD)

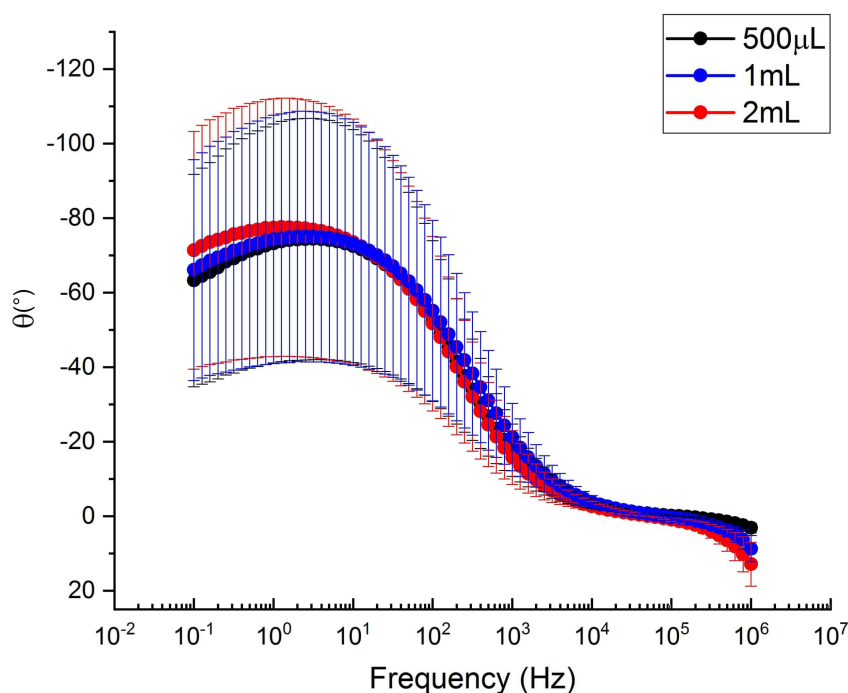


Figure 4.7: Phase plot of EIS experiments of Solution A with differing volumes ($n=5$, mean \pm SD)

It was observed in the resultant Nyquist (Figure 4.5) and bode plots (Figure 4.6 and Figure 4.7) that variations due to change in volume occurred. An increase in volume was associated with reduced Z' and Z'' , particularly with increasing frequency. In addition, a reduction in $|Z|$ was noticed with increasing volume that seemed to be relatively linear where, versus the 2mL volume, the increase in modulus in 1mL measurements were about 1.5-2 times higher and 3.5-4 higher in 0.5mL measurements. An increase in phase angle was also found with increased volume at lower frequencies ($<10\text{Hz}$) and a decrease at higher frequencies ($>10\text{Hz}$). These changes can be associated with a changing contact area with the electrodes (Trasatti & Petrii 1991) and indicated the need for a fixed contact surface. As a result, volumes used were fixed to 0.5mL when testing clinical samples (see next chapter). During the period when clinical measurements were performed, it was found that the minimum

volumes recorded were in the region of 1-2mL.

4.4.2 Artificial Peritoneal Exudate (APE)

In order to understand better what electrical behaviour may be exhibited using EIS in drain samples, a more complex artificial peritoneal exudate (APE), containing elements found in peritoneal fluid, was created as described in Section 3.2.2. As bacteria and low levels of blood contamination of clinical samples were expected to be the main cause of variation in clinical samples, samples of APE were also spiked with horse blood (HB) and 2 types of bacteria (*E. coli* strain DSM30083 and *P. aeruginosa* strain PA14), which have been found in previous studies, to help understand how the signal detected would be affected. Further details of the methodology can be found in Section 3.5.3. The average bacteria concentration added was 5.18×10^6 CFU/mL for PA14 and 6.88×10^6 CFU/ml for DSM30083 which was $>10^6$ CFU/mL that Fouda et al. (2011) found in patients with anastomotic leakage.

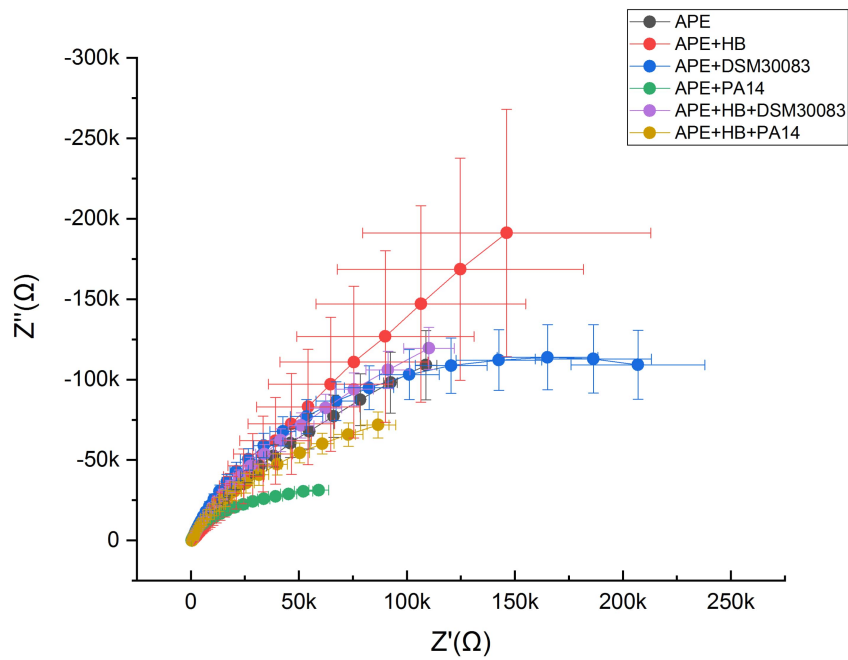


Figure 4.8: Nyquist plot of spiked artificial peritoneal exudate (APE) with horse blood (HB), *P. aeruginosa* (PA14) and *E. coli* (DSM30083). Mean \pm SD, n=4

Figure 4.8 shows the Nyquist plot of the averaged results of spiked solutions of APE (n=4). The addition of the various components caused observable variation in resistance and reactance as shown in Figure 4.8. ANOVA analyses were performed with Tukey post-hoc test which found significance between the differently spiked solutions in both resistance and reactance over different regions of frequency and this can be seen in Figure 4.9.

4.4. Electrochemical Impedance Spectroscopy (EIS)

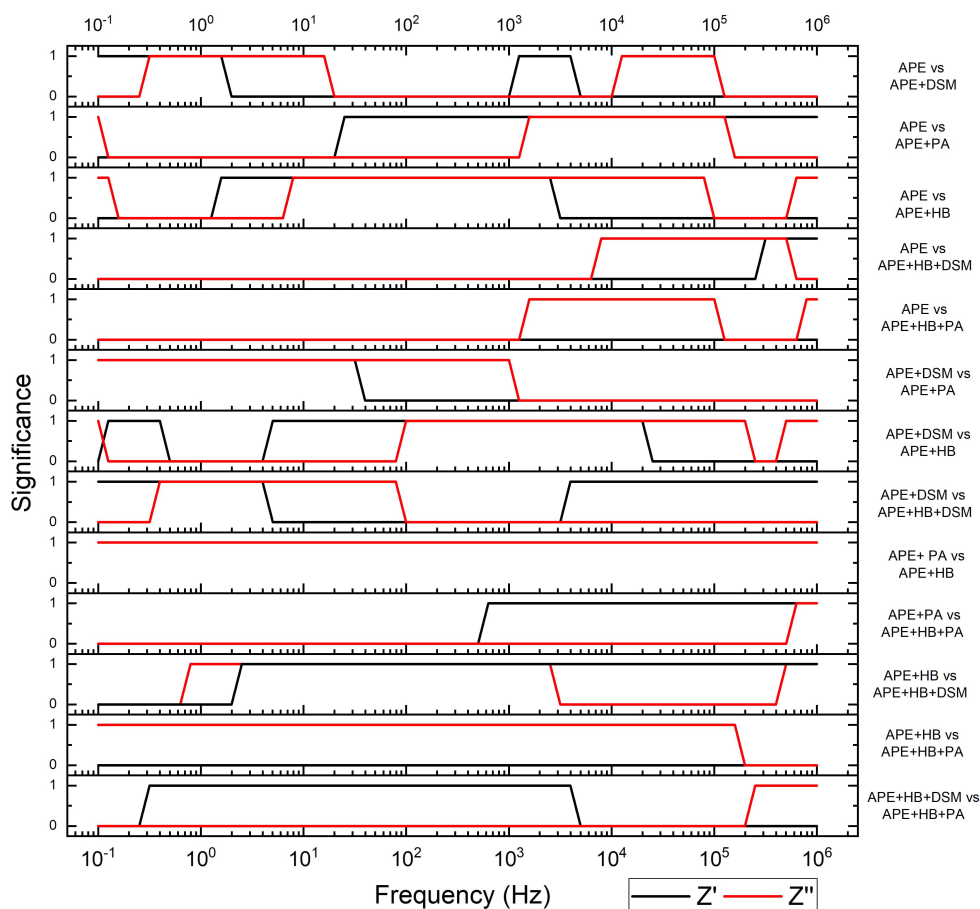


Figure 4.9: Graph showing significant differences between fluid spiked with horse blood(HB) and bacteria, *P. aeruginosa* and *E. coli*(DSM30083), over a frequency range of 0.1 and 1MHz

P. aeruginosa can be seen to cause a reduction in resistance and in reactance in Figure 4.8. When comparing the unspiked fluid to the fluid spiked only with PA14, there is a significant drop in resistance between $\approx 300\text{Hz}$ - 10^6Hz as well as a significant drop in reactance between ≈ 2 - 10^5Hz (Figure 4.9, Graph 2). For example, at 10kHz, the average resistance and reactance values of APE were 616.94 and -77.74Ω and for APE with PA14 was 417.96 and -15.199Ω . This could be explained by the fact that PA14 produces substances that are known to improve electron transfer, thus lowering both the resistance and re-

actance (Ali et al. 2017, Bosire et al. 2016).

Unlike *P. aeruginosa*, the presence of *E. coli* in the artificial fluid caused observable increases in resistance and reactance. For resistance, when comparing APE to APE spiked with DSM30083, an increase emerged in mid to low frequencies, significantly so at approximately 1000-4000Hz and 0.1-1.5Hz (Figure 4.9, Graph 1). For instance, at $\approx 2500\text{Hz}$ the average resistance of APE was 685.43Ω and the resistance of APE with DSM30083 was 544.96Ω . A matching trend was also seen in reactance values, though this was significant at relatively higher frequencies ($\approx 12\text{-}100\text{kHz}$ and $\approx 0.3\text{-}15\text{Hz}$). For example, at 100kHz , APE had an average reactance value of -22.63Ω whereas APE spiked with DSM had a value of -2.79Ω .

The addition of blood to the fluid caused significant increases over a large range of frequencies in resistance ($\approx 1.6\text{-}2500\text{Hz}$) and reactance ($\approx 10\text{-}80,000\text{Hz}$) versus a solution of just APE (Figure 4.9, Graph 3) as witnessed in Figure 4.8. This increase is much larger with decreasing frequency and can be explained by the fact that blood tends to adsorb onto surfaces (Gingell & Fornes 1976).

The addition of bacteria to the solution containing blood was found to decrease the reactance, which were particularly large with the addition of PA14 with decreasing frequency, with a drop of approximately $119,334\Omega$ being recorded at 0.1 Hz when comparing APE containing blood versus APE with blood and PA14 (Figure 4.9, Graph 12). Additionally, decreases in resistance were found with addition of DSM (Figure 4.9, Graph 11).

These results indicate that monitoring of specific frequencies may be useful in identifying differing elements in the clinical fluid.

It was noticed that the solution of APE and PA14 with the addition of blood

caused the electrochemical signature to be more aligned to the signature of just APE as observed in Figure 4.8 and reduced regions of significance indicated in Figure 4.9. As mentioned earlier, PA14 produces substances that improves electron transfer (Ali et al. 2017). However, blood tends to adsorb to the surface of material (Gingell & Fornes 1976, Khubutiya et al. 2010) (the electrodes in this case) and maybe reducing the utility of the substances produced by PA14 causing the increase in resistance and reactance.

The addition of blood to APE with DSM caused the electrochemical signature to be similar to APE, as seen in Figure 4.8 with significant increases only found in small regions at high frequencies (Figure 4.9, Graph 4). Changes with the addition of *E. coli* and blood can be associated with a known interaction between the two components (Fejes et al. 2018).

Phase and modulus plots were also produced of the spiked APE and are shown in Figure 4.10 and Figure 4.11. Similarly, to the Z' and Z'' plots, ANOVA tests were done using MATLAB to find if any significance occurred at each frequency. Where significant difference occurred can be seen in Figure 4.12. It can be seen in this figure that multiple areas of significance occurs between the variously spiked fluid, for example, the addition of *E.coli* to APE gave three regions of significant difference in phase results versus the non-spiked fluid.

4.4. Electrochemical Impedance Spectroscopy (EIS)

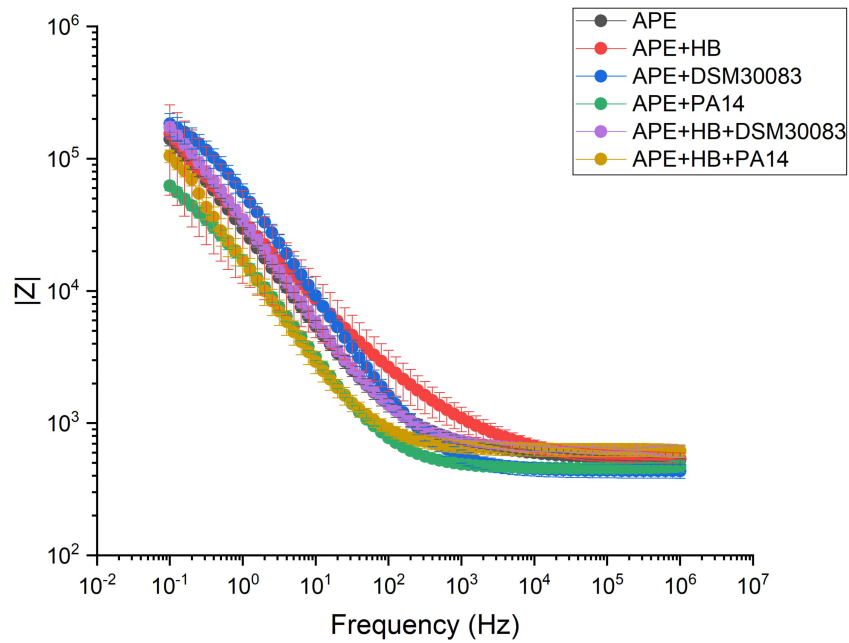


Figure 4.10: Averaged (\pm SD) modulus plot of spiked artificial peritoneal exudate (APE) with horse blood (HB), *P.aeruginosa* (PA14) and *E.coli* (DSM30083). Mean \pm SD

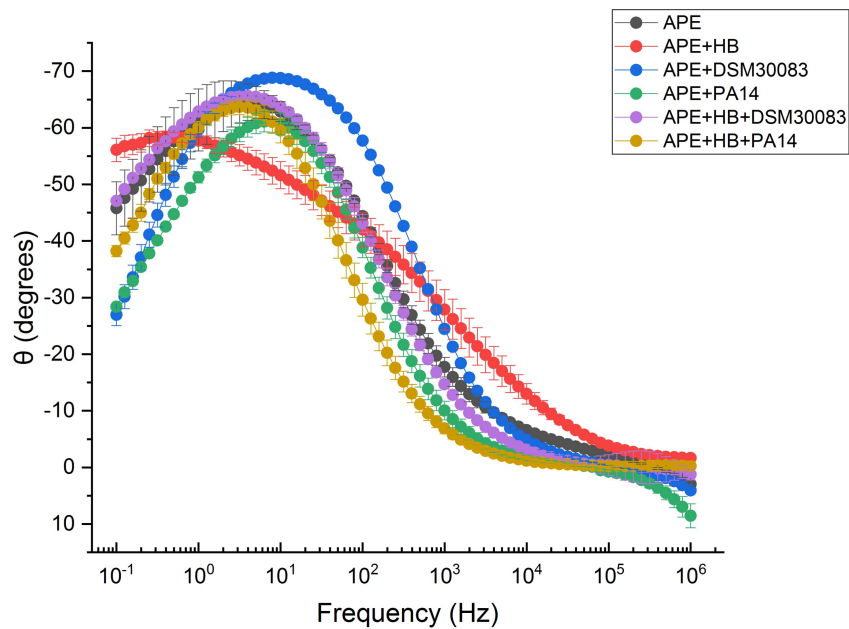


Figure 4.11: Averaged (\pm SD) phase plot of spiked artificial peritoneal exudate (APE) with horse blood (HB), *P.aeruginosa* (PA14) and *E.coli* (DSM30083). Mean \pm SD

4.4. Electrochemical Impedance Spectroscopy (EIS)

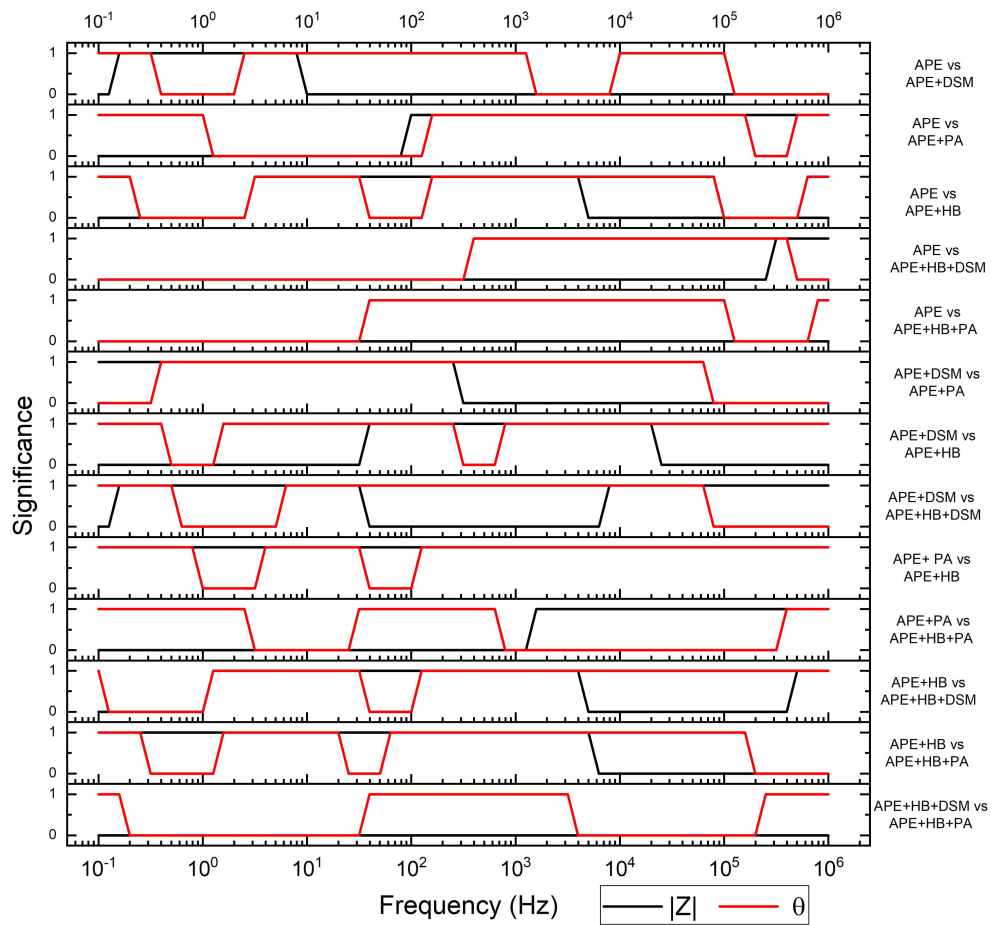


Figure 4.12: Graph showing significant differences in modulus and phase between fluid spiked with horse blood(HB) and bacteria, *P. aeruginosa* and *E. coli* (DSM30083), over a frequency range of 0.1 and 1MHz

In order for EIS to be useful technique to use for post-surgical monitoring, it must be able to distinguish between different components of the fluid it is monitoring. Examining the simulated fluid with components of blood and bacteria added in was an important step as it allowed understanding of how the signal was affected by these factors and that is it possible to distinguish between changes in the fluid composition. From the results given in this section, it can be seen that potentially looking at specific frequencies can help determine differing components like bacteria and blood. This may hold the key to allow for diagnosis of anastomotic leakage as well as potentially de-

tection and characterisation of complications. One way of better understanding and finding differences between the differing types of components is the use of normalisation techniques which is already being applied by the Medical Devices group at Strathclyde for identification of bacteria in wounds and lung sputum and is the subject of a University patent (Ward et al. 2014, 2018, Connolly & Shedden 2012).

Normalised Results

One method of observing changes that has been used successfully in previous studies (see section 1.5.5), is to normalise results versus a reference. For the results gained in this experiment, results were normalised versus the artificial peritoneal exudate that was not spiked (see section 3.6.2). Normalised modulus and phase plots are shown in 4.13 and 4.14. It can be seen in these figures that several points of interest could be attributed to the addition of various items. For example, the addition of horse blood caused a peak in the modulus at approximately 100Hz as well a peak at 10kHz in the normalised phase plot, which is unique versus the fluid spiked with other substances. Other trends that were noticed was that the addition of *E.coli* by itself would cause a normalised modulus peak at approximately 1Hz and a normalised phase peak at approximately 500Hz but the addition of blood negated the peaks of both the blood and *E.coli* may indicating a potential interaction between 2 elements.

Lastly, the addition of *P. aeruginosa* caused drops in the normalised modulus value at lower frequencies. Similar to the previous analysis with the raw data, the results given by normalisation for this experiment can allow EIS to determine the differing components of fluids (e.g. blood and bacteria) by looking for changes at particular frequencies that can be related to a particular

component. The use of normalisation also has the added advantage of making it easier/faster to pinpoint at which frequency that the largest changes occur due to a particular component such as blood at approximately 100Hz when looking at modulus.

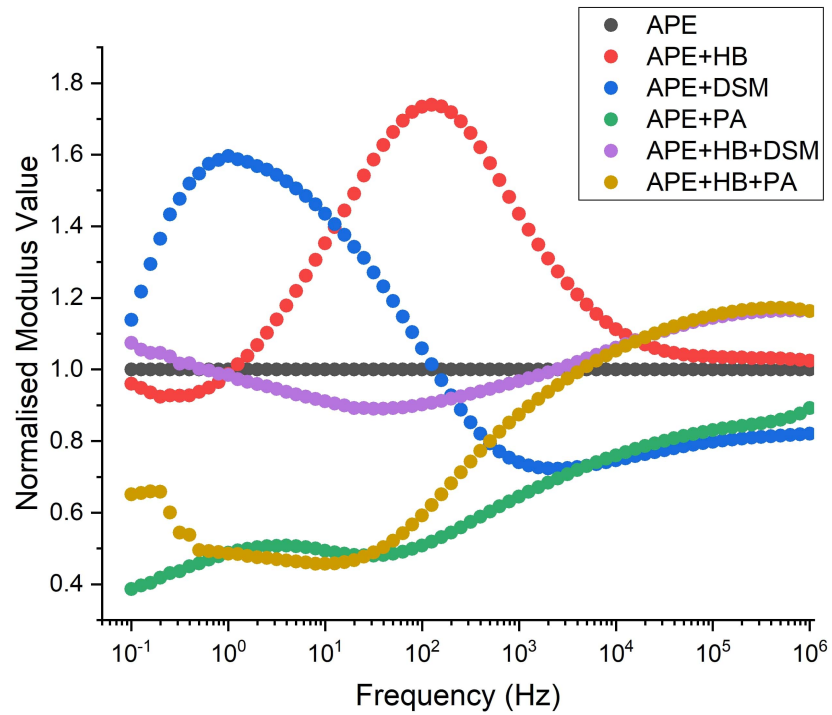


Figure 4.13: Normalised modulus results of variously spiked artificial peritoneal exudate (APE) vs unspiked APE. HB - Horse Blood, DSM -*E.coli* Strain, PA - *P.aeruginosa* strain PA14

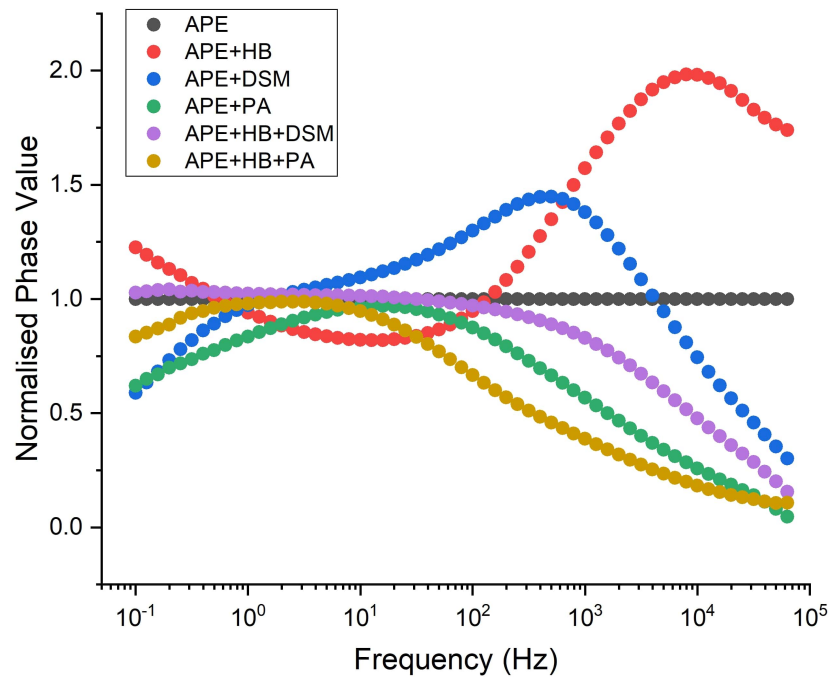


Figure 4.14: Normalised phase results of variously spiked artificial peritoneal exudate (APE) vs unspiked APE. HB - Horse Blood, DSM -*E.coli* Strain, PA - *P.aeruginosa* strain PA14

Modelling

Another way to analysis EIS results is to model the data as an electrical circuit. Attempts were therefore made to model the results obtained from the solution of artificial peritoneal fluid. Initially, a Randles model was used but was found not to fit correctly. However, by changing the capacitor in a Randles circuit into a constant phase element (CPE) (as explained in Section 2.4.1), a good fit was found when coded and approximated using MATLAB (Section 3.6.3). An example of the fitting is given in Figure 4.15.

The mathematical model of the circuit can be found in Section 2.4.1. Solution resistance, faradaic resistance, capacitance and phi of the CPE were approximated by MATLAB and are shown in Figures 4.16-4.19.

4.4. Electrochemical Impedance Spectroscopy (EIS)

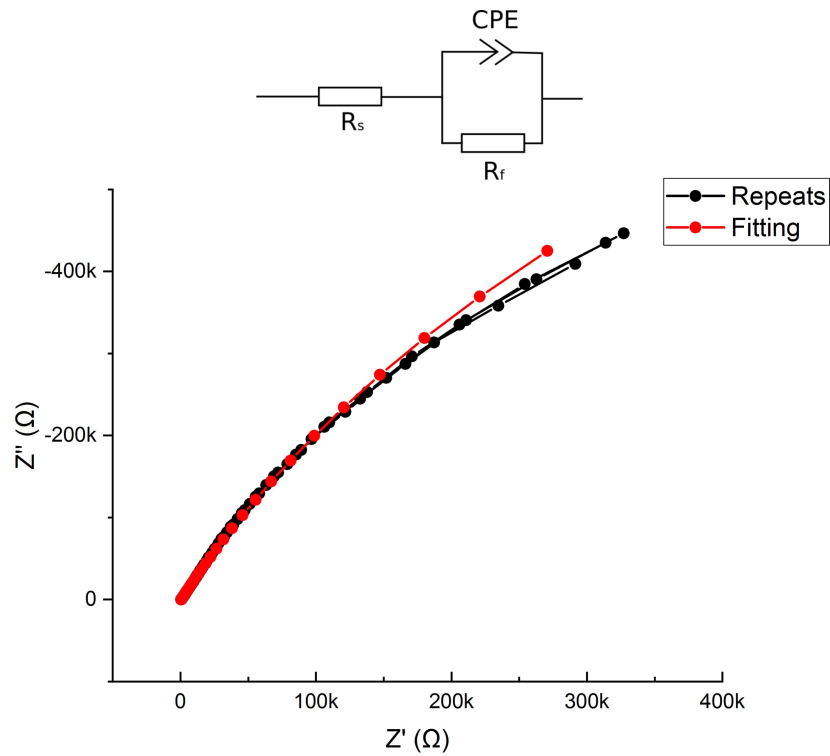


Figure 4.15: (Top) Circuit diagram of selected model of simulated fluid. R_s is solution resistance, R_f is faradaic resistance and CPE is the constant phase element. (Bottom) Example fitting of model to data gained from EIS measurement of APE + *E.coli*.

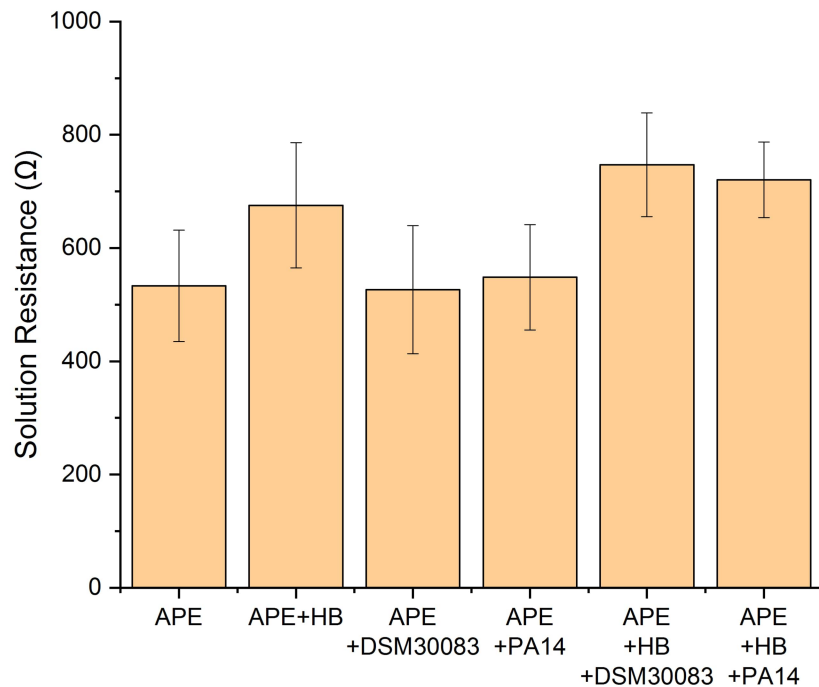


Figure 4.16: Solution resistance of spiked artificial peritoneal exudate(APE) with horse blood (HB), *P.aeruginosa* (PA14) and *E.coli* (DSM30083). Mean \pm SD, n=4.

It can be observed in Figure 4.16 that the addition of blood caused increased solution resistance. ANOVA tests were performed to find differences between the groups and found some significant changes. Tukey post-hoc tests found that APE+HB+DSM30083 was significantly different to APE and APE+DSM30083 ($\alpha < 0.05$) which potentially shows that the addition of blood and *E. coli* together may have substantial interaction with each other causing a large increase in solution resistance.

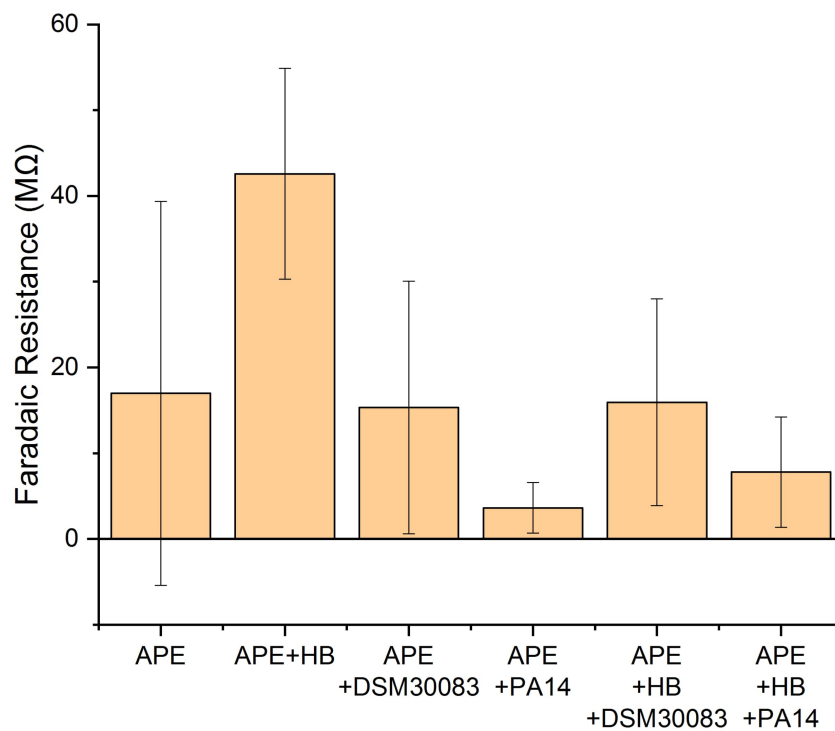


Figure 4.17: Faradaic resistance of spiked artificial peritoneal exudate(APE) with horse blood (HB), *P.aeruginosa* (PA14) and *E.coli* (DSM30083). Mean \pm SD, n=4.

Figure 4.17 shows the faradaic resistance of the various solutions tested. Large variations occurred as indicated by the large SD shown in the chart. Visually, PA14 seems to cause reductions in the faradaic resistance and the addition of blood causes the opposite. ANOVA analysis found significance and Tukey post-hoc tests found differences between APE+HB vs APE+HB+PA14 and APE+PA14 ($\alpha < 0.05$). This indicates that there is an effect on the electrode

by *P. aeruginosa* and is maybe able act to improve electron transfer from the solution to the electrode and thus reducing the faradaic resistance whereas the addition of blood has the opposite effect.

Figures 4.18 and 4.19 show the CPE capacitance and phi values of the various solutions. Though PA14 seemed to cause an increase, ANOVA tests found no significance in CPE capacitance between groups. However, significance was found in phi values and Tukey showed a difference between APE+HB versus APE+HB+PA14 and APE+PA14 ($\alpha < 0.05$). Phi is a value that indicates how capacitive the capacitor is, where 1 indicates the component is purely capacitive, whereas 0 indicates a purely resistive component. This indicates that the addition of blood (reducing the phi value) causes the electrode to behave more like a resistor whereas the addition of PA causes the electrode to act more capacitively.

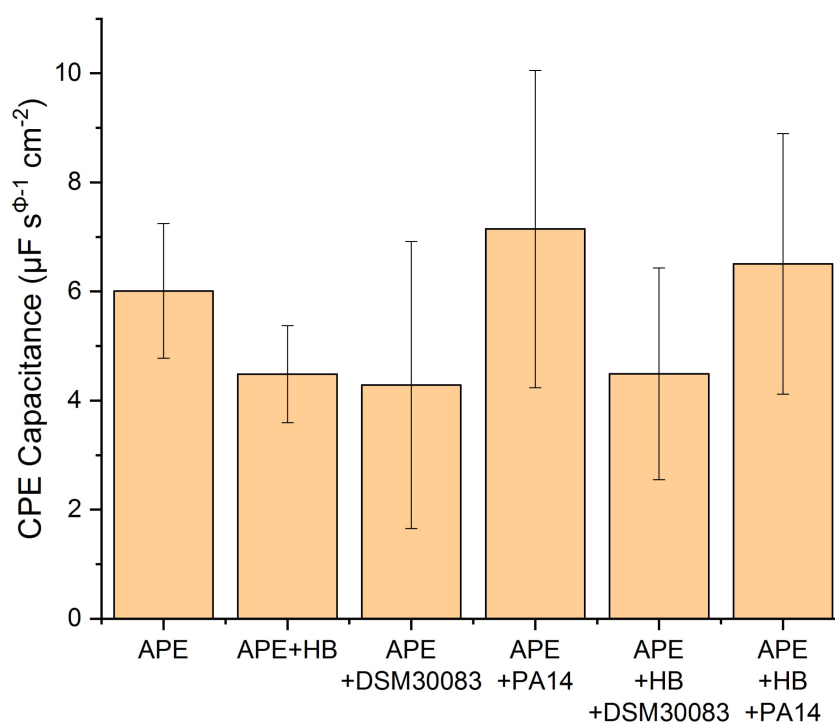


Figure 4.18: Capacitance term of CPE of spiked artificial peritoneal exudate(APE) with horse blood (HB), *P.aeruginosa* (PA14) and *E.coli* (DSM30083). Mean \pm SD, n=4.

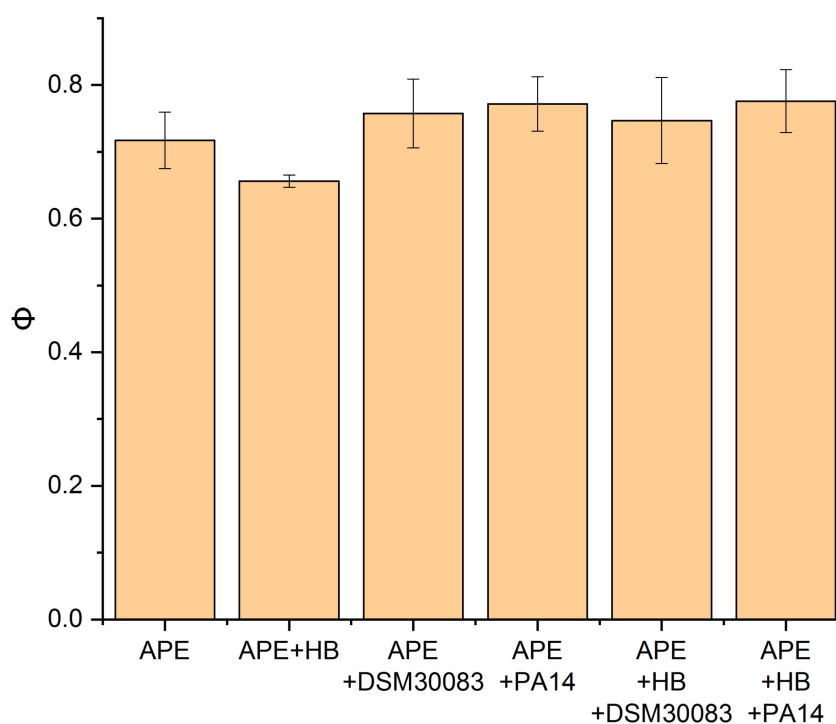


Figure 4.19: Phi (ϕ) term of CPE of spiked artificial peritoneal exudate(APE) with horse blood (HB), *P.aeruginosa* (PA14) and *E.coli* (DSM30083). Mean \pm SD, n=4.

In summary, EIS has been used previously to identify and understand biological systems. In this section, preliminary tests were performed to see how useful EIS could be in understanding the clinical fluid that was to be received from the fluid. Results show the need to maintain a fix volume of fluid to make results comparable as well as show that EIS can be used to determine/distinguish between differing elements of the fluid and an indication of how to run the analysis to reveal this information.

4.5 Cyclic Voltammetry

Cyclic voltammetry is a technique used to identify and investigate redox reactions as well as electron transfer reactions in a substance (see Section 2.4.1) and was used to see whether it was possible to identify any reactions that

could be associated with post-operative complications.

4.5.1 Initial Testing

As mentioned in the previous electrochemical impedance section, the volume of patient samples to be collected was expected to be minimal (<2mL). Increases in volume cause increases in the contact area of the electrode which in turn causes the current to increase as a result. In order to understand the limits of the measurable current that would occur in a scan, cyclic voltammetry was performed on volumes of 0.5mL, 1mL and 2mL with scan rates of 25, 50 and 100mV/s. Further details on the methodology can be seen in Section 3.5.5. Results were analysed as described in Section 3.6.4.

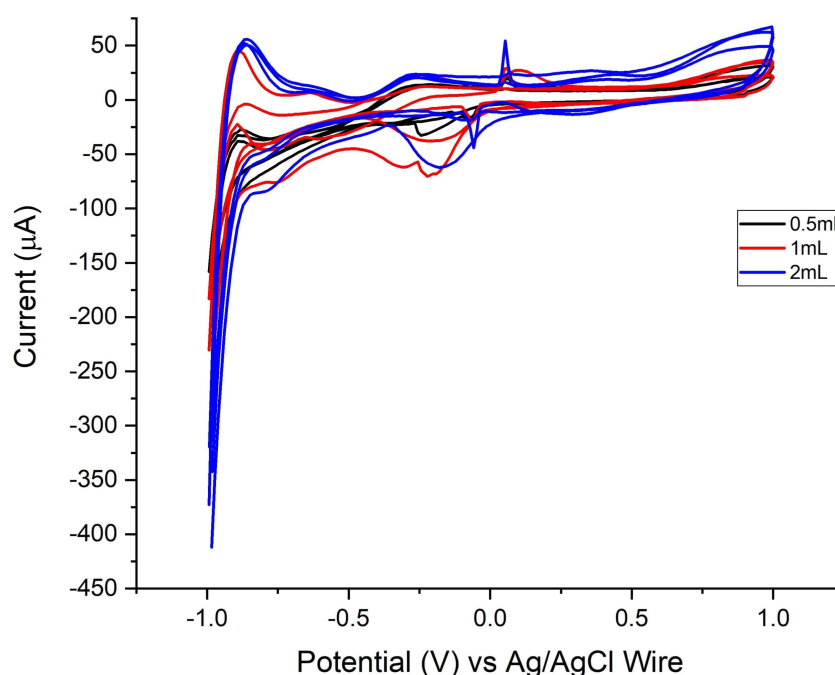


Figure 4.20: Cyclic Voltammetry of Solution A with different volumes in a 24 well plate. Scan rate of 25mV/s (n=3)

A couple of peaks can be seen in the results (Figure 4.20). The most notable is at -0.25V where a reduction peak can be seen which can be attributed in

adsorption onto platinum. There was also a reversible peak on one of the 2mL repeats at approximately 0V which can be associated with oxidation and reduction of CO₂. A large negative current occurred at potentials lower than approximately -0.8V. This change can be associated with the disassociation of water. Changes due to differing scan rates were not seen but the increase in volume did cause increases in current as expected, particularly in identifying peaks such as the reversible peak at approximately 0V. However, due to the expected lack of volume from samples from patients, it was decided that 0.5mL would be the volume to be used for clinical testing. It was found later that minimum amount received from patients were in the range of 1-2mL.

4.5.2 Artificial Peritoneal Fluid

Cyclic voltammetry was performed with the simulated fluid to see if any reactions could be captured by the technique and determine any regions of interest for clinical samples. Samples were cycled from -1V to 1V at 25, 50 and 100mV scan rates (section 3.5.6 for more details). Other than the disassociation of water at potentials lower than approximately -0.8V, no distinct peaks or substantial changes could be determined with the attempted removal of the baseline non-faradaic current (Figure 4.21), as described in Section 3.6.4, or with changes due to differing scan rates. This is not entirely surprising and is most likely caused by the complex environment of the fluid with interactions between ions, bacteria and blood that could be masking any signals from appearing. However, it was suggested early in the study that electrochemical scanning or single point potential sensors maybe unlikely to be useful for clinical monitoring due to this complex environment.

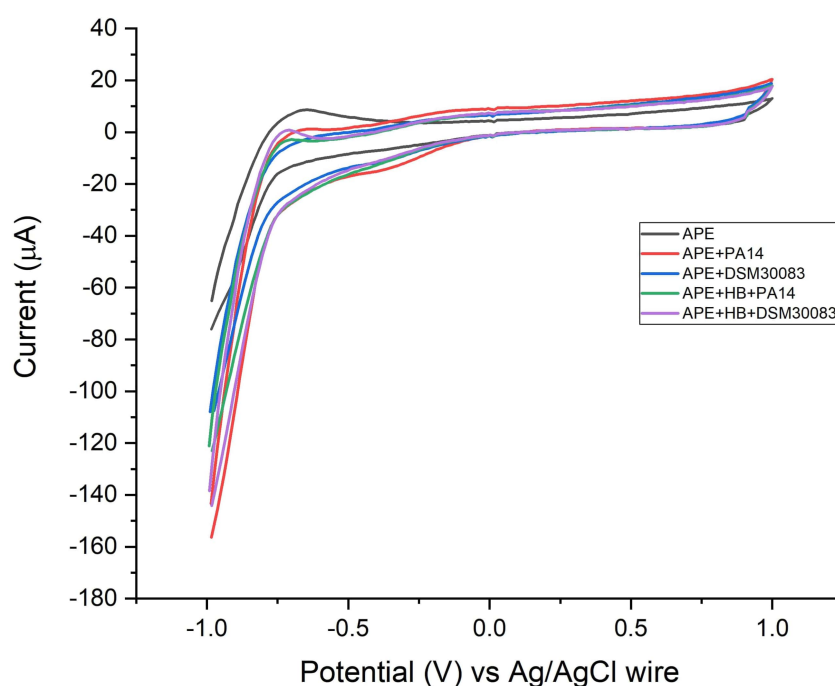


Figure 4.21: Cyclic Voltammetry (25mV/s scan rate) of variously spiked samples of artificial peritoneal exudate(APE) with horse blood(HB), *P.aeruginosa* (PA14) and *E.coli* (DSM30083)

4.6 Summary

In this chapter, preliminary tests were performed to develop methodology to measure glucose and lactate as well as looking at the usefulness of EIS and cyclic voltammetry for use in clinical samples. Both the glucose and lactate assays were characterised successfully for use in clinical patient samples. EIS testing showed promising results with some ability to distinguish between differing components of the fluid, such as blood and bacteria, which would be useful in the use of post-operative monitoring of patients to determine any complications such as anastomotic leakage. On the other hand, cyclic voltammetry showed to be less promising with a low ability to distinguish between differing components in the more complex model fluid. In the next chapter, clinical results are presented.

Chapter 5

Clinical Results

5.1 Introduction

The aim of this thesis was to determine a method of monitoring patients for anastomotic leakage after colorectal surgery and therefore prevent potentially serious consequences of this problem. In the previous chapter, preliminary experiments were performed to test proposed methodologies to be used for clinical samples. Based on these results, methods were finalised for use with clinical drain samples to be received from the hospital. In this chapter, the results from collecting and testing patients' drain samples during the post-op period where glucose, lactate, pH and electrochemical monitoring were performed.

5.2 Ethics and Patient Demographics

A biorepository ethics application was submitted to the West Node of the NHS Scotland Biorepository Service and was approved prior to collection of patient samples (Ref: 300, see appendix). All patients involved in the study were being treated at the Royal Alexandra Hospital and were consented by Good Clinical Practice (GCP) trained clinicians under the terms of the biorepository ethics application. Twenty-one patients were considered for the study for which drain fluids were collected and transported to the university, as described in Section 3.2.8. Three patients did not give enough sample volumes for experiments to be performed (Patients 9, 10 and 11). Therefore, a total of eighteen patients were included, with an age range of 48-78, of which the majority of patients underwent an anterior resection. Most drains were left in for 3-4 days (range: 1-6 days) with an average length of 3.33 days. The majority of patients underwent resection for cancer except for one

who underwent surgery for recurrent diverticulitis. Further details of patient demographics and procedures performed are given in Table 5.1.

Patients were checked for up to 30 days post-op for anastomotic leakage of which one patient (Patient 5) developed on post-op day 6, resulting in an incidence rate of 5.56%. However, due to an unfortunate accident, the drain was prematurely taken out by the patient after the first post-op drain sample was taken. Other post-operative conditions occurred in other patients and are noted in Table 5.2.

Table 5.1: Demographics and procedures undergone by patients included in the study

Variable	n
Sex	
Female	10
Male	8
Age	
46-55	3
56-65	3
66-75	11
76-85	1
Pre-operative Conditions	
Anal Stenosis	1
Chronic Kidney Disease - Stage 3	2
Chronic Obstructive Pulmonary Disease (COPD)	2
Coeliac Disease	1
Depression	4
Diabetic	5
Diverticular Disease	2
Gastro-Oesophageal Reflux Disease (GORD)	3
Hypertension	9
Hypothyroidism	3
Prolonged QTc	1
Reason for Surgery	
Colon Cancer	2
Recurrent Diverticulitis	1
Rectal Cancer	6
Recto-sigmoid Cancer	4
Sigmoid Cancer	5
Type of Surgery	
Abdominoperineal Resection	1
Anterior Resection	13
Extended Right Hemi-colectomy	1
Hartmann's Procedure	1
Proctocolectomy	1
Sigmoid Colectomy	1
Other Procedures	
Defunctioning Ileostomy	2
Loop Ileostomy	4
Partial Omentectomy	1
Stoma Formation	8
Laparoscopic converted to Open Surgery	1
Duration of Drain Collection (Days)	
≤2	4
3-4	12
≥5	2

Table 5.2: Post-operative complications in patients in study groups

Patient	Post-operative complications
1	Low haemoglobin levels
5	Anastomotic Leak
12	Lower respiratory tract infection (LRTI) Ileus
18	Ileus Portal vein thrombosis
19	Lower respiratory tract infection (LRTI) Ileus
21	Urinary tract infection

5.3 Lactate

Ischaemia, which is thought to occur prior to the onset of anastomotic leakage, occurs as a result of limited blood supply, and therefore oxygen, being transported to the tissue. When a reduction of oxygen occurs, tissues respire anaerobically for which the main product is lactate. The anaerobic respiration process is also thought to act as a trigger for healing processes. In addition to this, other processes such as aerobic glycolysis due to cell proliferation, inflammation and combatting of infections also produce lactate. Therefore, lactate was measured in patient drain samples to monitor its trend and to see if any deviations from these trends could be related to post-operative complications as described in Section 3.3.3 using enzymatic assays. Figure 5.1 shows the results of lactate levels for all patients.

A large range of values were measured from patients, with results generally below 30mM. A general decrease in lactate concentration was found over time with an average day one concentration of 17.06mM which dropped to 10.28mM on day 4. This trend was expected as a peak lactate concentration

should occur due to the aforementioned reasons (anaerobic respiration, cell proliferation and leucocytes combatting bacterial infections/inflammation). The reduction in lactate concentration over time occurs due to the reduction of these process as well as more tissues respire aerobically with angiogenesis providing oxygen that was previously limited, resulting in reduced lactate production.

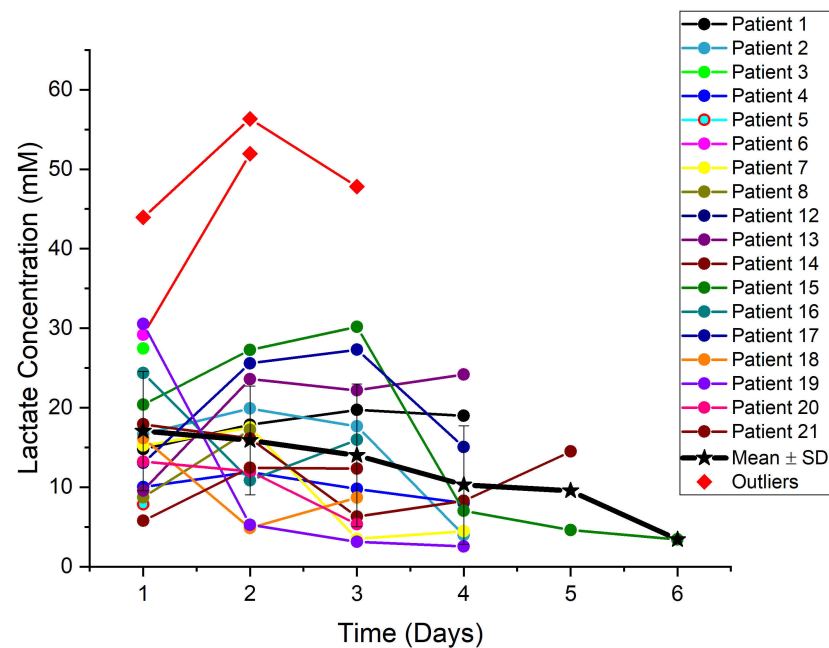


Figure 5.1: Measured lactate concentrations of patients from drain fluid. Points in red diamonds are outliers. Average line is mean \pm SD.

Patient 12 and patient 6 (on day two) were found to be outlying data, based on the equation stated in section 3.6.1, with concentrations greater than 40mM being recorded. Patient 12 was noted to have post-operative conditions of lower respiratory tract infection (LRTI) and an ileus which coincide with this high glucose level. Patient 6, on the other hand, was noted not to have any post-operative conditions so the increase in their lactate level is surprising. Whether this is anomalous or an asymptomatic event that resolved by itself is difficult to establish.

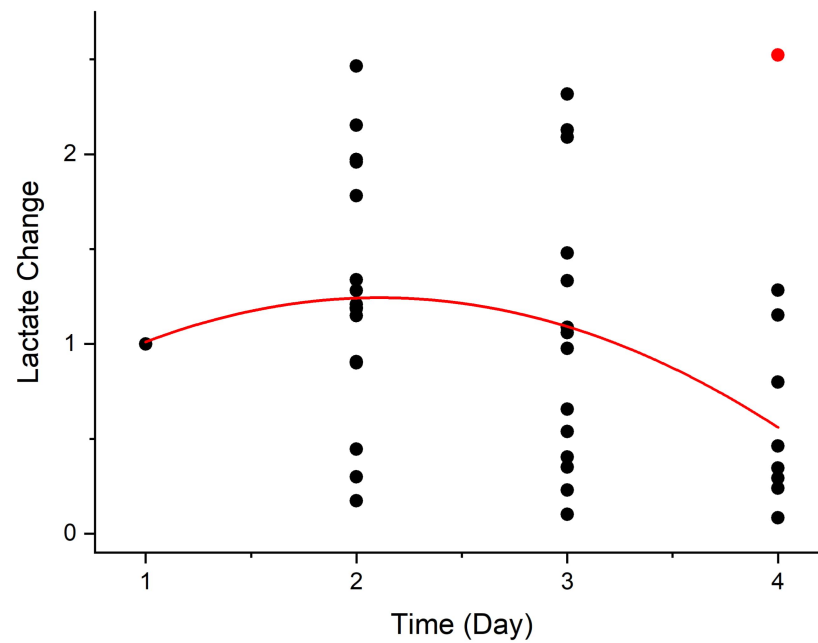


Figure 5.2: Polynomial fitting of normalised lactate results. Red line is the polynomial fitting (order=2) of the results ($R^2=0.145$) Outliers (patients 6 and 12) not included in the analysis

Patient data was normalised, as described in Section 3.6.2, to allow for comparison between patients and a trend line was fitted (represented in Figure 5.2 by red line) in the form of:

$$y = A + Bx + Cx^2$$

A quadratic fitting equation was used as it was expected that lactate levels would accumulate soon after surgery as a consequence of damaged tissues producing lactate through anaerobic respiration. As healing of the wound continues, angiogenesis occurs resulting in tissues respiring aerobically meaning reduced lactate production (Trabold et al. 2003).

The fitting results gave $A=0.3945$, $B=0.8057$ and $C=-0.1912$. The R^2 value of the fitting was found to be 0.145, indicating a weak trend and suggests that lactate

may not be a suitable method of detecting post-operative complications due to its high variability between patients.

To ensure that no large items ($>0.22\mu\text{m}$ e.g. red blood cells) interfered with the assay, samples that were filtered (from patient 13 onwards) were also measured for lactate concentration but no significant differences could be found between filtered and unfiltered samples ($p>0.39$) indicating these large molecules did not affect the assay.

Lactate Summary

Lactate in drain fluid was found to drop in concentration over time after an initial peak at the beginning of the post-op period, for which this trend that can be related to the reduction of healing process over time. However, this was found to be a relatively weak trend due to the large variability between patient lactate levels. No differences were found between the unfiltered and filtered samples meaning that none of the large molecules removed (red blood cells, bacteria, etc.) interfered with the assay.

5.4 Glucose

As mentioned previously, ischaemia is one of the most cited reasons for anastomotic leakage (see section 1.4.2). Glucose is main molecule involved in the respiration process and documenting its changes with regards to the healing process was thought to be worth monitoring to see if there were any deviations that could be related to post-operative complications.

5.4.1 Unfiltered Samples

Glucose concentrations of patient drain samples, once received from the hospital, as described in Section 3.2.8, were measured using an enzymatic assay that was characterised in Section 4.3. Further details of the methodology used can be found in Section 3.3.3.

Figure 5.3 shows the data gained from glucose measurements of patient drain samples over time. It was found that glucose concentrations generally drop over time post-surgery with an average concentration of approx. 9.75mM on day 1 falling to 2.17mM on day 4, a reduction of approximately 78%. An increase from day 4 to 5 in mean concentration was observed before a drop on day 6 but with few samples in this region (n=2 on day 5 and n=1 on day 6), it cannot be reasonably assumed that this is representative of glucose concentrations for these days. This peak of glucose during the early post-operative stage could be due a stress-response due to the trauma of surgery causing effects on normal metabolic/hormonal processes increasing the levels of glucose availability which is also required for tissues to heal. The reduction of glucose levels over time could be associated to the healing process as tissues are repaired and start functioning as normal, the response due to trauma is reduced leading to lower glucose levels being found. This could be represented using either linear or power curve where a peak occurs immediately after surgery and a rapid drop occurs over time.

Several outliers were found using the equation detailed in section 3.6.1, with patients 8 and 12 having outlying results on days 2 and 3 with concentrations of 17.21mM (patient 8, day 2), 34.76mM (patient 12, day 2) and 35.15mM (patient 12, day 3), which is much higher than other results which recorded

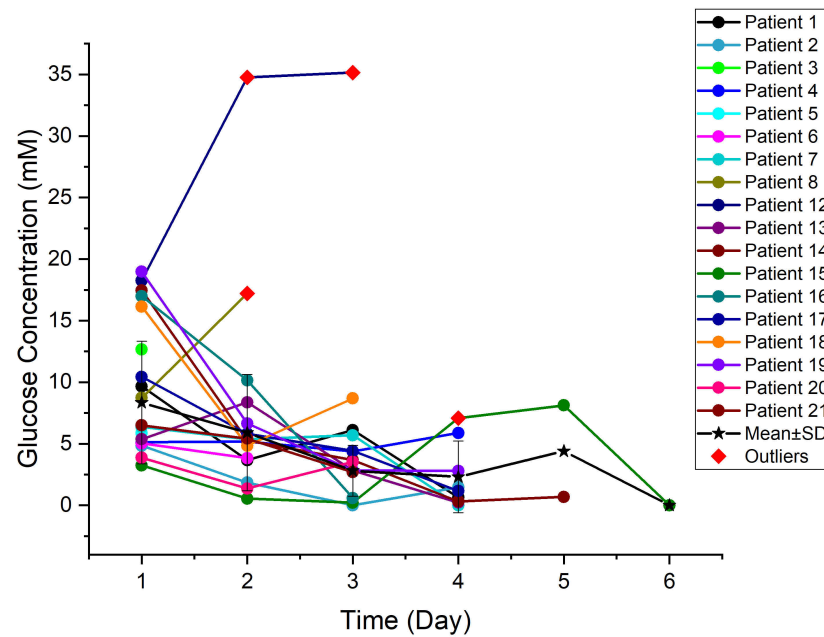


Figure 5.3: Glucose change over time for patient drain samples. Points shown as a red diamond are considered outliers. Mean±SD is of patients who did not have post-op complications.

concentrations of approximately 10mM or lower on these days. While patient 8 was noted not to have any post-operative complications/asymptomatic, patient 12 was found to have lower respiratory tract infection (LRTI) and an ileus.

Another observation was that several of the patients had an increase or plateau on at least 1 day before a reduction in glucose resumed, for example, patient 13 had a rise in concentration from 5.36mM on day 1 to 8.37mM on day 2 before glucose levels drop to close to 0mM on day 4. This could be related to the patients changing to a solid food diet. However, patient fifteen's glucose levels, while following this trend, had a substantial increase from 0.21mM on day 3 to 7.07mM on day 4, an approximately 34-fold increase, and 8.11mM on day 5, before a decrease to 0mM on day 6. Patient 15 was noted not to have any post-operative complications, though it cannot be ruled out that a minor

asymptomatic event occurred that resolved itself.

Results were normalised to the patient's day one value to allow of comparison between patients, as described in Section 3.6.2, for which the results are shown in Figure 5.4. The general downward trend was fitted excluding outliers (represented by a red line in Figure 5.4) using a linear fit of equation;

$$y = mx + c$$

Day 5 and 6 values were excluded from the fitting due to the lack of numbers on these days. Using origin, the gradient, m , was found to be -0.2881 and the intercept, c , was found to be 1.2544 . The R^2 value of the line was found to be 0.5787 indicating a moderately strong linear relationship indicating there is some relationship between time and a drop in glucose levels.

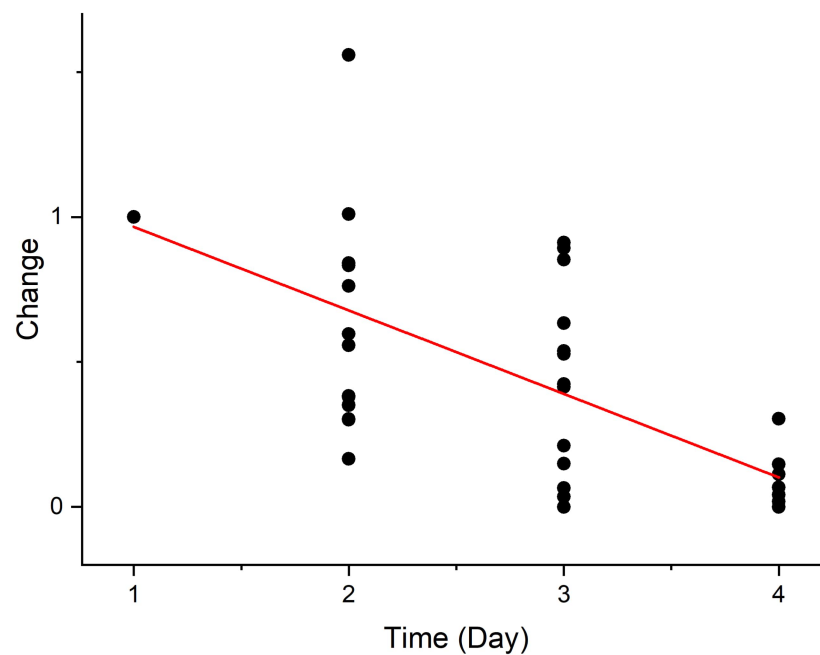


Figure 5.4: Fitting of glucose results from patient samples. Red line shows fitting of equation $y = mx + c$. Outliers (patients 8 and 12) not included in line fitting

5.4.2 Filtered Samples

After the first several patients had been tested (patient 1-12), a recurring observation was made that day 1 samples seemed to have visually higher levels of blood than that was originally expected, and when compared to other days. As red blood cells are known to interfere with the measurement of glucose levels when present in high concentrations, it was decided that testing of filtered samples should also be performed to see if there were changes in measured glucose levels. Samples were filtered by a $0.22\mu\text{M}$ syringe filter which would remove red blood cells ($\approx 7\mu\text{M}$ in size) as well as bacteria and proteins (see section 3.3.3).

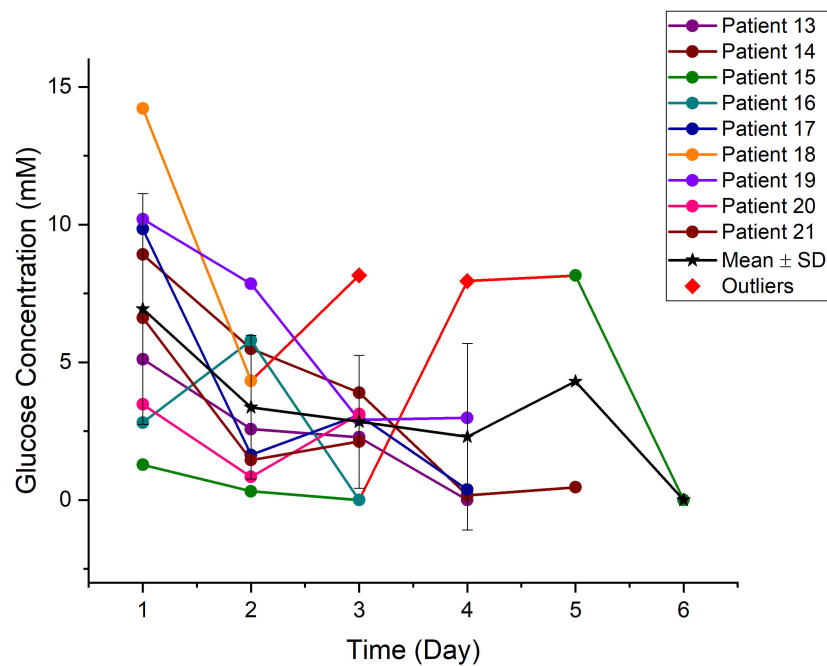


Figure 5.5: Glucose concentrations found in filtered patient samples. Red diamonds indicate points that were considered outliers.

Figure 5.5 shows the reported glucose concentrations from patient samples that were filtered prior to testing ($n=9$). A general reduction in glucose concentrations over time was observed, with an average concentration of 6.94mM

on day 1 decreasing down to 2.29mM on day 4. Differences could be observed between measurements of filtered and unfiltered samples on day 1 and were found to be significantly different ($p=0.045$) with a mean reduction of 4.06mM with the filtering of samples when one-way repeated measures ANOVA tests were performed. This supports the hypothesis that the higher levels of blood in samples on day one could be affecting measurements. Other days were found not to be significantly different.

Filtered samples were also normalised to their patient's day 1 value (as described in the methodology) and is shown in Figure 5.6. With the removal of outliers, it was found that a power curve could be fitted in the form of;

$$y = x^A$$

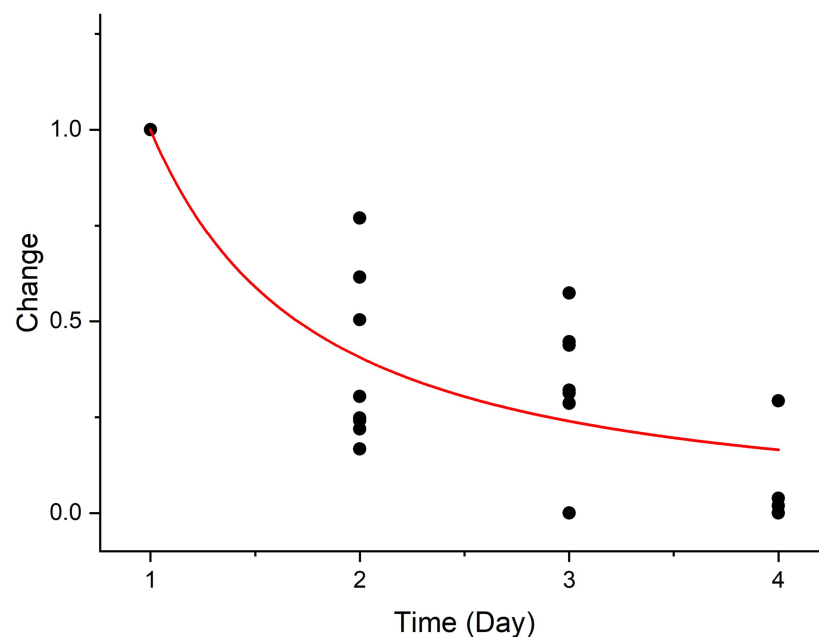


Figure 5.6: Glucose concentrations found in filtered patient samples. Outliers not included in line fitting

A power curve seemed appropriate for fitting. This was because the trauma

of surgery causes an immediate stress response that results in an increase of glucose. The glucose levels drop greatly soon after surgery due to no more surgical trauma occurring and the stress response being reduced (Duggan et al. 2017, Finnerty et al. 2013, Butler et al. 2005).

As seen in Figure 5.6, Origin was used to fit the plotted points and found A to be -1.30 (represented by a red line). The fitting was found to give a R^2 value of 0.81659 which is indicative of a strong trend. This drop in glucose levels (which was also found in unfiltered samples, figure 5.4) could be related to the healing process/surgery. As mentioned previously, the trauma of surgery causes a stress-induced response that affects metabolic and hormonal process that can cause glucose to accumulate causing the initial peak soon after surgery. As tissues heal, they start respiring aerobically and the stress-induced response is reduced resulting in a reduced glucose concentration. This strong trend in glucose reduction could potentially be useful later as it may help determine complications that may occur during the post-op period at an early stage, for example, patient 12 who had glucose levels that were considered outliers had post-operative complications. A similar trend could be established with patients with anastomotic leakage, with some previous studies that used micro dialysis tubes also noting a change in glucose between patients with and without leakage (Matthiessen et al. 2007, Pedersen et al. 2014), but as little data from patients with anastomotic leakage was gained, this could not be established here.

Glucose Summary

Glucose was monitored in drain fluid and a trend was found with the reduction of glucose over time that could be attributed to the healing pro-

cess/trauma due to surgery. In addition, it was found that measuring fluid that was filtered prior to assay testing had a significant difference in measurement of glucose concentration on samples collected on the first post-op day (most likely due to the observed high levels of red blood cells causing interference).

5.5 pH

When anaerobic respiration occurs, the resultant products cause pH levels to drop. The monitoring of this change in pH over time could potentially help understand what happens during the post-op period and how it changes with complications. Typically, the pH of peritoneal fluid is approximately 7.5-8 (DiZerega & Rodgers 1992). Measurements of pH were performed as described in section 3.4 in unfiltered (all patients) and on filtered samples (from patient 13 onwards). Results are shown in Figure 5.7 (unfiltered) and Figure 5.9 (filtered) and were normalised with respect to day 1 using the methodology described in Section 3.6.2 to allow for comparison between patients (Figure 5.8).

No obvious trends could be determined in either the unfiltered or filtered samples with most of the patients staying at approximately the same pH over the post-op period. This was slightly surprising as it would be expected, in uncomplicated post-op, that there would a slight drop in pH representing the anaerobic respiration of cell followed by an increase and plateau once cells have healed and aerobic respiration occurs as indicated in previous studies.

Several samples did drop in pH on day 3, with patients 1 and 17 dropping below a pH of 7 before a rise occurring on day 4, with patient 1 having a post-

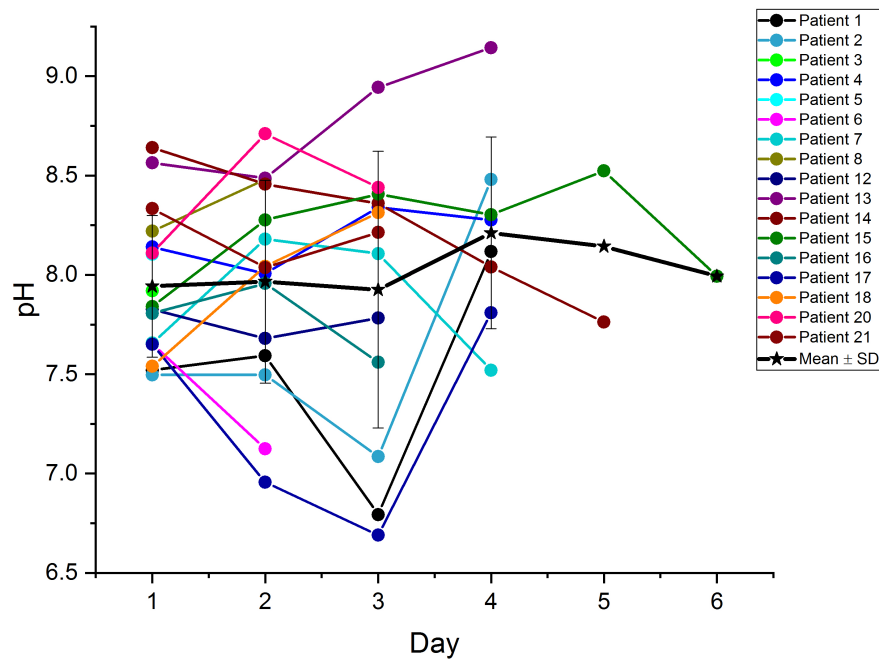


Figure 5.7: Unfiltered clinical pH results

operative complication (low haemoglobin levels) but patient 17 not having any known post-operative conditions. A larger variation of results seemed to occur on day 3, with standard deviations of 0.69 and 0.74 for unfiltered and filtered respectively. Prior and post this day, standard deviation values are <0.5 . Previous papers have mentioned that significant differences occurred on day 3 between anastomotic leakage and non-leakage patients with pH levels being lower than 7 in anastomotic leakage in one paper (Yang et al. 2013). However, in this case a healthy patient and a patient with another complication also dropped below this threshold, questioning the reliability of this threshold.

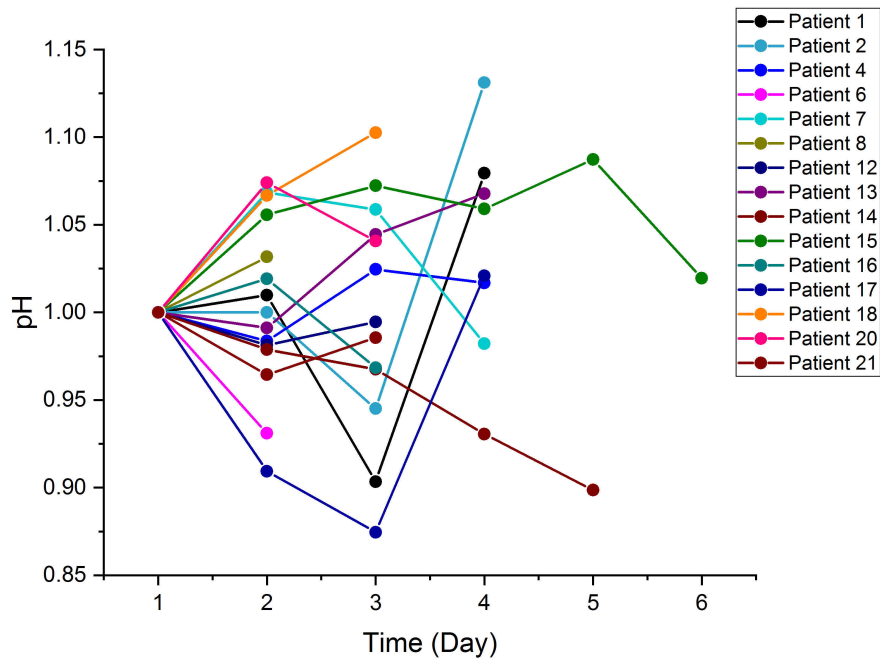


Figure 5.8: pH change versus day 1 values in clinical samples.

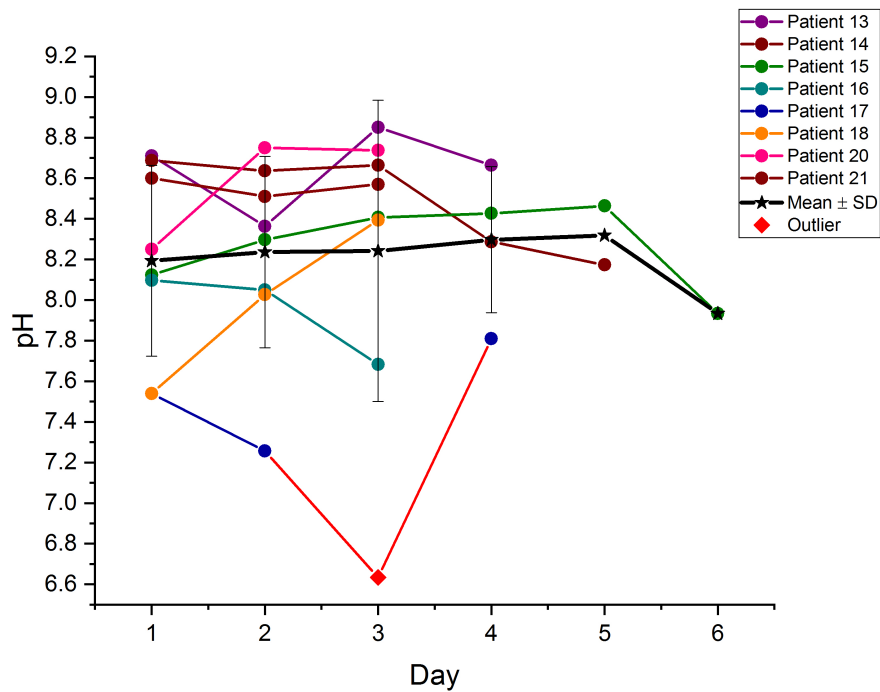


Figure 5.9: Filtered clinical pH results

It was found that day 1 samples were significantly different between filtered and unfiltered samples when 1-way repeated-measures ANOVA tests were performed (p-value=0.03689), with filtering causing a mean increase in pH of approximately 0.133 suggesting these large molecules, most likely blood which has a lower pH level (approx. 7.4) compared to peritoneal fluid, which was observed to be in high concentrations, influence the pH.

pH Summary

To summarise, pH was measured in drain fluid, but no trends could be determined. The only significant difference that was found between unfiltered and filtered samples on day 1 post-op samples indicating, most likely, that the heavy presence of blood that was observed was influencing the pH level.

5.6 EIS

EIS is a diagnostic electrochemical technique that has been used to understand/characterise biological systems such as identifying bacteria, metabolites, differing types of cells etc. (such as identifying cancerous cell) in a sample (see Section 1.5.5). This is done by applying a small potential perturbation at various frequencies and measuring the resultant response as impedance, which then can be represented on Nyquist plots (real vs imaginary impedance) or on Bode plots (magnitude/phase shift of impedance over the measured frequency) for which changes in results could be related to an element in the item of interest. Further information can be found in Section 2.4.1. EIS measurements were performed to see how the electrochemical signal of the drain fluid changed over time during the post-op period and see if any changes could be related to particular elements in clinical samples. Tests

were performed as described in Section 3.5.7 and the results are presented in this section.

5.6.1 Patients with Uncomplicated Post-op

This section looks at the drain fluid of patients who had no post-op complications.

Unfiltered Results

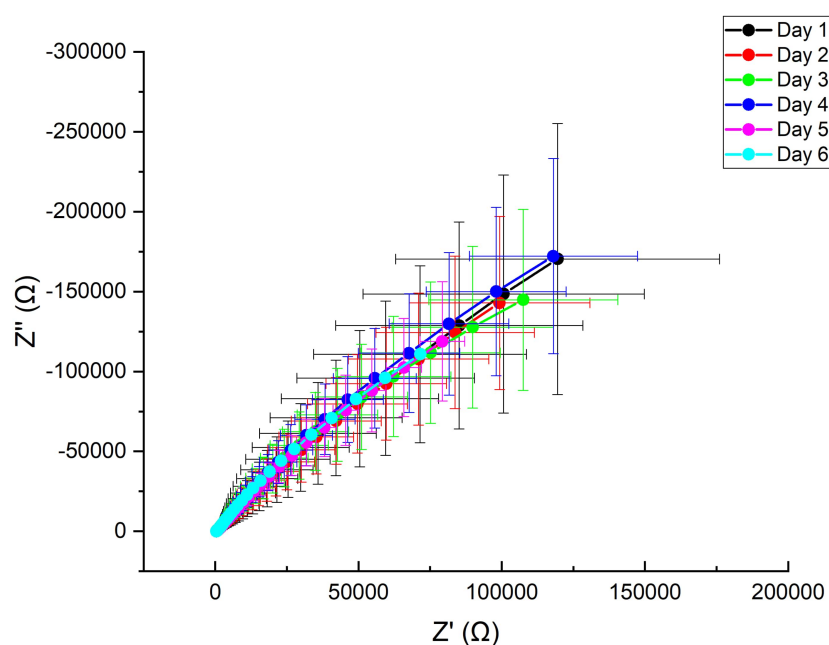


Figure 5.10: Average (\pm SD) Z' vs Z'' of clinical samples from uncomplicated post-op patients on each post-op day.

Figure 5.10 is a Nyquist plot of averaged values of all patients over time. It was observed that the EIS signature over time stayed relatively similar over time, which was slightly surprising as it was observed that the fluid composition seemed to change over time (e.g. visually higher amount of blood in day 1 samples, changes in glucose and lactate level shown in previous sections, etc.) and therefore it was thought that the results gained over time would also

change as a result.

Two-way repeated measures ANOVA tests were performed (Days 1-4), but no significant differences could be found in resistance and reactance indicating that for patients with no complications after post-op, the EIS signal stays relatively similar over time.

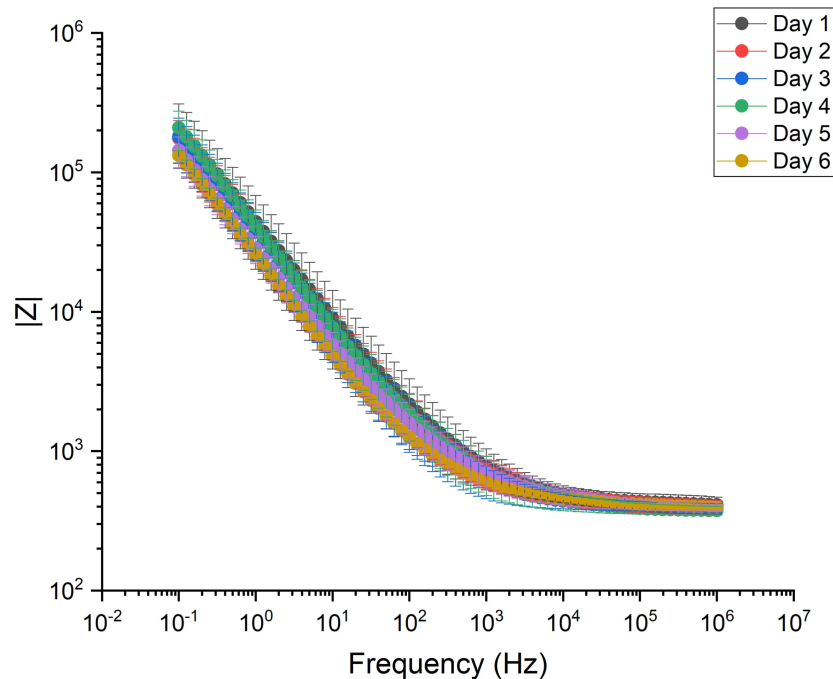


Figure 5.11: Average (\pm SD) modulus of clinical samples from uncomplicated post-op patients on each post-op day.

To see how the impedance changed as a result of frequency, bode plots were also created from the results and are shown in Figure 5.11 and Figure 5.12. Again, results between days appear to be similar, though there looked to be some separation of modulus results at lower frequencies and for phase at approximately 100Hz-10kHz. To confirm, 2-way repeated measures ANOVAs were also performed on the modulus and phase data, but no significance was found also reinforcing the point that the EIS signal stays similar over time for non-complicated patients.

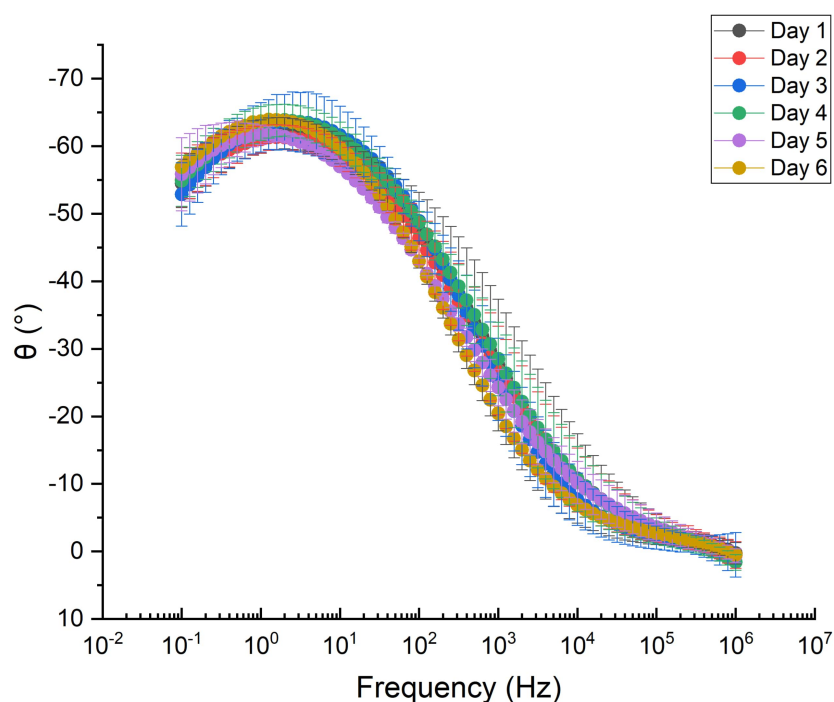


Figure 5.12: Average (\pm SD) phase of clinical samples from uncomplicated post-op patients on each post-op day.

Filtered Samples

In order to further understand how the fluid behaved electrochemically, some of the samples received from patient 13 onwards were filtered and then measured by EIS. Samples were filtered by a $0.22\mu\text{M}$ syringe filter, which was expected to predominantly remove bacteria, proteins and blood cells. The results of these measurements are shown in Figure 5.13.

Unlike samples that were not filtered, more variation over time seemed to occur, particularly at lower frequencies on day 2. Both resistance and reactance values were observed to change over time, particularly as the frequency dropped. Two-way repeated-measures ANOVAs found significant differences between some of the days at 0.1-0.25119Hz for resistance and 0.1-0.39811Hz for reactance results. The measurements of these frequencies can be seen in

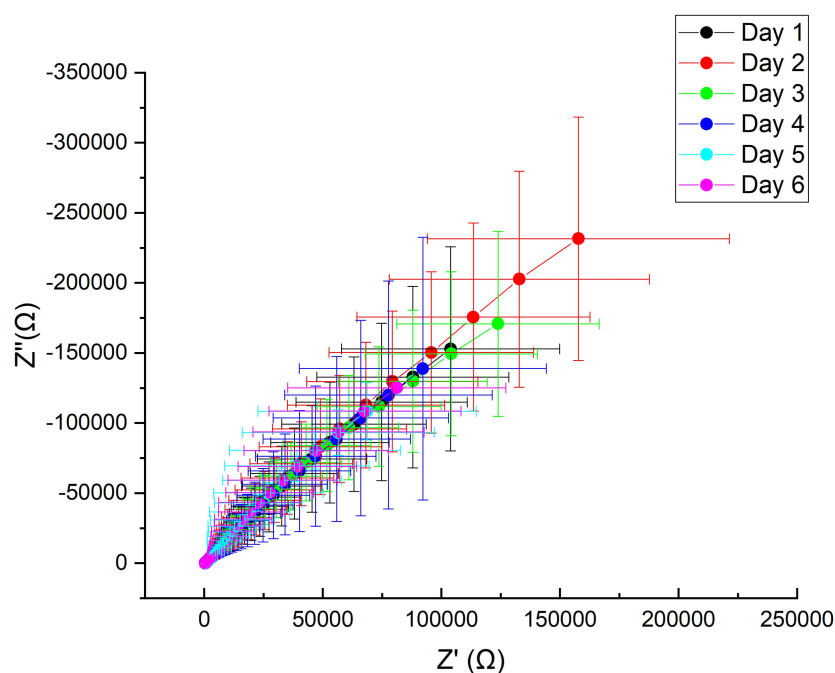


Figure 5.13: Average (\pm SD) Nyquist plot of filtered clinical samples from uncomplicated post-op patients on each post-op day.

Figure 5.14 and Figure 5.15 where an increase in resistance and reactance occurs before a continuous drop in values to a low point on day 4. An exception to this trend occurred in the resistance values at 0.19953Hz where values drop from day 1 to a low point on day 3 before increasing on day 4. At these low frequencies, changes are usually attributed to interactions of the cell membrane to its environment (e.g. metabolic changes, etc.).

Modulus and phase plots were produced and are presented in Figure 5.16 and Figure 5.17. The averaged modulus plot shows that results over time seem very similar over time though some separation could be observed at lower frequencies. Additionally, the phase plot shows some separation between day 1-4 and days 5 and 6 at mid to low frequencies (≈ 10 -10,000Hz), as well as day 4 results having a lower phase change versus the other days at low frequencies (< 1 Hz).

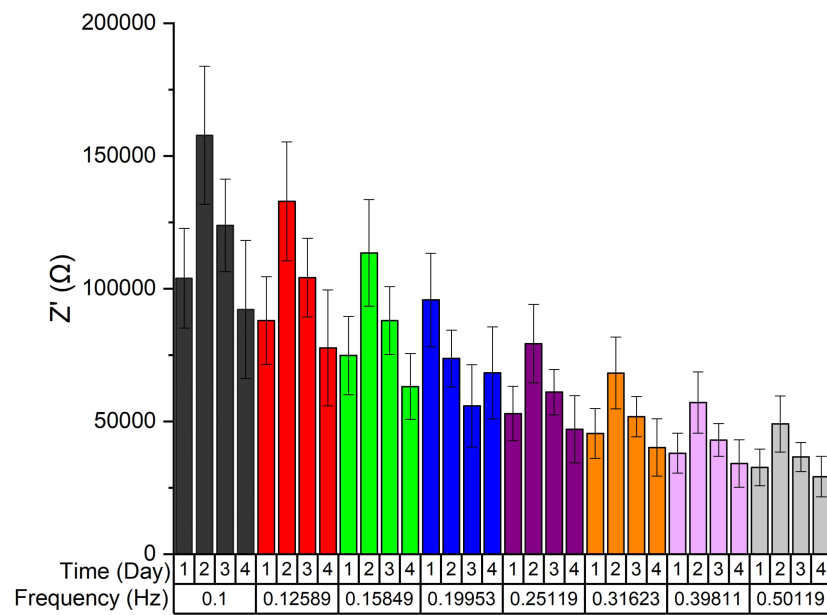


Figure 5.14: Resistance changes in regions that showed significance in filtered samples (Average \pm SE).

Once again, ANOVA analyses were performed for patients for both modulus and phase plots. Significance was found in modulus values at low frequencies (0.1-0.39811Hz) between some of the days also indicating changes in metabolites/ interactions of the cell membrane to the environment. The values of these frequencies over time are given in Figure 5.18 where modulus values increase on day 2 before dropping.

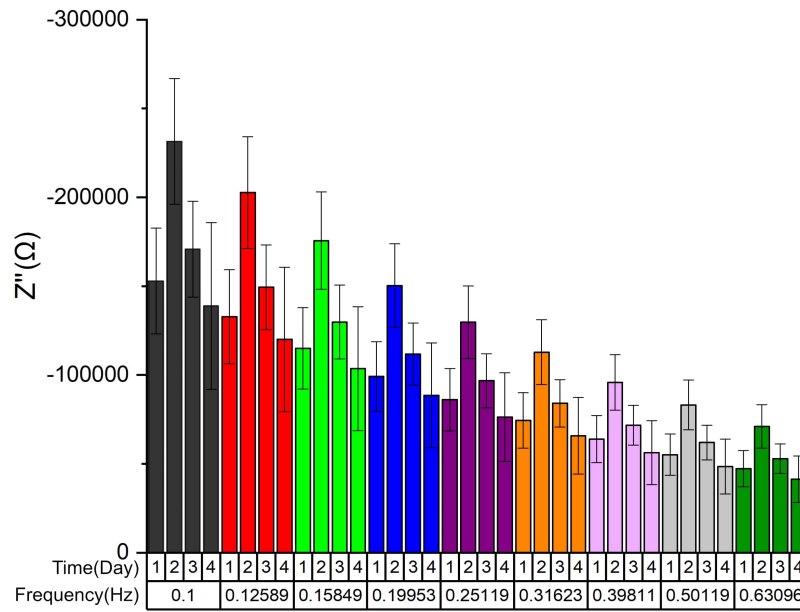


Figure 5.15: Reactance changes in regions that showed significance in filtered uncomplicated post-op patient samples (Average \pm SE).

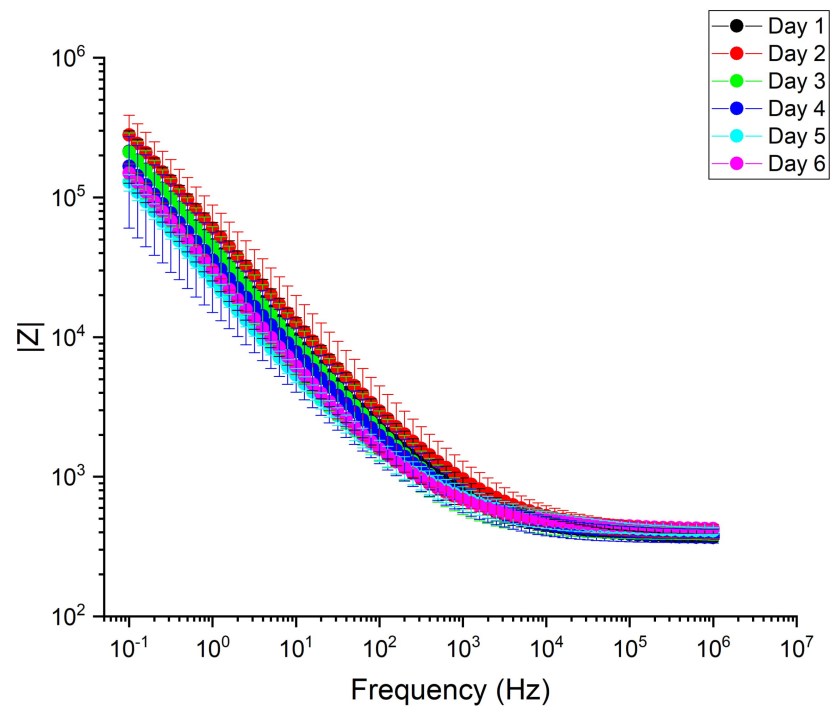


Figure 5.16: Average (\pm SD) modulus plot of filtered clinical samples from uncomplicated post-op patients on each post-op day.

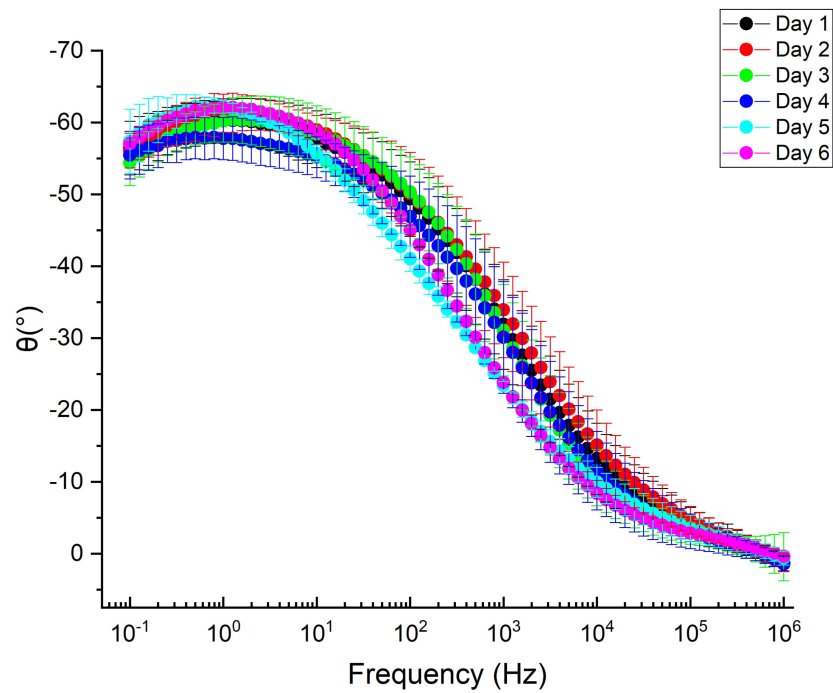


Figure 5.17: Average (\pm SD) phase plot of filtered clinical samples from uncomplicated post-op patients on each post-op day.

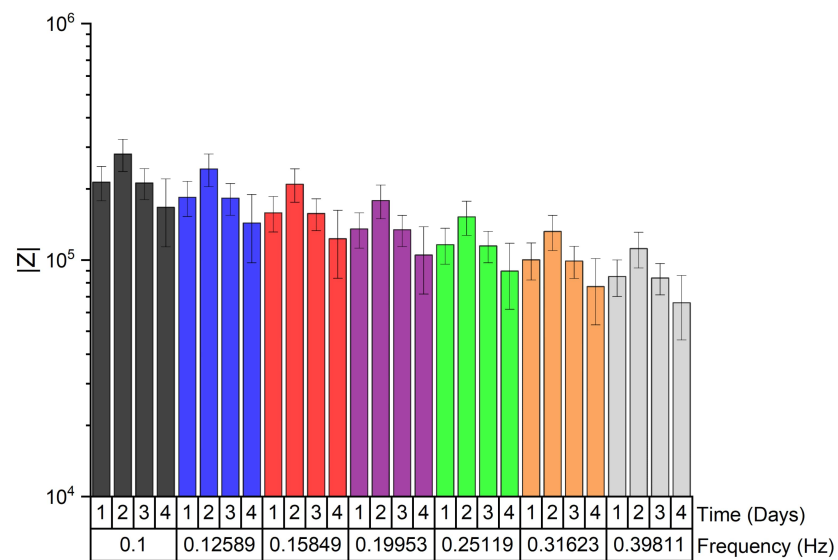


Figure 5.18: Modulus changes in regions that showed significance in filtered uncomplicated post-op patient samples (Average \pm SE).

Differences between Unfiltered vs Filtered data

The results of the filtered and unfiltered measurements were compared against each to other (on a day by day basis using 2-way repeated measures ANOVA) to determine how much of a difference the removal of large elements of the fluid such as bacteria, blood, proteins, etc. would make to the electrochemical signature. Analysis in this section is only done with patients 13 onwards as these were the patients with both unfiltered and filtered results.

As mentioned previously, the effect of filtering was observed to cause values of resistance and reactance to change, particularly at low frequencies (Figure 5.10 and Figure 5.13) and was confirmed to be significantly different using ANOVA tests.

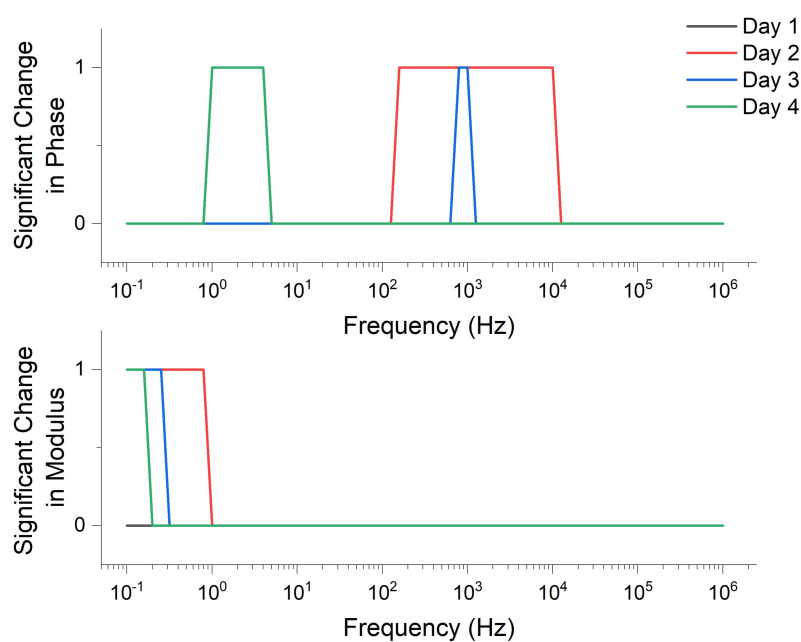


Figure 5.19: Regions where significant difference was found between unfiltered and filtered results for modulus and phase results of patient samples using 2-way repeated-measures ANOVA tests.

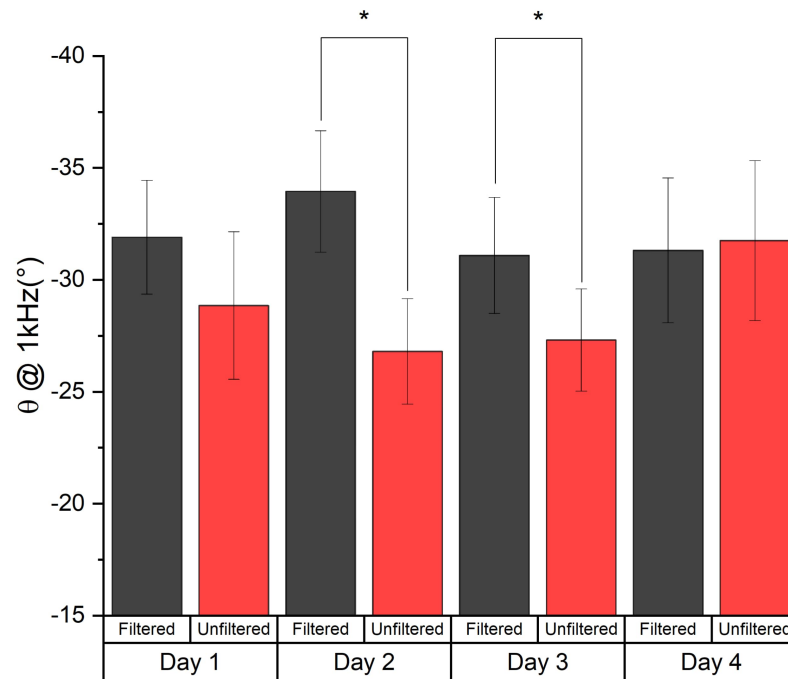


Figure 5.20: Changes in phase at 1kHz as a result of filtering over time. Significant differences occurred on Days 2 and 3. Bars are mean \pm SE.

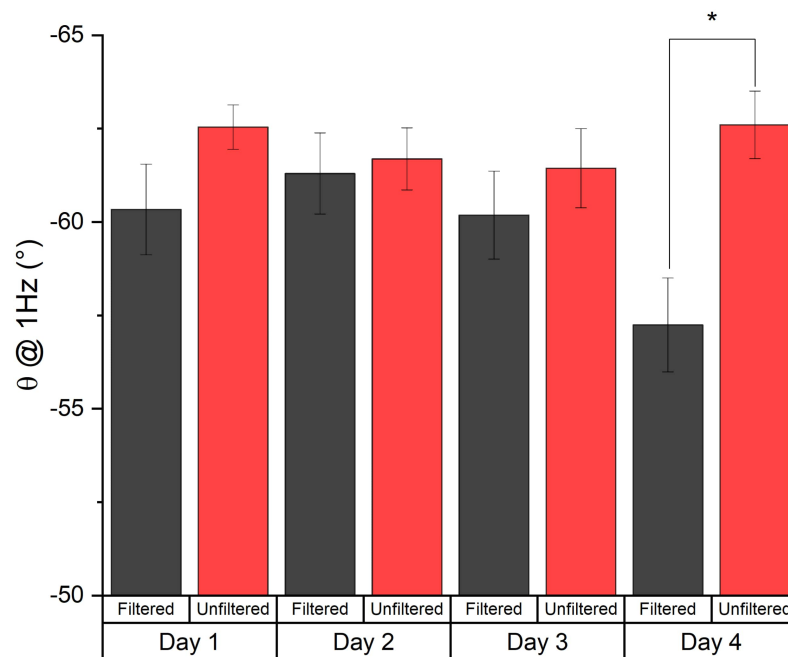


Figure 5.21: Changes in phase at 1Hz as a result of filtering over time. Significant differences occurred on Day 4 (indicated by star). Bars are mean \pm SE.

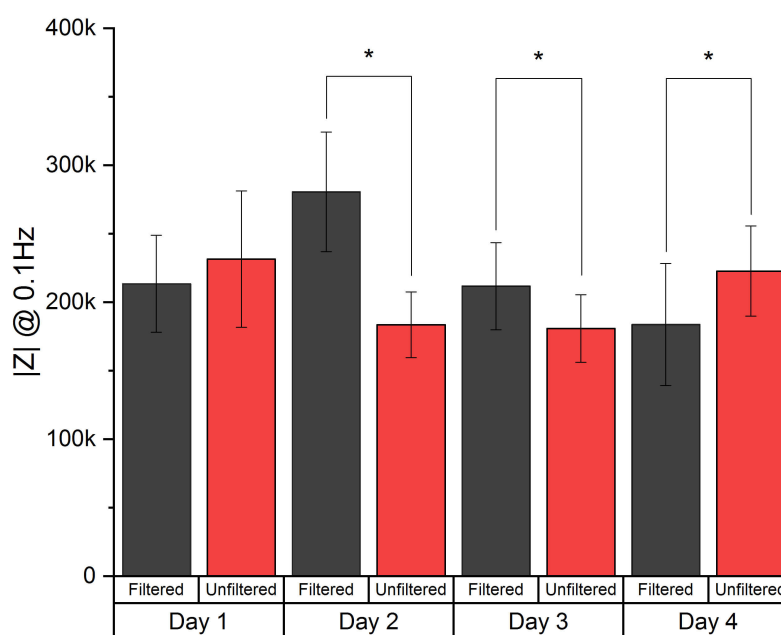


Figure 5.22: Changes in modulus at 0.1Hz as a result of filtering over time. Significant differences occurred on Days 2,3 and 4. Bars are mean \pm SE.

Differences were found between the unfiltered and filtered results at different regions of phase and modulus as shown in Figure 5.19. For phase, it was noted that a change occurred at mid frequencies ($\approx 500-10,000\text{Hz}$), where an increase in phase angle occurred, on days 2 and 3, when samples were filtered. Changes in this range are usually attributed to differing cellular structure interactions occurring which is not surprising seeing as the removal of cells would cause interactions to change.

On day 4 however, the inverse occurs in low frequency regions (around 1-7Hz). Examples of these changes can be seen in Figure 5.20 and Figure 5.21. Modulus values were found to be significantly different at low frequencies, with frequencies at 0.15849Hz and lower found to be different on days 2, 3 and 4. At these frequencies, it was found that filtered values were higher on days 2 and 3 but the inverse happened on day 4. An example of this is shown in Figure 5.22 at 0.1Hz. Changes at low frequencies are associated with alpha

dispersions (i.e. interactions at cell membranes, metabolites, etc.).

5.6.2 Post-operative Conditions

Results of patients who exhibited complications after surgery are investigated in this section. Complications of patients are listed in Table 5.2.

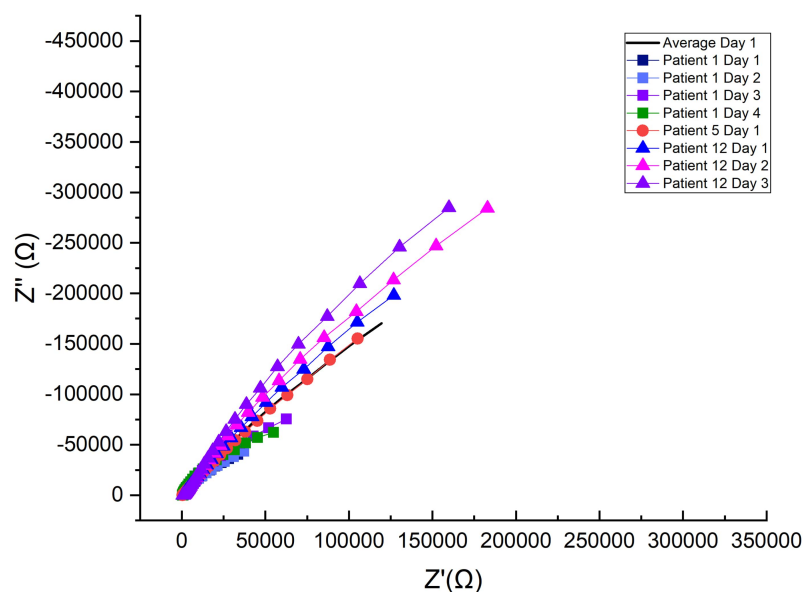


Figure 5.23: Nyquist Plots of unfiltered samples from Patients 1, 5 and 12.

It can be seen in Figure 5.23 and Figure 5.24 that several of the patients who had post-op complication had changes in their EIS signature, particularly patients 1, 12 and 19.

Patient 1, who was found to have low haemoglobin counts, exhibited notably lower resistance and reactance values versus uncomplicated patients (Figure 5.23). The resultant bode plots found that this patient's modulus values were low at higher frequencies (Figure 5.25) and phase values were found to be particularly low between 10-10,000Hz (Figure 5.26).

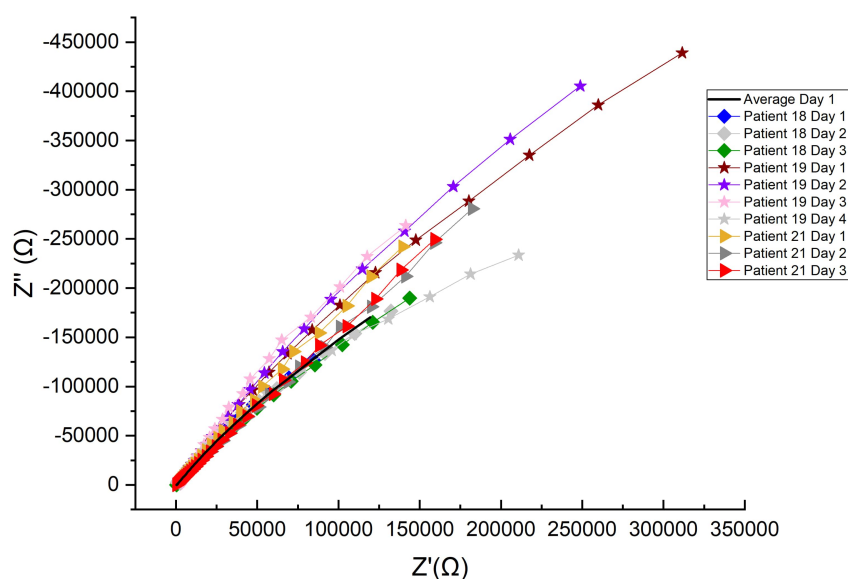


Figure 5.24: Nyquist Plots of unfiltered samples from Patients 18, 19 and 21.

Patients 12 and 19 (who had similar post-operative conditions) exhibited considerably higher resistance and reactance values, particularly at lower frequencies, versus patients with uncomplicated course of post-op for days 1 to 3. However, differences could be seen in their bode plots. Patient 12 exhibited higher modulus values at lower frequencies versus patient 19 and uncomplicated patients as well as lower phase values at approximately 100-10,000Hz. Patient 19 on the other hand had an unusual phase plot. While most phase plots from other patients had a peak at approximately 1-10Hz, patient 19 had something that resembled a double peak on day 4; one at approximately 200Hz and another at approximately 1Hz. It was also seen that when this day 4 sample was filtered, the peak at 1Hz disappeared. Changes in patient 19's results were seen more clearly when phase was normalised to day 1 results (Figure 5.28). From this figure, it can be seen that large changes were seen at higher frequencies which was also found with patient 12 who had changes of about 1.4 and 1.2 on days 2 and 3 respectively (at 10^5 Hz unfiltered). However, Patient 19 had a substantially large drop at high frequencies on day 4.

Other changes due to filtering were investigated but changes associated were insignificant.

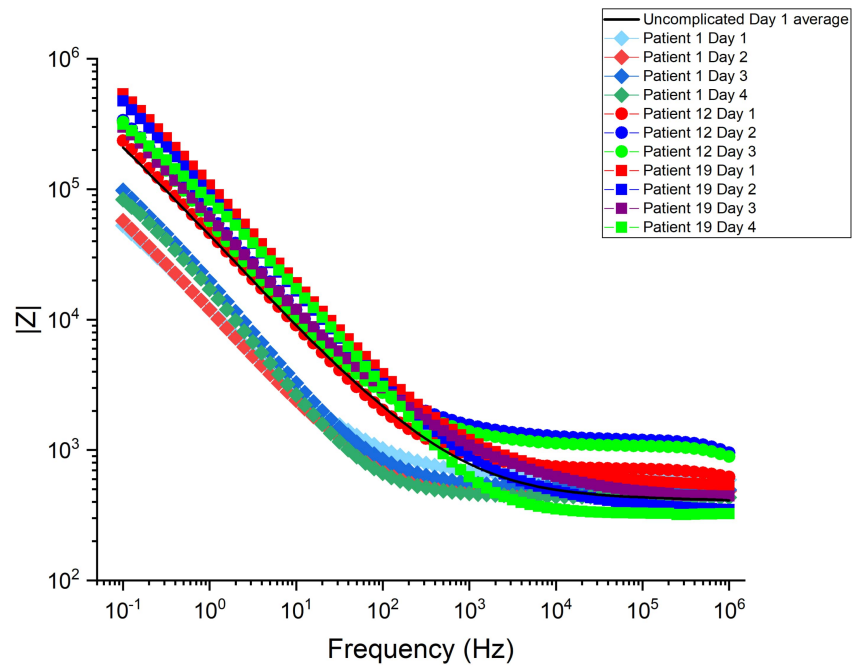


Figure 5.25: Modulus Plots of unfiltered samples from patients 1, 12 and 19.

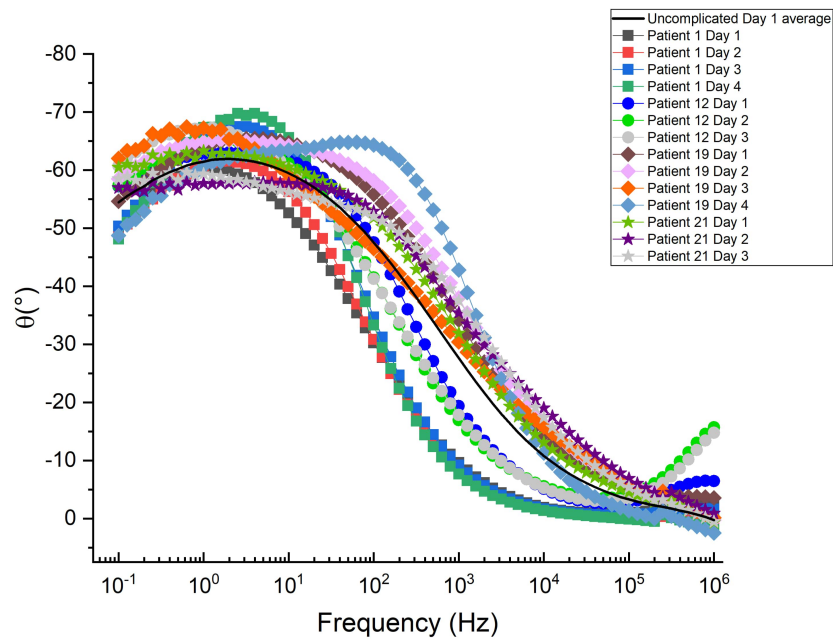


Figure 5.26: Phase plots of unfiltered samples from patients 1, 12, 19 and 21

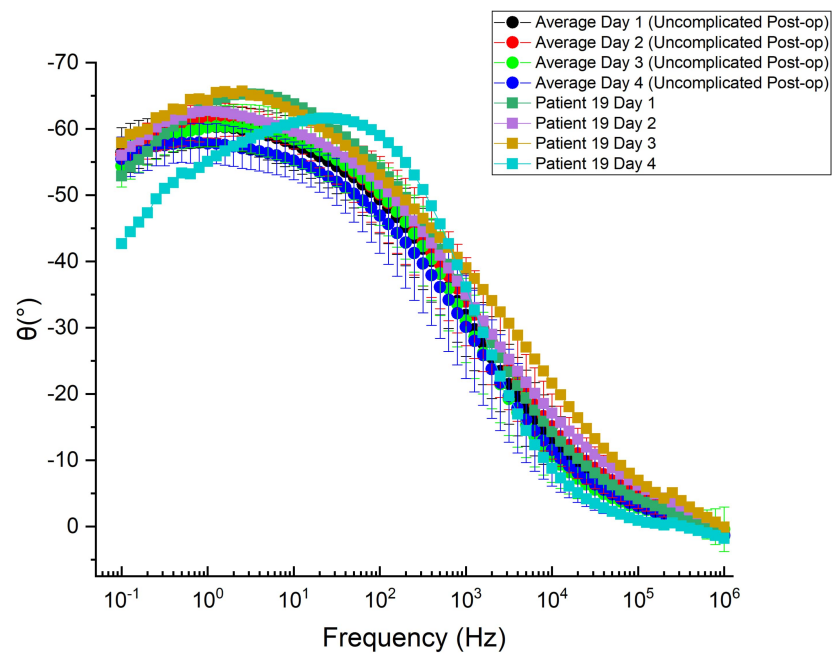


Figure 5.27: Phase plots of filtered samples from patient 19 versus uncomplicated cases

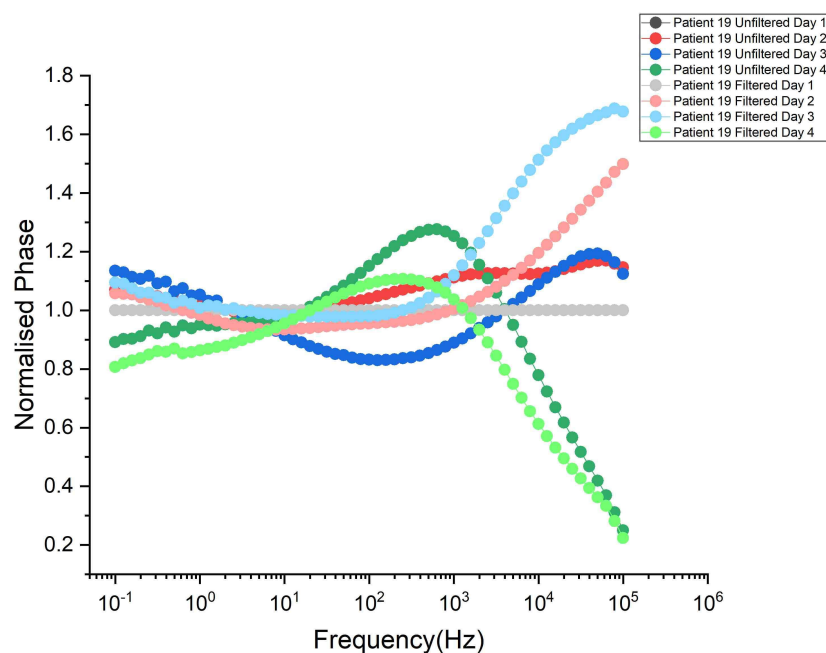


Figure 5.28: Normalised phase plots for patient 19

5.6.3 Modelling

Samples were fitted using MATLAB as described in Section 3.6.3 using a Randles' circuit using a constant phase element (CPE) to further understand what was happening at the electrodes and in solution. An example fitting is given in Figure 5.29 where the fitted circuit model is shown at the top of the figure. The parallel section of the CPE and the faradaic resistance (R_f) represents the resistance and capacitance at the electrode-electrolyte interface, and the remaining resistor connected represents the solution resistance (R_s). Further details can be found in Section 2.4.1. The results can be seen in Figures 5.30-5.33.

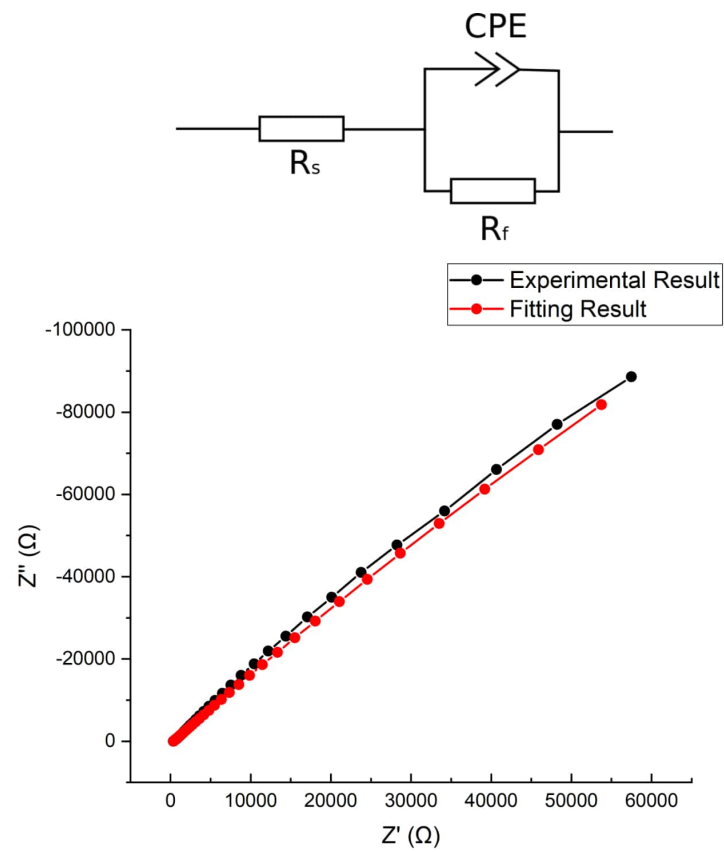


Figure 5.29: Example of modelling patient data

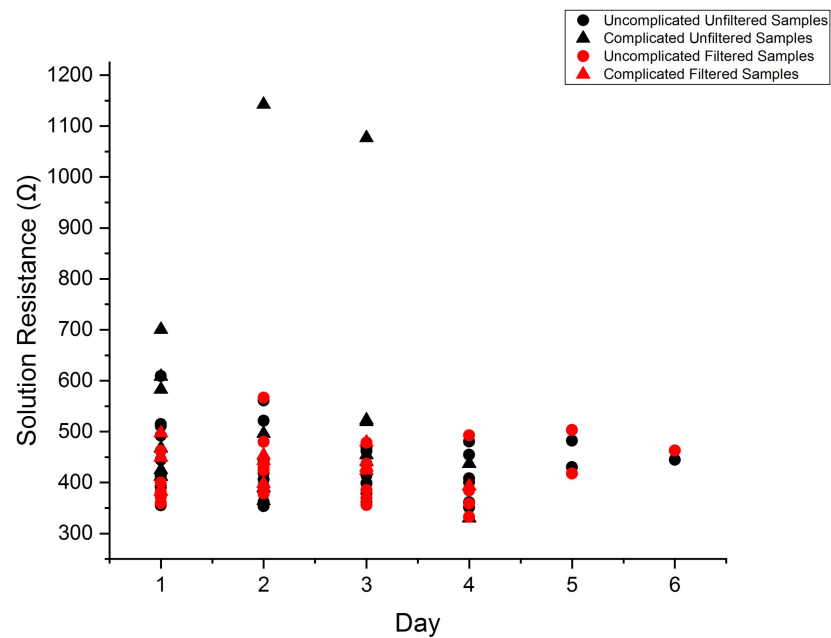


Figure 5.30: Calculated solution resistances from modelling

Calculated solution resistances of patients were found to stay within a relatively tight band with unfiltered samples having an average (mean \pm SD, time not a factor) solution resistance of $426.35\pm 57.85\Omega$ and $416.61\pm 57.46\Omega$ for filtered samples. Patient 12 (who had post-operative complication) produced higher solution values, particularly on days 2 and 3 with values of above 1000Ω and were considered outliers. No other trends/significant differences could be determined.

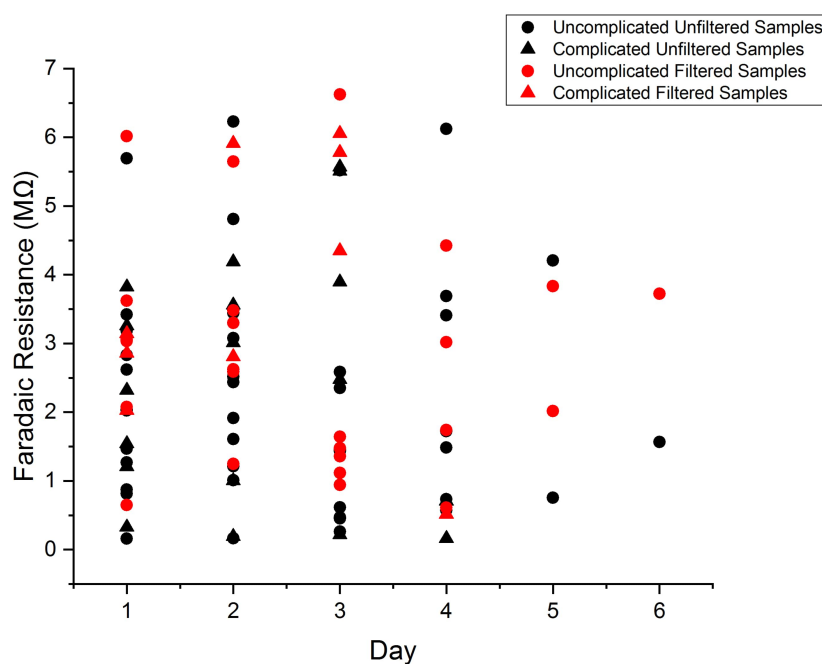


Figure 5.31: Calculated faradaic resistances from modelling

Larger variations were seen in faradaic resistance with range of 1.6 to $6.62\text{M}\Omega$ with average values (\pm SD) of $2.24\pm 1.66\text{M}\Omega$ for unfiltered samples and $3.19\pm 1.64\text{M}\Omega$ for filtered samples. No changes could be seen that were due to time, post-operative complications or whether the samples were filtered or not.

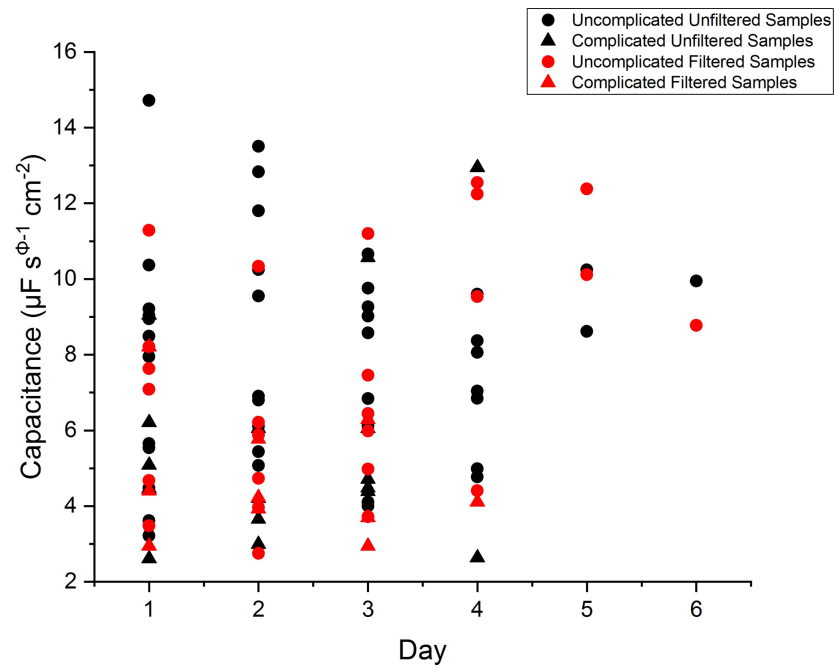


Figure 5.32: Calculated capacitance term of constant phase element from modelling

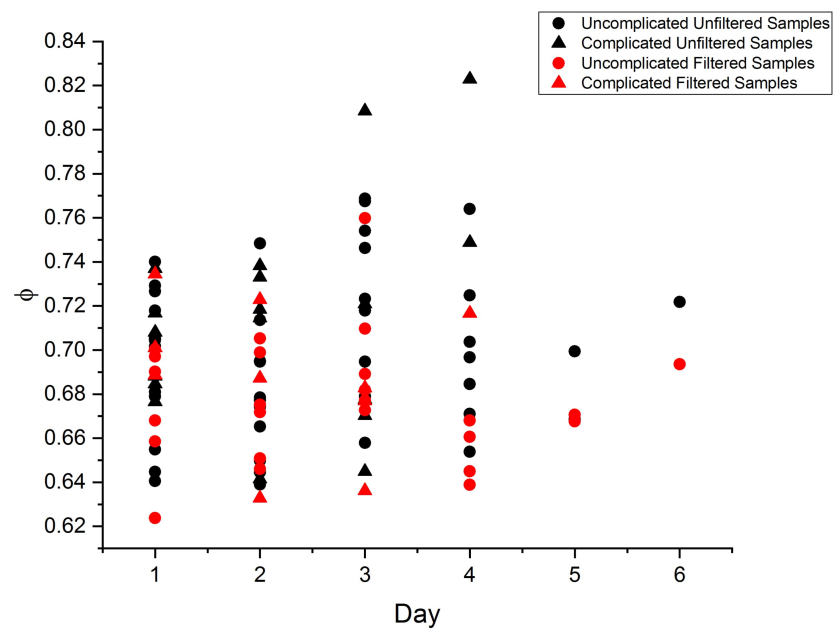


Figure 5.33: Calculated phi term of constant phase element from modelling

Capacitance and phi values were found to all be within a tight range of approximately 2-20 μ F and 0.64-0.76 respectively. When comparing samples with filtered and unfiltered measurements, it was found that a significant difference occurred on day 2 ($p=0.026$) with a mean drop of 2.64 μ F when samples were filtered indicating that a larger molecule/s (e.g. red blood cells, bacteria, etc.) may have been present in high enough quantities to affect the capacitance. Another observation that was noted is that the 2 of the values of phi were above 0.801, which was the outlier threshold. Both values were found to be patient one's day 3 and day 4 values who was found to have low haemoglobin levels. No other changes were detected.

5.6.4 Timed Experiment

As seen in the previous sections, some of the changes in the electrochemical impedance signature were thought be potentially due to blood, bacteria and/or proteins. As a result, and based on previous work in the group looking at bacteria, a timed experiment was performed where samples were measured by EIS as soon as they were received from the hospital as well as 6 and 24 hours later (Section 3.5.7).

Figure 5.34 shows the 3D Nyquist plot of changes in EIS signature over time. Patient 21 results showed particularly low resistance values on day 2 and the initial reading on day 3. This could be seen much more clearly in the 3D bode plots in Figure 5.35 and Figure 5.36.

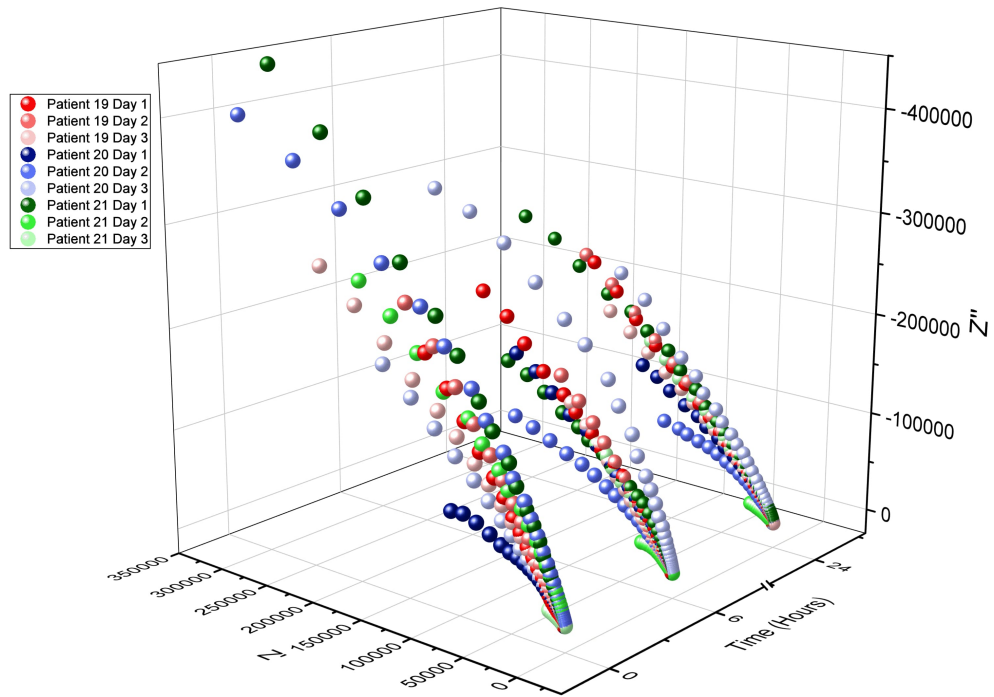
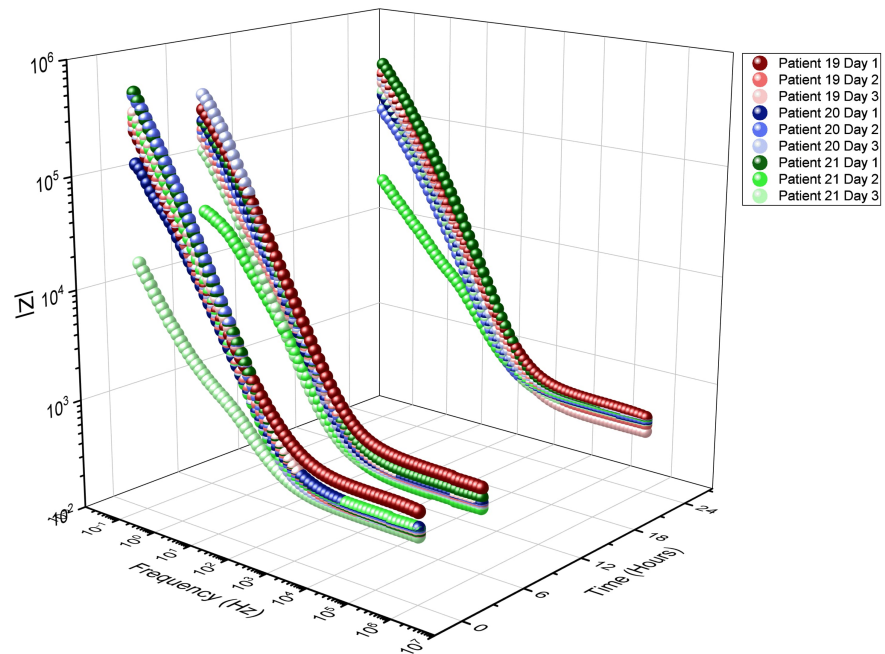
Figure 5.34: 3D Z' vs Z'' of timed experiment

Figure 5.35: 3D modulus of timed experiment

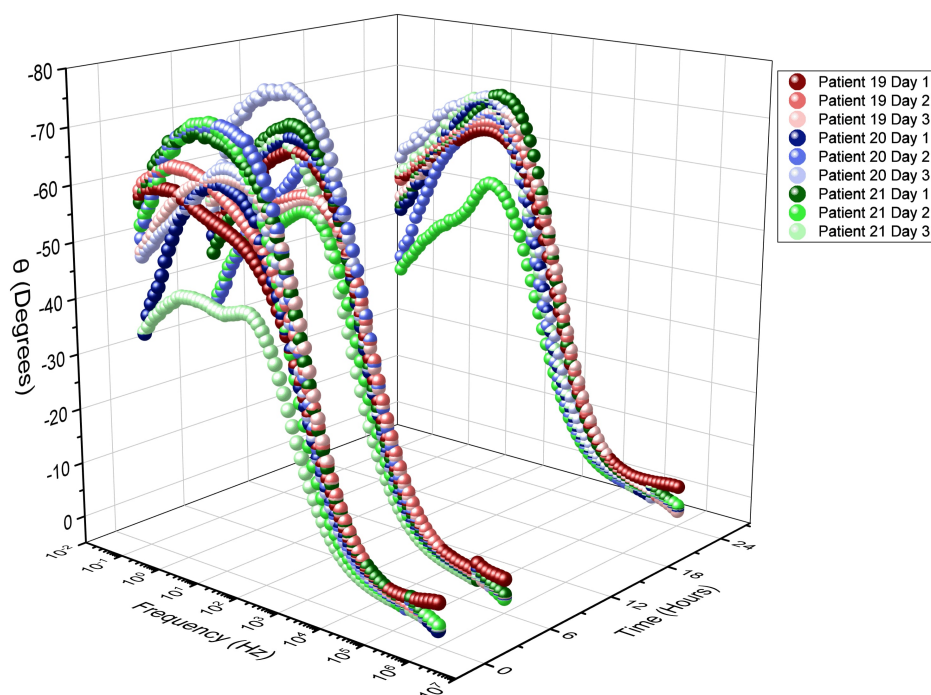


Figure 5.36: 3D phase of timed experiment

In order to try to better observe the changes that were happening between days, each patients' modulus and phase data were normalised, using a method implemented in previous biological impedance studies to identify various elements in fluid such as bacteria, cells, etc., to their day 1 results (see Section 3.6.2 for further details). Results were normalised by dividing the result at each time point by the first time point, which in this case is hour zero.

It was evident from the normalised results that large changes occurred in patient 21, particularly on day 3. Figure 5.37 shows the normalised modulus results where it can be seen that large changes occurred for patient 21 on day 3 with increases of ≈ 7 -11 times higher versus the initial reading at lower frequencies. Similar trends were seen in normalised Z' and Z'' results. Similar increases in patient 21 (day 3) were seen in normalised phase results though they were not to the same magnitude (Figure 5.38). The large changes in

patient 21 could be as a result of the patient having a urinary tract infection. Changes similar to this has been seen in previous work in the Medical Devices group at Strathclyde that have been related to bacteria.

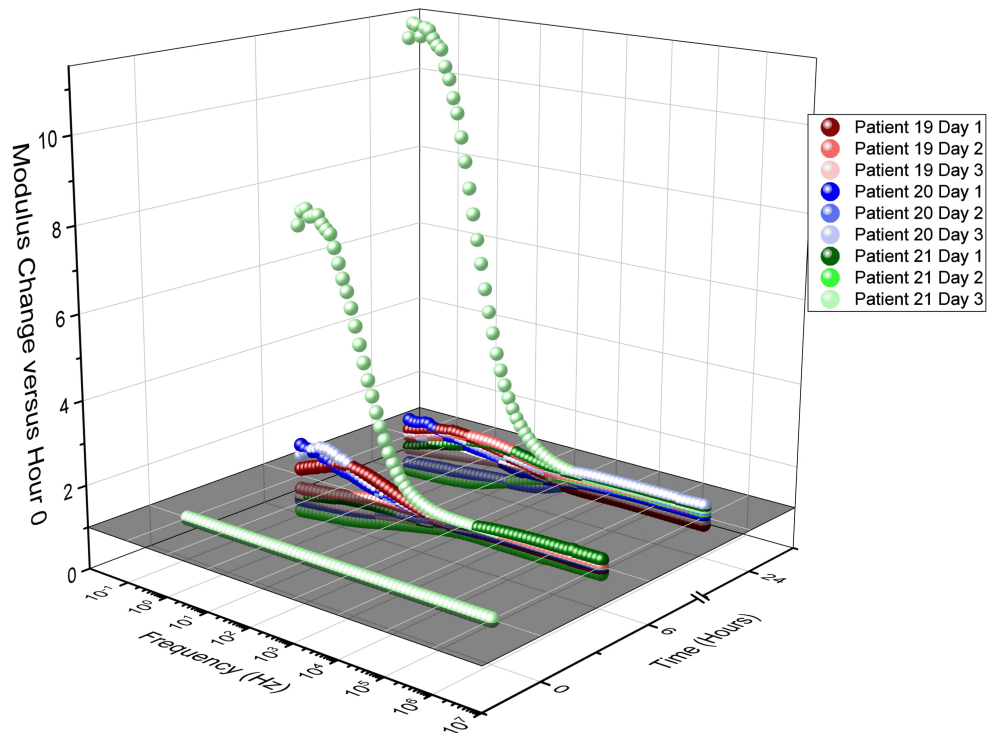


Figure 5.37: Normalised modulus of timed experiment

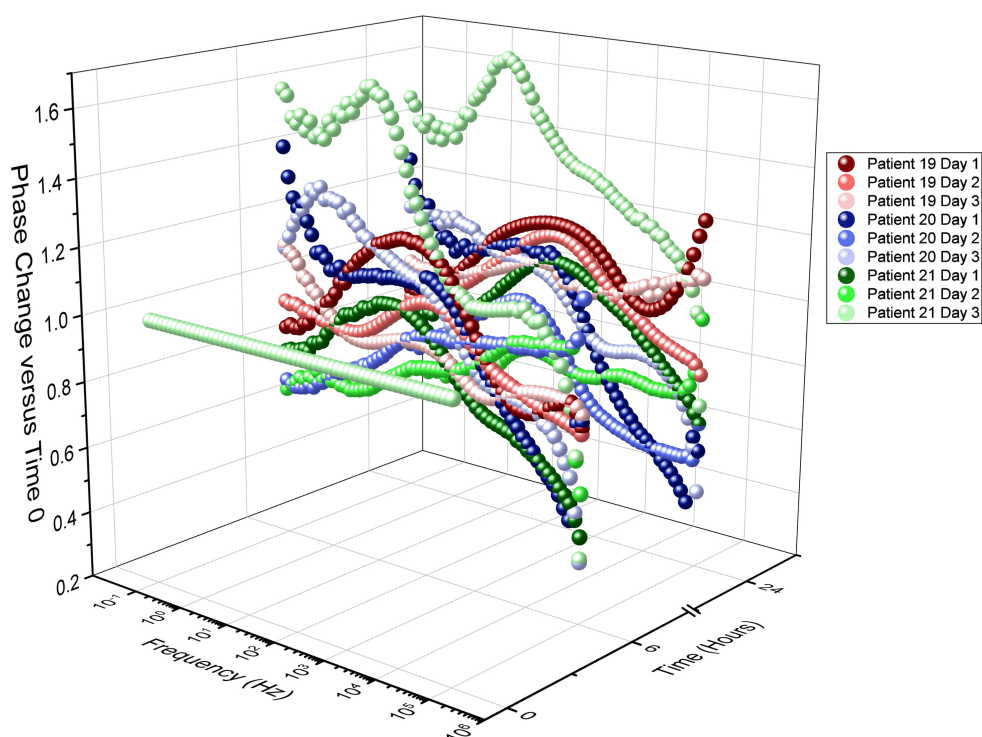


Figure 5.38: Normalised phase of timed experiment

EIS Summary

EIS was employed to diagnose collected patient samples. Potential interesting trends were found including differences due to filtering as well as changes that could be associated with post-operative conditions.

5.7 Cyclic Voltammetry

Finally, cyclic voltammetry tests were performed on both unfiltered and filtered results. Cyclic voltammetry was used to try to see if there were any redox reactions that were present in the fluid and whether they could be related to non-complicated and complicated post-op.

3 scan rates were used for the experiment: 25, 50 and 100mV/s. An ex-

ample cyclic voltammogram is shown in Figure 5.39. Large drops/rises at approximately -0.8V which is most likely due to the water disassociation. No peaks or troughs that could represent redox reactions could be determined from any of the patients. This was expected given the complexity of the fluid may cause masking of reactions while measurements took place which was similarly seen during the preliminary experiments (Section 4.5.2).

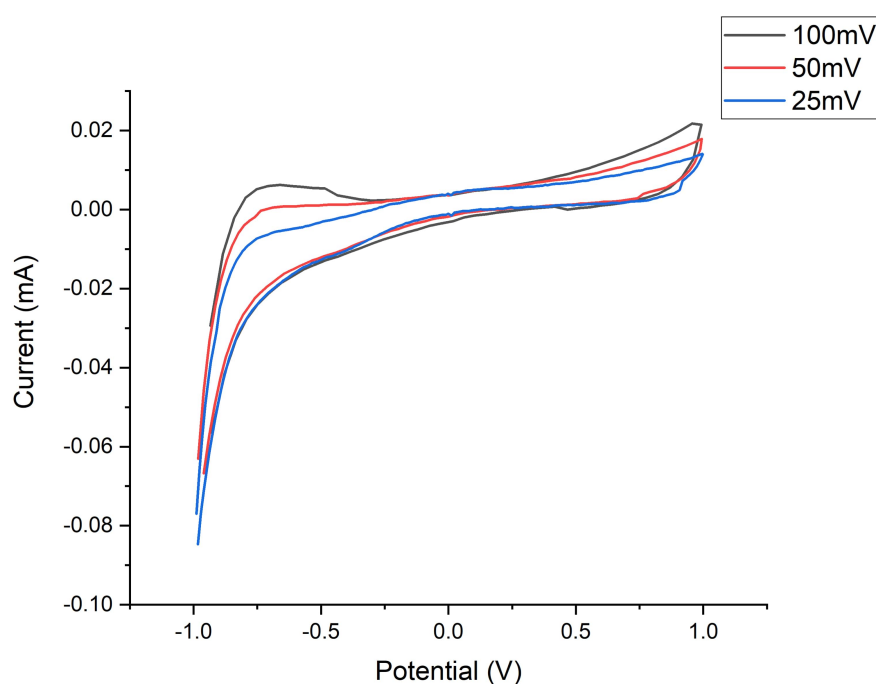


Figure 5.39: Example of patient cyclic voltammetry result (patient 17 day 1)

5.8 Summary

In this chapter, clinical samples were tested for glucose, lactate, pH and by EIS and cyclic voltammetry techniques based on developed methods that were tested in Chapter 4. Several interesting results were acquired including a strong downward trend in glucose concentration as well as outlying results that could be related to post-operative conditions. In the next chapter, results in both Chapters 4 and 5 are discussed in detail.

Chapter 6

Discussion and Conclusions

6.1 Introduction

Anastomotic leakage is a devastating post-operative complication and, if not treated early enough, can be fatal. Reports in the literature have shown that delays in treatment increases the risk of fatality, but current methods of detection are inadequate and often relies on patients exhibiting symptoms, by which time it could be potentially too late to treat effectively. In addition to this, anastomotic leakage has been associated with higher hospital costs, due to longer stays and interventions required, and reduced cancer survival rates (see Chapter 1 for more details). Overall, the effect on the patient's quality of life can be significant both in the short and long-term. Therefore, the aim of this thesis was to determine a suitable method to detect anastomotic leakage at an early stage to allow clinician to manage the complication and minimise further issues from occurring.

In this study it was decided that monitoring changes in fluid obtained from drains placed close to the anastomosis could potentially determine a reliable way of diagnosing anastomotic leakage at an early stage. Several biomarkers were chosen to be measured in this fluid. In addition to this, a couple of electrochemical techniques were also chosen to garner further information about the fluid. Methodologies were developed in Chapter 3 (for which the background theory is explained in Chapter 2), tested in Chapter 4 and were then used to measure the chosen parameters in patient samples in Chapter 5. While there was one patient who did exhibit anastomotic leakage, little information was gained as the drain was removed after the first post-op day. Other information was gathered on patients who had uncomplicated post-op courses as well as a few others who had other postoperative conditions (see

Table 5.2) which may prove useful in further studies in the area. Therefore in this chapter, the results obtained and presented in Chapters 4 and 5 are discussed. The usefulness of biomarkers and techniques used will be evaluated, conclusions drawn, and from this, future lines of enquiry will be suggested.

6.2 Ischaemic Markers

As mentioned in Chapter 1, ischaemia is a commonly cited as a major reason for anastomotic leakage. It would be expected that (in any case) tissues damaged at the anastomotic site, due to the trauma of surgery, would exhibit some level of hypoxia triggering healing processes. As damage tissues heal, it would be expected that effects due to ischaemia become less pronounced, with tissues ceasing to be hypoxic (Thompson et al. 2006, Bosmans et al. 2015).

While the whole process of anastomotic leakage is not fully understood, it is thought that tissues at the site of the anastomosis do not heal correctly, meaning that the effects of ischaemia (i.e. the release/production of certain molecules) would have a differing profile compared to a patient who undergoes an uncomplicated post-op recovery (Hallböök et al. 1996, Boyle et al. 2000). Therefore, it was decided that looking at several of these markers (glucose, lactate and pH) may give some insight into the anastomotic healing process as well as help identify patients with other post-operative complications.

6.2.1 Lactate

Lactate is a major biochemical marker that is produced in response to ischaemia and tissue injury, where a reduced blood supply to the tissues (and

therefore lack of oxygen) causes cells to switch from aerobic to anaerobic respiration, from which lactate is produced and accumulates. In addition to this effect, levels of lactate are further elevated due to rapidly proliferating cells exhibiting 'aerobic glycolysis', as well as being a by-product from leucocytes that are combatting bacterial species which occurs after colorectal surgery due to release of bacteria that is present in the colon (Stavrou & Kotzampassi 2017, Matthiessen et al. 2007).

A rise in lactate levels at healing sites is considered to be an important factor as it stimulates several important molecules/factors that are required for wound healing (Heiden et al. 2009, Porporato et al. 2012, Ryoo & Kim 2018). Therefore, it was thought important to monitor its levels over the post-operative period to understand how it changes in the healing process with regards to colorectal resection and how it may deviate in post-operative complications such as anastomotic leakage.

Initial Testing

Initially, a methodology was developed to measure the levels of lactate based on a commercially available kit (Section 3.3). The kit measures lactate levels using colorimetric methods where reactions with lactate oxidase, and consequently with hydrogen peroxide, produce a colour change for which the measured absorbance at a particular frequency (540nm in this case) is proportional to the concentration of lactate (more details are found in section 2.5).

As it was expected that low volumes of the drain fluid from patients would be received (potentially <2mL), the kit was adapted to accommodate for these volumes. To test the initial methodology and characterise the assay, calibra-

tion curves were produced from a range of 0-30mM using the methodology described in Section 3.3. The upper range of 30mM was chosen as it was expected that the linearity of the kit would cease at about 20-25mM and measuring up to 30mM would allow for observation of non-linearity and therefore, the limit of the kit.

From the results seen in Figure 4.1, a good linear region occurred up to 20mM after which, at 25 and 30mM, the standard deviation of the assay increased substantially from 0.081 at 20mM to 0.2906 and 0.1515 at 25 and 30mM respectively, meaning that the precision of assay at these ranges was reduced. As a result, 20mM was chosen to be the upper limit of the assay. The observation that a good linear region occurred between 0-20mM was supported using regression analysis where an R^2 value of approximately 0.997, indicating a very strong trend for which almost all the variations in results could be accounted by the line of best fit. In addition, a limit of detection was established at 3.24 μ M.

While it was expected that lactate levels would typically fall below 20mM based on previous literature that has quoted values up to approx. 15mM (Trabold et al. 2003, Porporato et al. 2012), there was the possibility that some of the values may measure higher than this. This has been indicated by a study by Wright (2019), who found lactate levels in drain fluid could exceed 25mM in some patients. Therefore, it was decided for use in clinical samples, samples would be diluted and then measured concentration be multiplied up to take into account the level of dilution. It was found later that some of the concentrations measured from patient samples were higher than 40mM.

The assay was also checked against an industrially produced standard (Figure 4.2) and was found to have no significant difference between the standard and

the calibration fit when a one-sample t-test was applied indicating that the adapted assay was as accurate as a known industrially-made standard (see Section 2.5.1 for further explanation).

Overall, a lactate assay was developed for use with small volumes of patient samples and was successfully characterised for use in clinical samples.

Clinical Results

After characterising the assay, the next step was to measure patient samples with the developed assay. Patient samples were transported from the hospital to the lab at the university using approved UN3373 packaging as described in Section 3.2.8. The methodology for measuring lactate in clinical samples is found in Section 3.3.3 for which the results are presented in Section 5.3.

When no damage to tissues has occurred (i.e. no surgical trauma, etc.), lactate levels are expected to be low, with the concentration in peritoneal fluid typically between 0.5-2.5mM (Porporato et al. 2012, Heiden et al. 2009, Trabold et al. 2003, Verma et al. 2014, Pucino et al. 2017). From results presented in Section 5.3, it was found that the lactate concentrations in drain fluid were substantially higher than the norm during the post-op recovery period with day one levels being at their peak, with an average concentration of 17.06mM (Figure 5.1).

This initial high level of lactate concentration was expected as (mentioned previously); firstly, tissue damage, due to the invasiveness of surgery, causes tissues, which are lacking oxygen, to respire anaerobically which as a consequence produce lactate; secondly, tissues during the healing process have been found to exhibit 'aerobic glycolysis' when rapidly proliferating, which produces lactate; lastly, lactate is produced when leucocytes are combatting

bacterial species which would likely have been released from the colon during surgery (Porporato et al. 2012, Hunt et al. 2007, Britland et al. 2012). All of these factors would contribute to the accumulation of lactate in the peritoneal fluid.

While elevated levels of lactate were expected during the initial post-op period, some of the values garnered from testing were surprisingly high when compared to previous studies. Levels of lactate in wounds and peritoneal fluid when abdominal surgery occurred have been reported to be up to 12-15 mM before a drop (Trabold et al. 2003, Porporato et al. 2012) and while many patients were around these values, some patients were notably higher with seven patients being above 20mM at some point during the post-operative period. Previous papers that looked at anastomotic leakage specifically, such as published by Pedersen et al. (2009) and Daams et al. (2014), reported much lower levels of lactate in patients without complications with Pedersen reporting a range of 0-6.6mM and Daams finding an average of 3.2mM. Though, a study by Wright (2019) also found high levels (>25mM) in a few patients which included patients who did not exhibit any post-operative complications.

Variations between lactate levels found in this thesis and previously published papers looking at anastomotic leakage could be due to measurement techniques. In this thesis, unlike previous studies, has been measured directly using colorimetric techniques. The aforementioned papers mentioned used microdialysis techniques which involves the use of semi-permeable tubes placed near the site of interest. Tubes have a fluid which is pumped through at a known rate and analytes passively diffuse into this fluid through the membrane which can be analysed using various techniques. However, in this the-

sis, measurements were performed directly on fluid taken from drains placed near the anastomotic site. While microdialysis tubes can be used to measure the quantity and distribution of analytes, a major drawback to that they often give a fraction of the actual concentration of the environment they are measuring. This is due to the fact that the flow rates used for the removal of an analyte is quicker than the replenishment of the analyte at the microdialysis surface ($>0.1\mu\text{L}/\text{min}$) (Chefer et al. 2009, Shippenberg & Thompson 1997, Turkina et al. 2017) and could explain the difference in levels found.

Another reason could be attributed to the timing of testing. In this thesis, samples had to be transported from the hospital to the University for testing. The time taken for transport is approximately (on average) 30 mins. During this time, there is the possibility that items in the fluid, such as bacterial metabolism may be increasing the levels of lactate during the transport period (Wright 2019, Jurtshuk 1996). In order to check that this is an issue or not, future testing should look at the effect of testing with respect to time.

Large variations were noticed between patients with standard deviations ranging from 6.85 to 9mM depending on the day. This could be as a result of patient factors, which have been shown to affect the healing process. For example, there was a relatively large age range of patients in the study (48-78). It is known that older patients ($\approx >60$) have been found to have delayed or altered wound healing. Therefore, it could be that varying lactate levels between patients over the initial post-op period could be due to the fact they are healing at differing rates, affecting the lactate levels. Other factors that have been found to affect the wound healing process include (but are not limited to) stress, depression, smoking, alcoholism and obesity (Guo & DiPietro 2010, Gouin & Kiecolt-Glaser 2011, McDaniel & Browning 2014) for which some of

the patients in this study had. This could be confirmed with a larger study where non-parametric tests such as Principal Component Analysis (PCA) can be used.

Another trend that was noted and expected was that lactate levels from patients were found to drop over time (see Figure 5.1). The reduction (after the initial increase) in lactate over time can similarly be attributed to the healing process, where angiogenesis provides blood supply to the surgical site resulting in restoration of normal oxygen levels in the tissue, allowing for aerobic respiration to occur. In addition, a reduction of proliferating cells would also start occurring, resulting in reduced aerobic glycolysis and therefore lower amounts of lactate being produced. Lactate present in the peritoneum is either drained away or converted to other molecules (e.g. oxaloacetate) causing a consequential decrease in its concentration (Ryoo & Kim 2018).

When an outlier test was implemented (as stated in Section 3.6.1), it was found that two of the patients tested had values that were highly dissimilar to the others; patients 6 and 12. Patient 6 had an increase on day 2 that was considered an outlier. Though this patient did not have any known post-operative conditions, they did however have chronic obstructive pulmonary disease (COPD), which has been associated with higher lactate levels versus a healthy subject (Engelen et al. 1995, Durmuş et al. 2018) and could explain this anomaly. Another patient also had COPD (Patient 3) but only one sample was taken on post-op day 1 so it was not possible if the same increase occurred in this patient.

Patient 12 had lactate levels that were considered outliers for all the days measured. This could be because the patient had post-operative complications (lower respiratory tract infection and ileus). How this patient got an infection

could be due bacteria, if released due to surgery and was not taken up by the lymphatic system, ending up in the vicinity of the diaphragm due to convective forces in the peritoneum (DiZerega & Rodgers 1992). Bacteria causing the infection could be producing lactate, as well the lactate produced by leucocytes as a result of combatting infections, in addition to healing processes that produce lactate (Porporato et al. 2012, Hunt et al. 2007, Sun et al. 2017). However, it should be noted that patient 19 also experienced the same post-op complications as patient 12 but, after an initial high (but not considered outlier) lactate concentration on day one, their levels dropped substantially, whereas patient 12 was consistently high. This could be due to numerous reasons such as the vector of infection (differing bacteria species, etc.), the type of lower respiratory infection, etc. or either patient could be anomalous. More patients with these morbidities would be required to understand this more, as well as microbiology studies of patient samples.

Patient 12 indicates a potential issue with measuring lactate for use in detection of anastomotic leakage. Here, patient 12 had elevated lactate levels due to an infection and/or an ileus. If future work finds that anastomotic leakage also increases lactate levels, it should be checked that the increases can be differentiated from increases due to other conditions. Whether this is done by looking at solely at lactate levels, or in conjunction with other results (e.g. glucose results) would need to be determined.

It was initially observed with the first few patients that higher levels of blood contamination were found in samples than expected. To check that this was not affecting the overall lactate measurement, samples were also filtered from patient 13 using a 0.22 μ M syringe filter and compared to unfiltered results. The use of this size of filter results in removal of red blood cells (which are

usually 7-8 μ M) as well as bacteria and other large elements but does not inhibit the movement of lactate or glucose through the filter (Bruil et al. 1995, Chen et al. 2016). No significant differences were found between the filtered and unfiltered results indicating that red blood cells (or any other large components) were not affecting lactate absorbance values.

One way to make it easier to compare patients and determine trends is to normalise the data versus a reference. For lactate assay results, the data was normalised to the patient's day 1 result as described in Section 3.6.2, for which the results are shown in Figure 5.2. When a curve was fitted to normalised data, it yielded a polynomial fitting (order of 2) which had a particularly low R^2 value (0.145). This low R^2 value indicates a weak/no trend, likely due to the fact that the high levels of variation between patients' lactate level. Due to this lack of fitting/inability to determine a trend, the use of lactate to determine post-operative conditions such as anastomotic leakage may be severely diminished as it would be substantially more difficult to determine differences between non-complicated and complicated post-op patients.

Summary

A methodology was developed, tested and used to test lactate levels in peritoneal drain fluid. A weak trend was found where lactate levels dropped over time during the post-op period. Though there were a couple patients with outlying results that could be related to their pre/post – operative conditions, larger studies are required to confirm these trends. As no data was gained with regards to anastomotic leakage was gained, it is difficult to say whether monitoring this marker would be useful, but due to lack of trends and large variations between patients over time, it seems unlikely to be a useful marker.

6.2.2 Glucose

In aerobic respiration, glucose is converted into pyruvate and produces large amounts of ATP which provides energy for normal physiological processes. However, when cells are lacking oxygen and or damaged, anaerobic respiration occurs instead, where glucose is converted into lactate with lower amounts of ATP being produced (Matthiessen et al. 2007, Muller et al. 2012). Therefore, monitoring of this molecule was thought to be important as a way of understanding how it behaves during the healing period and if it alters with respect to anastomotic leakage (see Section 1.5.1).

Initial Testing

Akin to the lactate assay, a methodology was developed for testing glucose concentrations using a commercially available kit that used colorimetric means to measure glucose, which reacts with enzyme glucose oxidase, for which one of the products is hydrogen peroxide that then undergoes another reaction to produce a colour change which can be measured and related to concentration to glucose (see Section 2.5 for more details).

Similarly, to the lactate assay, the kit had to be adapted for use for small volumes that could be received from patients. To characterise the glucose assay with the proposed smaller volumes to be used, the assay methodology was tested between 0-30mM concentrations of glucose, using the methodology described in Section 3.3, to determine a linear region for which the assay could be used. The upper range of 30mM was used as it was expected the assay would lose linearity at approximately 20-25mM, for which going past this range would allow observation of the loss of linearity. The results of this are presented in Section 4.3.

From Figure 4.3, it was observed that between 25-30mM, the gradient of the graph changes versus the gradient seen between 0-25mM. In addition, at 30mM, the precision of the assay is seen to reduce as indicated by the standard deviation of 0.0534, which is approximately double the standard deviation at 25mM (0.0237). Due to these reasons, it was decided that the upper limit of the assay was 25mM. When line fitting was performed between 0-25mM (as shown by the red line in Figure 4.3), an R^2 value of 0.993 was found which indicates a strong fit where almost all the data points could be accounted for by the line of fit. The glucose results to be gained from clinical samples were expected to within this range based on previous literature such as by Daams et al. (2014) who found glucose levels at approximately 8mM. However, there was the possibility that values could result higher than this 25mM limit so, as a precaution, it was decided that samples would be diluted and the values multiplied up to reflect the dilution. It was found later that some of the glucose values garnered from patients were higher than 25mM with the highest measurement found at approximately 35mM.

As a way to determine accuracy, the assay was also used to determine the concentration of an industrially produced reference to measure its accuracy versus a known standard. The standard was labelled at being at a concentration of 5.56mM. Looking at Figure 4.4, the assay found the concentration of reference to be of a similar value. To ensure this, a one sample t-test was performed and found no significant difference between the measurements and the reference value indicating the assay could be considered accurate.

Overall, based on evaluating the parameters of linearity, range, accuracy, precision, etc. it was thought that use of this glucose assay (between 0-25mM) would be suitable for use in clinical samples to be received from the hospital.

Clinical Results

The protocol developed and characterised in Section 4.3 was then used on clinical samples that was transported to the university using approved biological packaging and tested as described in Sections 3.2.8 and 3.3.3 for which the results are presented in Section 5.4.

Initial results found that glucose levels were at a peak at shortly after post-op with a high on day one of approximately 9.75mM as shown in Figure 5.3. The initial peak found could be related to the stress-response due to the trauma of surgery. Due to the shock of surgery, the nervous system triggers a host of mechanisms that leads to the production of several types of hormones being released. This includes cortisol and growth hormone, which cause increased levels of glucose to be produced, as well as catecholamines to be produced which, in addition to increasing glucose level, also inhibits insulin secretion (Duggan et al. 2017, Finnerty et al. 2013, Butler et al. 2005). After this initial peak on day 1, it can be seen that levels in glucose dropped over time with an average glucose concentration of 2.17mM on day 4 which can be attributed to the reduction of the nervous system response to the trauma of surgery resulting in less glucose being produced.

Pedersen et al. (2009) found glucose levels to be 8mM (on average) when initial measurements were made. This value is similar to the average value in this study of 9.75mM on day 1 though several patients were substantially higher than this with 5 patients being approximately 15-20mM on day 1. However, the profile of glucose over time is somewhat different between what was found in Pedersen et al. paper and this thesis. Pedersen et al. found that glucose levels dropped slightly over time to 7mM (on average) and dropped

further in patients with anastomotic leakage, whereas in this thesis, levels drop more considerably, with an average glucose concentration of 2.17mM on day 4 being found. It should be noted only 2 patients had anastomotic leakage in this study. Matthiessen et al. (2007) also found similar results to Pedersen et al. with a similar glucose concentration throughout the time period (6 days) of 7mM but in leakage patients, the level dropped on day 5 and 6 to 4mM. However, Daams et al. (2014), found glucose levels stayed at a constant level regardless. Differences could be associated to the measuring technique used in these papers versus what was used in this experiment. In this experiment, measurements were done directly on drain samples whereas in all the papers mentioned here, microdialysis tubes were used. As mentioned as a potential problem in lactate measurements as well, microdialysis techniques often measure lower concentrations versus the environment they are in due to fact that the flow rate is set such that not enough of the analyte is taken up by the dialysate fluid (Chefer et al. 2009, Shippenberg & Thompson 1997, Turkina et al. 2017). Another problem that should be noted in this experiment that might cause a difference compared to previous studies is that measurements were taken after a period of time due to transport of material from the hospital to the university and, therefore it is plausible that levels of glucose may have changes due to cellular/bacterial/etc. processes. A future experiment should be conducted to see if this occurs and if so, how much of a difference it makes to the overall result.

Results were normalised to allow for comparison between patients and to determine any trend. This was done by dividing the patient's results by their day one value (see Section 3.6.2 for further details) for which the results are presented in Figure 5.4. It could be seen there was a linear downward trend in

glucose concentration and when a linear trendline was fitted (as represented by a red line in the figure), the R^2 value was found to be 0.5787, indicating a moderately strong trend between glucose concentration and time.

However, it was observed that the levels of blood, particularly on day 1, seemed to be high. Red blood cells have been known to affect the measured glucose concentrations with many studies investigating blood glucose measurement finding differences between measuring glucose in whole blood and in plasma which is attributed to the differing water content levels between red blood cells and plasma (Kim 2016, Sidebottom et al. 1982, Carstensen et al. 2008).

To check whether this was affecting results, samples from patient 13 onwards were also measured after being put through a $0.22\mu\text{m}$ filter, as described in Section 3.5.7, which would remove intact red blood cells, as well as bacteria and proteins (Bruil et al. 1995, Chen et al. 2016). Using a paired t-test, it was found that a significant difference occurred between the 2 sets of samples on day 1 ($p=0.045$) with a mean reduction of 4.06mM in measured glucose concentration when samples were filtered. This is thought to be due to the red blood cells observed at higher levels on day one. In order to confirm this suspicion, future tests should also record the levels of red blood cells in the samples and compare results between unfiltered and filtered with respect to this additional parameter. If this it is the case that red blood cells do cause the disparity between filtered and unfiltered measurements, it may be the case that a relationship can be determined between unfiltered and filtered results, such as in blood glucose measurements where there is a normally an 11% difference between whole blood and serum measurements (Kim 2016). Other days were found to be not significantly different which can be explained by

previous studies which have found blood in the peritoneal cavity is removed quickly, either by being taken up by the lymphatic system (mostly red blood cell through this route) or through blood capillaries (DiZerega & Rodgers 1992, Mengert et al. 1951).

While there was a slight difference between filtered and unfiltered results, the overall trend over time remained the same (i.e. a drop in glucose over time). When the same normalisation was applied to filtered results in a similar manner to results gained with unfiltered samples, it was observed that the change over time followed a power law relationship. When a power law line was fitted, it was found that the R^2 value was approximately 0.82, a high value indicating a strong trend which was also higher than the value found the linear trend found in unfiltered samples. The use of a power law relationship seemed appropriate as it was expected glucose levels would be at their highest immediately after surgery due to the aforementioned trauma causing an immediate increase in glucose. As the surgical trauma is stopped, the glucose levels would drop quickly over the post-op period to a plateau value (Duggan et al. 2017, Finnerty et al. 2013, Butler et al. 2005).

The strong trend found here could be useful as it could help determine post-operative complication if a patient's glucose level do not follow this trend. In this study, several patients had outlying results: patients 8, 12 and 15.

Patient 12 had high levels of glucose of which days 2 and 3 were considered outliers based on the equation shown in section 3.6.1 (patient also had high levels of lactate on the same days). This patient was found to have a lower respiratory tract infection and an ileus. This increase in glucose is could be due to the fact the presence of infection triggers an inflammatory response/stress response. Infection causes the release of growth hormone, cortisol and inflam-

matory cytokines which as a result, has been found to inhibit insulin and/or increase glucose levels (Jeon et al. 2008, Rayfield et al. 1982). It should be noted however, that patient 19 was found to have similar postoperative conditions and did not exhibit the high levels of glucose found with patient 12, meaning either patient could be anomalous and more patients with similar conditions would need to be tested to determine if there is any utility to this. Further larger studies with these conditions would need to be performed to determine any trends.

Patient 8 was found to have a high level of glucose on day 2 that was considered anomalous. Though this patient did not have any post-operative conditions, they did have Stage 3 chronic kidney disease for which, there is evidence that glucose metabolism is commonly compromised due to insulin resistance (de Boer 2008, Siew & Ikizler 2008). While not necessarily diagnosing any post-operative conditions, it could be seen that monitoring glucose can be a useful tool, particularly when there is evidence to show high levels of glucose can cause issues with healing by interfering with growth factors, cytokines, etc. In addition, high levels of glucose can provide a medium for bacteria to proliferate (Cuomo et al. 2019, Patel 2008). Control of glucose levels is therefore important during the post-op period to allow healing to occur and prevent conditions such as anastomotic leakage from occurring and therefore real-time monitoring of this parameter is important.

Patient 15 exhibited an unusual rise in glucose levels on day 4 and 5, where on Figure 5.3, an increase of 7-8mM occurs. This is a very unusual increase and was considered anomalous. There could be several reasons for this. The first could be that this could coincide with when the patient switched to solid foods. Many of the patients are seen to have a slight increase/plateau in glu-

cose measurements which could be associated with this switch. Patient 15 potentially could have a much more notable peak versus other patients. Another reason could be that a minor event occurred, such as a minor asymptomatic anastomotic leak, which resolved itself and no adverse problems were noted by the patient or clinicians. Proving this in future work maybe challenging however as it may require the use of a CT scan when a similar event occurs, which could be hard to justify, particularly when the risks of CT scan are considered.

Summary

An assay was developed, tested and used to measure glucose peritoneal drain concentrations. Glucose levels peaked on day 1 after post-op which then dropped over time for which, a strong trend was found. It was found that there was a difference in glucose levels when samples were filtered prior to testing on day 1 samples, most likely due to higher levels of blood contamination. Larger studies are required to confirm the trends found as well as to see if any post-operative conditions could be linked to outlying glucose measurements as shown by patients 8, 12 and 15. No information was gained with glucose trends with regards to anastomotic leakage so it was difficult to tell whether this marker can be used for diagnosis but maybe worth further exploring to see whether differences can be found between patients with and without leakage in a similar vain to outlying patients found in this study.

6.2.3 pH

Another outcome of ischaemia is a reduction in pH due to the consequences of anaerobic respiration, such as lactate production. This drop in extracellular

pH has been found to be an important factor in healing of tissues, particularly in literature with regards to skin wound healing, for which healing of colorectal tissue is thought to be analogous to (see Section 1.4.2). Lower pH values (neutral/acidic) have been found to be associated with reduced risk of chronic wound due to enhancing the inflammatory response. In addition, the reduction of pH is also associated with reduced infections as bacteria cannot effectively colonise the wound. However, prolonged reduction of pH may cause more harm than good with evidence to show that molecules such as neutrophils exhibiting an amplified and sustained response which can negatively affect growth factors and can cause degradation of the extracellular matrix leading to chronic wounds (Schneider et al. 2007, Jones et al. 2015, Millan et al. 2006, Nagoba et al. 2015).

The pH within the large intestine varies depending on location with the lowest pH normally found at the caecum, with a pH of about 6.4, that rises gradually across the large intestine to about 7.5 at the rectum (Nugent et al. 2001, Evans et al. 1988). The pH of peritoneal fluid is approximately 7.5-8 (DiZerega & Rodgers 1992) so it could be plausible that leakage from the colon could also contribute the lowering of pH levels in drain fluid that could be detected.

It was therefore decided, it may be worth looking at pH due to the aforementioned reasons to see if any trends could be associated to post-operative leakage. pH was measured using a standard glass pH probe using the methodology described in Section 3.4.2 (theory of pH measurement can be found in section 2.4.3). Looking at the results presented in Section 5.5, no discernible trend could be established from either unfiltered or filtered results which was not expected due to the reasons mentioned above (reduced pH to aid in healing before recovering to normal levels in uncomplicated cases) and based from

the limited literature and data that had looked into pH due to anastomotic leakage. In addition, a large range of values were found which has not been indicated by previous studies (see Section 5.5).

Little literature exists on measuring the pH as a diagnostic tool for anastomotic leakage. Yang et al. (2013) found, when measuring drain fluid in patient after rectal surgery, that a significant drop on pH on day 3 was associated with anastomotic leakage and proposed a threshold of 6.978 on day 3 to determine whether a patient was going to have an anastomotic leakage which was determined to have a high sensitivity (98.7%) and specificity (94.7%). However, in the paper, Yang et al. (2013) provided very little information with regards to pH and anastomotic leakage with only mean values being provided (errors bars are provided but it is unclear whether this is standard deviation, standard error or something else). In this study, more information was gained such as the range of measurements, which were seen to be large during the post-op period. The large range of values found may dispute whether the high levels sensitivity and specificity found by Yang et al. (2013). Similar results were found by Millan et al. (2006), using balloon tonometry, who claimed that there was an increased risk if the pH within the colon near the surgical site was below 7.28.

In this study, a couple of patients were found to be below both thresholds that were determined by Millan et al. (2006) and Yang et al. (2013). Patient 17 who had the lowest pH value on day 3 of 6.7 was found to have no complications after surgery. The other patient who also was below this threshold was patient 1 who had post-op complications of having low haemoglobin levels. This does make some sense as with reduced haemoglobin levels, less carbon dioxide (being produced due to respiration) is being removed. Increased carbon

dioxide results in reduced pH (Arthurs & Sudhakar 2005). This highlights the fact that while anastomotic leakage may cause a drop in pH, other complications could also cause this drop and care must be taken when analysing results.

In this thesis, no changes/trends in pH could be determined. pH of the peritoneal fluid may have dropped versus the patients normal pH. The way to test this would be to acquire peritoneal fluid from the patient prior to surgery but there are ethical issues with this approach.

An observation that was made with the first several samples was the high levels of blood contamination that was present in day 1 samples. As a check, some of the later fluid collected from patient 13 onwards were filtered and also measured using the glass pH probe. It was found when stats tests were performed that there was a significant difference between filtered and unfiltered day 1 samples with a mean decrease of 0.133 in pH when samples are filtered. There are a couple of reasons for this occurring: first, blood has a pH of approximately of 7.4 (Aoi & Marunaka 2014) which is lower than that of peritoneal fluid. Due to the high levels of blood contamination observed in these day 1 samples, it could be possible that enough blood is present to bring the overall pH down. A second possibility is potentially there is a higher presence of blood, bacteria, etc. in these day 1 samples undergoing processes (e.g. anaerobic respiration, etc.) that causes the pH to drop during the transport of samples from the hospital to the university. In order to understand better what is occurring to cause the drop in pH, a more detailed look at the microbiology is most likely required and potentially an experiment looking at the effect of time on the sample is needed.

Based on these results, it would seem that pH would have a low utility for

determining anastomotic leakage or other post-op conditions, though a larger study would be needed to confirm this. Though pH measurements in this experiment did not yield any trends in terms of diagnosing anastomotic leakage or other post-operative condition, a potential alternative that could yield more success is measuring the pH both intraluminal and extraluminal (or drain fluid) of the anastomotic site. Anastomotic leakage could be confirmed if the pH of both measurements are similar to each other.

6.3 Electrochemical Testing

6.3.1 EIS

Electrochemical Impedance Spectroscopy (EIS) is a well-known technique used to diagnose systems. This is done by inputting a potential perturbation to the system and measuring its impedance response over a range of frequencies. Several biological phenomena have been found previously with alpha, beta and gamma dispersions being characterised and related to characteristics such as permanent dipoles, etc. Several studies have investigated looking at identifying and characterising various components of biological fluids such as identifying differing types of bacteria, looking at metabolites, distinguishing between cancerous and non-cancerous tissue, etc. Therefore, EIS was used in this thesis to understand and to investigate peritoneal fluid and to see if any trends could be identified that could be related to components of the fluid and if that could be related to post-operative complications after colorectal resection.

Preliminary Experiments

Initial Testing with Solution A

Initial tests of the proposed methodology were performed with Solution A, a simulated wound fluid exudate, to test the initial methodology would work with low volumes (0.5, 1 and 2mL) that maybe received from the hospital (see Section 3.5.5).

It was clear to see from Figures 4.5, 4.6 and 4.7 that changes in volume resulted in changes in resistance, reactance, magnitude and phase values. More specifically, reduction in volume resulted in higher resistance, reactance and modulus values. In addition, phase values were higher with lower volumes low (<10Hz) and lower at higher frequencies (>10Hz). The results from this were expected due to the fact that the change in volume would result in changing contact areas which would affect the current and highlighted the need for a fixed contact area. As it was thought that samples from patients would be low, it was decided that using a volume of 500 μ L would be adequate for the technique.

Testing of a More Representative Drain Model Fluid

While Solution A was a good starting point to test methodologies, its main disadvantage in this case is that it does not represent the complexity of the fluid to be collected from patients and therefore the results gained in the previous experiment may not be representative. To try to understand the electrochemical behaviour that maybe determined from patient samples an artificial peritoneal exudate (APE) was created which had several of the ions at appropriate concentrations. This was based on a paper by Kelton et al. (1978) which provided the concentration of various items found in human peritoneal

fluid samples (See Section 3.2.2). It was expected that blood contamination and/or bacteria may be the main elements that change the results in patient fluid. As a result, this artificial fluid was then spiked with horse blood and/or bacteria to further simulate what could happen due to surgical trauma and/or leakage of colon contents to see if it was possible to attribute changes in results to these components. This was performed as described in Section 3.5.6.

From Figures 4.8, 4.10 and 4.11, it was observed that the addition of various components to the simulated fluid caused changes to the results gained through EIS testing in resistance, reactance, modulus and phase values. This was further reinforced when ANOVA analysis found differences in various frequencies between the variously spiked fluids in all the plots as shown in Figures 4.9 and 4.12. For example, changes between APE and APE with PA could be found by observing the resistance at frequencies higher than 20Hz whereas changes between APE and APE with *E.coli* could be observed by looking at resistances below 20Hz.

For EIS to be a useful method of post-operative monitoring, it should be able to distinguish between various components of the fluid. Here it could be seen that distinctions could be made between variously spiked samples at multiple frequencies. This indicates that potentially for clinical samples that monitoring changes at frequencies could be related to an item in sample that in turn could aid in diagnosing anastomotic leakage or other post-operative conditions. However, due to the multiple regions where changes can be observed, it may be best to try to find a single or narrowband of frequencies that is related to a component of the fluid or reduce the amount and time required to perform the analysis. One way of doing this is to normalise the results.

Normalisation of Artificial Peritoneal Exudate

One of method that has been used to distinguish between elements in a test sample is the use of normalisation, where results are standardised against a reference. In this case, using a patented technique, data gained from patients were normalised against their day one result at each frequency tested for the EIS measurements (see Section 3.6.2 for further details).

It could be seen in the resultant modulus and phase plots (Figure 4.13 and 4.14) that it was easier to spot changes that were occurring that could be attributed to how the fluid was spiked. For example, the addition of *E.coli* to the artificial exudate caused a peak change in modulus change at low frequencies (<1Hz) and a peak change in phase at approximately 400Hz. Whereas, the addition of blood caused a peak modulus change at approximately 100Hz. These results gave an indication that it may be possible to monitor specific frequencies to distinguish between components but would also allow a method to reduce the amount of data/work required for future analysis in a potential device.

Modelling of Artificial Peritoneal Exudate

Results from EIS measurements can be used to fit equivalent circuits. This circuit can be used to model various aspects of the fluid and set-up, e.g. electrodes (see section 2.4.1). In this experiment, it was found that the resultant EIS signatures could be modelled like a modified Randles circuit with a Constant Phase Element (CPE) instead of a capacitor as shown on the top of Figure 4.15.

The need to replace capacitor with a CPE was not surprising as it has been found in previous literature that solid electrodes, like the platinum wires used

in this experiment, have been shown to cause frequency-dependant dispersions (Lasia 2014).

From the model that was approximated, the following parameters are given and displayed in Table 6.1: Solution resistance, faradaic resistance and the capacitive and phi term of the CPE (see section 2.4.1 for further information about the mathematical model of the Randles circuit with CPE).

Table 6.1: Calculated parameter values of spiked solutions (mean \pm SD)

	Mean Solution Resistance/ Ω	Mean Faradaic Resistance/ $M\Omega$	Capacitance / μF	Phi
APE	533.32 \pm 98.43	10.69 \pm 20.24	6.01 \pm 1.23	0.72 \pm 0.04
APE+HB	675.44 \pm 110.67	40.26 \pm 10.23	4.49 \pm 0.89	0.66 \pm 0.01
APE+E.Coli	526.67 \pm 113.09	10.53 \pm 10.47	4.28 \pm 2.63	0.76 \pm 0.05
APE+P.Aeruginosa	548.46 \pm 93.08	3.63 \pm 2.94	7.15 \pm 2.91	0.77 \pm 0.04
APE+HB+E.Coli	746.92 \pm 91.67	10.59 \pm 10.21	4.49 \pm 1.94	0.75 \pm 0.06
APE+HB+P.Aeruginosa	720.51 \pm 66.61	7.79 \pm 6.40	6.51 \pm 2.39	0.78 \pm 0.04

Solution resistance could be seen to particularly change with respect to the addition of blood at first glance (Figure 4.16) where increases could be seen. It was found that significant differences were found in between APE+HB+E.coli versus unspiked APE and APE+E.coli. A similar trend was seen with PA but was not considered significant. Why the addition E.Coli and blood caused a significant increase in solution resistance could be as a result of interactions that occur between blood (particularly platelets) and *E.coli* (Fejes et al. 2018, Matus et al. 2017).

Faradaic resistance was found to drop substantially with the addition of *P.aeruginosa* (PA) and increase with the addition of blood. Significant differences were found between APE+HB vs APE+PA and APE+HB+PA. The capacitance term of the CPE was found to be similar between all the sam-

ples but the phi value of the CPE was found to decrease with the addition of blood and increase with PA. Significant differences were found, similar to what was found in faradaic resistance, between APE+HB versus APE+PA and APE+PA+HB. The phi term represents how much of a deviation the component is from a purely capacitive component where 1 equals a purely capacitive component and 0 equals a purely resistive component.

The drop in faradaic resistance and increase in the phi term of the CPE with the addition of PA could be explained by the fact PA is able to affect electron transfer through metabolites it produces such as phenazine-1-carboxylic acid and pyocyanin which can act as electron mediators (Ali et al. 2017, Bosire et al. 2016). By being able to improve electron transfer at the interface between solution and electrode, PA is able to reduce the faradaic resistance and increase phi. This also indicates in turn that blood must inhibit electron flow and thus increases the faradaic resistance and causes the CPE to act more as a resistor which may be due to the fact that cells in blood tend to adsorb onto the surface of materials (Gingell & Fornes 1976, Khubutiya et al. 2010, Vogler 2012).

Previous studies that have investigated other bodily fluids have found some values to be of similar magnitudes to results found here. For example, Ribaut et al. (2009) found values of $526\text{-}746\Omega$ and $1.53\text{-}7.79\text{M}\Omega$ for solution and faradaic resistance. Silue et al. (2017) found vitreous humor to have a similar solution resistance to what was found here (659.83Ω) as well as a similar CPE capacitance of $1.18\mu\text{F}$. However, differences have been found as well with Ribaut et al. finding the capacitance of the double layer to be a magnitude of 10 lower at $0.65\mu\text{F}$ and the associated phi value was found to be at approximately 0.95 (higher than found here of approx. 0.7) and both the faradaic

resistance and the phi values were found to be much lower in vitreous humor when compared to peritoneal fluid (24.49k Ω and 0.54) (Silue et al. 2017). Additionally, Muñoz-Berbel et al. (2007) found solution resistances of *E.coli* suspensions to be approximately 230 Ω with CPE capacitance and phi values to be approximately 0.13 μ F and 0.90. Differences can be attributed to the differing make up of fluids tested. In addition, the lower phi values found in this thesis could be attributed to the electrodes. Muñoz-Berbel et al. (2007) used a disk electrode and Ribaut et al. (2009) used microelectrodes whereas here, platinum rods were used.

When the above parameters were later compared to patient samples, it was found that values obtain were of similar magnitude (Table 6.2). For example, the average faradaic resistance from patients with uncomplicated post-op courses was 2.24 \pm 1.66M Ω and the range of values obtained from the variously spiked values ranged from 1.53-7.79M Ω . This indicates that the created simulated fluid could be used as a good starting point for preliminary testing for other experiments looking at peritoneal fluid.

The results found in this section indicate that changes to each of the parameters could be related to a component in the fluid such as bacteria or blood. Previous studies have been done to relate changes in models to the addition of disease or other substances (explained further in clinical modelling section). Therefore, monitoring of these parameters maybe useful in clinical samples as it could be linked to post-operative conditions.

Clinical Results

After preliminary testing, samples were collected and transported to the hospital as described in Section 3.2.8.

Uncomplicated Post-op Patients

Patient drain samples were tested in a similar way to the artificial peritoneal exudate. It was found that the patients' who had an uncomplicated post-op had EIS signatures that were similar to each other and tests found no significant changes over time (Figures 5.10, 5.11 and 5.12). This is surprising considering that it would be expected that, due to the changing composition of the fluid over time, the EIS results would also change. For example, one obvious change was the observed reduction of blood contamination in the patient samples over time that affected the glucose results. Previous studies have also indicated differences in ion and protein concentrations as well as indications that the rheology of the peritoneal fluid changing over time during the post-op period after abdominal surgery (Bhusal et al. 2018).

The fact that the EIS signals received over time remained similar could indicate that though changes are most likely taking place in the fluid between each time point in (at least) patients with uncomplicated post-op, the amount of change occurring is relatively minimal that it causes little to no influence on the signal and/or is being dominated by other substances such that it does not register on the signal.

To try and further understand how the fluid behaved, the fluid was filtered using 0.22 μ m filter. The use of a 0.22 μ m filter removes larger items in the fluid such as red blood cells ($\approx 7\mu$ m) and bacteria ($>0.22\mu$ m) (Bruil et al. 1995, Chen et al. 2016). When samples were filtered by a 0.22 μ m filter, more separation of signals were noticed over the post-op period as seen in the Nyquist and bode plots shown in Figures 5.13, 5.16 and 5.17, particularly on day 2. The filter allows ions and small molecules such as glucose and lactate through. This therefore indicates the changes in received signals in filtered samples

are due to ionic components/metabolites which maybe being hidden behind items that have a greater influence on the signal. This is further indicated by the fact that when statistical tests were performed, significant changes were found at lower frequencies as shown in the resistance, reactance and modulus value as shown in Figures 5.14, 5.15 and 5.18, where an increase occurs from day 1 to 2 before dropping on days 3 and 4. As stated previously in Section 2.4.1, at these low frequencies, changes are usually associated with cell membranes and the surrounding environment and are known as alpha dispersions. Changes associated to this can be due to a number of possibilities including metabolic exchange and ions present in the item of interest (Dean et al. 2008, Kuang & Nelson 1998, Schwan 1957). It is most likely that this change was as a result of due to the trauma of surgery. Initial thoughts looked at comparing the trends of glucose and lactate to results found here, however, lactate and (more so) glucose were found to drop immediately after day 1 post-op making them unlikely targets. Other molecules that could be candidates for this change include inflammatory markers (such as cytokines), potassium, growth factors, etc. which have been shown to increase due to surgical trauma (Bhusal et al. 2018, Brokelman et al. 2011, Haney 2000).

In order to narrow down the candidates that could be responsible for this change, future studies should monitor various metabolites/ions and see if they follow the same trend or continue to measure patients in a similar manner with EIS and see if this changes with regards to a particular post-operative condition and/or pre-operative condition.

Data gained from unfiltered and filtered samples were also investigated to try and identify trends in how they varied. Several significant changes were found, particularly in the phase measurement as shown in Figure 5.19. One

significant difference found that, around the 1kHz region, the average mean phase value on days 2 and 3 increased when samples were filtered, as shown in Figure 5.20, with a larger change on day 2 which decreased on day 3. Changes in this region can be associated with β -dispersions which are changes that are associated to cellular structures and how they interact. It could be plausible that this change could be associated to a larger molecule that maybe present in high enough quantities to affect the unfiltered signal. However, one more likely possibility is that this could be due to the presence of bacteria which can present in the fluid due to its release from the colon during the surgery (Komen et al. 2014). Previous studies have found bacteria caused changes in phase measurements with time, for example in Ward et al. (2018) found that *S. aureus* caused a large change in phase angle at around 1kHz in the phase plot (approx. peak change of 9%).

It is possible that the bacteria released from the colon starts replicating during the first post-op day to cause a significant change on day 2, before being combated by the immune response, causing a reduced change on day 3 prior to no significant changes occurring on day 4 due to the reduction of bacteria. Patients in this study who went through an uncomplicated course were not given antibiotics. Both Komen et al. (2014) and Junger et al. (1996) found increases to bacteria between days 2 to 4. This in turn could also explain why there was a significant difference in low frequency values of impedance modulus on days 2, 3 and 4 as the bacteria may have produced/secreted various items, for example, *P. aeruginosa* produces pyocyanin which has been shown to have an effect on impedance measurements. Some of these by-products can pass through the filter which could explain the significant differences (Ward et al. 2014, Singh et al. 2010). In order to confirm this suspicion, microbiology

studies of samples would need to be done.

Complicated Post-op Patients

When looking at the EIS results from patients with complications, several patients' signals stood out as being substantially different to patients who did not experience a post-op complication: Patient 1, 12 and 19.

When Patient 1's sample was tested, it was noticed that the both the resistance and reactance values found for all the days were substantially lower than the average uncomplicated patient sample. For example, the average Z' and Z'' for patients with uncomplicated post-op on day 1 at 1Hz was $215,511\Omega$ and $-38,568\Omega$ whereas, patient 1's day 1 value at the same frequency was 5947Ω and $-10,492\Omega$, a 36-fold difference in resistance and 4-fold difference in reactance (seen in Figure 5.23). This patient was also found to have low haemoglobin levels during the post-op period. This drop in measured resistance and reactance was similar to what was found in Section 4.4.2 where artificial peritoneal exudate exhibited higher impedance values when it was spiked with horse blood. Previous studies have also found that an increase in haemoglobin also causes an increase in resistance (Tran et al. 2018).

Both patient 12 and particularly patient 19 were recorded to have higher resistance and reactance, particularly at lower frequencies (for example at 0.1Hz Day 1 uncomplicated patient average $Z'=119,509\Omega$, $Z''=170,425\Omega$. Patient 12 day 1 $Z'=126,907\Omega$, $Z''=-197,923\Omega$. Patient 19 day 1 $Z'=311,565\Omega$, $Z''=-439,065\Omega$) as shown in Figures 5.23 and 5.24. Both patients experienced the same post-operative conditions (lower respiratory tract infection and ileus).

Both patient 12 and 19 had changes in the high frequency range of the phase plot (seen in patient 19 normalised graph – Figure 5.28). Changes in this

range are due to cellular structure interactions which could indicate bacteria associated with the infection or another marker that is associated with ileus, potentially inflammatory markers/IL-1 signalling pathway (Vilz et al. 2015).

Patient 19 had something that represented a double peak on day four with a second peak at approximately 1kHz which showed up as a peak of approximately 1.3 when normalised in Figure 5.28. This peak coincides with a bacterial peak that has been seen previously in other studies such as Ward et al. (2018) who found a normalised peak change of approximately 0.09 in phase at 1kHz with the addition of *S. aureus*. This is further indicated by the fact that this peak is reduced from approx. 1.3 to 1.09 when the sample was filtered (which would have removed bacteria) and measured.

The results here show that it may be possible to determine post-operative conditions via the application of EIS and mathematical normalisation of impedance parameters. However, to confirm this belief, more, larger studies are required as well as microbiology studies of samples, particularly in regards to post-operative conditions that may be as a result of bacterial infections.

Modelling of Patient Samples

Results from EIS experiments can be used to create representative electrochemical models for which several parameters can be determined (see Section 2.4.1). In Section 4.4.2, it was found that the use of a modified Randles circuit (where the capacitor was replaced with a constant phase element) fitted the artificial peritoneal exudate. The same circuit was therefore used to fit results gained from the EIS measurements on clinical samples for which 4 parameters were calculated; Solution resistance, faradaic resistance, capacitance and phi. The average values for patients with non-complicated post-op

courses are found in Table 6.2.

Table 6.2: Average modelling parameter values obtained from clinical samples. Mean \pm SD

	Solution Resistance / Ω	Faradaic Resistance / $M\Omega$	Capacitance / μF	Phi
Average from unfiltered uncomplicated patient samples	426.34 \pm 57.85	2.24 \pm 1.66	7.91 \pm 2.72	0.70 \pm 0.04
Average from filtered uncomplicated patient samples	416.61 \pm 57.47	2.80 \pm 1.64	7.44 \pm 3.07	0.68 \pm 0.03

Solution resistance for most patients were found to be within a relatively tight band with mean value of 426.35(\pm 57.85) Ω for unfiltered samples and 416.61(\pm 57.46) Ω for filtered samples. Patient 12's solution resistance values were found to be high versus other patients, particularly on days 2 and 3 ($>1k\Omega$), as seen in Figure 5.30. Patient 12 was found to have an ileus and a lower respiratory tract infection. This increase could potentially due to the higher levels of glucose and lactate that was found earlier for patient 12 which follow the same trend. Glucose has been found to increase solution resistance to a point in previous papers in simpler fluid such as in Olarte et al. (2014) who found a sharp rise up to approx. 70mg/dL glucose. In order to confirm this, a future experiment where patient samples were spiked with either glucose or lactate for which an EIS measurement occurred before and after this step could be done.

Unlike results for solution resistance, large variations were found in faradaic resistance with values ranging from 1.6 to 6.62 $M\Omega$ (Figure 5.31). The large range in values could be due to the large number and variation of items that could be present in the clinical samples that interact with the electrode and affect its resistance. Capacitance and its associated phi value for the constant phase element were found to stay within a narrow band of values during the

time period (2-20 μ F, 0.64-0.76)(Figures 5.32 and 5.33).

However, it was found that there was a significant difference in capacitance between unfiltered and filtered samples on day 2 with a mean drop of 2.64 μ F when filtered indicating that an element that was filtered out was contributing to capacitance value such as bacteria which has shown to affect the capacitance in previous studies (Kim, Kang, Lee & Yoon 2011, Ward et al. 2018). Another difference that was found was that the phi values for patient 1 were relatively high on days 3 and 4 (>0.8). Patient 1 was found to have low haemoglobin levels during the post-op period and follows a similar trend found during the initial testing where the removal of horse blood caused increases in phi values (Section 4.4.2). While this was not significant between APE and APE spiked with blood, it could be worth monitoring in future testing with patients also exhibiting the same post-operative condition. In order to confirm this and the changes in capacitance, microbial studies of the samples would be needed for future studies.

Previous studies have looked at different fluids and how they are affected by differing conditions such as the study by Ribaut et al. (2009) used modelling to investigate red blood cells and how values given from models were affected by malaria. On top of the solution resistance, faradaic resistance and double layer capacitance, other components were added to represent the red blood cell (additional resistance and capacitance). It was found that the solution resistance and faradaic resistance of blood to be 470 Ω and 2M Ω with the use of gold electrodes, which is similar magnitude to values found here (526-746 Ω , 1.53-7.79M Ω). The capacitance of the double layer was however found to be a magnitude of 10 lower at 0.65 μ F and the associated phi value was found to be at approximately 0.95 (higher than found here of approx. 0.7). It was found

that the faradaic resistance as well as other components that were also included to represent the red blood cell varied were found to drop as a result of the malaria. Vitreous humor has also been modelled with an additional CPE element for characterisation studies for future studies in associated issues related with the eye (e.g. retinal detachment). This has also been found to have a similar solution resistance to what was found here (659.83Ω) as well as a similar CPE capacitance of $1.18\mu\text{F}$. However, both the faradaic resistance and the phi values were found to be much lower when compared to peritoneal fluid ($24.49\text{k}\Omega$ and 0.54) (Silue et al. 2017). Though only one outlying event maybe related to a patient in these results, it maybe continuing to monitor the parameters in larger scale studies to see if any of the parameters can be used to determine any post-op complications.

While models were found to fit well a limitation of the model is that it is quite simple. It describes the interface between the electrode and solution as a CPE and resistor in parallel, and the solution itself is described as resistance. More complex modelling could potentially improve the fitting by including the electrochemical behaviour of components in the solutions such as cells by modelling the cell membrane and its contents as a capacitor and resistor like what was done in Ribaut et al. (2009). While the EIS modelling in this thesis is relatively basic, its strength is in its simplicity and allows for quick evaluation of several parameters. More work should be performed to see how the parameters change with post-op complications, but the model used here provides a good foundation to further develop more complex models if required.

Timed Experiment

Previous studies have looked at bacteria and its effect on the EIS signal over

time (Ward et al. 2014, 2018). This has been done by monitoring the same fluid over a period of time and looking at the changes that have been exhibited. A timed experiment was therefore performed where fluid was measured initially when received, as well as 6 and 24 hours later for which the results are presented in Section 5.6.4.

An interesting result that was yielded from this experiment involves patient 21. It could be seen that large changes could be seen in this patient's resistance, reactance, modulus and phase values over time as seen in Figures 5.34, 5.35 and 5.36.

Results were then normalised, as described in Section 3.6.2, as previous studies have found that this can be used to help identify various components of samples. When results were normalised, the changes in patient 21's signal that were noted earlier became much more exaggerated, particularly in day 3 modulus and phase values where changes of 7-11 times were seen at low frequencies with a peak change at 0.126Hz in the modulus results and at 12.58Hz in the phase results (Figures 5.37 and 5.38).

This change in patient 21's signal could be attributed to the fact that they had a urinary tract infection and the bacteria causing this infection could be the cause of the signal changes. It is difficult to say how the drain fluid contained the bacteria causing the UTI, but this maybe as a result of a hospital acquired infection, which tends to happen at a higher frequency compared to other operations (Sheka et al. 2016), where the bacteria was introduced to urinary tract and the peritoneum in a similar time period.

From the initial experiments in Chapter 4 (Figure 4.14), it was seen that the addition of *E.coli* to the artificial peritoneal exudate (APE) caused a similar

peak in modulus of approximately 1.6 times higher than a unspiked APE at a similar frequency ($\approx 0.5\text{Hz}$) to the result gained by patient 21 on day 3. It should also be noted that in the same figure that the addition of blood with *E.coli* also caused this peak to be masked, so it could be plausible that if samples from patient 21 on days 1 and 2 had only blood removed and were then tested, a similar result could have been produced on these days. Similar changes in phase have been found in papers by Ward et al. (2014, 2018) where changes were found in phase and resistance at low frequencies due to the addition of bacteria (*P. aeruginosa* and *S. aureus*). In order to confirm that bacteria are causing these changes, future testing should include streaking samples on agar plates when received from the hospital on top of using the testing performed here. This will allow identification of bacterial species in the samples as well as the concentration of bacteria in the sample.

Summary

EIS methods were developed, tested and used in clinical peritoneal samples to identify components that could be related to post-operative conditions. Some results indicate that changes in the EIS could be related to post-operative conditions such as bacterial infection. However, more larger scale studies are required with further understanding of the microbiology of the samples.

6.3.2 Cyclic Voltammetry

Initial Testing

Initial experiments looked at the limits of measurable current with regards to changing volumes. A couple of peaks were found in one or two of the peaks. One at approximately -0.25V which can be associated with adsorption

onto platinum. A large drop in current can also be seen at potentials below -0.8V which can be associated with the dissociation of water (Patzner et al. 1989). Current limits were found to be in the micro-ampere range and the experiment highlighted the need to keep a clean electrode surface.

After this experiment was performed on an artificial peritoneal exudate to see if it was possible to see if any reactions/regions of interest that maybe worth looking at for use in clinical sample collection. Like in the volume graphs, the drop in current below -0.8V could be associated with water dissociation. Other than this, it was found that no reactions could be determined from the results. This indicated that utility of cyclic voltammetry maybe limited as redox reactions may not be able to overcome the noise in the signal and be seen in the voltammogram.

Clinical Testing

When the same technique was applied to the clinical drain samples, it was found in both the unfiltered and filtered results with no discernible peaks appearing (Section 5.7). The lack of changes (peaks) in the current-voltage graphs was not particularly surprising based on the initial testing in section 4.4.2 for the similar reason that there is a multitude of substances in the fluid causing a large enough noise for which any redox reactions which may have occurred not appearing during testing. In order to overcome this, the use of differing electrodes which are specific for certain molecules may be required. For example, a metal electrode could be coated with a glucose oxidase enzyme to measure for glucose.

6.4 Conclusions and Future Work

Anastomotic leakage is a potentially life-threatening complication for which there is no universally accepted method of diagnosing. The aim of this thesis was to work towards determining a biomarker/method of determining anastomotic leakage so clinicians can intervene at an early stage with the appropriate action. Several biomarkers and methods were investigated in peritoneal drain fluid: Glucose, Lactate, pH, EIS and cyclic voltammetry. It was thought that there would be a high potential to generate a method to detect anastomotic leakage with a view of a developing a point-of-care device.

Initially, methodologies for testing patient samples had to be developed. For glucose and lactate, a commercially available assay kit was modified for use and characterised successfully for use with patient samples. EIS and CV methodologies were also tested and gave an indication of how to perform analysis of patient samples.

After testing developed methodologies were used to test patient samples who had undergone colorectal resection. One patient did experience anastomotic leakage but due to unfortunate circumstances, little data was procured from this patient. However, information about how patients who underwent an uncomplicated post-operative as well a few patients who experienced other post-operative complications was acquired.

Based on the analysis, it is thought that the methods that have a high potential of determining anastomotic leakage (and other post-op conditions for that matter), would be looking at glucose concentrations or EIS results over the post-op period. Glucose produced a strong trend during the post-operative period. Therefore, it would be worth into further with a larger scale study to

see if it deviates from this trend when post-operative conditions occur. While one patient who had a post-op condition in this study did exhibit anomalous data, more data to see if that is a reoccurring trend.

Table 6.3: Changes found possibly due to post-op complications

Patient	Post-op condition	Deviations
1	- Low-Hb count	- Reduced resistance and reactance values in EIS results
12	- LRTI - Ileus	- High (outlying) Glucose on days 2 and 3 - High (outlying) Lactate on days 2 and 3 - High resistance and reactance EIS values
19	- LRTI - Ileus	- High resistance and reactance EIS values - Large changes in normalised EIS modulus and phase values
21	- Urinary Tract Infection	- Large changes in normalised modulus and phase values in timed EIS measurements (day 2 and particularly day 3)

Analysed EIS data produced some interesting trends which could help understand how peritoneal fluid changes during the post-operative period. Some changes were found in a few of the patients with post-operative conditions that included lower respiratory tract infections, urinary infections and low haemoglobin counts, indicating its potential but more work with larger scale studies being required as well as further understanding of how the fluid behaves in uncomplicated patients and then in patients with postoperative patients. Further understanding could be achieved by looking in more detail into the microbiology for example, bacterial studies of the drain fluid, and relating changes to the drain fluid. In addition, further work could look into the use of artificial intelligence to analyse the data and spot trends that may be otherwise be missed.

Lactate, pH and cyclic voltammetry were also looked into but based on the results, providing weak to no trends, future work in these areas should be discouraged with regards to post-operative monitoring of post-operative conditions.

A Potential Device for Continuous Post-surgical Monitoring

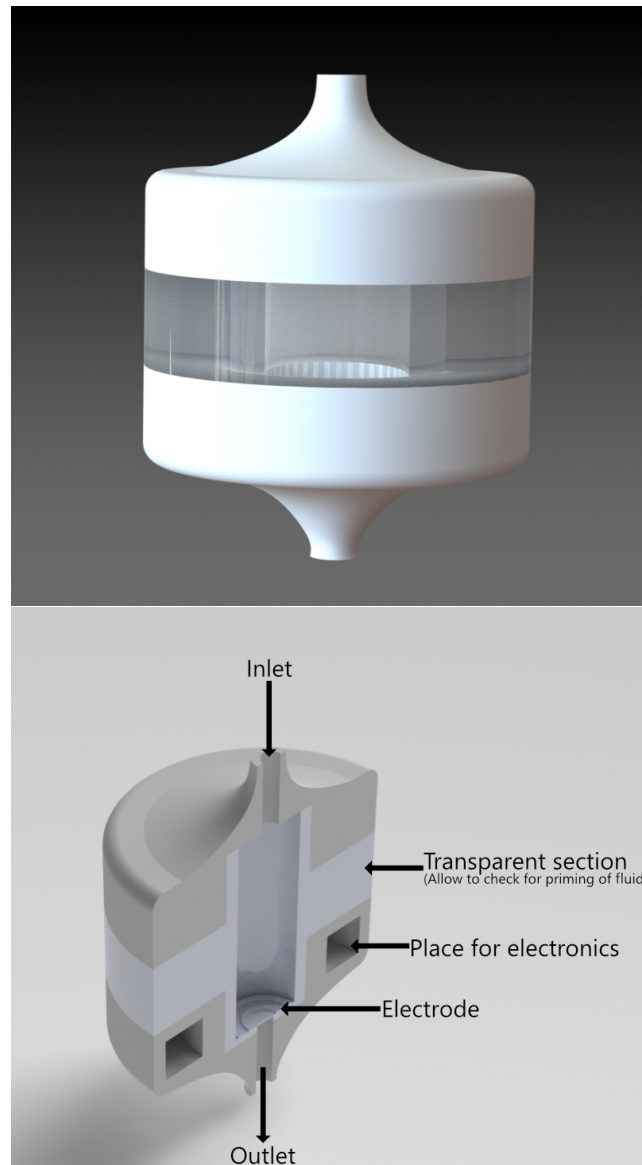


Figure 6.1: Potential device for post-op monitoring

Assuming that a robust method/biomarker of determining anastomotic leakage can be achieved and demonstrated in a larger scale study, the next step would be to develop a device that would allow for monitoring of the peritoneal drain exudate *in situ*. One way of achieving this is to develop device that can attach onto existing drain tubes such as conceptualised in Figure 6.1.

Drain tubes can be attached to either end to allow flow from the patient to the drain bags while sensors can monitor changes in the fluid as it flows through. This device could be linked to a computer system which can alert clinicians when deviations to the expected signal occurs and would therefore allow for early intervention of issues.

Development of a device towards an early warning system to diagnose anastomotic leakage and/or other post-op complication could potentially help avoid/reduce mortalities of patients. This thesis provided some interesting insight which could help towards this goal but further work is required.

References

- 2015 European Society of Coloproctology Collaborating Group (2020), 'Predictors for Anastomotic Leak, Postoperative Complications, and Mortality After Right Colectomy for Cancer: Results From an International Snapshot Audit.', *Diseases of the colon and rectum* **63**(5), 606–618.
URL: <http://www.ncbi.nlm.nih.gov/pubmed/32032201>
- Abbas, M. A. (2010), 'Endoscopic management of acute colorectal anastomotic complications with temporary stent.', *JLS : Journal of the Society of Laparoscopic Surgeons* **13**(3), 420–4.
- Ahmad, S. S., Duke, S., Jena, R., Williams, M. V. & Burnet, N. G. (2012), 'Advances in radiotherapy', *BMJ* **345**(dec04 1), e7765–e7765.
- Alcamo, I. E. & Warner, J. M. (2010), *Schaum's outline of microbiology*, 2 edn, McGraw Hill, New York.
- Ali, N., Anam, M., Yousaf, S., Maleeha, S. & Bangash, Z. (2017), 'Characterization of the Electric Current Generation Potential of the Pseudomonas aeruginosa Using Glucose, Fructose, and Sucrose in Double Chamber Microbial Fuel Cell', *Iranian Journal of Biotechnology* **15**(4), 216–223.
- Almeida, A., Faria, G., Moreira, H., Pinto-de Sousa, J., Correia-da Silva, P. & Maia, J. C. (2012), 'Elevated serum C-reactive protein as a predictive factor

- for anastomotic leakage in colorectal surgery', *International Journal of Surgery* **10**(2), 87–91.
- Althumairi, A. A. & Gearhart, S. L. (2015), 'Local excision for early rectal cancer: transanal endoscopic microsurgery and beyond.', *Journal of gastrointestinal oncology* **6**(3), 296–306.
- Alves, A., Panis, Y., Trancart, D., Regimbeau, J.-M., Pocard, M. & Valleur, P. (2002), 'Factors associated with clinically significant anastomotic leakage after large bowel resection: multivariate analysis of 707 patients.', *World journal of surgery* **26**(4), 499–502.
- Aoi, W. & Marunaka, Y. (2014), 'Importance of pH homeostasis in metabolic health and diseases: crucial role of membrane proton transport.', *BioMed research international* **2014**(598986), 1–8.
- Arezzo, A., Verra, M., Passera, R., Bullano, A., Rapetti, L. & Morino, M. (2015), 'Long-term efficacy of endoscopic vacuum therapy for the treatment of colorectal anastomotic leaks', *Digestive and Liver Disease* **47**(4), 342–345.
- Arezzo, A., Verra, M., Reddavid, R., Cravero, F., Bonino, M. A. & Morino, M. (2012), 'Efficacy of the over-the-scope clip (OTSC) for treatment of colorectal postsurgical leaks and fistulas.', *Surgical endoscopy* **26**(11), 3330–3.
- Arthurs, G. J. & Sudhakar, M. (2005), 'Carbon dioxide transport', *Continuing Education in Anaesthesia, Critical Care and Pain* **5**(6), 207–210.
- Ashraf, S. Q., Burns, E. M., Jani, A., Altman, S., Young, J. D., Cunningham, C., Faiz, O. & Mortensen, N. J. (2013), 'The economic impact of anastomotic leakage after anterior resections in English NHS hospitals: are we adequately remunerating them?', *Colorectal Disease* **15**(4), e190–e198.

- Association of Surgeons of Great Britain and Ireland & The Association of Coloproctology of Great Britain and Ireland (2016), Prevention, Diagnosis and Management of Colorectal Anastomotic Leakage, Technical report.
- Baker, E. A., El Gaddal, S., Aitken, D. G. & Leaper, D. J. (2003), 'Growth factor profiles in intraperitoneal drainage fluid following colorectal surgery: relationship to wound healing and surgery.', *Wound repair and regeneration : official publication of the Wound Healing Society [and] the European Tissue Repair Society* **11**(4), 261–7.
- Baker, S., Griffiths, C. & Nicklin, J. (2011), *Microbiology*, 4 edn, Garland Science, New York, London.
- Bard, A. J. & Faulkner, L. R. (2000), *Electrochemical Methods: Fundamentals and Applications*, 2nd edn, Wiley Textbooks, New York.
- Baskar, R., Dai, J., Wenlong, N., Yeo, R. & Yeoh, K.-w. (2014), 'Biological response of cancer cells to radiation treatment', *Frontiers in Molecular Biosciences* **1**(November), Article 24.
- Benoist, S., Panis, Y., Alves, A. & Valleur, P. (2000), 'Impact of obesity on surgical outcomes after colorectal resection', *The American Journal of Surgery* **179**(4), 275–281.
URL: <https://linkinghub.elsevier.com/retrieve/pii/S0002961000003378>
- Bertram, P., Junge, K., Schachtrupp, A., Götze, C., Kunz, D. & Schumpelick, V. (2003), 'Peritoneal Release of TNF α and IL-6 After Elective Colorectal Surgery and Anastomotic Leakage', *Journal of Investigative Surgery* **16**(2), 65–69.

- Betts, J. G., Young, K. A., Wise, J. A., Johnson, E., Poe, B., Kruse, D. H., Korol, O., Johnson, J. E., Womble, M. & DeSaix, P. (2018), *Anatomy & Physiology*, OpenStax, Houston, Texas.
- Bhusal, P., Rahiri, J. L., Sua, B., McDonald, J. E., Bansal, M., Hanning, S., Sharma, M., Chandramouli, K., Harrison, J., Procter, G., Andrews, G., Jones, D. S., Hill, A. G. & Svirskis, D. (2018), 'Comparing human peritoneal fluid and phosphate-buffered saline for drug delivery: do we need bio-relevant media?', *Drug delivery and translational research* **8**(3), 708–718.
- Blausen.comstaff (2014), 'Medical gallery of Blausen Medical 2014'.
URL: https://en.wikiversity.org/wiki/WikiJournal_of_Medicine/Medical_gallery_of_Blausen_Medical_2014
- Blumetti, J. & Abcarian, H. (2015), 'Management of low colorectal anastomotic leak: Preserving the anastomosis', *World Journal of Gastrointestinal Surgery* **7**(12), 378–383.
- Bockris, J. O. & Reddy, A. K. N. (2002), *Modern Electrochemistry 1*, Kluwer Academic Publishers, Boston.
- Bosire, E. M., Blank, L. M. & Rosenbaum, M. A. (2016), 'Strain- and Substrate-Dependent Redox Mediator and Electricity Production by *Pseudomonas aeruginosa*.', *Applied and environmental microbiology* **82**(16), 5026–38.
- Bosmans, J. W. A. M., Jongen, A. C. H. M., Bouvy, N. D. & Derikx, J. P. M. (2015), 'Colorectal anastomotic healing: why the biological processes that lead to anastomotic leakage should be revealed prior to conducting intervention studies', *BMC Gastroenterology* **15**(1), 180.

- Boyle, N. H., Manifold, D., Jordan, M. H. & Mason, R. C. (2000), 'Intraoperative assessment of colonic perfusion using scanning laser Doppler flowmetry during colonic resection.', *Journal of the American College of Surgeons* **191**(5), 504–10.
- Bray, C., Bell, L. N., Liang, H., Haykal, R., Kaiksow, F., Mazza, J. J. & Yale, S. H. (2016), 'Erythrocyte Sedimentation Rate and C-reactive Protein Measurements and Their Relevance in Clinical Medicine.', *WMJ : official publication of the State Medical Society of Wisconsin* **115**(6), 317–21.
- British Pharmacopoeia (1995), *Sodium chloride and calcium chloride solution*, HMSO, London.
- Britland, S., Ross-Smith, O., Jamil, H., Smith, A. G., Vowden, K. & Vowden, P. (2012), 'The lactate conundrum in wound healing: Clinical and experimental findings indicate the requirement for a rapid point-of-care diagnostic', *Biotechnology Progress* **28**(4), 917–924.
- Brokelman, W. J. A., Lensvelt, M., Borel Rinkes, I. H. M., Klinkenbijnl, J. H. G. & Reijnen, M. M. P. J. (2011), 'Peritoneal changes due to laparoscopic surgery.', *Surgical endoscopy* **25**(1), 1–9.
- Brouwer, N. P. M., Bos, A. C. R. K., Lemmens, V. E. P. P., Tanis, P. J., Hugten, N., Nagtegaal, I. D., de Wilt, J. H. W. & Verhoeven, R. H. A. (2018), 'An overview of 25 years of incidence, treatment and outcome of colorectal cancer patients.', *International journal of cancer* **143**(11), 2758–2766.
URL: <http://www.ncbi.nlm.nih.gov/pubmed/30095162><http://www.pubmedcentral.nih.gov/articlerender.fcgi?artid=PMC6282554>
- Bruce, J., Krukowski, Z. H., Russell, E. M. & Park, K. G. M. (2001), 'System-

atic review of the definition and measurement of anastomotic leak after gastrointestinal surgery', *British Journal of Surgery* **88**, 1157–1168.

Bruil, A., Beugeling, T., Feijen, J. & van Aken, W. G. (1995), 'The mechanisms of leukocyte removal by filtration', *Transfusion Medicine Reviews* **9**(2), 145–166.

URL: <https://linkinghub.elsevier.com/retrieve/pii/S0887796305800537>

Butler, S. O., Btaiche, I. F. & Alaniz, C. (2005), 'Relationship between hyperglycemia and infection in critically ill patients.', *Pharmacotherapy* **25**(7), 963–76.

Cancer Research UK (2015a), 'Surgery for colon cancer — Bowel cancer — Cancer Research UK'.

URL: <https://www.cancerresearchuk.org/about-cancer/bowel-cancer/treatment/surgery/surgery-colon-cancer>

Cancer Research UK (2015b), 'Types of surgery for bowel cancer'.

URL: <http://www.cancerresearchuk.org/about-cancer/type/bowel-cancer/treatment/surgery/which-surgery-for-bowel-cancer>

Cancer Research UK / Wikimedia Commons (2014a), 'File:Diagram showing a local resection of an early stage bowel cancer CRUK 068.svg'.

URL: https://commons.wikimedia.org/wiki/File:Diagram_showing_a_local_resection_of_an_early_stage_bowel_cancer_CRUK_068.svg

Cancer Research UK / Wikimedia Commons (2014b), 'File:Diagram showing T stages of bowel cancer CRUK 276.svg'.

URL: https://commons.wikimedia.org/wiki/File:Diagram_showing_T_stages_of_bowel_cancer_CRUK_276.svg

- Carstensen, B., Lindström, J., Sundvall, J., Borch-Johnsen, K. & Tuomilehto, J. (2008), 'Measurement of blood glucose: comparison between different types of specimens', *Annals of Clinical Biochemistry* **45**(2), 140–148.
- Castilla, D. M., Liu, Z.-J. & Velazquez, O. C. (2012), 'Oxygen: Implications for Wound Healing', *Advances in Wound Care* **1**(6), 225–230.
- Chadi, S. A., Fingerhut, A., Berho, M., DeMeester, S. R., Fleshman, J. W., Hyman, N. H., Margolin, D. A., Martz, J. E., McLemore, E. C., Molena, D., Newman, M. I., Rafferty, J. F., Safar, B., Senagore, A. J., Zmora, O. & Wexner, S. D. (2016), 'Emerging Trends in the Etiology, Prevention, and Treatment of Gastrointestinal Anastomotic Leakage', *Journal of Gastrointestinal Surgery* **20**(12), 2035–2051.
- Chefer, V. I., Thompson, A. C., Zapata, A. & Shippenberg, T. S. (2009), 'Overview of brain microdialysis.', *Current protocols in neuroscience* (Unit7.1).
- Chen, P.-C., Chen, C.-C. & Young, K.-C. (2016), 'Characterization of thermo-plastic microfiltration chip for the separation of blood plasma from human blood', *Biomicrofluidics* **10**(5), 054112.
URL: <http://aip.scitation.org/doi/10.1063/1.4964388>
- Choi, H.-K., Law, W.-L. & Ho, J. W. C. (2006), 'Leakage After Resection and Intraperitoneal Anastomosis for Colorectal Malignancy: Analysis of Risk Factors', *Diseases of the Colon & Rectum* **49**(11), 1719–1725.
- Chopra, S. S., Mrak, K. & Hünerbein, M. (2009), 'The effect of endoscopic treatment on healing of anastomotic leaks after anterior resection of rectal cancer', *Surgery* **145**(2), 182–188.

- Christensen, J. (1991), *Gross and Microscopic Anatomy of the Small Intestine*, in S. Phillips, J. Pemberton & R. Shorter, eds, 'The Large Intestine: Physiology, Pathophysiology, and Disease', Raven Press, Ltd., New York, chapter 2, pp. 13–35.
- Chu, K. M. (2010), *Epidemiology and Risk Factors of Colorectal Cancer*, in S. L. Gearhart & N. Ahuja, eds, 'Early Diagnosis and Treatment of Cancer Series: Colorectal Cancer', 1st edn, Elsevier, Philadelphia, chapter 1, pp. 1–11.
- Connolly, P. & Shedden, L. (2012), 'A System and Method for Cell Characterisation'.
- Constantinides, V. A., Heriot, A., Remzi, F., Darzi, A., Senapati, A., Fazio, V. W. & Tekkis, P. P. (2007), 'Operative Strategies for Diverticular Peritonitis', *Annals of Surgery* **245**(1), 94–103.
URL: <http://journals.lww.com/00000658-200701000-00015>
- Costedio, M. M. & Hyman, N. H. (2008), 'Outcomes of Colorectal Anastomosis', *Seminars in Colon & Rectal Surgery* **19**, 37–40.
- Cuomo, R., Nisi, G., Brandi, C., Giardino, F. R. & Grimaldi, L. (2019), 'Future Directions to Limit Surgical Site Infections.', *Journal of investigative surgery : the official journal of the Academy of Surgical Research* **0**, 1–3.
- Daams, F., Luyer, M. & Lange, J. F. (2013), 'Colorectal anastomotic leakage: Aspects of prevention, detection and treatment', *World Journal of Gastroenterology* **19**(15), 2293–2297.
- Daams, F., Wu, Z., Cakir, H., Karsten, T. M. & Lange, J. F. (2014), 'Identification

- of anastomotic leakage after colorectal surgery using microdialysis of the peritoneal cavity', *Techniques in Coloproctology* **18**, 65–71.
- de Boer, I. H. (2008), 'Vitamin D and glucose metabolism in chronic kidney disease.', *Current opinion in nephrology and hypertension* **17**(6), 566–72.
- Dean, D. A., Ramanathan, T., Machado, D. & Sundararajan, R. (2008), 'Electrical Impedance Spectroscopy Study of Biological Tissues.', *Journal of electrostatics* **66**(3-4), 165–177.
- DeArmond, D. T., Carswell, A., Loudon, C. L., Simmons, J. D., Bayer, J., Das, N. a. & Johnson, S. B. (2013), 'Diagnosis of anastomotic leak: Electrolyte detection versus barium fluoroscopy', *Journal of Surgical Research* **182**(2), 192–197.
- DeArmond, D. T., Cline, A. M. & Johnson, S. B. (2010), 'Anastomotic Leak Detection by Electrolyte Electrical Resistance', *Journal of Investigative Surgery* **23**(4), 197–203.
- den Dulk, M., Noter, S. L., Hendriks, E. R., Brouwers, M. A. M., van der Vlies, C. H., Oostenbroek, R. J., Menon, A. G., Steup, W. H. & van de Velde, C. J. H. (2009), 'Improved diagnosis and treatment of anastomotic leakage after colorectal surgery', *European Journal of Surgical Oncology* **35**(4), 420–426.
- den Dulk, M., Witvliet, M. J., Kortram, K., Neijenhuis, P. A., de Hingh, I. H., Engel, A. F., van de Velde, C. J., de Brauw, L. M., Putter, H., Brouwers, M. A. & Steup, W.-H. (2013), 'The DULK (Dutch Leakage) and modified DULK score compared: actively seek the leak', *Colorectal Disease* **15**, e528–e533.
- Denost, Q., Rouanet, P., Faucheron, J.-L., Panis, Y., Meunier, B., Cotte, E., Meurette, G., Kirzin, S., Sabbagh, C., Loriau, J., Benoist, S., Mariette, C.,

- Sielezneck, I., Lelong, B., Mauvais, F., Romain, B., Barussaud, M.-L., Germain, C., Picat, M.-Q., Rullier, E. & Laurent, C. (2017), 'To Drain or Not to Drain Infraperitoneal Anastomosis After Rectal Excision for Cancer', *Annals of Surgery* **265**(3), 474–480.
URL: <http://journals.lww.com/00000658-201703000-00009>
- Dickens, E. & Ahmed, S. (2018), 'Principles of cancer treatment by chemotherapy', *Surgery (Oxford)* **36**(3), 134–138.
- DiZerega, G. S. & Rodgers, K. E. (1992), *The Peritoneum*, Springer New York, New York, NY.
- Duggan, E. W., Carlson, K. & Umpierrez, G. E. (2017), 'Perioperative Hyperglycemia Management: An Update.', *Anesthesiology* **126**(3), 547–560.
- Durmuş, U., Doğan, N. Ö., Pekdemir, M., Yılmaz, S., Yaka, E., Karadaş, A. & Güney Pınar, S. (2018), 'The value of lactate clearance in admission decisions of patients with acute exacerbation of COPD', *The American Journal of Emergency Medicine* **36**(6), 972–976.
URL: <https://linkinghub.elsevier.com/retrieve/pii/S0735675717309105>
- El-Azeem, A. A., Hamdy, G., Saraya, M., Fawzy, E., Anwar, E. & Abdulattif, S. (2013), 'The role of procalcitonin as a guide for the diagnosis, prognosis, and decision of antibiotic therapy for lower respiratory tract infections', *Egyptian Journal of Chest Diseases and Tuberculosis* **62**(4), 687–695.
- Emile, S. H. & Abd El-Hamed, T. M. (2017), 'Routine Drainage of Colorectal Anastomoses: An Evidence-Based Review of the Current Literature', *Gastroenterology Research and Practice* **2017**, 1–7.
URL: <https://www.hindawi.com/journals/grp/2017/6253898/>

- Engelen, M. P., Casaburi, R., Rucker, R. & Carithers, E. (1995), 'Contribution of the Respiratory Muscles to the Lactic Acidosis of Heavy Exercise in COPD', *Chest* **108**(5), 1246–1251.
- Epstein, F. H. & Parrillo, J. E. (1993), 'Pathogenetic Mechanisms of Septic Shock', *New England Journal of Medicine* **328**(20), 1471–1477.
- Erb, L., Hyman, N. H. & Osler, T. (2014), 'Abnormal Vital Signs Are Common after Bowel Resection and Do Not Predict Anastomotic Leak', *Journal of the American College of Surgeons* **218**(6), 1195–1199.
- Ernst, H. & Knoll, M. (2001), 'Electrochemical characterisation of uric acid and ascorbic acid at a platinum electrode', *Analytica Chimica Acta* **449**(1-2), 129–134.
URL: <https://linkinghub.elsevier.com/retrieve/pii/S0003267001013502>
- Evans, D. F., Pye, G., Bramley, R., Clark, A. G., Dyson, T. J. & Hardcastle, J. D. (1988), 'Measurement of gastrointestinal pH profiles in normal ambulant human subjects', *Gut* **29**(8), 1035–1041.
- Fejes, A. V., Best, M. G., van der Heijden, W. A., Vancura, A., Verschueren, H., de Mast, Q., Wurdinger, T. & Mannhalter, C. (2018), 'Impact of Escherichia coli K12 and O18:K1 on human platelets: Differential effects on platelet activation, RNAs and proteins', *Scientific Reports* **8**(1), 16145.
URL: <http://www.nature.com/articles/s41598-018-34473-w>
- Fernández, M. R., Ruiz, F. R., López, A. F., Segurola, C. L., Cebrián, J. M. F. & de la Portilla de Juan, F. (2017), 'C Reactive Protein as a Predictor of Anastomotic Leakage in Colorectal Surgery. Comparison Between Open and Laparoscopic Surgery', *Cirugía Española (English Edition)* **95**(9), 529–535.

- Finnerty, C. C., Mabvuure, N. T., Ali, A., Kozar, R. A. & Herndon, D. N. (2013), 'The surgically induced stress response.', *JPEN. Journal of parenteral and enteral nutrition* **37**(5 Suppl), 21S–9S.
- Fouda, E., El Nakeeb, A., Magdy, A., Hammad, E. a., Othman, G. & Farid, M. (2011), 'Early detection of anastomotic leakage after elective low anterior resection.', *Journal of gastrointestinal surgery : official journal of the Society for Surgery of the Alimentary Tract* **15**(1), 137–144.
- Fracalvieri, D., Biondo, S., Saez, J., Millan, M., Kreisler, E., Golda, T., Frago, R. & Miguel, B. (2012), 'Management of colorectal anastomotic leakage: differences between salvage and anastomotic takedown', *The American Journal of Surgery* **204**(5), 671–676.
- Gahring, L. C., Carlson, N. G., Kulmer, R. A. & Rogers, S. W. (1996), 'Neuronal Expression of Tumor Necrosis Factor Alpha in the Murine Brain', *Neuroimmunomodulation* **3**(5), 289–303.
- Garcia-Granero, A., Frasson, M., Flor-Lorente, B., Blanco, F., Puga, R., Carratalá, A. & Garcia-Granero, E. (2013), 'Procalcitonin and C-Reactive Protein as Early Predictors of Anastomotic Leak in Colorectal Surgery', *Diseases of the Colon & Rectum* **56**(4), 475–483.
- Gersing, E. (1998), 'Impedance spectroscopy on living tissue for determination of the state of organs', *Bioelectrochemistry and Bioenergetics* **45**(2), 145–149.
- Gessler, B., Eriksson, O. & Angenete, E. (2017), 'Diagnosis, treatment, and consequences of anastomotic leakage in colorectal surgery', *International Journal of Colorectal Disease* **32**(4), 549–556.

- Giaccaglia, V., Salvi, P. F., Cunsolo, G. V., Sparagna, A., Antonelli, M. S., Nigri, G., Balducci, G. & Ziparo, V. (2014), 'Procalcitonin, as an early biomarker of colorectal anastomotic leak, facilitates enhanced recovery after surgery', *Journal of Critical Care* **29**(4), 528–532.
- Gingell, D. & Fornes, J. A. (1976), 'Interaction of red blood cells with a polarized electrode: evidence of long-range intermolecular forces', *Biophysical Journal* **16**(10), 1131–1153.
- Ginsberg, B. H. (2009), 'Factors Affecting Blood Glucose Monitoring: Sources of Errors in Measurement', *Journal of Diabetes Science and Technology* **3**(4), 903–913.
- Girard, E., Messenger, M., Sauvanet, A., Benoist, S., Piessen, G., Mabrut, J.-Y. & Mariette, C. (2014), 'Anastomotic leakage after gastrointestinal surgery: Diagnosis and management', *Journal of Visceral Surgery* **151**(6), 441–450.
- Gouin, J.-P. & Kiecolt-Glaser, J. K. (2011), 'The Impact of Psychological Stress on Wound Healing: Methods and Mechanisms', *Immunology and Allergy Clinics of North America* **31**(1), 81–93.
URL: <https://linkinghub.elsevier.com/retrieve/pii/S0889856110000810>
- Gröne, J., Koch, D. & Kreis, M. E. (2015), 'Impact of intraoperative microperfusion assessment with Pinpoint Perfusion Imaging on surgical management of laparoscopic low rectal and anorectal anastomoses', *Colorectal Disease* **17**, 22–28.
URL: <http://doi.wiley.com/10.1111/codi.13031>
- Guo, S. & DiPietro, L. A. (2010), 'Critical review in oral biology & medicine: Factors affecting wound healing', *Journal of Dental Research* **89**(3), 219–229.

- Habib, K., Gupta, A., White, D., Mazari, F. A. K. & Wilson, T. R. (2015), 'Utility of contrast enema to assess anastomotic integrity and the natural history of radiological leaks after low rectal surgery: systematic review and meta-analysis', *International Journal of Colorectal Disease* **30**(8), 1007–1014.
- Hakkarainen, T. W., Steele, S. R., Bastaworous, A., Dellinger, E. P., Farrokhi, E., Farjah, F., Florence, M., Helton, S., Horton, M., Pietro, M., Varghese, T. K. & Flum, D. R. (2015), 'Nonsteroidal Anti-inflammatory Drugs and the Risk for Anastomotic Failure', *JAMA Surgery* **150**(3), 223.
URL: <http://archsurg.jamanetwork.com/article.aspx?doi=10.1001/jamasurg.2014.2239>
- Hallböök, O., Johansson, K. & Sjö Dahl, R. (1996), 'Laser Doppler blood flow measurement in rectal resection for carcinoma—comparison between the straight and colonic J pouch reconstruction.', *The British journal of surgery* **83**(3), 389–92.
- Halter, R., Hartov, A., Heaney, J., Paulsen, K. & Schned, A. (2007), 'Electrical Impedance Spectroscopy of the Human Prostate', *IEEE Transactions on Biomedical Engineering* **54**(7), 1321–1327.
- Hammond, J., Lim, S., Wan, Y., Gao, X. & Patkar, A. (2014), 'The Burden of Gastrointestinal Anastomotic Leaks: an Evaluation of Clinical and Economic Outcomes', *Journal of Gastrointestinal Surgery* **18**(6), 1176–1185.
- Haney, A. F. (2000), Peritoneal Fluid, in G. S. DiZerega, ed., 'Peritoneal Surgery', Springer New York, New York, NY, pp. 51–64.
- Heiden, M. G. V., Cantley, L. C. & Thompson, C. B. (2009), 'Understanding the

- Warburg Effect: The Metabolic Requirements of Cell Proliferation', *Science* **324**(5930), 1029–1033.
- Herigstad, B., Hamilton, M. & Heersink, J. (2001), 'How to optimize the drop plate method for enumerating bacteria', *Journal of Microbiological Methods* **44**(2), 121–129.
- Herwig, R., Glodny, B., Kühle, C., Schlüter, B., Brinkmann, O. a., Strasser, H., Senninger, N. & Winde, G. (2002), 'Early identification of peritonitis by peritoneal cytokine measurement.', *Diseases of the colon and rectum* **45**(4), 514–21.
- Hirano, Y., Omura, K., Tatsuzawa, Y., Shimizu, J., Kawaura, Y. & Watanabe, G. (2006), 'Tissue oxygen saturation during colorectal surgery measured by near-infrared spectroscopy: Pilot study to predict anastomotic complications', *World Journal of Surgery* **30**(3), 457–461.
- Hugh, R. & Leifson, E. (1964), 'The proposed Neotype Strains of *Pseudomonas Aeruginosa* (Schroeter 1872) Migula 1900', *International Bulletin of Bacteriological Nomenclature and Taxonomy* **14**(2), 69–84.
- Hunt, T. K., Aslam, R. S., Beckert, S., Wagner, S., Ghani, Q. P., Hussain, M. Z., Roy, S. & Sen, C. K. (2007), 'Aerobically derived lactate stimulates revascularization and tissue repair via redox mechanisms.', *Antioxidants & redox signaling* **9**(8), 1115–24.
- Hyman, N., Manchester, T. L., Osler, T., Burns, B. & Cataldo, P. a. (2007), 'Anastomotic leaks after intestinal anastomosis: it's later than you think.', *Annals of surgery* **245**(2), 254–258.
- Iyer, S. S. & Cheng, G. (2012), 'Role of interleukin 10 transcriptional regulation

- in inflammation and autoimmune disease.', *Critical reviews in immunology* **32**(1), 23–63.
- Jabłońska-Trypuć, A., Matejczyk, M. & Rosochacki, S. (2016), 'Matrix metalloproteinases (MMPs), the main extracellular matrix (ECM) enzymes in collagen degradation, as a target for anticancer drugs', *Journal of Enzyme Inhibition and Medicinal Chemistry* **31**(sup1), 177–183.
- Jeon, C. Y., Furuya, E. Y., Smaldone, A. & Larson, E. L. (2008), 'Post-admission glucose levels are associated with healthcare-associated bloodstream infections and pneumonia in hospitalized patients with diabetes.', *Journal of diabetes and its complications* **26**(6), 517–21.
- Jessup, J. M., Goldberg, R. M., Asare, E. A., Benson III, A. B., Brierley, J. D., Chang, G. J., Chen, V., Compton, C. C., Nardi, P. D., Goodman, K. A., Gress, D., Guinney, J., Gunderson, L. L., Hamilton, S. R., Hanna, N. N., Kakar, S., Kosinski, L. A., Negoita, S., Ogino, S., Overman, M. J., Quirke, P., Rohren, E., Sargent, D. J., Schumacher-Penberthy, T., L., Shibata, D., Sinicrope, F. A., Steele, S. R., Stojadinovic, A., Tejpar, S., Weiser, M. R., Welton, M. L. & Washington, M. K. (2017), Colon and Rectum, in M. B. Amin, S. Edge, F. Greene, D. R. Byrd, R. K. Brookland, M. K. Washington, J. E. Gershewald, C. C. Compton, K. R. Hess, D. C. Sullivan, J. M. Jessup, J. D. Brierley, L. E. Gaspar, R. L. Schilsky, C. M. Balch, D. P. Winchester, E. A. Asare, M. Madera, D. M. Gress & L. R. Meyer, eds, 'AJCC Cancer Staging Manual', 8th edn, Springer International Publishing, Basel, chapter 20, pp. 251–274.
- Jones, E. M., Cochrane, C. A. & Percival, S. L. (2015), 'The Effect of pH on the Extracellular Matrix and Biofilms', *Advances in Wound Care* **4**(7), 431–439.
- Jonker, D. J., O'Callaghan, C. J., Karapetis, C. S., Zalcberg, J. R., Tu, D., Au,

- H.-J., Berry, S. R., Krahn, M., Price, T., Simes, R. J., Tebbutt, N. C., van Hazel, G., Wierzbicki, R., Langer, C. & Moore, M. J. (2007), 'Cetuximab for the Treatment of Colorectal Cancer', *New England Journal of Medicine* **357**(20), 2040–2048.
- Junger, W., Junger, W. G., Miller, K., Bahrami, S., Redl, H., Schlag, G. & Moritz, E. (1996), 'Early detection of anastomotic leaks after colorectal surgery by measuring endotoxin in the drainage fluid.', *Hepato-gastroenterology* **43**(12), 1523–9.
- Jurtshuk, P. (1996), Bacterial Metabolism, in S. Baron, ed., 'Medical Microbiology', 4th edn, University of Texas Medical Branch at Galveston, Galveston (TX).
- Jutesten, H., Draus, J., Frey, J., Neovius, G., Lindmark, G., Buchwald, P. & Lydrup, M. L. (2019), 'High risk of permanent stoma after anastomotic leakage in anterior resection for rectal cancer', *Colorectal Disease* **21**(2), 174–182.
- Karliczek, A., Benaron, D. A., Baas, P. C., Zeebregts, C. J., Wiggers, T. & Van Dam, G. M. (2010), 'Intraoperative assessment of microperfusion with visible light spectroscopy for prediction of anastomotic leakage in colorectal anastomoses', *Colorectal Disease* **12**(10), 1018–1025.
- Kehlet, H. (1997), 'Multimodal approach to control postoperative pathophysiology and rehabilitation', *British Journal of Anaesthesia* **78**(5), 606–617.
- Kelton, J. G., Ulan, R., Stiller, C. & Holmes, E. (1978), 'Comparison of chemical composition of peritoneal fluid and serum: a method for monitoring dialysis patients and a tool for assessing binding to serum proteins in vivo.', *Annals of internal medicine* **89**(1), 67–70.

- Khubutiya, M. S., Evseev, A. K., Kolesnikov, V. A., Goldin, M. M., Davydov, A. D., Volkov, A. G. & Stepanov, A. A. (2010), 'Measurements of platinum electrode potential in blood and blood plasma and serum', *Russian Journal of Electrochemistry* **46**(5), 537–541.
URL: <http://link.springer.com/10.1134/S1023193510050071>
- Kim, H. S. (2016), 'Blood Glucose Measurement: Is Serum Equal to Plasma?', *Diabetes & Metabolism Journal* p. 365.
- Kim, M. J., Shin, R., Oh, H.-K., Park, J. W., Jeong, S.-Y. & Park, J.-G. (2011), 'The Impact of Heavy Smoking on Anastomotic Leakage and Stricture After Low Anterior Resection in Rectal Cancer Patients', *World Journal of Surgery* **35**(12), 2806–2810.
URL: <http://link.springer.com/10.1007/s00268-011-1286-1>
- Kim, T., Kang, J., Lee, J. H. & Yoon, J. (2011), 'Influence of attached bacteria and biofilm on double-layer capacitance during biofilm monitoring by electrochemical impedance spectroscopy', *Water Research* **45**(15), 4615–4622.
- Kirchhoff, P., Clavien, P.-A. & Hahnloser, D. (2010), 'Complications in colorectal surgery: risk factors and preventive strategies', *Patient Safety in Surgery* **4**(1), 5.
- Komen, N., De Bruin, R. W. F., Kleinrensink, G. J., Jeekel, J. & Lange, J. F. (2008), 'Anastomotic leakage, the search for a reliable biomarker. A review of the literature', *Colorectal Disease* **10**(2), 109–115.
- Komen, N., Morsink, M., Beiboer, S., Miggelbrink, A., Willemsen, P., van der Harst, E., Lange, J. & van Leeuwen, W. (2009), 'Detection of colon flora in peritoneal drain fluid after colorectal surgery: Can RT-PCR play a role in di-

- agnosing anastomotic leakage?', *Journal of Microbiological Methods* **79**(1), 67–70.
- Komen, N., Slieker, J., Willemsen, P., Mannaerts, G., Pattyn, P., Karsten, T., de Wilt, H., van der Harst, E., de Rijke, Y. B., Murawska, M., Jeekel, J. & Lange, J. F. (2014), 'Acute phase proteins in drain fluid: a new screening tool for colorectal anastomotic leakage? The APPEAL study: analysis of parameters predictive for evident anastomotic leakage.', *American journal of surgery* **208**(3), 317–23.
- Komen, N., Slieker, J., Willemsen, P., Mannaerts, G., Pattyn, P., Karsten, T., de Wilt, H., van der Harst, E., van Leeuwen, W., Decaestecker, C., Jeekel, H. & Lange, J. F. (2014), 'Polymerase chain reaction for *Enterococcus faecalis* in drain fluid: the first screening test for symptomatic colorectal anastomotic leakage. The Appeal-study: Analysis of Parameters Predictive for Evident Anastomotic Leakage', *International Journal of Colorectal Disease* **29**(1), 15–21.
- Konishi, T., Watanabe, T., Kishimoto, J. & Nagawa, H. (2006), 'Risk factors for anastomotic leakage after surgery for colorectal cancer: results of prospective surveillance.', *Journal of the American College of Surgeons* **202**(3), 439–44.
URL: <http://www.ncbi.nlm.nih.gov/pubmed/16500248>
- Kornmann, V. N. N., van Ramshorst, B., Smits, A. B., Bollen, T. L. & Boerma, D. (2014), 'Beware of false-negative CT scan for anastomotic leakage after colonic surgery', *International Journal of Colorectal Disease* **29**(4), 445–451.
- Krurup, P.-M., Jorgensen, L. N. & Harling, H. (2014), 'Management of Anastomotic Leakage in a Nationwide Cohort of Colonic Cancer Patients', *Journal of the American College of Surgeons* **218**(5), 940–949.

- Kuang, W. & Nelson, S. O. (1998), 'Low-frequency Dielectric Properties Of Biological Tissues: A Review With Some New Insights', *Transactions of the ASAE* **41**(1), 173–184.
- Lamazza, A., Sterpetti, A., De Cesare, A., Schillaci, A., Antoniozzi, A. & Fiori, E. (2015), 'Endoscopic placement of self-expanding stents in patients with symptomatic anastomotic leakage after colorectal resection for cancer: long-term results', *Endoscopy* **47**(03), 270–272.
- Lasia, A. (2014), *Electrochemical Impedance Spectroscopy and its Applications*, Springer New York, New York, NY.
- Law, W. I., Chu, K. W., Ho, J. W. & Chan, C. W. (2000), 'Risk factors for anastomotic leakage after low anterior resection with total mesorectal excision.', *American journal of surgery* **179**(2), 92–6.
- Leslie, A. & Steele, R. J. C. (2003), 'The interrupted serosubmucosal anastomosis - still the gold standard', *Colorectal Disease* **5**(4), 362–366.
URL: <http://doi.wiley.com/10.1046/j.1463-1318.2003.00460.x>
- Li, Y.-D., He, K.-X. & Zhu, W.-F. (2019), 'Correlation between invasive microbiota in margin-surrounding mucosa and anastomotic healing in patients with colorectal cancer', *World Journal of Gastrointestinal Oncology* **11**(9), 717–728.
URL: <https://www.wjgnet.com/1948-5204/full/v11/i9/717.htm>
- Liu, H., Wang, J., He, T., Becker, S., Zhang, G., Li, D. & Ma, X. (2018), 'Butyrate: A Double-Edged Sword for Health?', *Advances in Nutrition* **9**(1), 21–29.
URL: <https://academic.oup.com/advances/article/9/1/21/4849000>

- Longo, W. E., Virgo, K. S., Johnson, F. E., Oprian, C. A., Vernava, A. M., Wade, T. P., Phelan, M. A., Henderson, W. G., Daley, J. & Khuri, S. F. (2000), 'Risk factors for morbidity and mortality after colectomy for colon cancer.', *Diseases of the colon and rectum* **43**(1), 83–91.
- Lopez-Castejon, G. & Brough, D. (2011), 'Understanding the mechanism of IL-1 β secretion', *Cytokine & Growth Factor Reviews* **22**(4), 189–195.
- Macdonald, J. (1987), 'Impedance spectroscopy and its use in analyzing the steady-state AC response of solid and liquid electrolytes', *Journal of Electroanalytical Chemistry and Interfacial Electrochemistry* **223**(1-2), 25–50.
- Mäkelä, J. T., Kiviniemi, H. & Laitinen, S. (2003), 'Risk factors for anastomotic leakage after left-sided colorectal resection with rectal anastomosis', *Diseases of the Colon and Rectum* **46**(5), 653–660.
- Marieb, E. N. & Hoehn, K. (2013), *Human Anatomy & Physiology*, 9th edn, Pearson, San Francisco.
- Markou, P. & Apidianakis, Y. (2014), 'Pathogenesis of intestinal *Pseudomonas aeruginosa* infection in patients with cancer.', *Frontiers in cellular and infection microbiology* **3**, 115.
URL: <http://www.ncbi.nlm.nih.gov/pubmed/24432250><http://www.pubmedcentral.nih.gov/articlerender.fcgi?artid=PMC3882663>
- Marres, C. C. M., van de Ven, A. W. H., Leijssen, L. G. J., Verbeek, P. C. M., Bemelman, W. A. & Buskens, C. J. (2017), 'Colorectal anastomotic leak: delay in reintervention after false-negative computed tomography scan is a reason for concern', *Techniques in Coloproctology* **21**(9), 709–714.

- Martin, E. (2015), *Concise Medical Dictionary*, 9th edn, Oxford University Press, Oxford.
- Martini, F. H., Nath, J. L. & Bartholomew, E. F. (2015), *Fundamentals of Anatomy & Physiology*, 10th edn, Pearson Education Limited, Harlow.
- Matheson, N. A. (1992), 'Prospective audit of an extramucosal technique for intestinal anastomosis', *British Journal of Surgery* **79**(8), 843–843.
URL: <http://doi.wiley.com/10.1002/bjs.1800790848>
- Mathew, A. J., Wann, V. C., Abraham, D. T., Jacob, P. M., Selvan, B. S., Ramakrishna, B. S. & Nair, A. N. (2010), 'The Effect of Butyrate on the Healing of Colonic Anastomoses in Rats', *Journal of Investigative Surgery* **23**(2), 101–104.
- Matthiessen, P., Henriksson, M., Hallböök, O., Grunditz, E., Norén, B. & Arberman, G. (2008), 'Increase of serum C-reactive protein is an early indicator of subsequent symptomatic anastomotic leakage after anterior resection.', *Colorectal disease : the official journal of the Association of Coloproctology of Great Britain and Ireland* **10**(1), 75–80.
- Matthiessen, P., Strand, I., Jansson, K., Törnquist, C., Andersson, M., Rutegård, J. & Norgren, L. (2007), 'Is Early Detection of Anastomotic Leakage Possible by Intraperitoneal Microdialysis and Intraperitoneal Cytokines After Anterior Resection of the Rectum for Cancer?', *Diseases of the Colon & Rectum* **50**(11), 1918–1927.
- Matus, V., Valenzuela, J. G., Hidalgo, P., Pozo, L. M., Panes, O., Wozniak, A., Mezzano, D., Pereira, J. & Sáez, C. G. (2017), 'Human platelet interaction with E. coli O111 promotes tissue-factor-dependent procoagulant activity,

- involving Toll like receptor 4', *PLOS ONE* **12**(9), e0185431.
URL: <https://dx.plos.org/10.1371/journal.pone.0185431>
- McDaniel, J. C. & Browning, K. K. (2014), 'Smoking, Chronic Wound Healing, and Implications for Evidence-Based Practice', *Journal of Wound, Ostomy and Continence Nursing* **41**(5), 415–423.
URL: <http://journals.lww.com/00152192-201409000-00003>
- McDermott, F. D., Collins, D., Heeney, A. & Winter, D. C. (2014), 'Minimally invasive and surgical management strategies tailored to the severity of acute diverticulitis', *British Journal of Surgery* **101**(1), e90–e99.
URL: <http://doi.wiley.com/10.1002/bjs.9359>
- McGrath, A. (2005), Anatomy and Physiology of the Bowel and Urinary Systems, in 'Stoma Care', Wiley-Blackwell, chapter 1, pp. 1–16.
- Mengert, W. F., Cobb, S. W. & Brown, W. W. (1951), 'Introduction of blood into the peritoneal cavity; an experimental study.', *Journal of the American Medical Association* **147**(1), 34–7.
- Millan, M., García-Granero, E., Flor, B., García-Botello, S. & Lledo, S. (2006), 'Early prediction of anastomotic leak in colorectal cancer surgery by intramucosal pH', *Diseases of the Colon and Rectum* **49**(5), 595–601.
- Miller, K., Arrer, E. & Leitner, C. (1996), 'Early detection of anastomotic leaks after low anterior resection of the rectum', *Dis Colon Rectum* **39**(10), 1081–1085.
- Mitry, E., Rachet, B., Quinn, M. J., Cooper, N. & Coleman, M. P. (2008), 'Survival from cancer of the colon in england and wales up to 2001', *British Journal of Cancer* **99**, S26–S29.

- Moran, G. W., Leslie, F. C., Levison, S. E. & McLaughlin, J. T. (2008), 'Enteroendocrine cells: Neglected players in gastrointestinal disorders?', *Therapeutic Advances in Gastroenterology* **1**(1), 51–60.
- Muller, M., Mentel, M., van Hellemond, J. J., Henze, K., Woehle, C., Gould, S. B., Yu, R.-Y., van der Giezen, M., Tielens, A. G. M. & Martin, W. F. (2012), 'Biochemistry and Evolution of Anaerobic Energy Metabolism in Eukaryotes', *Microbiology and Molecular Biology Reviews* **76**(2), 444–495.
URL: <https://mmbbr.asm.org/content/76/2/444>
- Muñoz-Berbel, X., Vigués, N., Mas, J., Jenkins, A. T. A. & Muñoz, F. J. (2007), 'Impedimetric characterization of the changes produced in the electrode-solution interface by bacterial attachment', *Electrochemistry Communications* **9**(11), 2654–2660.
- Nagoba, B. S., Suryawanshi, N. M., Wadher, B. & Selkar, S. (2015), 'Acidic environment and wound healing: A review', *Wounds* **27**(1), 5–11.
- National Bowel Cancer Audit Project Team (2020), National Bowel Cancer Audit - Annual Report 2019, Technical report.
- National Cancer Registration and Analysis Service & Cancer Research UK (2017), *Chemotherapy, Radiotherapy and Tumour Resections in England: 2013-14 workbook*, NCRAS, London.
- Nemati, M., Hamidi, A., Maleki Dizaj, S., Javaherzadeh, V. & Lotfipour, F. (2016), 'An Overview on Novel Microbial Determination Methods in Pharmaceutical and Food Quality Control', *Advanced Pharmaceutical Bulletin* **6**(3), 301–308.

- Nesbakken, A., Nygaard, K., Lunde, O. C., Blücher, J., Gjertsen & Dullerud, R. (2005), 'Anastomotic leak following mesorectal excision for rectal cancer: True incidence and diagnostic challenges', *Colorectal Disease* **7**(6), 576–581.
- Nguyen, M. D. & Venton, B. J. (2015), 'Fast-scan Cyclic Voltammetry for the Characterization of Rapid Adenosine Release.', *Computational and structural biotechnology journal* **13**, 47–54.
URL: <http://www.ncbi.nlm.nih.gov/pubmed/26900429><http://www.pubmedcentral.nih.gov/articlerender.fcgi?artid=PMC4720017>
- NICE (2011), 'Colorectal cancer: the diagnosis and management of colorectal cancer'.
- Noel, M. S. (2017), 'Biologics in bowel cancer', *Journal of Gastrointestinal Oncology* **8**(3), 449–456.
- Nugent, S. G., Kumar, D., Rampton, D. S. & Evans, D. F. (2001), 'Intestinal luminal pH in inflammatory bowel disease: possible determinants and implications for therapy with aminosalicylates and other drugs.', *Gut* **48**(4), 571–7.
- Office for National Statistics (2019), Cancer survival by stage at diagnosis for England, Technical report.
- Okuda, J., Hayashi, N., Okamoto, M., Sawada, S., Minagawa, S., Yano, Y. & Gotoh, N. (2010), 'Translocation of *Pseudomonas aeruginosa* from the intestinal tract is mediated by the binding of ExoS to an Na,K-ATPase regulator, FXYD3.', *Infection and immunity* **78**(11), 4511–22.
URL: <http://www.ncbi.nlm.nih.gov/pubmed/20805335><http://www.pubmedcentral.nih.gov/articlerender.fcgi?artid=PMC2976341>

- Olarte, O., Barbe, K., Van Moer, W. & Van Ingelgem, Y. (2014), Glucose characterization based on electrochemical impedance spectroscopy, *in* '2014 IEEE International Instrumentation and Measurement Technology Conference (I2MTC) Proceedings', IEEE, pp. 833–837.
- Pasternak, B., Matthiessen, P., Jansson, K., Andersson, M. & Aspenberg, P. (2010), 'Elevated intraperitoneal matrix metalloproteinases-8 and -9 in patients who develop anastomotic leakage after rectal cancer surgery: a pilot study.', *Colorectal disease : the official journal of the Association of Coloproctology of Great Britain and Ireland* **12**(7), e93–8.
- Patel, K. L. (2008), 'Impact of tight glucose control on postoperative infection rates and wound healing in cardiac surgery patients.', *Journal of wound, ostomy, and continence nursing : official publication of The Wound, Ostomy and Continence Nurses Society* **35**(4), 397–404.
- Patzer, J. F., Yao, S. J., Wolfson, S. K. & Ruppel-Kerr, R. (1989), 'Urea oxidation kinetics via cyclic voltammetry', *Bioelectrochemistry and Bioenergetics* **22**(3), 341–353.
URL: <https://linkinghub.elsevier.com/retrieve/pii/0302459889870515>
- Pedersen, M. E., Qvist, N., Bisgaard, C., Kelly, U., Bernhard, A. & Møller Pedersen, S. (2009), 'Peritoneal microdialysis. Early diagnosis of anastomotic leakage after low anterior resection for rectosigmoid cancer.', *Scandinavian journal of surgery : SJS : official organ for the Finnish Surgical Society and the Scandinavian Surgical Society* **98**(3), 148–54.
- Pedersen, M. E., Qvist, N., Fristrup, C. & Mortensen, M. B. (2014), 'Mediastinal microdialysis in the diagnosis of early anastomotic leakage after resec-

- tion for cancer of the esophagus and gastroesophageal junction.', *American journal of surgery* **208**(3), 397–405.
- Pedrazzani, C., Moro, M., Mantovani, G., Lazzarini, E., Conci, S., Ruzzenente, A., Lippi, G. & Guglielmi, A. (2017), 'C-reactive protein as early predictor of complications after minimally invasive colorectal resection', *Journal of Surgical Research* **210**, 261–268.
- Peel, A. L. G. & Taylor, E. W. (1991), 'Proposed definitions for the audit of postoperative infection : a discussion paper', *Annals of the Royal College of Surgeons of England* **73**, 385–388.
- Peters, W. R., Smallwood, N. & Hyman, N. H. (2019), Prevention, Diagnosis, and Management of Anastomotic Leak, in C. J. Yeo, ed., 'Shackelford's Surgery of the Alimentary Tract, 2 Volume Set', eighth edn, Elsevier, Philadelphia, chapter 177, pp. 2137–2146.
- Pine, J. & Stevenson, L. (2017), 'Intestinal stomas', *Surgery (Oxford)* **35**(3), 165–170.
- Popescu, G., Sala, D., Gliga, M., Ciulic, S., Neagoe, R. M. & Mureşan, M. (2017), 'The Incidence and Mortality of Anastomotic Leakage after Colorectal Cancer Surgery', *Jurnalul de Chirurgie* **13**(3).
- URL:** <https://www.omicsonline.org/open-access/the-incidence-and-mortality-of-anastomotic-leakage-after-colorectal-cancer-surgery-1584-9341-1.php?aid=95884>
- Porporato, P. E., Payen, V. L., De Saedeleer, C. J., Pr eat, V., Thissen, J.-P., Feron, O. & Sonveaux, P. (2012), 'Lactate stimulates angiogenesis and accel-

- erates the healing of superficial and ischemic wounds in mice', *Angiogenesis* **15**(4), 581–592.
- Price, C. P. (2001), 'Regular review: Point of care testing', *BMJ* **322**(7297), 1285–1288.
- Pucino, V., Bombardieri, M., Pitzalis, C. & Mauro, C. (2017), 'Lactate at the crossroads of metabolism, inflammation, and autoimmunity', *European Journal of Immunology* **47**(1), 14–21.
- Quiding-Järbrink, M., Smith, D. A. & Bancroft, G. J. (2001), 'Production of matrix metalloproteinases in response to mycobacterial infection.', *Infection and immunity* **69**(9), 5661–70.
- Radiopaedia (2014), 'Anastomotic leak — Radiology Case — Radiopaedia.org'.
- URL:** <https://radiopaedia.org/cases/anastomotic-leak?lang=gb>
- Radiopaedia (2017), 'Rectovesical fistula and rectal anastomotic leak — Radiology Case — Radiopaedia.org'.
- URL:** <https://radiopaedia.org/cases/rectovesical-fistula-and-rectal-anastomotic-leak?lang=gb>
- Rahbari, N. N., Weitz, J., Hohenberger, W., Heald, R. J., Moran, B., Ulrich, A., Holm, T., Wong, W. D., Tiet, E., Moriya, Y., Laurberg, S., den Dulk, M., van de Velde, C. & Büchler, M. W. (2010), 'Definition and grading of anastomotic leakage following anterior resection of the rectum: A proposal by the International Study Group of Rectal Cancer', *Surgery* **147**(3), 339–351.
- Rayfield, E. J., Ault, M. J., Keusch, G. T., Brothers, M. J., Nechemias, C. &

- Smith, H. (1982), 'Infection and diabetes: the case for glucose control.', *The American journal of medicine* **72**(3), 439–50.
- Reisinger, K. W., Poeze, M., Hulsewé, K. W., van Acker, B. a., van Bijnen, A. a., Hoofwijk, A. G., Stoot, J. H. & Derikx, J. P. (2014), 'Accurate Prediction of Anastomotic Leakage after Colorectal Surgery Using Plasma Markers for Intestinal Damage and Inflammation', *Journal of the American College of Surgeons* **219**(4), 744–751.
- Ribaut, C., Reybier, K., Reynes, O., Launay, J., Valentin, A., Fabre, P. L. & Nepveu, F. (2009), 'Electrochemical impedance spectroscopy to study physiological changes affecting the red blood cell after invasion by malaria parasites', *Biosensors and Bioelectronics* **24**(8), 2721–2725.
- Richards, C. H., Campbell, V., Ho, C., Hayes, J., Elliott, T. & Thompson-Fawcett, M. (2012), 'Smoking is a major risk factor for anastomotic leak in patients undergoing low anterior resection', *Colorectal Disease* **14**(5), 628–633.
URL: <http://doi.wiley.com/10.1111/j.1463-1318.2011.02718.x>
- Rullier, E., Laurent, C., Garrelon, J., Michel, P., Saric, J. & Parneix, M. (1998), 'Risk factors for anastomotic leakage after resection for rectal cancer', *British Journal of Surgery* **85**, 355–358.
- Ryoo, S. M. & Kim, W. Y. (2018), 'Clinical applications of lactate testing in patients with sepsis and septic shock', *Journal of Emergency and Critical Care Medicine* **2**(4), 14–14.
- Sak, K. (2012), 'Chemotherapy and Dietary Phytochemical Agents', *Chemotherapy Research and Practice* **2012**, 11 pages.

- Schardey, H. M., Kamps, T., Rau, H. G., Gatermann, S., Baretton, G. & Schildberg, F. W. (1994), 'Bacteria: a major pathogenic factor for anastomotic insufficiency.', *Antimicrobial Agents and Chemotherapy* **38**(11), 2564–2567.
- Schneider, L. A., Korber, A., Grabbe, S. & Dissemond, J. (2007), 'Influence of pH on wound-healing: A new perspective for wound-therapy?', *Archives of Dermatological Research* **298**(9), 413–420.
- Schwan, H. P. (1957), 'Electrical Properties of Tissue and Cell Suspensions', *Advances in Biological and Medical Physics* **5**, 147–209.
- Senagore, A. J., Delaney, C. P., Madboulay, K., Brady, K. M., Fazio, V. W. & Fazio, C. V. W. (2003), 'Laparoscopic colectomy in obese and nonobese patients.', *Journal of gastrointestinal surgery : official journal of the Society for Surgery of the Alimentary Tract* **7**(4), 558–61.
URL: <https://linkinghub.elsevier.com/retrieve/pii/S1091255X02001245><http://www.ncbi.nlm.nih.gov/pubmed/12763416>
- Sevim, Y., Celik, S. U., Yavarifar, H. & Akyol, C. (2016), 'Minimally invasive management of anastomotic leaks in colorectal surgery', *World Journal of Gastrointestinal Surgery* **8**(9), 621.
- Sheka, A. C., Tevis, S. & Kennedy, G. D. (2016), 'Urinary tract infection after surgery for colorectal malignancy: risk factors and complications.', *American journal of surgery* **211**(1), 31–9.
URL: <http://www.ncbi.nlm.nih.gov/pubmed/26298687><http://www.pubmedcentral.nih.gov/articlerender.fcgi?artid=PMC6039384>
- Sheridan, W. G., Lowndes, R. H. & Young, H. L. (1987), 'Tissue oxygen ten-

- sion as a predictor of colonic anastomotic healing.', *Diseases of the colon and rectum* **30**(11), 867–871.
- Shippenberg, T. S. & Thompson, A. C. (1997), 'Overview of Microdialysis', *Current Protocols in Neuroscience* p. Unit7.1.
- Shogan, B. D., Carlisle, E. M., Alverdy, J. C. & Umanskiy, K. (2013), 'Do We Really Know Why Colorectal Anastomoses Leak?', *Journal of Gastrointestinal Surgery* **17**(9), 1698–1707.
- Shroyer, N. F. & Kocoshis, S. A. (2011), *Anatomy and Physiology of the Small and Large Intestines*, 4th edn, Elsevier.
- Sidebottom, R. A., Williams, P. R. & Kanarek, K. S. (1982), 'Glucose determinations in plasma and serum: potential error related to increased hematocrit.', *Clinical chemistry* **28**(1), 190–2.
- Siew, E. D. & Ikizler, T. A. (2008), 'Determinants of insulin resistance and its effects on protein metabolism in patients with advanced chronic kidney disease.', *Contributions to nephrology* **161**, 138–144.
- Silue, T., Minnikanti, S. & Peixoto, N. (2017), Randles Model of Vitreous Humor, in 'Proceedings of the 10th International Joint Conference on Biomedical Engineering Systems and Technologies', Vol. 2017-Janua, SCITEPRESS - Science and Technology Publications, pp. 156–162.
- Silva, P. B. M., Oliveira, K. A. & Coltro, W. K. T. (2016), 'Colorimetric Detection of Glucose in Biological Fluids Using Toner-Based Microzone Plates', *Journal of the Brazilian Chemical Society* .
URL: <http://www.gnresearch.org/doi/10.5935/0103-5053.20160164>

- Silvestre, J., Rebanda, J., Lourenço, C. & Póvoa, P. (2014), 'Diagnostic accuracy of C-reactive protein and procalcitonin in the early detection of infection after elective colorectal surgery - a pilot study.', *BMC infectious diseases* **14**, 444.
- Singh, G., Wu, B., Baek, M. S., Camargo, A., Nguyen, A., Slusher, N. A., Srinivasan, R., Wiener-Kronish, J. P. & Lynch, S. V. (2010), 'Secretion of *Pseudomonas aeruginosa* type III cytotoxins is dependent on pseudomonas quinolone signal concentration.', *Microbial pathogenesis* **49**(4), 196–203.
- Sørensen, L. T., Jørgensen, T., Kirkeby, L. T., Skovdal, J., Vennits, B. & Wille-Jørgensen, P. (1999), 'Smoking and alcohol abuse are major risk factors for anastomotic leakage in colorectal surgery.', *The British Journal of Surgery* **86**(7), 927–931.
- Stavrou, G. & Kotzampassi, K. (2017), 'Gut microbiome, surgical complications and probiotics.', *Annals of gastroenterology* **30**(1), 45–53.
- Steele, S. R., Hull, T. L., Read, T. E., Saclarides, T. J., Senagore, A. J. & Whitlow, C. B. (2016), *The ASCRS Textbook of Colon and Rectal Surgery*, Springer International Publishing, Cham.
- Stumpf, M., Klinge, U., Wilms, A., Zabrocki, R., Rosch, R., Junge, K., Kroenes, C. & Schumpelick, V. (2005), 'Changes of the extracellular matrix as a risk factor for anastomotic leakage after large bowel surgery', *Surgery* **137**(2), 229–234.
- Sun, S., Li, H., Chen, J. & Qian, Q. (2017), 'Lactic Acid: No Longer an Inert and End-Product of Glycolysis', *Physiology* **32**(6), 453–463.
URL: <https://www.physiology.org/doi/10.1152/physiol.00016.2017>

- Szumlowicz, U. M. & Hull, T. L. (2011), Colonic Physiology, in D. Beck, P. Roberts, T. Saclarides & A. Senagore, eds, 'The ASCRS Textbook of Colon and Rectal Surgery', 2 edn, Springer New York, New York, NY, pp. 23–39.
- Tanaka, T., Narazaki, M. & Kishimoto, T. (2014), 'IL-6 in inflammation, immunity, and disease.', *Cold Spring Harbor perspectives in biology* **6**(10), a016295.
- Thomas, M. & Margolin, D. (2016), 'Management of Colorectal Anastomotic Leak', *Clinics in Colon and Rectal Surgery* **29**(02), 138–144.
- Thompson, S. K., Chang, E. Y. & Jobe, B. A. (2006), 'Clinical review: Healing in gastrointestinal anastomoses, Part I', *Microsurgery* **26**(3), 131–136.
URL: <http://doi.wiley.com/10.1002/micr.20197>
- Tobias, J. & Hochhauser, D. (2014), Tumours of the small and large bowel, in 'Cancer and its Management', 7th edn, John Wiley & Sons, Ltd., Chichester, chapter 16, pp. 308–320.
- Toutouzas, K., Kleidi, E. S., Drimousis, P. G., Balla, M., Papanikolaou, M. N., Larentzakis, A., Theodorou, D. & Katsaragakis, S. (2009), 'Anastomotic leak management after a low anterior resection leading to recurrent abdominal compartment syndrome: a case report and review of the literature', *Journal of Medical Case Reports* **3**(1), 125.
- Trabold, O., Wagner, S., Wicke, C., Scheuenstuhl, H., Hussain, M. Z., Rosen, N., Seremetiev, A., Becker, H. D. & Hunt, T. K. (2003), 'Lactate and oxygen constitute a fundamental regulatory mechanism in wound healing.', *Wound repair and regeneration : official publication of the Wound Healing Society [and] the European Tissue Repair Society* **11**(6), 504–9.

- Tran, A. K., Sapkota, A., Wen, J., Li, J. & Takei, M. (2018), 'Linear relationship between cytoplasm resistance and hemoglobin in red blood cell hemolysis by electrical impedance spectroscopy & eight-parameter equivalent circuit.', *Biosensors & bioelectronics* **119**(August), 103–109.
- Trasatti, S. & Petrii, O. A. (1991), 'Real surface area measurements in electrochemistry', *Pure and Applied Chemistry* **63**(5), 711–734.
URL: <https://www.degruyter.com/view/journals/pac/63/5/article-p711.xml>
- Tsujinaka, S. & Konishi, F. (2011), 'Drain vs No Drain After Colorectal Surgery', *Indian Journal of Surgical Oncology* **2**(1), 3–8.
URL: <http://link.springer.com/10.1007/s13193-011-0041-2>
- Turkina, M. V., Ghafouri, N., Gerdle, B. & Ghafouri, B. (2017), 'Evaluation of dynamic changes in interstitial fluid proteome following microdialysis probe insertion trauma in trapezius muscle of healthy women', *Scientific Reports* **7**(1), 43512.
URL: <http://www.nature.com/articles/srep43512>
- U. S. National Institutes of Health - National Cancer Institute (2001), 'Mucosa: Image Details - NCI Visuals Online'.
URL: <https://visualsonline.cancer.gov/details.cfm?imageid=1781>
- Uchida, K. & Kamikawa, Y. (2007), 'Muscularis mucosae - the forgotten sibling.', *Journal of smooth muscle research = Nihon Heikatsukin Gakkai kikanishi* **43**(5), 157–77.
- Uğraş, B., Giriş, M., Erbil, Y., Gökpınar, M., Çitlak, G., İşsever, H., Bozbora, A. & Öztezcan, S. (2008), 'Early prediction of anastomotic leakage after

- colorectal surgery by measuring peritoneal cytokines: Prospective study', *International Journal of Surgery* **6**(1), 28–35.
- van Berge Henegouwen, M. I., van der Poll, T., van Deventer, S. J. & Gouma, D. J. (1998), 'Peritoneal cytokine release after elective gastrointestinal surgery and postoperative complications.', *American journal of surgery* **175**(4), 311–6.
- van Koperen, P. J., van Berge Henegouwen, M. I., Rosman, C., Bakker, C. M., Heres, P., Slors, J. F. M. & Bemelman, W. A. (2009), 'The Dutch multicenter experience of the endo-sponge treatment for anastomotic leakage after colorectal surgery.', *Surgical endoscopy* **23**(6), 1379–83.
- Veloso, N., Dinis Silva, J., Carvalho, M., Rosa, I., Medeiros, I., Gonçalves, L., Godinho, R. & Viveiros, C. (2013), 'Endo-SPONGE® treatment for anastomotic leakage after colorectal surgery', *GE Jornal Português de Gastrenterologia* **20**(3), 132–135.
- Verma, I., Kaur, S., Goyal, S., Goyal, S., Multani, J. S. & Narang, A. P. (2014), 'Diagnostic value of lactate levels in acute abdomen disorders', *Indian Journal of Clinical Biochemistry* **29**(3), 382–385.
- Vermeer, T., Orsini, R., Daams, F., Nieuwenhuijzen, G. & Rutten, H. (2014), 'Anastomotic leakage and presacral abscess formation after locally advanced rectal cancer surgery: Incidence, risk factors and treatment', *European Journal of Surgical Oncology (EJSO)* **40**(11), 1502–1509.
- Vignali, A., Fazio, V. W., Lavery, I. C., Milsom, J. W., Church, J. M., Hull, T. L., Strong, S. A. & Oakley, J. R. (1997), 'Factors associated with the occurrence

- of leaks in stapled rectal anastomoses: a review of 1,014 patients.', *Journal of the American College of Surgeons* **185**(2), 105–13.
- Vignali, A., Gianotti, L., Braga, M., Radaelli, G., Malvezzi, L. & Carlo, V. D. (2000), 'Altered microperfusion at the rectal stump is predictive for rectal anastomotic leak', *Diseases of the Colon & Rectum* **43**(1), 76–82.
- Vilz, T. O., Roessel, L., Chang, J., Pantelis, D., Schwandt, T., Koscielny, A., Wehner, S. & Kalff, J. C. (2015), 'Establishing a biomarker for postoperative ileus in humans - Results of the BiPOI trial.', *Life sciences* **143**, 58–64.
- Vogler, E. A. (2012), 'Protein adsorption in three dimensions', *Biomaterials* **33**(5), 1201–1237.
URL: <https://linkinghub.elsevier.com/retrieve/pii/S0142961211012634>
- Walker, K. G., Bell, S. W., Rickard, M. J. F. X., Mehanna, D., Dent, O. F., Chappuis, P. H. & Bokey, E. L. (2004), 'Anastomotic leakage is predictive of diminished survival after potentially curative resection for colorectal cancer.', *Annals of Surgery* **240**(2), 255–259.
- Wang, J. (2006), *Analytical Electrochemistry*, John Wiley & Sons, Inc., Hoboken, NJ, USA.
- Wang, L. & Gu, J. (2010), 'Risk Factors for Symptomatic Anastomotic Leakage After Low Anterior Resection for Rectal Cancer with 30 Gy/10 f/2 w Pre-operative Radiotherapy', *World Journal of Surgery* **34**(5), 1080–1085.
URL: <http://link.springer.com/10.1007/s00268-010-0449-9>
- Ward, A. C., Connolly, P. & Tucker, N. P. (2014), 'Pseudomonas aeruginosa Can Be Detected in a Polymicrobial Competition Model Using Impedance Spectroscopy with a Novel Biosensor', *PLoS ONE* **9**(3), e91732.

- Ward, A. C., Hannah, A. J., Kendrick, S. L., Tucker, N. P., MacGregor, G. & Connolly, P. (2018), 'Identification and characterisation of *Staphylococcus aureus* on low cost screen printed carbon electrodes using impedance spectroscopy', *Biosensors and Bioelectronics* **110**(January), 65–70.
- Warschkow, R., Steffen, T., Thierbach, J., Bruckner, T., Lange, J. & Tarantino, I. (2011), 'Risk Factors for Anastomotic Leakage after Rectal Cancer Resection and Reconstruction with Colorectostomy. A Retrospective Study with Bootstrap Analysis', *Annals of Surgical Oncology* **18**(10), 2772–2782.
URL: <http://link.springer.com/10.1245/s10434-011-1696-1>
- Webb, C. R., Koboziev, I., Furr, K. L. & Grisham, M. B. (2016), 'Protective and pro-inflammatory roles of intestinal bacteria', *Pathophysiology* **23**(2), 67–80.
- Weledji, E. P. & Ngowe, M. N. (2013), 'The challenge of intra-abdominal sepsis', *International Journal of Surgery* **11**(4), 290–295.
- Wikimedia Commons (2008), 'File:Electric double-layer (BMD model) NT.PNG'.
URL: [https://commons.wikimedia.org/wiki/File:Electric{_}double-layer{_}\(BMD{_}model\){_}NT.PNG](https://commons.wikimedia.org/wiki/File:Electric{_}double-layer{_}(BMD{_}model){_}NT.PNG)
- Wilson, J. A. & Clark, J. J. (2004), 'Obesity: Impediment to Postsurgical Wound Healing', *Advances in Skin & Wound Care* **17**(8), 426–432.
URL: <http://journals.lww.com/00129334-200410000-00013>
- Wood, J. D. (2019), Normal Anatomy, Digestion, Absorption, in 'Adult Short Bowel Syndrome', Elsevier, pp. 1–16.
- Wright, E. C. (2019), The development of novel biomarker techniques for the

- early detection of colorectal anastomotic breakdown, Md, The University of Glasgow.
- Wu, G. (2010), *Assay Development*, John Wiley & Sons, Inc., Hoboken, NJ, USA.
- Yamamoto, T., Umegae, S., Matsumoto, K. & Saniabadi, A. R. (2011), 'Peritoneal cytokines as early markers of peritonitis following surgery for colorectal carcinoma: A prospective study', *Cytokine* **53**(2), 239–242.
- Yanase, S., Yasuda, K. & Ishii, N. (2018), 'Small-Scale Colorimetric Assays of Intracellular Lactate and Pyruvate in the Nematode *Caenorhabditis elegans*.' , *Journal of visualized experiments : JoVE* (140).
URL: <http://www.ncbi.nlm.nih.gov/pubmed/30371679><http://www.pubmedcentral.nih.gov/articlerender.fcgi?artid=PMC6235533>
- Yang, L., Huang, X.-E., Xu, L., Zhou, X., Zhou, J.-N., Yu, D.-S., Li, D.-Z. & Guan, X. (2013), 'Acidic Pelvic Drainage as a Predictive Factor For Anastomotic Leakage after Surgery for Patients with Rectal Cancer', *Asian Pacific Journal of Cancer Prevention* **14**(9), 5441–5447.
- Zeeh, J., Inglin, R., Baumann, G., Dirsch, O., Riley, N. E., Gerken, G., Büchler, M. W. & Egger, B. (2001), 'Mycophenolate mofetil impairs healing of left-sided colon anastomoses.' , *Transplantation* **71**(10), 1429–35.
URL: <http://journals.lww.com/00007890-200105270-00013><http://www.ncbi.nlm.nih.gov/pubmed/11391231>
- Zhang, J.-M. & An, J. (2007), 'Cytokines, inflammation, and pain.' , *International anesthesiology clinics* **45**(2), 27–37.

Appendix 1 : Biorepository Ethics Approval



University of Glasgow | School of
Medicine



Friday, 11 August 2017

Joshua Paulinus
Dept of Biomedical Engineering
University of Strathclyde
106 Rottenrow
Glasgow
G4 ONW

Dear Joshua,

Biorepository Application Number: 300

Study Title: Collection and use of surplus ascetic fluid from patients undergoing colorectal resection.

On behalf of the NHS GG&C Biorepository Management Committee I am pleased to provide approval for the acquisition of tissue for the above application. This approval is on the basis described in your application and supporting documents.

The committee would be grateful for an update on the progress of the use of the tissue and for information on the publications which arise from this work. At the end of the study Biorepository staff may also contact you for this information.

If your project is eligibly funded we will transcribe your application onto an IRAS R&D form for the R&D financial return. It will also be included in the national R&D database, CPMS.

In addition we would ask you to acknowledge the NHS GG&C Bio-repository in any publications.

Thank you for collaborating with the NHS GG&C Biorepository. We wish you every success with this work.

Yours sincerely,

James Going, MB PhD, MRCP, FRCPath
Consultant Pathologist and Director of NHSGGC Biorepository
cc Jane Hair, Fiona Graham

Dr James Going, MB PhD, MRCP, FRCPath
University Pathology Unit
L2b – 106
Laboratory Medicine Building, Southern General Hospital
Govan Road, Glasgow, G51 4TF

Tel: +44 (0)141 354 9437
E-mail: james.going@glasgow.ac.uk